



**University of
Reading**

**SUMOylation Regulates Focal Adhesions in
Cancer Cell Migration**

Zhiyao Huang

THESIS SUBMITTED TO THE SCHOOL OF BIOLOGICAL SCIENCES AT THE
UNIVERSITY OF READING FOR THE DEGREE OF DOCTOR OF PHILOSOPHY

Ph.D. Thesis

June 2017

Declaration

I confirm that this is my own work and the use of all materials from other sources has been properly and fully acknowledged.

Signature:

Date:

Contents

| | |
|---|-------|
| Contents | 3-7 |
| Abbreviations | 8-11 |
| Figures and Tables | 12 |
| Abstract | 13-14 |
| Chapter 1- Introduction | |
| 1.1 Cancer Cell Metastasis | 15 |
| 1.2 SUMOylation and its Post-Translational Protein Modification Cycle..... | 19 |
| 1.3 SUMOylation and Cancer..... | 21 |
| 1.4 General Aspects of SUMOylation and its Role in Cellular Physiology..... | 23 |
| 1.5 Crosstalk between SUMOylation and other PTMs and other SUMO Motifs..... | 24 |
| 1.6 The Fundamental Proteins in Facilitating Cancer Cell Metastasis: the Integrin-Focal Adhesions Signalling in Cell Migration Machinery..... | 26 |
| 1.7 Talin and Vinculin..... | 34 |
| 1.8 The Inhibitors Used in this Study | 36 |
| 1.9 Cell Lines Used for this Study..... | 39 |
| 1.10 The Hypothesis: SUMOylation Plays an Important Role in the Regulation of Focal Adhesions, which are Essential in Cell Migration..... | 39 |
| Chapter 2 - Materials and Methods | |
| 2.1 – 2.4 Cell Culture..... | 41 |
| 2.1 Media Preparation | |
| 2.2 Routine Cell Passage | |
| 2.3 Haemocytometry | |
| 2.4 Freezing and Thawing the Cells | |
| 2.5 DNA Plasmid Extraction and Purification: HA SUMO-2, GFP-Vinculin, mEmerald-Vinculin and GFP-Talin..... | 43 |
| 2.5.1 LB Media and Bacto Agar Preparation | |
| 2.5.2 The Selection of the Antibiotics-resistant DNA Plasmids and the Growth of the Bacterial Broth | |
| 2.5.3 Maxiprep Kit | |
| 2.6 Drug Treatment: Ginkgolic Acid, Gossypetin and 2-D08 | 47 |
| 2.7 Focal Adhesion Turnover Assay..... | 48 |
| 2.7.1 DNA Plasmid Transfection | |
| 2.7.2 Non-Compressed Collagen Coating | |
| 2.7.3 2.5D Cell Culture | |
| 2.8 Immunocytochemistry..... | 49 |
| 2.8.1 Cell Growth on Coverslips | |
| 2.8.2 Immunocytochemistry Staining | |

| | |
|---|----|
| 2.8. 3 Experimental Controls | |
| 2.8. 4 Primary and Secondary Antibodies for IHC Experiments | |
| 2.9 Confocal Microscopy and Live-Cell Imaging..... | 51 |
| 2.10 Phase-Contrast Live-Cell Timelapse..... | 51 |
| 2.10. 1 Cell Growth in 3D Collagen Matrix | |
| 2.10. 2 Drug Treatments | |
| 2.10. 3 Live-Cell Timelapse Microscopy | |
| 2.11 Western Blotting..... | 53 |
| 2.11. 1 Bradford Protein Assay | |
| 2.11. 2 Western Blotting Buffers (Manually Prepared) | |
| 2.11. 3 Electrophoresis | |
| 2.11. 4 Membrane Transfer | |
| 2.11. 5 Blocking | |
| 2.11. 6 Primary and Secondary Antibodies | |
| 2.11. 7 Band Detection | |
| 2.11. 8 Primary and Secondary Antibodies for WB Experiments | |
| 2.12 Ubc9 siRNA Knockdown and Western Blotting..... | 55 |
| 2.12. 1 GAPDH siRNA Knockdown | |
| 2.12. 2 Ubc9 siRNA Knockdown | |
| 2.13 Quantitative Data Analysis: Image J..... | 59 |
| 2.14 Statistics..... | 60 |

Chapter 3 - SUMOylation Plays an Important Role in the Dynamics and Turnover Rate of Focal Adhesions and Cell Migration

| | |
|---|----|
| 3.1 Introduction and Hypothesis | 61 |
| 3. 2 Blocking SUMOylation with GA Leads to Increased Number of Talin Containing FAs..... | 64 |
| 3. 3 Inhibition of SUMOylation with GA in MDA-MB-231 Cells Grown on the Top of 2mg/ml Collagen Causes Increased Number, Size or Turnover of Focal Adhesions..... | 67 |
| 3. 3. 1. GA 2hrs Treatment Increases the Mean Talin Containing FAs Number, Size or Turnover Time | |
| 3. 3. 2. GA 2hrs Treatment Increases the Mean FAK Containing FAs Number, Size or Turnover Time | |
| 3. 3. 3. GA 2hrs Treatment Increases the Mean Vinculin Containing FAs Number, Size or Turnover Time | |
| 3. 4 GA at 25, 50 or 100µM Leads to Decreased Speed of Cell Migration and Reduced Total Cell Migration Length..... | 74 |
| 3. 5 Ubc9 siRNA Knockdown Reduces the Ubc9 Expression..... | 76 |
| 3. 6 Ubc9 siRNA 48hrs Treatment Alone Leads to Increased Talin Number and Size Similarly to the GA 100µM Treatment; However, Ubc9 siRNA Treatment Also Causes Cell Membrane Ruffling..... | 78 |
| 3. 7 Combining 100µM GA and 25nM Ubc9 siRNA Treatment does not further Increase the FAs Number or Size..... | 80 |
| 3. 8 Ubc9 siRNA Knockdown Leads to Reduced Speed of Cell Migration for Both 25h and 48h Timelapse..... | 82 |
| 3. 9 Other SUMOylation Inhibitors Also Cause an Increase in the Mean FAs Number or Size..... | 86 |
| 3. 9. 1. GA, Gossypetin or 2-D08 1hour Treatments Cause an Increase in the Mean Number or Size of Vinculin Containing FAs | |
| 3. 9. 2. GA, Gossypetin or 2-D08 1 hour Treatments Cause an Increase in the Mean Number or Size of Talin Containing FAs | |
| 3. 9. 3. GA or 2-D08 15 Minutes Treatments Caused an Increase in the Mean Number of Vinculin Containing FAs | |

- 3. 9. 4. GA or Gossypetin 1 hour Treatments Caused an Increase in the Mean Number of Vinculin Containing FAs; 2-D08 Caused an Increase in the Mean Size of Vinculin Containing FAs
- 3. 9. 5. GA or 2-D08 15 Minutes Treatments Caused an Increase in the Mean Number of Talin Containing FAs
- 3. 9. 6. GA or 2-D08 1 hour Treatments Caused an Increase in the Mean Number of Talin Containing FAs; 2-D08 Caused an Increase in the Mean Size of Talin Containing FAs

Discussion.....98-106

Chapter 4 – SUMOylation of Talin and Vinculin

| | |
|--|-----|
| 4. 1 Introduction and Hypothesis..... | 107 |
| 4.2 Method Development..... | 110 |
| 4.2. 1 Antibodies for IP and WB Experiments..... | 111 |
| 4.2. 2 Immunoprecipitation and Western Blotting (IP and WB) | 112 |
| IP Preparation with Whole Cell Lysates: 6-well Plates for GA 15, 30 or 60 Minutes | |
| IP Preparation with Whole Cell Lysates: T25 Flasks | |
| IP and Reverse IP with the Whole Cell Lysates Only | |
| 4.2. 3 pcDNA3 HA SUMO-2 WT Plasmid Transfection, Immunoprecipitation and Western Blotting..... | 114 |
| HA SUMO-2 Plasmid Transfection / 6-well Plates and IHC | |
| HA SUMO-2 Plasmid Transfection / T25 Flasks | |
| Immunoprecipitation Using the HA SUMO-2 Plasmid | |
| Western Blotting with Fluorescence | |
| Fluorescent Scanning | |
| 4.2. 4 VIVA Bind™-SUMO Kit and Western Blotting..... | 118 |
| Wcl Preparations for Non-Flushed Cells with Fibronectin Coating | |
| VIVA Bind™-SUMO Matrix Preparation | |
| VIVA Bind™-SUMO Assay | |
| Elution of Captured SUMOylated Proteins | |
| 4.2. 5 Isolation of Focal Adhesions with the VIVA Bind™-SUMO Kit and Western Blotting..... | 120 |
| 4.2. 6 Co-Immunoprecipitation..... | 122 |
| Stripping and Re-blotting with the Isolated FA Samples | |
| 4.2. 7 Co-Transfection with siRNA and HA SUMO-2 Plasmid..... | 123 |
| 4. 3. 1 IP and WB Reveals Talin is SUMOylated..... | 124 |
| 4. 3. 2 IP and WB Reveals Vinculin is SUMOylated | 125 |
| 4. 3. 3 HA-tag SUMO-2 Plasmid Transfection Shows the Expression of SUMO-2 in the Cytoplasm and in the Nucleus of the MDA-MB-231 Cells..... | 125 |
| 4. 3. 4 GAPDH or Akt are not SUMOylated..... | 126 |
| 4. 3. 5 HA-tag SUMO-2 IP Detects both Full-length SUMOylated Talin and Fragments of Talin..... | 126 |
| 4. 3. 6 HA-tag SUMO-2 IP Detects SUMOylated Vinculin..... | 129 |
| 4.3. 7 SUMO VIVA™ Binding Assay and IP SUMOylated Talin or SUMOylated Vinculin in Isolated FAs..... | 130 |
| 4. 3. 8 Ubc9 siRNA Transfection with HA-tag SUMO-2 plasmid Transfection | 135 |
| 4. 3. 9 Effect of Gossypetin and 2-D08 Treatments on Talin SUMOylation..... | 137 |
| 4.3. 10 Focal Adhesion Expression was not Affected after GA or Ubc9 siRNA Treatment..... | 138 |
| 4.3. 11 Talin is SUMOylated in U2OS Cells..... | 140 |
| 4.3. 12 HA-tag SUMO-2 IP Detects SUMOylated Full-Length Talin and Fragments of Talin..... | 141 |

| | |
|--|---------|
| 4.3. 13 SUMOylation may Cause an Interruption of the FA Proteins Complex | 141 |
| 4.3. 14 Determination of Inhibition of SUMOylated FAs on FA Protein-Protein Interaction in U2OS Cells..... | 144 |
| Discussion | 147-157 |

Chapter 5 – The Identification of the Focal Adhesion Proteins Which Can be SUMOylated

| | |
|---|---------|
| 5.1 Introduction and Hypothesis..... | 158 |
| 5.2 Mass Spectrometry..... | 161 |
| 5.3 The Predictions of SUMOylated Talin Using SUMO-plot and GPS SUMO Programmes..... | 164 |
| 5.4 The Predictions of SUMOylated Vinculin Using SUMO-plot and GPS SUMO Programmes..... | 166 |
| 5.5 Mass Spectrometry Analysis Identifies Focal Adhesions can be SUMOylated..... | 168 |
| 5.6 STRING Data Analysis Shows the Protein-Protein Interactions in Focal Adhesions..... | 173 |
| 5.7 Validation of Filamin-A (Filamin-1) as a SUMOylation Substrate | 177 |
| 5.8 The Predicted SUMO Modified Sites in Known SUMOylated Substrates: p53, Rac1, FAK and Actin, Cytoplasmic 1 Using SUMOplot and GPS SUMO Programmes..... | 180 |
| Discussion | 184-193 |

Chapter 6 – The Regulation of SUMOylation in Focal Adhesions in Platelets and the Megakaryocyte-like CMK11-5 Cells

| | |
|--|---------|
| 6.1 Introduction and Hypothesis..... | 194 |
| 6.2 Methods..... | 197 |
| 6.2. 1 Treating CMK11-5 Cells for Spreading and Immunostaining Experiments | |
| 6.2. 2 CMK11-5 Cells: siRNA Treatment | |
| 6.2. 3 Platelets Spreading Assays | |
| 6.2. 4 Immunoprecipitation and Western Blotting with Platelets | |
| 6.2. 5 Platelets with the VIVAbind™-SUMO Kit | |
| 6.3 Inhibition of SUMOylation Causes Increased Number and Size of Talin Containing FAs in CMK11-5 Cells..... | 200 |
| 6.4 Ubc9 siRNA Transfection Significantly Reduced the Ubc9 Enzyme Expression in CMK11-5 Cells..... | 202 |
| 6.5 Ginkgolic Acid Reduces Platelet Adhesion and Spreading upon Fibrinogen Binding..... | 204 |
| 6.6 GA Treatment of Platelets Induces Cleavage of Talin | 207 |
| 6.7 SUMO VIVA™ Binding Kit and Western Blotting Show SUMOylated Talin in Platelets..... | 208 |
| Discussion | 210-215 |

| | |
|---|---------|
| Chapter 7 - Overall Discussion and Future Perspectives | 216-222 |
| 7.1 De-SUMOylation and its Focus..... | 216 |
| 7.2 SUMOylation and Ubiquitination..... | 218 |
| 7.3 Future Perspective of SUMOylation | 220 |
| 7.3. 1 The Potential Drug Targets for Metastatic Cancers and Other Findings | |
| 7.3. 2 The Potential Drug Targets for Anti-Platelets Therapy | |
| Acknowledgement | 223 |
| Bibliography | 224-245 |

Abbreviations (A-Z)

2-D08 2',3',4'-trihydroxyflavone

3-B08, Gossypetin, Goss 3,5,7,8,3',4'-hexahydroxyflavone

ANOVA Analysis of Variance

AD Alzheimer's disease

ASDs Atrial septal defects

ADP adenosine diphosphate

ALT Alternative lengthening of telomeres

AGC Automatic gain control

ABD Actin binding domain

BSA Bovine serum albumin

BRCA1 Breast cancer type 1 susceptibility protein

Br Bradford reagent

Co-IP Co-immunoprecipitation

CHDs Congenital heart defects

CNS Central neuron system

CMV Cytomegalovirus

Cdc42 Cell division control protein 42 homolog

CHO Chinese hamster ovary

CID Collision-induced dissociation

DTT Dithiothreitol

DAG Diacylglycerol

DMEM Dulbecco's Modified Eagle's Medium

DMSO Dimethyl sulfoxide

D2S Distance to start

ERK1/ERK2 Extracellular signal-regulated kinase 1/2

ECM Extracellular matrix

EGFR Epidermal growth factor receptor

EMT Epithelial-mesenchymal transition

EGF Epidermal growth factor

E1 SUMO-conjugating enzyme SAE1/2 SUMO-activating enzyme subunit 1/2

ER Oestrogen receptor

FAs Focal adhesions

FAK Focal adhesion kinase

FBS Fetal bovine serum

FoxM1 Forkhead transcription factor

FDR False discovery rate

GA Ginkgolic acid
GEFs Guanine nucleotide exchange factor
GPS SUMO Group-based prediction system algorithm SUMO
GPIb Glycoprotein Ib
GS Goat serum
GPIIb/IIIa (platelet Integrin α IIb β 3) glycoprotein IIb/IIIa
HA-tag Hemagglutinin tag
HSFs Heat shock factor families
HER-2 /neu oncogene/ERBB2 human epidermal growth factor receptor 2
HUVECs Human umbilical vein endothelial cells
HEK293T Human embryonic kidney 293
HRP Horseradish Peroxidase
HDAC Histone deacetylase
HGF Hepatocyte growth factor
hFN human Fibronectin
IHC Immunocytochemistry
IP Immunoprecipitation
Ig Immunoglobulin
IBS2 Integrin binding site 2
LB medium Luria-Bertani medium
LC-MALDI-MS/MS Liquid chromatography-Matrix-assisted laser desorption/ionization-Mass spectrometry
mAb Monoclonal antibody
MET Mesenchymal-epithelial transition
MMPs Matrix metalloproteinases
MAPK Mitogen-activated protein kinase
MLCK Myosin light-chain kinase
MCC Matthews correlation coefficient
MEF2A Myocyte-specific enhancer factor 2A
N-terminal FERM Protein 4.1, ezrin, radixin and moesin homology
NEM N-Ethylmaleimide
OS Osteosarcoma
ox-LDL Oxidized low-density lipoprotein
OSCC Oral squamous cell carcinoma
PTMs Post-translational modifications
PBS Phosphate buffered saline
PEI Polyethylenimine

PKC Protein kinase C
PARP poly ADP ribose polymerase
p130Cas p130 CRK-associated substrate
PVDF Polyvinylidene difluoride membrane
Penstrep Penicillin/Streptomycin
PFA Paraformaldehyde
PIAS1 Protein inhibitor of activated STAT1
PDSM Phosphorylation dependent sumoylation motif, ψ KxExxSP
PTB Phosphotyrosine binding
PDGF Platelet-derived growth factor
PI-3'K Phosphoinositide 3-kinase
PIC Protein inhibitor cocktail
PTK Protein tyrosine kinase
PIP5K1C Phosphatidylinositol-4-phosphate 5-kinase, type I, gamma
PtdIns(4,5)P₂, PIP₂ Phosphatidylinositol-4,5-bisphosphate
PtdIns (3,4,5)P₃, PIP₃ Phosphatidylinositol (3,4,5)-trisphosphate
PMA Phorbol 12-myristate 13-acetate treatment
PCNA Proliferating cell nuclear protein
RIAM GTPase Rap1-interacting adaptor molecule
ROCK Rho kinase
RanGAP1 RanGTPase-activating protein
SUMO small ubiquitin-related modifier
SIM SUMO-interaction motif
SBM SUMO-binding motif
SFKs Src family kinases
shRNAs short hairpins RNAs
siRNA small interfering RNA
SNPs Single nucleotide polymorphisms
SH2 Src-homology 2
SFKs Src family kinases
SDS Sodium dodecyl sulphate
SEM Standard error of the mean
TEA Triethanolamine
TBS Tris buffer saline
TBST TBS-Tween-20
TRAP Thrombin receptor activator peptide
TXA₂ Thromboxane A₂

TGF- β Transforming growth factor beta
TRF1, TRF2 Telomeric repeat-binding factor 1 or 2
Ulp/SEN1 Ubiquitin-like protease/sentrin-specific protease family
UBLs Ubiquitin-like proteins
UCH-L1 Ubiquitin C-terminal hydrolase-L1 deubiquitinating enzyme
Ubc9 SUMO-conjugating enzyme (E2)
VBSs Vinculin binding sites
VSDs Ventricular septal defects
VEGF Vascular endothelial growth factor
VASP Vasodilator-stimulated phosphoprotein
vWF von Willebrand factor
wcl Whole cell lysate
WB Western blotting
WASP Wiskott-aldrich syndrome protein

Figures and Tables

Chapter 1: Figure 1-12

Chapter 2: Table 1-5

Chapter 3: Figure 13-34, Table 6

Chapter 4: Figure 35-59, Table 7-11

Chapter 5: Figure 60-66, Table 12-26

Chapter 6: Figure 67-76, Table 27

Abstract

Metastasis is a multistep process which involves the tumour cells invasion through extracellular matrix (ECM) barriers and finding new spaces for colonization and proliferation. Focal adhesions (FAs) are important structures in facilitating cell migration and invasion. FAs can be modified through post-translational modifications (PTMs) and one of them is SUMOylation. In this study, MDA-MB-231 breast carcinoma and U2OS osteosarcoma cells have been used to study the regulation of FAs in the cancer cells and a regulatory mechanism of SUMOylation has been proposed. Later, the platelets and a megakaryocyte-like cell line (CMK11-5 cells) were used.

Firstly, a SUMOylation inhibitor ginkgolic acid (GA) was used in MDA-MB-231 cells, which significantly increased the mean number, size and turnover time of FAs; GA at 25, 50 and 100 μ M significantly decreased the speed of cell migration in MDA-MB-231 cells after 24 hours. Ubc9 (SUMO-conjugating enzyme) siRNA was used in MDA-MB-231 cells to knock down Ubc9, which also significantly increased the mean number and size of FAs; the combination of GA and Ubc9 siRNA did not further increase the mean number and size of FAs. 25nM Ubc9 siRNA reduced the speed of cell migration after 25 and 48 hours. All SUMOylation inhibitors including ginkgolic acid, 2-D08 and gossypetin significantly increased the FAs mean number or size in U2OS cells and in MDA-MB-231 cells.

Bioinformatics software, such as SUMOplot and GPS SUMO predicted that talin and vinculin were SUMOylated. Three different immunoprecipitation methods (IP) have been developed as endogenous IP, HA-tagged SUMO-2 IP and using a SUMO-VIVATM binding assay. The IP and western blotting showed that talin could be SUMOylated in both MDA-MB-231 and U2OS cells; vinculin SUMOylation was determined in MDA-MB-231 cells and in the co-immunoprecipitation experiments (co-IP). The effects of inhibiting SUMOylation on FA cleavage were further investigated in the IP and co-IP experiments in both cancer cells. For example, in the IP and co-IP experiments, talin appeared at the intact molecular weight 250kDa (230kDa using different antibodies) as well as 47kDa and other molecular weights (such as 220kDa and 100kDa) during inhibitor treatments, suggesting that talin could be cleaved and the inhibitor treatment either inhibited the intact talin protein or the cleaved products of talin. A Mass Spectrometry study was conducted to identify and confirm the previously SUMOylated proteins in all three cell lines: MDA-MB-231, CMK11-5 and platelets; talin SUMOylation was identified in all three cell lines. Furthermore, *fila.min-1* was identified and confirmed in the experimental conditions.

Finally, the regulatory mechanism of SUMOylation in talin was studied in CMK11-5 cells and platelets. GA significantly increased the mean number and size of talin containing FAs in CMK11-5 cells and the effects of talin cleavage in platelets were further investigated.

In summary, SUMOylation plays an important role in the regulation of focal adhesions and cell migration.

Key words: focal adhesions, focal adhesion number, size & turnover, SUMOylation, cancer cell migration, talin, vinculin, filamin-1, focal adhesion cleavage, ginkgolic acid, 2-D08, gossypetin, Ubc9 siRNA, MDA-MB-231, U2OS, CMK11-5, platelets

Chapter 1 – Introduction

1.1 Cancer Cell Metastasis

The six hallmarks of cancer have been summarised as the ‘acquired capabilities of cancer’ firstly in 2000 and revised in 2011 (Hanahan and Weinberg, 2011) in Figure 1, which are categorised as sustained proliferative signalling, resistance to cell death, induced angiogenesis, replicative immortality, evading growth suppressors and activated invasion and metastasis. In addition to the six hallmarks of cancer pathogenesis there are two emerging hallmarks, deregulation of cellular energetics, which is the capability to modify or reprogram cellular metabolism to support neoplastic proliferation, the other is avoiding immune destruction i.e. the cancer cells can escape and evade immunological destructions by T and B lymphocytes, macrophages and natural killer cells. Two enabling characteristics have also been proposed as genome instability and mutation, which could provide cancer cells with genomic instability and mutability driving neoplasia; the other is tumour-promoting inflammation.

Therapeutic targets have been developed and introduced into the clinic; these include VEGF signalling inhibitors targeting angiogenesis; PARP inhibitors, which target genome instability and mutations; EGFR inhibitors, which target the sustained proliferative signalling; HGF/c-Met inhibitors targeting invasion and metastasis; cyclin-dependent kinase inhibitors, proapoptotic BH3 mimetics, telomerase inhibitors, selective anti-inflammatory drugs, small molecule monoclonal antibodies i.e. immune activating anti-CTLA4 mAb (Hanahan and Weinberg, 2011).

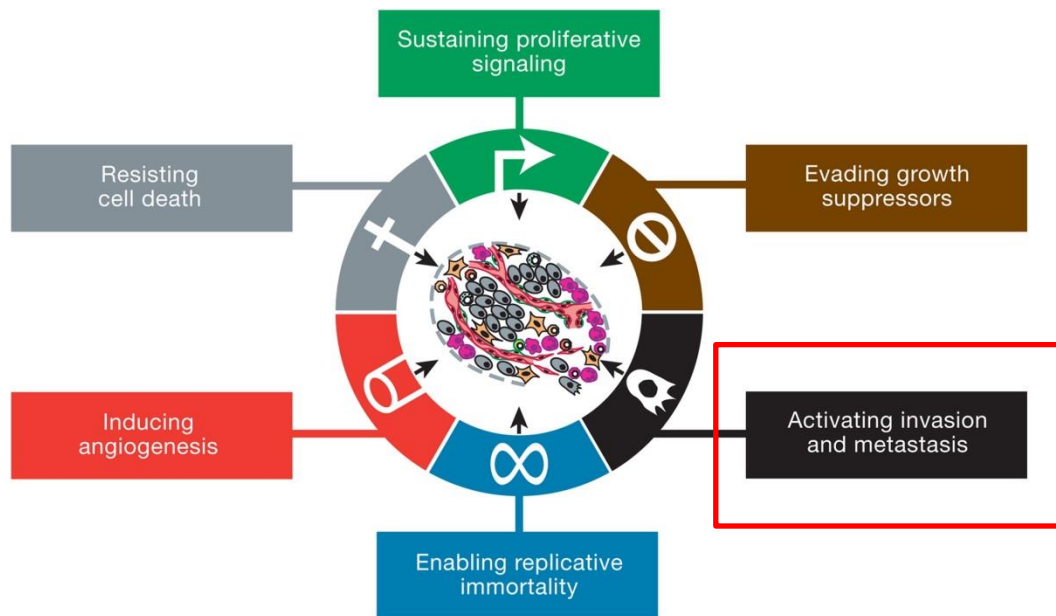


Figure 1. The rationalized and favoured six hallmarks described by Hanahan and Weinberg, taken from (Hanahan and Weinberg, 2011) describing: 1. Chronic proliferation signalling maintenance 2. Evasion of the tumour growth suppressors, i.e. circumvention of the tumour suppressor genes encoding the proteins RB (retinoblastoma-associated) and TP53 also known as p53 proteins, corruption of the TGF- β pathway etc 3. Attenuation of the natural barrier of programmed cell death by apoptosis 4. Permission of replicative immortality 5. Inducing angiogenesis 6. activation of invasion and metastasis – metastasis will be the main focus for this study

Tumour cell invasion and metastasis is thought to be responsible for 90% of cancer-associated deaths, which remains one of the most perplexing aspects of this disease, more specifically, the secondary tumours but not the primary neoplasia are the main threat to cancer mortality (Leber and Efferth, 2009b, Chaffer and Weinberg, 2011).

Metastasis is a multistep process where the tumour cells disseminate, invade local or adjacent tissues, intravasate at the primary site, proliferate and survive in the blood or lymphatic circulation, extravasate and colonize to the distant parts of the body (Friedl, 2011).

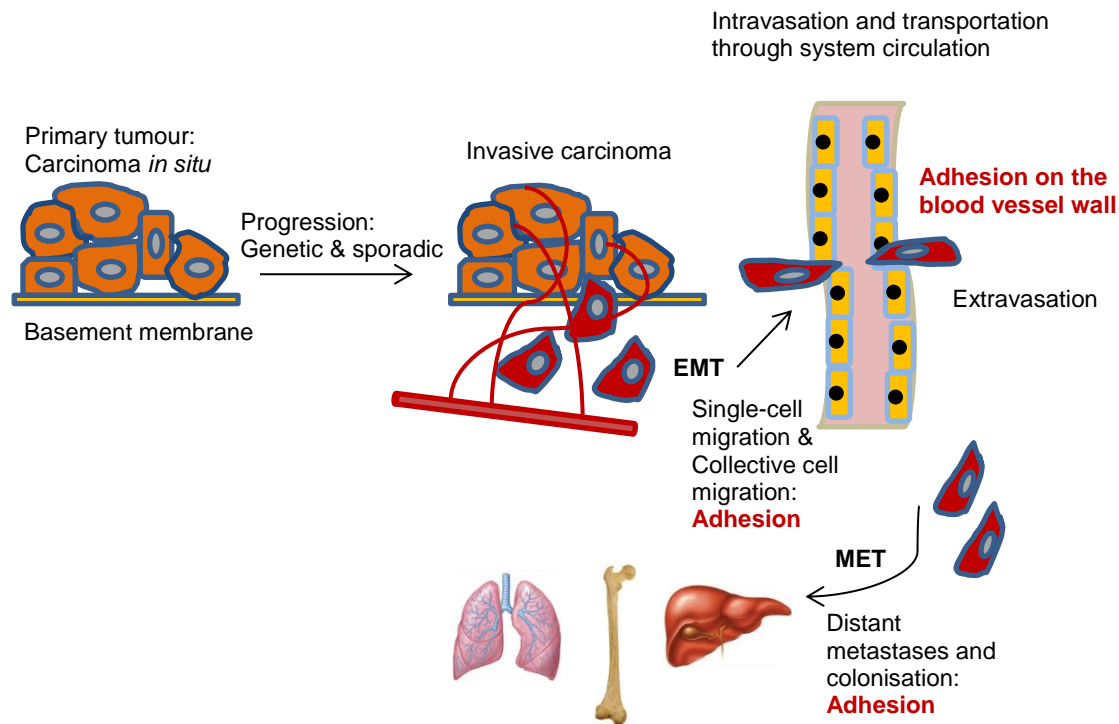


Figure 2. Epithelial-mesenchymal transition (EMT) is a mechanism important for promoting primary tumour cell invasion, where the tumour cells proliferate and supplied with oxygen and nutrients through angiogenesis; when a group of cancer cells detached from the primary tumours and could breach through the blood vessel wall, various signalling factors and multiple complicated signalling cascades are involved, the cancer cells could switch back through mesenchymal-epithelial transition (MET) after extravasation finding a space to colonize and form macro-metastases in the distant parts of the body, modified from Robert A. Weinberg, 2007, *The Biology of Cancer, Chapter 14: Invasion and Metastasis, Figure 14.17b*. Focal adhesions play an important role in the cancer cell metastasis

In Figure 2, EMT has been shown to be one of the main mechanisms for cancer cell migration and metastasis. Several modes of cell migration have been noted; single cell migration includes the mesenchymal \leftrightarrow amoeboid transition for both directions; multicellular cell migration includes the mesenchymal \leftrightarrow multicellular streaming/collective transition on both directions or collective-to-amoeboid transition (Friedl, 2010). Focal adhesions (FAs) are an important functional group of proteins that play an important role in the transition of cell migration. These adhesions include talin, vinculin, paxillin, focal adhesion kinase (FAK), zyxin, VASP (vasodilator-stimulated phosphoprotein), α -actinin and over 100 FA specific proteins have been identified (Kim et al., 2012).

The tumour local microenvironment or the extracellular matrix (ECM) is essential in tumour cell migration and metastasis, where in the primary tumour niche, ECM can stimulate and enable micro- and macro-metastasis and promote cancer progression (Ram, 2005). Aberrant ECM remodelling activities and metabolism can lead to changes in the organization, composition, topography and biochemical properties of the ECM (Lu, 2012). There are several main promoters/contributors involved in metastasis such as ECM

degrading enzymes matrix metalloproteinases (MMPs), stromal cells, immune cells, cancer-associated fibroblasts, cytokines, growth factors, epithelial cells and mesenchymal stem cells etc (Lu, 2012, Friedl, 2011, Ngoc, 2012). The ECM is crucial in establishing and maintaining tissue polarity and architecture, where the cells in the epithelial or solid organs have distinct polarity that are vital in distinguishing tissue or organ formation and function; this ECM-maintained tissue architecture prevents tumour cell invasion (Lu, 2012).

One of the two mechanisms in tumour single-cell migration has been demonstrated as the EMT *in vivo* in Figure 2 (Grunert et al., 2003, Friedl, 2011, Wolf, 2003). Abnormal or deregulated ECM dynamics can promote EMT, which facilitates the primary polarised epithelial tumour cells to invade through the basement membrane, undergo multiple biochemical changes resulting in mesenchymal transition leading to invasion and metastasis (Lu, 2012, Wirtz et al., 2011). The tumours are often surrounded by highly concentrated collagen-containing matrices, which the surrounding tissue is more rigid or isotropic (Lu, 2012, Geiger, 2011). Therefore, EMT type of cell migration plays an important role in tumour cell migration.

The EMT epithelial-mesenchymal transition has been proposed and classified into three types and markers have been denoted for the epithelial or the mesenchymal phenotype; specifically, type 3 EMT occurs in neoplastic cells which have undergone genetic and epigenetic changes previously and these mesenchymal cells express markers such as vimentin, desmin, N-cadherin, fibronectin, β -catenin, syndecan-1, $\alpha 5\beta 1$ integrin and so on; moreover, the full spectrum of signalling events which contribute to EMT in carcinoma development is complex and the signal is likely originated from the tumour-ECM associated stroma notably HGF, EGF, PDGF and TGF- β (Kalluri and Weinberg, 2009). The metastatic capacity of the tumours might be inherent; therefore, the understanding of the molecular mechanisms of the metastatic processes is essential (Weigelt et al., 2005). The phenotypic and biochemical alterations during the metastasis are concerned with various aspects including cell-cell adhesion, growth factor signalling, gene expression, motility and so on (Leber and Efferth, 2009a). Focal adhesions have been studied in this study.

1.2 SUMOylation and its Post-Translational Protein Modification Cycle

SUMOylation has been known for the last 30 years as a type of protein post-translational modifications (PTMs). SUMO (small ubiquitin-related modifier) families are ubiquitin-related small proteins, which are 10~18kDa and can be conjugated to cellular substrates in the same way as ubiquitin, but the SUMO proteins share less than 20% amino acid sequence identity with ubiquitin; SUMOylation is regulated through a controlled cycle by E1, E2 and E3 enzymes (Geiss-Friedlander and Melchior, 2007). SUMO is covalently conjugated to a variety of proteins and de-conjugated by SUMO-specific proteases; SUMO modifications of proteins regulates crucial cell signalling, factors and functional parameters of proteins; specifically, like ubiquitin, SUMO has been found to be covalently attached to certain lysine residues of specific proteins (Hilgarth et al., 2004, Hay, 2005). SUMO is critically important in early embryonic development whilst SUMO is also present throughout development (Nie et al., 2009). More proteins have been identified to be SUMO modified through protein-protein interactions, genetic networks and proteomics; more than 1000 proteins have been identified as potential SUMO-conjugation (SUMOylation) targets (Makhnevych et al., 2009, Wang and Dasso, 2009).

Four SUMO homologues have been described. SUMO-1 is found mainly in the nucleus; SUMO-2/-3 are predominantly present in the cytosol, where SUMO-2 and -3 are 95% similar to each other and SUMO-1 is more distinct, being only ~45% similar to SUMO-2/3 (Azuma et al., 2003); the important distinctions between SUMO-2/3 and SUMO-1 conjugation pathways have been quantitatively and qualitatively characterized (Saitoh and Hinchey, 2000). SUMO-1 and SUMO-2 protein conjugates can be distinct but also overlapping as some proteins can only be modified by SUMO-1 or SUMO-2 only and some proteins can be modified by both SUMO-1 and SUMO-2 (Vertegaal et al., 2006). SUMO-4 has been described with restrict pattern of expression with the highest in the kidney reported (Gill, 2004, Bohren et al., 2004).

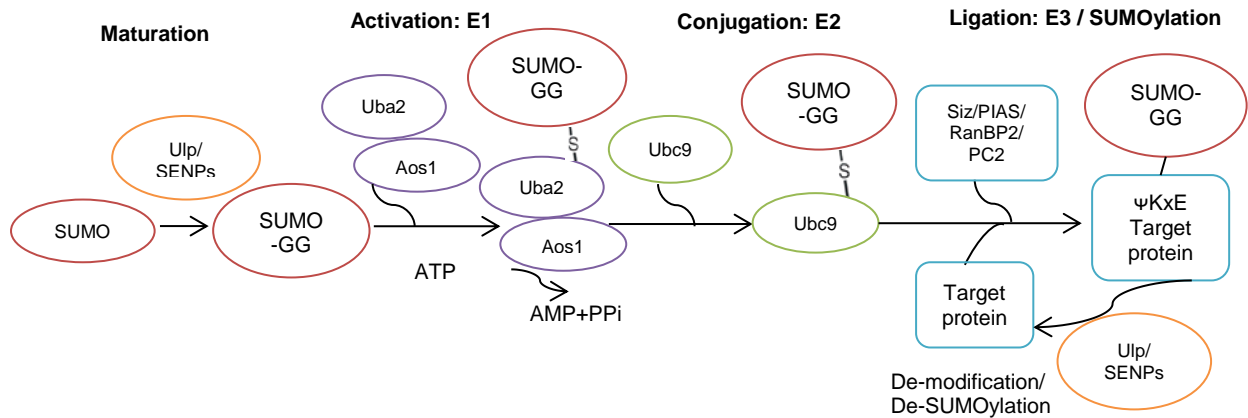


Figure 3. The SUMOylation pathway in studying the SUMOylation of protein substrates: the ~100 amino acid SUMO has to be cleaved by a carboxyterminal hydrolase, Ulp or a SUMO protease to expose the carboxy-terminal glycine SUMO-GG. Then, a thioester conjugation is formed between the SUMO-GG and the E1 activating enzyme via cysteine (Aos1/Uba2) in the presence of ATP. This pathway is continuously processed where a thioester intermediate conjugation is formed between active SUMO-GG and the E2 conjugating enzyme Ubc9 via active cysteine. This modification is ligated through E3 ligases such as PIAS or RanBP2 acting as an adaptor between the Ubc9 and the target protein. The isopeptidase SENPs are active in protein deSUMOylation, therefore SUMOylation or de-SUMOylation could happen in balance within the SUMO cycle, modified from (Seeler and Dejean, 2003)

In Figure 3, the covalent SUMO conjugation involves three enzymatic reactions: firstly, SUMO family proteins must be post-translationally modified by SUMO proteases to expose the COOH-terminal diglycine motif in a ATP-dependent manner; and with the catalytic cysteine of E1 activating enzyme which forms a thioester bond between SUMO family proteins and their substrate targets; the E1 enzyme known as the SUMO-activating enzyme SAE1/SAE2 heterodimer, also as Aos1 and Uba2 in yeast; secondly, this is followed by the activated SUMO conjugation to the E2-conjugating enzyme Ubc9 via the second thioester bond formation; thirdly, an isopeptide bond is formed between SUMO family proteins and their substrates via the mutual co-operative reaction between Ubc9 and E3 protein ligases (known as Siz1p, Siz2p/Nfi1p and Mms21p in yeast; PIAS in higher eukaryotes) (Bossis and Melchior, 2006, Hay, 2005, Boggio et al., 2004, Makhnevych et al., 2009, Rouleau et al., 2008, Vertegaal et al., 2006, Wilkinson and Henley, 2010). The SUMO-conjugating E2 enzyme Ubc9 is the only E2 enzyme in the SUMO conjugation pathway and as such is an important target in studying SUMOylation.

SUMO conjugated proteins are susceptible to specific sumo isopeptidases cleavage including the Ulp family in yeast (Ulp1 and Ulp2) and the SENP proteins (SEN1-8), resulting in de-sumoylation (Bossis and Melchior, 2006, Drag and Salvesen, 2008, Hang and Dasso, 2002). The endogenous constitutively active SENPs can rapidly deconjugate SUMO

from its substrates, creating a dynamic balance between SUMO addition and deconjugation; prevention of deSUMOylation in *Schizosaccharomyces pombe* has resulted in slow growth and increased sensitivity to replicative stress, suggesting that the deSUMOylation dynamics is important to the SUMO cycle (Békés et al., 2011).

Many targeted conjugates contain the SUMO consensus motif ψ KxE; ψ is a large hydrophobic residue, K is the acceptor lysine and x is any residue (Hay, 2005). SUMO-1 also contains consensus sequences for Ubc9 direct binding which is critical for SUMO-1 modifications (Sampson et al., 2001). SUMOylation can also occur at lysine residues outside the consensus motifs and not all ψ KxE motifs can be SUMOylated (Wilkinson and Henley, 2010). Non-consensus motifs have been identified, for example, the GTPase Rac1 was found within the polybasic region non-consensus sites for SUMO conjugation mainly (Castillo-Lluva et al., 2010).

1.3 SUMOylation and Cancer

The SUMOylation substrates include proteins encoded by oncogenes and tumour suppressor genes, which are important in cell growth, differentiation and apoptosis; given by these SUMO-substrates, SUMOylation is expected to play regulatory roles in tumorigenesis (Alarcon-Vargas and Ronai, 2002). One study showed that Ubc9 could promote breast cancer MD-MB-231 cell invasion and metastasis in a SUMOylation-independent manner (S Zhu et al., 2009). Ubc9 is also up-regulated in breast, ovarian head and neck and lung cancer (Wu et al., 2009). More evidence has shown that Ubc9 can promote cell proliferation in epithelial ovarian cancer cells *in vitro* (Dong et al., 2013); Ubc9 could promote lung and breast cancer cell invasion and metastasis *in vivo* (Dong et al., 2013, Wu et al., 2009, Li et al., 2013a). Alterations in Ubc9 expression may be responsible for tumour chemo-sensitivity (Mo et al., 2004). Since SUMOylation has been implicated in many types of cancers, where Ubc9 plays a central role in the SUMO pathway, it has led to potential studies in rational drug design, virtual screening and more approachable interactive partners in SUMOylation (Duan et al., 2009).

Mutations in the BRCA1 gene have been previously shown to associate with increased risk for inherited breast and ovarian cancers (Qin et al., 2011); Yunlong Qin et al. study showed that the wildtype BRCA1a proteins can bind to nuclear chaperone Ubc9 E2 enzyme, which can suppress ovarian cancer cell growth; mutant BRCA1a is dysregulated with Ubc9 binding and this leads to mislocalization of mutant BRCA1 proteins, loss of ER- α repression and loss of growth suppression of BRCA1 proteins causing hereditary and sporadic ovarian cancers (Qin et al., 2012).

A number of oncogenes and tumour suppressor genes encoded proteins including PML, Mdm2, p53, c-Myb, c-Jun and Rb etc, undergo SUMOylation (Baek, 2006). SUMOylation is important in cellular responses to DNA damage and key oncogenic pathways driven by c-Myc and K-Ras mutations may be addicted to SUMOylation; Myc may also regulate SUMOylation and marked increase in the expression of genes which encode regulators of the SUMOylation pathway were found in human Myc-driven lymphomas resulting in hyper-SUMOylation in these tumours (Hoellein et al., 2014). Recent findings suggest that SUMO modifications of transcriptional responses may be required for tumour invasion and SUMOylated proteins may be potentially molecular markers for metastatic tumours, such as in melanoma (Ganesan et al., 2007). Many more SUMOylation substrates include p53, p63, p73, Mdm2, c-Jun, NFκB, IκBα, viruses including cytomegalovirus (CMV), herpes simplex virus and human papillomavirus E1 (Uchimura et al., 2004, Buschmann et al., 2001, Da Silva-Ferrada et al., 2012, Alarcon-Vargas and Ronai, 2002).

For other examples, oncogenic activities of MafA gene is negatively regulated by SUMOylation; dysregulated transcriptional MafA contributes to multiple myeloma (MM) in humans (Kanai et al., 2010). In MM patients plasma cell lysates samples, UBE21 was elevated hence SUMOylation was markedly enhanced; p53 was found to be SUMOylated in the MM patients and MM cell lines; several other signalling molecules are also Ubc9 target substrates including Smad4, c-Jun, NFκB etc (Driscoll et al., 2010, Li et al., 2013a). In Myc-high human breast cancers i.e. MDA-MB-231, loss of SAE1/2 enzymatic activities by using SAE1/2 gene shRNAs (short hairpins RNAs) has the strongest synthetic lethality upon Myc hyperactivation; clinically, depletion or low SAE2 express may correlate with less aggressive tumours and longer metastasis-free survival in patients, where active SAE2 is required for mitotic spindle functions in Myc-dependent tumour growth (Kessler et al., 2012). The tumour suppressor HIC1 gene was also shown that 314 lysine residue to be the same target for both SUMOylation and acetylation, which is also a direct gene target for p53 (Stankovic-Valentin et al., 2007).

The transcription factor p53 is well known to be mutated in various tumour cell types; p53 was shown to be modified by SUMO-1 at C-terminal with a single motif K386 (Rodriguez et al., 1999, Gostissa et al., 1999, Kwek et al., 2001, Müller et al., 2000). FAK has been known as a tumorigenic marker, which also has a binding site in the N-terminal proline-rich domain of p53 (Golubovskaya et al., 2008). c-Jun is modified by SUMO-1 at a single lysine residue K229, which may be negatively regulated by SUMO-1 (Müller et al., 2000). Both p53 and c-Jun are regulated by the ubiquitin-proteasome pathway; p53 mutant showed unaltered ubiquitination but defective SUMO-1 conjugation and slightly impaired apoptotic activity,

where modification of p53 by SUMO-1 and Ubc9 may be important for its full biological activity (Müller et al., 2000).

1.4 General Aspects of SUMOylation and its Role in Cellular Physiology

SUMOylation plays a vast role in the cell participating in nearly all parts of cellular physiology. Some examples have been listed here. The RanGTPase-activating protein, RanGAP1, was first evidence reported and found to be modified by SUMO-1 but can also be conjugated by SUMO 2/3 through compensatory adaptation, which regulates RanGAP1 localization to the nuclear pore complex also together with Ubc9 and nucleoporin Nup358/RanBP2 interactions (Bernier-Villamor et al., 2002). RanGAP1 later has been used as positive control in some studies in the discovery of protein SUMOylation.

There are studies which have been done in the neurons of the CNS (central neuron system) suggesting that SUMOylation can modulate neuronal differentiation, synapse formation control in order to regulate synaptic transmission and neuronal cell survival (Henley et al., 2014). Accumulating evidence grows and shows that perturbations in neuronal SUMOylation can contribute numerous pathological conditions, including Parkinson's disease, Alzheimer's disease (AD), Huntington's disease and so on (Martin et al., 2007). α -synuclein can be SUMOylated by SUMO-1 and SUMO 2/3 and its pathogenic mechanism is involved in protein aggregation in Parkinson's disease; SUMOylation may react as a prohibition mechanism in the huntingtin protein accumulation in Huntington's disease; SAE2, Ubc9 and SENP3 are involved in Alzheimer's disease, where SNPs (single nucleotide polymorphisms) in these genes can co-segregate with AD; the protein tau can be SUMOylated, the proportion of SUMOylated tau or ubiquitinated tau can regulate its accumulation or degradation balance in AD (Schorova and Martin, 2016).

The balanced SUMOylation and deSUMOylation pathway is also critical for normal cardiac development (Wang and Schwartz, 2010); one of Wang's studies showed that both heterozygous and homozygous SUMO-1 knockout mice displayed congenital heart defects (CHDs), atrial septal defects (ASDs) and ventricular septal defects (VSDs) with high mortality rates however both were rescued by the cardiac re-expression of the SUMO-1 transgene, which was critical in the developing embryonic heart (Wang et al., 2011).

In another study, a serum response factor (SRF)-dependent cofactor, myocardin, its activity was strongly enhanced by SUMO-1 modification on K445 lysine and co-expressed PIAS1 association via its E3 ligase activity, which SUMO modification acted to promote myocardin

transactivation of the cardiac muscle specific gene expressions in 10T1/2 fibroblasts (Wang et al., 2007).

SUMOylation has been extensively known as predominantly a nuclear modification, where it was found in the nuclear bodies and chromatin, modifying a large number of chromatin-remodelling complexes and in the response to DNA damage, of all the proteins, ~66% proteins were modified by SUMO were nuclear (Hendriks and Vertegaal, 2016, Hendriks et al., 2015c). SUMO modifications play critical roles in many cellular reactions, including cell cycle progressions both in invertebrates and mammals, for example, SUMO 2/3 was found to localize to centromeres and condensed chromosomes whereas SUMO-1 was localized to the mitotic spindle and spindle mid-zone; transcription factor modifications such as human topoisomerase I and II in mitosis and histone post-translational modification i.e. HDAC1 and 4 (histone deacetylase), polycomb group genes, chromatin remodelling, maintaining genome stability i.e. SUMO involvement in DNA replication and damage repairing, also in cellular, nuclear and vesicle-mediated protein transport i.e. exosomal sorting of microRNA and mRNA metabolism (Collavin et al., 2004, Azuma et al., 2003, David et al., 2002, Makhnevych et al., 2009, Shiio and Eisenman, 2003, Zhang et al., 2008a, Denison et al., 2005, Kirsh et al., 2002).

1.5 Crosstalk between SUMOylation and other PTMs and other SUMO Motifs

Competition between SUMOylation, acetylation, phosphorylation or ubiquitination lysine residues for protein-protein interactions, protein conjugation or crosstalk signalling has also been known (Wilkinson and Henley, 2010). Global mass spectrometric analysis (MS) has been used to uncover the high density and variety of PTMs with the protein substrates being modified by different groups covalently (Hunter, 2007). Positive crosstalk is defined as one PTM serves as a signal for the addition or removal of a second PTM or serves for a binding protein recognition to transmit a second modification; negative crosstalk is defined as direct competition for modification of a single residue in a protein or indirect effects, whereas one PTM modification can mask the recognition site for a second PTM; there can also be combinatorial effects in the binding domains of PTMs crosstalk (Hunter, 2007). SUMOylation can be regulated by phosphorylation, ubiquitination and oxidation both positively and negatively; acetylation negatively; examples include MEF2A and I κ B α , where phosphorylation of these substrates close to lysine can inhibit SUMOylation; MEF2A can also be acetylated on the same lysine residue, hence antagonizing SUMOylation; this is the same for ubiquitination where it can target the same lysine residue such as PCNA, a single lysine can be modified by ubiquitination or SUMOylation through negative crosstalk regulation (Martin et al., 2007, Grégoire et al., 2006, Hunter, 2007). The SUMOylation

pathway is very similar to ubiquitination, where ubiquitination can regulate proteasomal degradation of some SUMOylation substrates (Yang et al., 2007, Wilkinson and Henley, 2010).

Using high-resolution MS, global SUMOylation has been studied in a site-specific manner in human cells, indicating that SUMOylated lysines can be ubiquitinated, acetylated or methylated therefore in this more specific way, many hundreds of sites have been identified to be regulated by SUMOylation, ubiquitination or acetylation (Hendriks et al., 2014). Site-specific identification has also revealed SUMO-2 targets in cells with not only consensus motifs but also with inverted SUMOylation consensus motifs; direct mass spectrometric evidence has identified that crosstalk between phosphorylation and SUMOylation with a preferred four residues spacer between the SUMOylated lysine and the phosphorylated serine (Matic et al., 2010).

The E3 SUMO protein ligase PIAS1 (protein inhibitor of activated STAT) proteins function as SUMO-1-tethering proteins and zinc-finger dependent E3 SUMO protein ligases and are found to regulate and modulate a number of transcription factors and PIAS-like proteins such as AR, p53, c-Jun, septins, and the DJ-1 protein, which are modified by SUMO-1 conjugation (Kotaja et al., 2002). Non-covalent interactions with SUMO modifications can be regulated through SUMO-1, Ubc9 and PIAS1 (Martin et al., 2007). Recently, a SUMO-binding motif (SBM/SIM) was also identified serving as the receptor for binding SUMO-modified proteins with the SUMO moiety (Rouleau et al., 2008). PDSM (phosphorylation dependent sumoylation motif, ψ KxExxSP) is discovered in the majority of transcriptional regulators including the erythroid transcription factor GATA-1, MEF2A (myocyte-specific enhancer factor 2A) and heat shock factor families (HSFs) (Hietakangas et al., 2006, Grégoire et al., 2006). As more new SUMO-conjugating moieties are discovered, this will provide valuable information to predict more novel SUMO substrates.

1.6 The Fundamental Proteins in Facilitating Cancer Cell Metastasis: the Integrin-Focal Adhesions Signalling in Cell Migration Machinery

Integrins are transmembrane heterodimers which are critical for bi-directional signalling as 'outside-in' or 'inside-out' signalling (Delon and Brown, 2007). 'Outside-in' or 'inside-out' integrin signalling with FAs is important in EMT migration and metastasis (Grunert et al., 2003). 'Outside-in' integrin signalling is induced by binding of an ECM ligand which causes conformational change and integrin clustering, leading to intracellular alterations such as phosphorylation; also when the cancer cells were encountering in their microenvironment, extracellular signals activation can influence cell survival and proliferation, cytoskeletal structure and polarity, focal adhesions, migration and invasion (Anthis and Campbell, 2011). 'Outside-in' signalling can be triggered by clustering of integrin i.e. the heterodimers forming hetero-oligomers, which stimulates and recruits multivalent protein complexes to integrin cytoplasmic domains; these have been activated previously by the binding of the extracellular ligands to the ectodomains of integrins and these intracellular recruitment of protein complexes can include focal complexes and focal adhesions (Shattil et al., 2010).

Cell migration on extracellular matrix ECM requires the turnover of integrin formed focal adhesions, i.e. in the assembly and disassembly process (Carragher et al., 2003, Chao et al., 2010); integrins consist α - and β -subunits which bind to collagens, laminins, fibronectin, fibrin and vitronectin according to each α , β subunit combination (Geiger, 2011); deletion in the highly conserved β_1 gene confers defects in adhesions, cell proliferation and survival (Legate et al., 2006). Understanding the mechanism of integrin signalling is important in cellular physiology, as they have been shown to regulate a diverse range of cellular functions including initiation, progression and metastasis in solid tumours.

Different cell lines express different types of integrin isoforms. For example, integrin $\alpha_5\beta_1$, $\alpha_v\beta_3$, $\alpha_v\beta_6$ can be upregulated in some tumours but their normal expressions are low or usually undetectable in most adult epithelia, which make them attractive therapeutic drug targets (Desgrosellier and Cheresh, 2010). $\alpha_5\beta_1$ integrin is bound with fibronectin adhesively and they are tensioned by actin and myosin II in two forms: the relaxed adhesive bonds or tensioned adhesive bonds; inhibitors of actin and myosin II could block the $\alpha_5\beta_1$ integrin/fibronectin tensioned adhesive bonding, parallel with a dose-dependent reduction of FAK phosphorylation on Y397 downstream (Friedland et al., 2009). The bidirectional outside-in and inside-out $\alpha_v\beta_3$ integrin-mediated signalling cascade transcends through the extracellular signal-regulated kinase (ERK1/ERK2), mitogen-activated protein kinase (MAPK) and phosphoinositide 3-kinase (PI-3'K) in MDA-MB-231 breast cancer cells, which could regulate breast cancer cell proliferation and survival (Vellon et al., 2006). The $\alpha_v\beta_3$ integrin

expression was altered and higher expression of $\alpha\text{v}\beta\text{3}$ with actin were shown in primary breast cancer cells, correlated with their higher motility requirements indicating the malignant potential of the breast cancers (Havaki et al., 2007), in particular, tumour-specific integrin $\alpha\text{v}\beta\text{3}$ contributes to spontaneous breast tumour metastasis to the bone (Sloan et al., 2006).

Integrin signalling is involved the clustering of integrins and the recruitment of kinases as well as scaffolding molecules, such as FAK, Src family kinases (SFKs), p130 CRK-associated substrate (p130Cas), a ternary complex containing an integrin-linked kinase (ILK), the adaptor proteins PINCH (particularly interesting Cys-His-rich protein) and parvin required for integrin-mediated functions in cell migration, angiogenesis and survival (Desgrosellier and Cheresh, 2010, Legate et al., 2006, Kim et al., 2011). Cancer cell invasion and migration require regulated integrin-mediated focal adhesions. The regulation molecules include the RIAM (Rap1-GTP-interacting adaptor molecule), which mediates the recruitment of talin to the integrin-cell membrane in FA dynamics (Goult et al., 2013b).

Collagen, fibronectin, fibrinogen, gelatin have been used in the study of cell migration. Collagen was the basis of extracellular matrix ECM used *in vitro* to study cancer cell metastasis and invasion, as the cancer cells required their ECM microenvironment niche to disseminate (Ngoc, 2012, Lu, 2012). 2 mg/ml collagen has been used to form the collagen matrix, as this concentration has been suggested to form a matrix mesh size ($<1\mu\text{m}$), which was significantly smaller than the cell body and nucleus (Bloom et al., 2008). The use of reconstituted and polymerised rat tail type I collagen matrices can affect the formation, structure and rigidity of the collagen fibres, additionally, this has enabled the study of tumour cell behaviour, morphology and FAs formation in 3D environments (Artym and Matsumoto, 2010, Wolf, 2009). Type I collagen telopeptides contain critical lysine residues which after oxidation support collagen covalent cross-linking formation *in vitro* to maintain the matrix fibril structure (Sabeh et al., 2009, Wolf, 2009, Cukierman et al., 2002, Kim, 2005). The collagen matrix thickness, density, tension, orientation, stabilisation, the distance from the hard substrates and protein overexpression represent significant factors which can have an impact on the number, shape and composition of the adhesions in 3D observation (Zaman et al., 2006, Harunaga and Yamada, 2011).

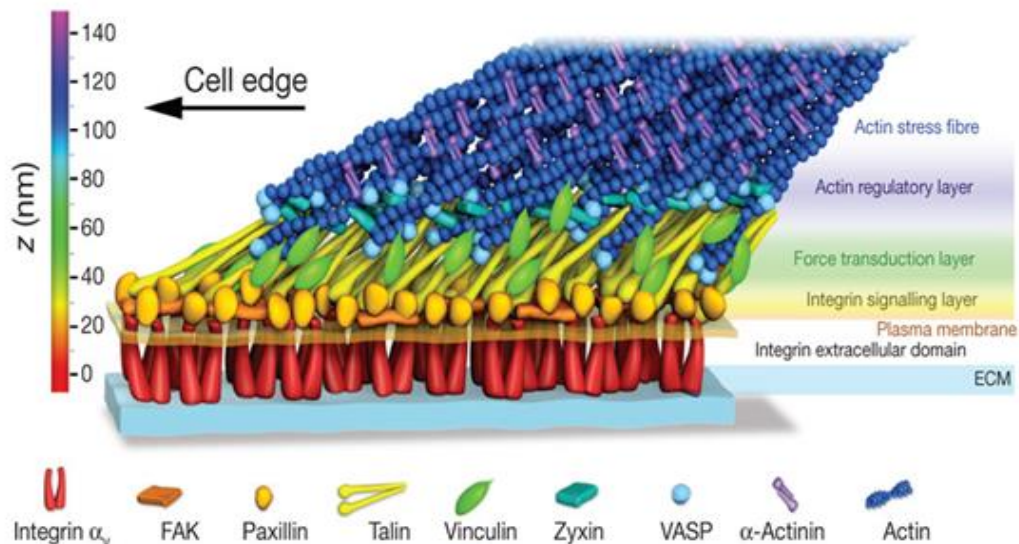


Figure 4. Schematic model of focal adhesions molecular architecture in three layers: the integrin signalling layer, the force transduction layer and the actin regulatory layer and the main FAs include the integrin, FAK, paxillin, talin, vinculin, zyxin, VASP, α -actinin in the integrin signalling and force transduction layers together associated with the actin to exert force on the cell edge, taken from (Kanchanawong et al., 2010)

Focal adhesions are discrete, elongated ‘plaques’ found at the peripheral or central parts of the cell usually associated to the ends of actin filament bundles (Huttenlocher, 2011). In Figure 4, many proteins have been identified and studied including talin, FAK (focal adhesion kinase), vinculin, paxillin, VASP, α -actinin, zyxin and so on.

The spatial nanoscale of protein organization in FAs has been mapped using 3D super-resolution fluorescence microscopy, revealing integrins and actin were vertically separated by a ~ 40 nm FA core region consisting three main functional layers: an integrin-mediated signalling layer in close proximity with the cell membrane and the extracellular domain ECM (integrin cytoplasmic tail, FAK and paxillin); an intermediate force transducing layer (talin and vinculin); an actin-filament regulatory layer (VASP, zyxin and α -actinin), illustrated as a model of the FA molecular architecture based on experimentally determined protein positions in Figure 4 (Kanchanawong et al., 2010). This has demonstrated a well-organized architecture of FAs, which provides valuable information on the study of protein-protein interactions and regulatory functions in FAs.

The initial steps of local invasion consist of dynamic changes in the cell-ECM matrix and cell-cell adhesion controlled by signalling pathways (Friedl, 2011). FAs are important in cell crawling movement, i.e. in mesenchymal cell migration, FAs dynamic activities, rapid assembly and disassembly processes are controlled and regulated spatiotemporally at the leading edge or the rear end of the migrating cell (Broussard et al., 2008, Chan et al., 2010);

lamellipodial structure is usually found at the leading edge to facilitate protruding and the interactions with the ECM signalling, where the cell protrusions also associate with 3D motility enhancement specifically (Meyer et al., 2012, Prass et al., 2006); actin-filament polymerisation directs lamellipodium formation and protrusion; also actin-filament converges with myosin-II motors which contracts and pulls on strong FAs generating traction forces, this causes upward bending, cell body translocation, adhesion release and turnover at the cell front, adhesion retraction and weak adhesion disassembly at the cell rear, all of which direct the cell movement forward (Lock, 2008, Parsons et al., 2010, Webb, 2002).

This adhesion turnover process has been presented in a simple diagram in Figure 5.

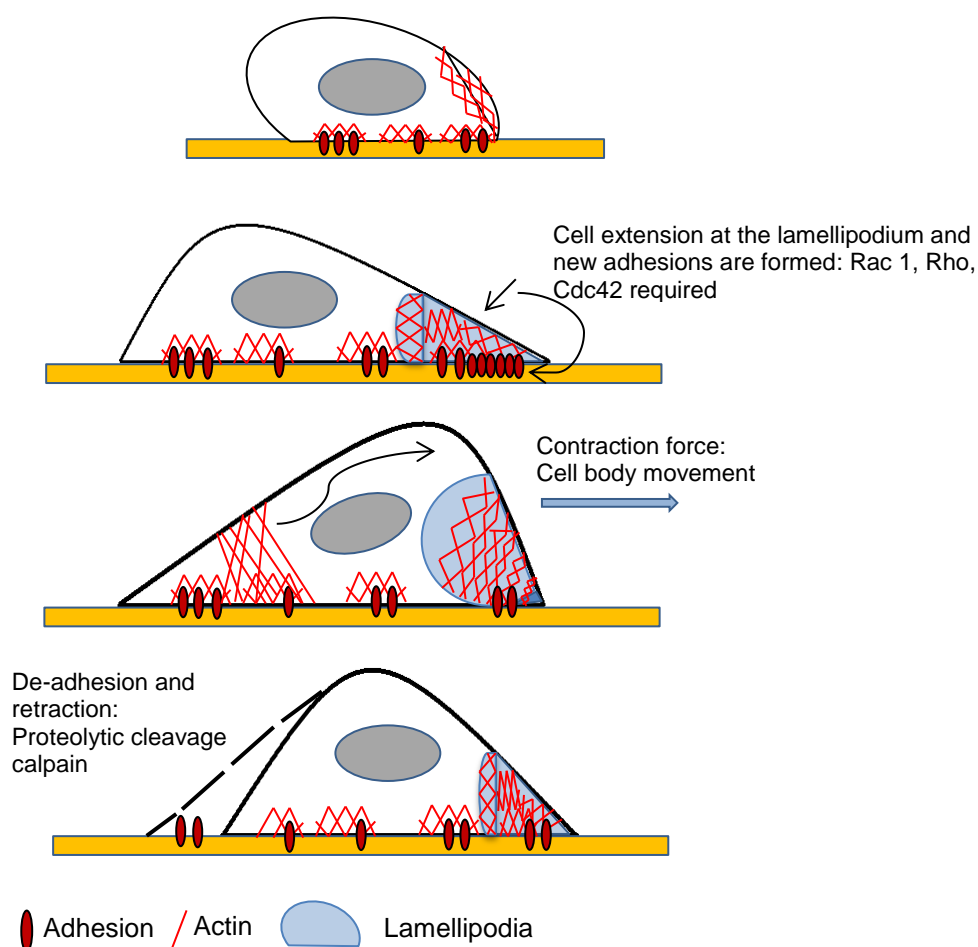


Figure 5. Simplified schematic diagram of FAs formation and assembly at the lamellipodial leading edge, where the cell-ECM substrate attachment and cell extension is processed at the lamellipodium and new FA are formed; for the cell to migrate in a directional manner, the cell needs to develop its filopodia/lamellipodia in response to a stimulus at the cell leading edge, the GTPases Rac 1, Rho and Cdc42 are required for the control of cell lamellipodia structural formation and regulation of the new FAs; The new formation of FAs close to cell leading edge provide traction force for the cell to move the cell body forward. This forward movement is also accompanied by the FAs retraction and disassembly at the cell rear end and these turned over FAs can be proteolytically cleaved by a family of calcium-activated proteases, calpains, therefore promoting FA disassembly and facilitating cell migration, modified from (Frame et al., 2002)

Figure 5 has shown a simplified diagram of the lifetime of FA turnover and cell migration. The FAs can form an adhesome at the local cell-ECM substrate coupling to the cytoplasmic integrin β tail at the transmembrane, together with actin stress fibres and myosin-II, which acts as a dynamic motor cell migration machinery.

It is thought that FA assembly is an event of sequential recruitment of individual or groups of adhesion components rather than stabilized large cytoskeletal complexes, occasionally adhesions may come into the contact simultaneously (Webb et al., 2002); Conversely, FA disassembly seems also not to be a simple reversal mechanism of the FA assembly event (Webb et al., 2002). The integrin, adhesion proteins and actin linkage becomes more organized in migrating cells, which indicates an increase in efficiency in adhesion signalling (Brown et al., 2006). The adhesion strength also affects the rate of migration spatiotemporally, where little adhesion provides insufficient tracking force and too much adhesion immobilizes cell movement (Gupton and Waterman-Storer, 2006). Several factors regulate the FA turnover and cell migration. The sequential recruitment order of FAs has been simplified in a diagram in Figure 6.

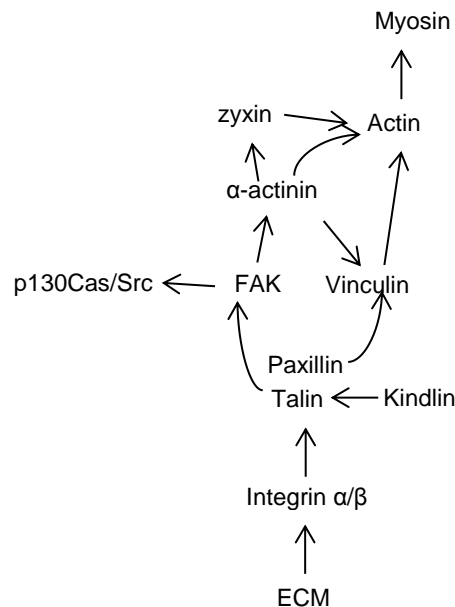


Figure 6. Schematic compositions of FAs: the integrin α/β interacts with the ECM at the focal contacts, which consist of structural and regulatory proteins that can transmit outside-in signals and also relay inside-out signals to obtain activated integrin state at the ECM-substrate surfaces. The kindlin family proteins have also been key players in assisting talin activation of integrins. The first binding of paxillin and talin recruits FAK and vinculin binding to the FA contacts. α -actinin can be phosphorylated by FAK and binds to vinculin and actin-myosin stress fibres; zyxin also binds to α -actinin and the actomyosin network but zyxin is only present in mature FA. The protein tyrosine kinase Src and the adaptor protein p130Cas are also associated with FAK in the FA contacts, modified from (Mitra et al., 2005)

Inside-out integrin signalling is dependent on talin and kindlin and inactivation is mediated by Src family kinases (SFKs) tyrosine phosphorylation of the β -tail and filamin binding (Shattil et al., 2010, Anthis and Campbell, 2011). Many signalling molecules can activate integrin including the ECM proteins i.e. fibronectin, laminin and collagen; GTPase Rap1A and RIAM (Critchley and Gingras, 2008, Kim et al., 2011, Anthis and Campbell, 2011). A simplified diagram is presented in Figure 7.

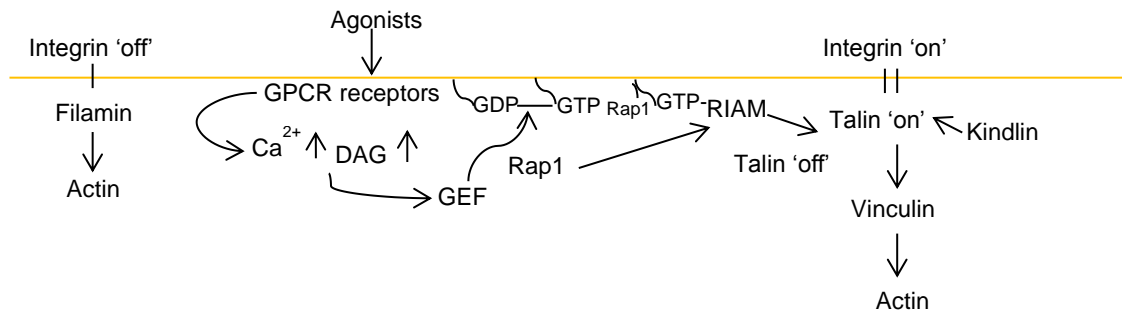


Figure 7. Simplified inside-out integrin signalling in the recruitment of talin to the cell membrane: the agonists bind to the G-protein coupled receptors and increase the concentration of calcium and DAG (diacyl glycerol) cellular level; this then activates a GEF (guanine nucleotide exchange factor) that activates the Rap1 (belonging to the GTPase family); Rap1 promotes the exchange of GDP to GTP, active Rap1 also interacts with RIAM and this recruits talin to the cell membrane; kindlin is also associated with talin to enhance integrin signalling. Inactivated integrin is stabilized by filamin binding to its β -tail, modified from (Anthis and Campbell, 2011)

Rap1-GTP recruits RIAM (the small GTPase Rap1-interacting adaptor molecule) to the membrane; RIAM binding to talin rod domain recruits talin to the membrane; talin binds and activates integrin, and recruits actin cytoskeleton; sequentially, conformational changes in the talin-RIAM complex binding causes competitive binding of vinculin head to talin, also vinculin tail binding links FAs to actin (Izard and Vorrhein, 2004, Goult et al., 2013b, Humphries et al., 2007). Upon FA recruitment, vinculin structure stays in an active conformation, which also leads to binding of vinexin, ponsin, VASP and actin-related proteins Arp 2/3 to the neck; actin, PIP2 and paxillin to the vinculin tail (Humphries et al., 2007, Zamir and Geiger, 2001).

Integrin-talin assembling also recruits FAK, which binds to Src in Figure 6; this dual kinase FAK-Src can bind and phosphorylate other scaffold proteins such as paxillin and p130Cas, which can regulate Src-FAK-Crk interactions with Rac, this is required for FA turnover, lamellipodia formation and cell migration (Mitra, 2006, Schaller, 2001, Kraynov et al., 2000, Westhoff et al., 2004). FAK also interacts with Arp 2/3 which is regulated by the Wiskott-Aldrich Syndrome Protein (WASP) (Pollard and Borisy, 2003). Arp2/3 initiates the new actin filaments polymerization (Galbraith et al., 2007). Calpain-2/FAK-Src is linked and regulated

in FAs network-actin disassembly, i.e. proteolysis of FAK (Westhoff et al., 2004). Also, RIAM dependent MEK-1 activation pathway was required for efficient FAs disassembly (Coló et al., 2012).

FAs also impact actin contraction and polarization through Rho GTPase protein (Huveneers and Danen, 2009). Rho GTPase hydrolysis (GTP to GDP) is regulated through the opposing activities of guanine nucleotide exchange factor (GEFs) (Huveneers and Danen, 2009).

Cell membrane protrusions/lamellipodial ruffling and spreading at the leading edge in migrating cells requires Rac1 (Rho GTPase family), Cdc42 and actin cytoskeleton at the cell front (Figure 5) (Petrie and Yamada, 2012); whereas in the retractive cell body and rear end, active RhoA is required to recruit ROCK which phosphorylates cytoskeletal proteins and generates actomyosin contractility by actin stress fibres; also proteolytic degradation of ECM is assisted with integrin-mediated directional cell migration (Ram, 2005, Wolf, 2003, Sahai, 2003). RhoA-ROCK-myosin II signalling dictates the mode of 3D cell migration (Petrie and Yamada, 2012).

Actin cytoskeleton-myosin linkage to FAs exerts tension and contractile forces which leads to cell motility (Hu et al., 2007, Giannone et al., 2007). Actin fibres have been shown to be polymerising along the leading edge of moving protrusions and pushing synchronously with primed $\beta 1$ integrin-mediated FAs sideways (Galbraith et al., 2007). In lamellipodia of the leading edge, actin polymerisation is regulated by WASP/WAVE family Arp2/3 complex, profilin, cortactin, cofilin, LIM kinase, Rho family GTPases, PtdIns (3,4,5)P₃, Rac and Cdc42 (Yamaguchi and Condeelis, 2007, Huveneers and Danen, 2009). Other signalling molecules such as the WASP-Arp 2/3 pathway, cofilin, Cdc42 are necessary for invadopodia protrusion formation and invasion of the cancer cells (Yamaguchi et al., 2005, Yamaguchi and Condeelis, 2007, Chan et al., 2009, Ridley, 2011).

1.6. 1 Post Translational Modifications of Focal Adhesions

Focal adhesions are known to be regulated by PTMs and the regulation of FAs may not be subjected to only one PTM, competitions or co-operative reactions can occur, which increases the complexity of the post-translational regulatory mechanism of FAs. For example, the focal adhesion kinase, FAK, a tyrosine kinase, was discovered to be a substrate of the viral Src oncogene initially and later identified to be a highly tyrosine-phosphorylated protein localized in the integrin-cell adhesion sites, which can enhance Src SH2 (Src-homology 2) domain binding to FAK through phosphorylation at Tyr-397 and further phosphorylation of FAK at Tyr-576/577 leading to full activation (Mittra, 2006, Chan et al., 2009, Hsia et al., 2003).

FAK has been associated with metastatic potential *in vivo* and reported in many tumours including breast, ovarian, colon, prostate, melanoma, thyroid, pancreatic, head and neck and so on (Chan et al., 2009, Golubovskaya et al., 2007, Cance et al., 2013, Cance et al., 2000). FAK has also several tyrosine phosphorylation sites including Tyr-397, 407, 576, 577, 861 and 925 (Mitra et al., 2005). Adhesion turnover involves many tyrosine kinases and phosphatases, which many of them are engaged in FAK signalling (Broussard et al., 2008). These are Src, p190RhoGAP, Rho kinase (ROCK), Cdc42 and myosin light chain kinase (MLCK) etc (Schober et al., 2007, Chan et al., 2009). FAK has been an important signalling factor which is involved in cancer cell adhesion and migration, tumour angiogenesis and progression (Mitra, 2006, Parsons, 2003). The N-terminal FERM (protein 4.1, ezrin, radixin and moesin homology) domain of FAK has been an active area for research, the FERM domain enables integrin-FAK activation, associates a signalling linkage from EGF (epidermal growth factor) receptors, PDGF (platelet-derived growth factor) receptors and G-protein coupled receptors and recently, the FERM domain of FAK was found to be covalently modified by SUMO at ϵ -amino position of lysine 152 (Mitra et al., 2005).

FAK is a protein substrate for SUMOylation. FAK has been shown to be SUMOylated (Yao et al., 2011, Kadaré et al., 2003). In the yeast two-hybrid screen, the N-terminal domain of FAK was found to interact with PIAS1, which promoted SUMO-1 conjugation to FAK at K152 and this enhanced its autophosphorylation (Yao et al., 2011, Kadaré et al., 2003). Autophosphorylation was an important function for FAK, which induced high affinity binding site for SH2 domain of Src (Kadaré et al., 2003). Moreover, Kadaré et al. study showed that SUMOylation of FAK occurred in the nucleus mostly and possibly independent of cell adhesion, as PIAS1 is a nuclear protein predominantly, suggesting that cytoplasmic FAK may undergo nucleocytoplasmic cycling, which allowed its nuclear SUMOylation at K152 in the presence of PIAS1 (Kadaré et al., 2003). In Yao et al. study, inhibiting protein SUMOylation after 6 hours ginkgolic acid treatment in HEK293T cells (human embryonic kidney 293) showed a significant decrease in SUMO1 and SUMO 2/3 conjugation and a reduction in Tyr-397 phosphorylation in the SUMOylated form of FAK. These may suggest SUMOylation of FAs, such as FAK, could alter protein localization; SUMOylation of FAK may additionally regulate signalling at the adhesion as well as in the nucleus. SUMOylation is critical in regulating FAK kinase activity and signalling and a global crosstalk for SUMOylation-modulated phosphorylation.

1.7 Talin and Vinculin

Talin is an important cytosolic protein associated with $\beta 1$ integrin to the cytoskeleton, found in the membrane-enriched fraction containing Golgi and endoplasmic reticulum (Martel et al., 2000). Talin in mammalian cells exists as 2 isoforms, talin 1 and talin 2, the role of talin in FA formation and maintenance is unique, where talin not only is required for linking integrin to actin filaments, but talin together with kindlin 1 and 2 are all required for integrin activation (Geiger et al., 2009, Montanez et al., 2008, Anthis and Campbell, 2011). Talin is a 270kDa molecule consisting of the N-terminal head domain (F0, F1, F2 and F3 subdomains/FERM domain) of 50kDa and the C-terminal rod domain (tail domain) of 220kDa, which the rod domain has binding sites for vinculin and actin and this leads to inside-out integrin activation (Anthis et al., 2009, Critchley and Gingras, 2008, García-Alvarez et al., 2003).

One study has described that intramolecular interactions of talin as an autoinhibition phase, disruption of talin autoinhibition could result in morphogenetic defects during fly development and a process involved in wound healing called dorsal closure was much delayed, moreover, this was resulted from reduced talin turnover (Ellis et al., 2013). Therefore, talin autoinhibition could provide a link and modulate adhesion turnover and adhesion stability critical for normal morphogenesis (Ellis et al., 2013).

Talin has been known to co-stimulate with integrin activation, regulate FA turnover and pathways have been elucidated: RIAM has been implicated in talin activation to activate $\beta 3$ integrin activation (Critchley and Gingras, 2008); the proteolysis of talin by the intracellular calcium-dependent protease, calpain has been shown to be critical for FA disassembly, specifically, the adhesion turnover was a rate-limiting step mediated by talin proteolysis and the disassembly of vinculin, paxillin and zyxin were dependent on the ability of calpain cleavage of talin (Franco et al., 2004); integrin signalling via FAK and Src promotes the binding of PIP kinase PIPK1 γ 90 to the F3 domain of talin and the translocation of talin to the plasma membrane, therefore, talin may activate integrin and provide the bridges to actin cytoskeleton (Critchley, 2004). The talin distribution in the cell not just found in the cell-ECM junctions, such as in the FA, but also found in the basal surface of the epithelial / endothelial cells in contact with basement membrane, in the myotendinous junctions of skeletal muscle cells, in the endothelial cell-cell junctions, neuromuscular junctions, in the platelets and so on (Critchley, 2004).

The molecular structure of talin and its binding partners have been elucidated and a simplified diagram of talin is presented in Figure 8.

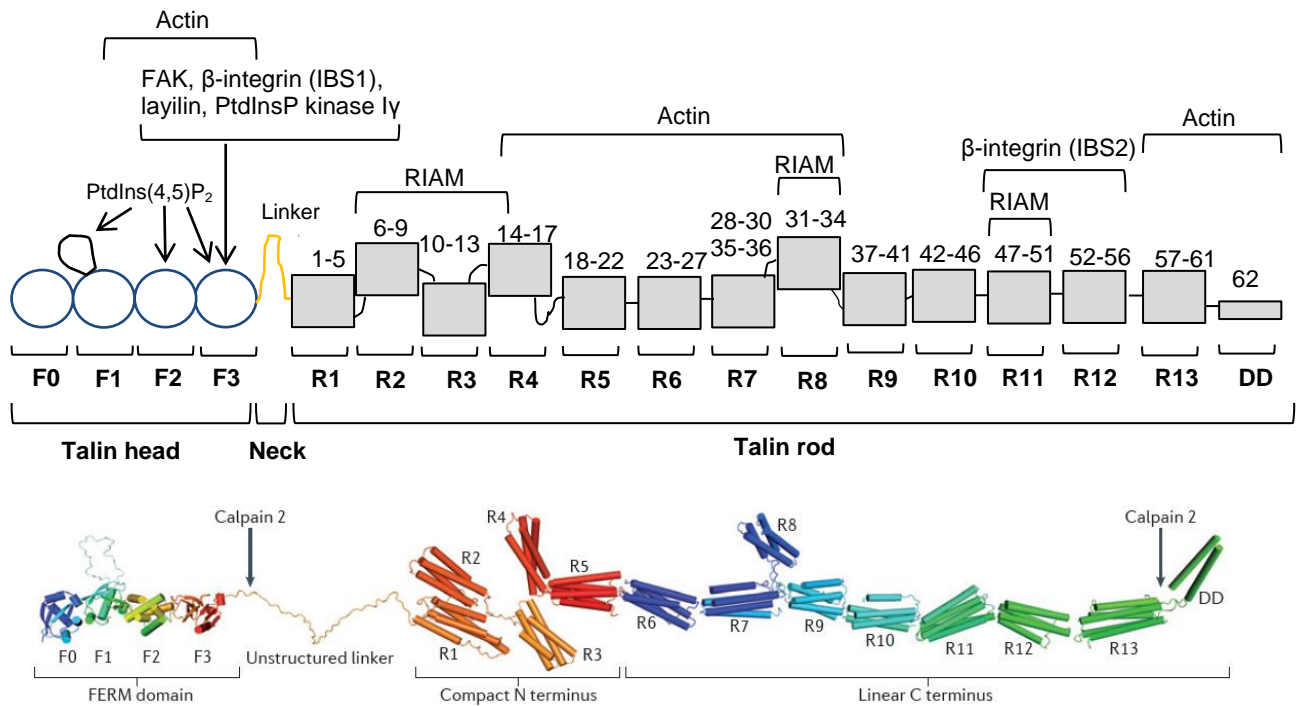


Figure 8. The structural model and binding domains of full-length talin 1: the atypical FERM N-terminal head domain of talin is linked to the flexible C-terminal talin rod by an unstructured linker of ~80 residues. At the linker/neck region, it contains a calpain-2 cleavage site (between Q433 and Q434). The talin rod contains 62 α -helices, which are grouped into 4- or 5-helix bundles (R1-R13) and a single helical dimerization domain (DD). The talin rod also contains multiple vinculin binding sites (R1 helix number 4, R2 helices 6, 9, R3 helices 11, 12, R6 27, R7 36, R8 33, R10 46, R11 50 and R13 58). Many domain binding partners have been mapped onto the structure of talin 1, such as F2F3 contains actin and FAK binding sites, F3 domain contains β -integrin (IBS1), PtdIns(4,5) P_2 and PtdInsP kinase 1 γ binding sites; talin rod also contains a second binding site for actin (R4-R8) and β -integrin (IBS2); the C-terminal contains the THATCH domain, where actin also binds and the dimerization domain (DD), modified from (Calderwood et al., 2013)

Figure 8 represents the structural model of talin 1. The F3 domain of talin contains a canonical phosphotyrosine binding (PTB) fold which can directly bind to the membrane proximal NPxY/F motif of the cytoplasmic β integrin tail; the F2/F3 domains have binding surface for the membrane and modify its orientation relative to the bilayer (Kalli et al., 2010, Domadia et al., 2010). The talin rod domain has also been revealed with a second integrin binding site, the integrin binding site 2 (IBS2), which is essential for linking integrin β subunits to the cytoskeleton (Rodius et al., 2008, Moes et al., 2007).

Talin contains ~11 vinculin binding sites (VBSs) in the rod domain and the rest of the rod denoted as the grey box numbers in Fig. 8 represents ~62 amphipathic helices (Patel et al., 2006). Talin can be cleaved by calpain-2 between the head and the rod domain, which has previously shown to be important in FA turnover (García-Alvarez et al., 2003, Bate et al., 2012). Vinculin could also be cleaved by calpain into fragments (Serrano and Devine, 2004).

From the SUMOplot analysis, which has speculated talin or vinculin could be both SUMOylated. Since the list of SUMOylated substrates is growing rapidly, whether FAs could be SUMOylated *in vitro* or *in vivo* will be crucial to understand cell migration. The talin-vinculin interactions is crucial in FA, since talin molecule has many VBSs binding sites and the structural vinculin binding domain with talin has been elucidated (Roberts and Critchley, 2009).

1.8 The Inhibitors Used in this Study

Small Molecule Inhibitors of Protein SUMOylation: Ginkgolic Acid

Until recently, very few small molecule probes were available to study the critical role of SUMOylation in cancer. Two small molecule inhibitors have been reported, which appear to both target the E1 SUMO-conjugating enzyme (SAE1/2), these are ginkgolic acid (Fukuda et al., 2009a) and Kerriamycin B (Fukuda et al., 2009b). Both inhibitors completely inhibit the SUMOylation of RanGAP1-C2 *in vitro* with GA at a concentration of 10 μ M and Kerriamycin B at a concentration of 20 μ M; moreover, both inhibitors directly bind to E1 and completely block the formation of the E1-SUMO-1 thioester intermediate both *in vitro* and *in vivo* with GA at a concentration of 10 μ M and Kerriamycin B at a concentration of 20 μ M, but without affecting ubiquitination (Fukuda et al., 2009a, Fukuda et al., 2009b).

The *Ginkgo biloba L.* is the oldest tree species and has survived over millions of years on earth (Bilia, 2002). The *Ginkgo biloba* leaf extracts and some of their constituents appear to have antitumor activities (DeFeudis et al., 2003). The *Ginkgo biloba* leaf extracts have also been shown to have antioxidant effects, cardiovascular protective effects, stress alleviating effects, antiangiogenic effects and prevention of neurodegenerative diseases (Ahlemeyer and Kriegelstein, 2003, DeFeudis and Drieu, 2004, Zhou et al., 2004). Ginkgolic acid (GA) is an extract from the *Ginkgo biloba* tree leaves, which appears to have allergenic properties and it is quantified in the Ginkgo extraction as less than 5 ppm, with two other main active compounds as flavonoids and terpenoids (Mahadevan and Park, 2008, Smith and Luo, 2004).

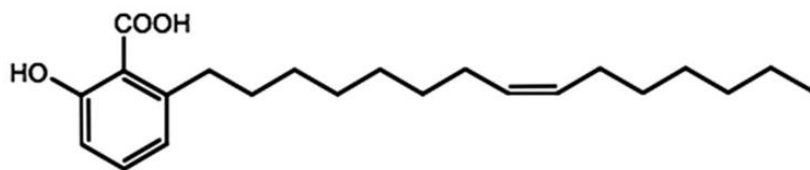
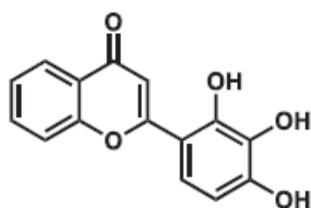


Figure 9. Showing the carboxylic COOH group and the long aliphatic chain in ginkgolic acid (15:1) (Fukuda et al., 2009a)

In Fukuda's study, they have shown that both the carboxylic group and the long aliphatic chain are important for binding to E1 and hence for inhibition of SUMOylation (the carboxylic group and the aliphatic chain of GA are shown in Figure 9); they have also shown that 100 μ M GA can inhibit the SUMOylation of p53; since p53 can be modified by SUMO-1 on lysine residue 386 *in vitro* and *in vivo* (Gostissa et al., 1999, Rodriguez et al., 1999).

2-D08 (2',3',4'-trihydroxyflavone)



2-D08

Figure 10. 2-D08, a synthetic oxygenated flavonoid (Kim et al., 2014)

A newly developed SUMOylation assay which used a microfluidic electrophoretic mobility shift system as a type of medium throughput kinetic screening between the protein substrate and the products of enzymatic reactions to directly monitor the product formation has found that out of 500 screened small molecules and compounds, 10 compounds showed more than 90% inhibition of SUMOylation reaction after 100 minutes performance; 2-D08 had the most potent inhibitory activities (Kim et al., 2013). 2-D08 was found to inhibit the conjugation of SUMO-1, SUMO-2 and SUMO-3 to I κ B α (Kim et al., 2013); additionally, 2-D08 was capable of inhibiting SUMOylated topoisomerase-I fragment with a concentration of 30 μ M *in vitro* and in two breast cancer cell lines ZR-75-1 and BT-474, pre-treatments with 2-D08 could inhibit the camptothecin-induced rapid accumulation of SUMOylated topoisomerase-I (Kim et al., 2013). 2-D08 was concluded a novel, cell permeable and mechanistically unique inhibitor of protein SUMOylation (Kim et al., 2014), however, its specific role in the inhibitory effects of protein SUMOylation is still unclear.

3-B08 or Gossypetin (3,5,7,8,3',4'-hexahydroxyflavone)

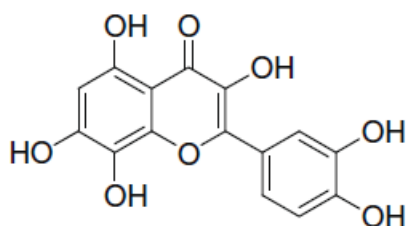


Figure 11. 3-B08, also known as gossypetin, the chemical structure of the commercially available flavone derivative (Jeong et al., 2009, Kim et al., 2013)

Gossypetin, also known as 3-B08, has been shown to have the second most potent inhibitory effects of protein SUMOylation alongside GA30 (30 μ M) being the positive control for the protein SUMOylation activity (Kim et al., 2013).

Gossypetin has originally been shown to have antimutagenic, antioxidant, antimicrobial and antiatherosclerotic effects (Chen et al., 2013, Jeong et al., 2009, Francis et al., 1989). Gossypetin was found to inhibit protein oxidation and lipid peroxidation (Chen et al., 2013); gossypetin had an atheroprotective role against the oxidized low-density lipoprotein (ox-LDL) induced injury in human umbilical vein endothelial cells (HUVECs) (Lin, 2015).

Spectomycin B1

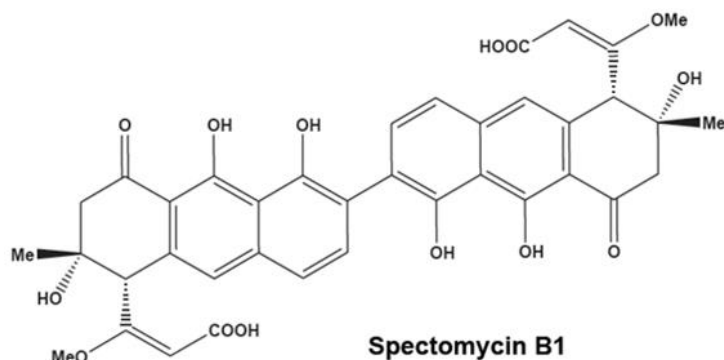


Figure 12. The structure of spectomycin B1 identified using an *in situ* cell-based screening system (Hirohama et al., 2013)

The first identified Ubc9 inhibitor known as spectomycin B1, which was shown to bind to the E2 enzyme, the Ubc9 enzyme directly and also exhibited to inhibit estrogen-dependent proliferation of MCF7 human breast cancer cells, leading to its potential to develop as a therapeutic agent against hormone dependent breast cancers (Hirohama et al., 2013). 10 μ M of spectomycin B1 can inhibit the SUMOylated RanGAP1 *in vitro* (IC₅₀ value is 4.4 μ M) and 100 μ M spectomycin B1 treatment for 24 hours can inhibit *in vivo* p53 SUMOylation; furthermore, 10 μ M of spectomycin B1 can inhibit the E2 Ubc9-SUMO-1 thioester bond intermediate formation but not the E1-SUMO-1, indicating that spectomycin B1 is a direct and selective target for binding to E2 Ubc9 enzyme (Hirohama et al., 2013).

1.9 Cell Lines Used for this Study

Breast cancer has been difficult to treat, as multiple mechanisms are involved and the tumour microenvironments are vital for its metastasis (Boudreau and Myers, 2003). In breast cancers, tumour induced angiogenesis has been considered the first evidence as the pre-invasive stage of high grade solid ductal carcinoma *in situ* (Boudreau and Myers, 2003). The most famous known HER-2 /neu oncogene (also known as the epidermal growth factor receptor 2 ERBB2) has been amplified in human breast cancer cell lines and is a significant indicator/predictor with the overall time to relapse or survival in breast cancer patients (Slamon et al., 1987). The histological different types of invasive breast carcinoma and possible models of breast cancer metastasis have been summarized (Weigelt et al., 2005). MDA-MB-231 cell line is a type of invasive and metastatic breast cancer cell line and has been used for this study.

Osteosarcoma (OS) is a type of highly malignant tumour, approximately one thirds of the patients are not responding to chemotherapy and the effective and alternative treatments are still missing due to its early onset mostly lacking a predisposing lesion, only < 2% shown with prevalence of inheritance with the majority of tumours being sporadic, high genetic heterogeneity and infrequency with enough patients cohorts to compensate for the high genetic variability, these are a few factors that make osteosarcoma a difficult tumour type to study and treat (Mohseny et al., 2011, Mohseny, 2012). The human osteosarcoma U2OS cell line was derived from a moderately differentiated sarcoma of the tibia of a 15 year old girl in 1964 (Niforou et al., 2008). Spectral karyotyping analysis and cytogenetic analysis have revealed chromosomal instability, structural rearrangements and alterations and high incidence of aneuploidy in the OS tumours and cell lines (Bayani et al., 2003). The U2OS cell line has been used in this study as a different type of tumour cell line to MDA-MB-231 cells.

1.10 The Hypothesis: SUMOylation Plays an Important Role in the Regulation of Focal Adhesions, which are essential in Cell Migration

From the literature, emerging evidence has shown that SUMOylation is critical in tumorigenesis. In this current study, SUMOylation has been hypothesized to play a critical role in regulating the dynamic activities of FAs in cancer cell migration.

To start with, several steps have taken place: SUMOylation inhibitors including ginkgolic acid (GA), 2-D08, gossypetin have been used in both MDA-MB-231 cells and U2OS cells to investigate their effects on FA number, size and turnover dynamics. The GA and the Ubc9 siRNA has been used in the MDA-MB-231 cell migration studies. The initial studies have led

to the study of the identification of which FA proteins could be SUMOylated in MDA-MB-231 cells and U2OS cells. Three different IP methods have been developed. Later, two additional cell lines were used, the CMK11-5 cells and the platelets. A mass spectrometry study was conducted to validate and confirm the FA protein SUMOylation. Finally, the mechanism of FA protein SUMOylation in different cell types has been compared. These study approaches have been used to investigate how the changes in the dynamic activities of FAs could affect cancer cell migration and metastasis, where SUMOylation has been hypothesized to regulate this diverse process.

Chapter 2 – Materials and Methods

2.1-2.4 Cell Culture

Three cell lines were used for studying SUMOylation in the regulation of focal adhesions. MDA-MB-231 human breast cancer cell line (ATCC), the U2OS human bone osteosarcoma cell line (ECACC, European Collection of Authenticated Cell Cultures) and the human megakaryocyte-like cell line, CMK11-5 cell line (purchased from the Health Sciences Research Resources Bank in Japan).

2.1 Media Preparation

MDA-MB-231 cells were maintained in DMEM (Dulbecco's Modified Eagle's Medium 1X) containing 1 g/L D-glucose, L-glutamine and pyruvate, 500 ml media (Gibco), which was supplemented with 10% (v/v) fetal bovine serum (FBS, 50 ml, Gibco) and 5.5 ml of 1% v/v Penicillin/Streptomycin (10,000 units/ml penicillin, 10,000 µg/ml streptomycin, Gibco). The cells were grown in T75 flasks at 37°C/5% CO₂ humidified environment. Serum free DMEM media was also made in a 50ml Falcon tube without FBS but added with Penicillin/Streptomycin for experiments.

CMK11-5 cells were maintained in RPMI media at 37°C/5% CO₂ environment. The RPMI media (containing L-glutamine, Gibco) was supplemented with 10% (v/v) fetal bovine serum (FBS, 50 ml, Gibco) only.

U2OS cells were routinely maintained in McCoy's 5A (Modified) Media 1X containing L-glutamine (500 ml, Gibco), which was supplemented with 10% (v/v) fetal bovine serum (FBS, 50 ml, Gibco) and 5.5 ml of 1% v/v Penicillin/Streptomycin (10,000 units/ml penicillin, 10,000 µg/ml streptomycin, respectively, Gibco). The cells were grown in T75 flasks at 37°C/5% CO₂ humidified environment. The serum free McCoy's 5A modified media was also made together in a 50ml Falcon tube.

PBS pH 7.4 (1x, phosphate buffered saline, Gibco) (with no CaCl₂ and MgCl₂) was used to wash the monolayer of MDA-MB-231 cells and U2OS cells grown in the T75 flask. OPTI-MEM I (1x, Gibco) reduced serum medium (containing HEPES, 2.4 g/L sodium bicarbonate and L-glutamine) was used for the siRNA transfection experiments.

2.2 Routine Cell Passage

For routine cell passage, the MDA-MB-231 cells were grown in T75 flasks and washed with 10 ml PBS once; the cells were trypsinized with 2 ml of 0.05% Trypsin-EDTA (1X, Gibco) at 37°C/5% CO₂ humidified environment for 5-10 minutes. The cells were detached from the bottom of the flask and were resuspended with 3 ml of fresh DMEM media to inactivate the trypsin. The cell suspension was mixed well to ensure single cell separation. The cells were seeded at 1:6 or 1:8 splitting ratio; 0.6-0.8 ml of the cell resuspension was added with 20 ml fresh DMEM media into a new T75 flask. The cells were incubated at 37°C/5% CO₂ humidified environment for 3-4 days until 80% confluence (2-4 x 10⁶ cells, 95% viability) and ready to be split again.

The growth media for U2OS cells was removed and the cells were washed with 10 ml PBS once. The cells were trypsinized with 2 ml of 0.05% Trypsin-EDTA (1X, Gibco) at 37°C/5% v/v CO₂ humidified environment for 5-10 minutes. The cells were resuspended with 3 ml fresh McCoy's 5A modified media and it was mixed well. The cells were seeded at 1:6 ratio. They were maintained in new T25 flasks at 37°C/ 5% v/v CO₂ humidified environment for 3-4 days until 80% confluence and ready to be split again.

The CMK11-5 cells were grown in cell suspension in RPMI media at 37°C/5% v/v CO₂ humidified environment. Some CMK11-5 cells could differentiate to spread and attach to the bottom of the flask. At 80% confluence, all the cells grown in suspension in the culture media was taken into a sterile 50 ml tube and the tube was spun down at 1500 rpm for 5 minutes. The differentiated cells stuck to the flask were thrown away. The media was removed from the 50 ml tube and the cell pellet was resuspended with 2 ml fresh RPMI media. The cells were split at 1:5 or 1:6 ratios depending on the confluency. 0.3-0.6 ml of the cell resuspension was added with 20 ml fresh RPMI media into a new T75 flask. The cells were incubated at 37°C/5% CO₂ humidified environment for 2-3 days until they were ready to split again.

2.3 Haemocytometry

The haemocytometer was moistened and affixed with a clean glass cover-slip, where the coverslip would adhere by suction to the centre. 25µl of a well-mixed cell suspension was pipetted at one edge of the coverslip and run through the empty space. The cells were counted in 4 large corner squares and the number was recorded.

A formula was used:

Average count of cells in 4 squares $\times 10^4$ (conversion factor) = cell concentration / ml
1 $\times 10^5$ cells was usually the starting number for experiments, the formula was as:

The number of cells wanted /cell concentration (C_1) \times Volume (ml)
The cell concentration obtained in the cell suspension (C_2)

2.4 Freezing and Thawing the Cells

Freezing buffer was prepared in FBS with 10% DMSO (i.e. 5 ml DMSO+45 ml FBS). The cells from 1 T75 flask (MDA-MB-231 vs. U2OS cells) were trypsinized with 2 ml trypsin, left for incubation for 10 minutes in the incubator and resuspended in 3 ml fresh media. They were transferred into 15 ml Falcon tubes and centrifuged down at 3000 rpm for 10 minutes. The supernatant was removed from each tube and the cell pellet was resuspended in 8 ml freezing buffer. 1.5 ml or 2 ml cell suspension in the freezing buffer was aliquoted into the cryo vials. The vials were labelled with the cell line name, the date and the initials. The vials were put into the 100% isopropyl alcohol-containing container Mr Frosty freezing container. This was to achieve $-1^\circ\text{C}/\text{minute}$ rate of cooling for cell preservation in the -80°C for 24 hours. Then the vials were wrapped in the metal wire and plastic rack and frozen in liquid nitrogen for long term storage.

The vials were taken up from liquid nitrogen and immediately put into the 37°C water bath for thawing. The 1.5 ml or 2 ml of the defrosted cell suspension was transferred into a 15 ml Falcon tube. 10 ml fresh media was added to the tube and mixed well with the cells. The tube was centrifuged down at 3000 rpm for 10 minutes. The supernatant was removed. 5 ml fresh media was added to the cell pellet and resuspended well. The 5 ml cell suspension was added into a new T75 flask with 20 ml fresh media in it. The flask was left in the incubator and the media was changed every 2 days. 1 week was needed for the cells to grow.

2.5 DNA Plasmid Extraction and Purification: HA SUMO-2, GFP-Vinculin, mEmerald-Vinculin and GFP-Talin

pcDNA3 HA-Sumo2 WT was a gift from Guy Salvesen (Addgene plasmid # 48967); pGFP(C3)-Vinculin was a gift from Klaus Hahn (Addgene plasmid # 30312); mEmerald-Vinculin-N-21 was a gift from Michael Davidson (Addgene plasmid # 54304); GFP-Talin 1 was a gift from Anna Huttenlocher (Addgene plasmid # 26724). HA SUMO-2, mEmerald/GFP-vinculin or GFP-talin 1 plasmids were bought from Addgene and obtained in

E.coli bacteria-containing stabs in small glass bottles. The bacterial stab contained the inserted DNA plasmid construct, which could be stored at 4°C for up to 2 weeks.

2.5. 1 LB Media and Bacto Agar Preparation

Luria-Bertani (LB) media was prepared by adding tryptone (10 g), yeast extract (5 g), NaCl (10 g) and 1 litre deionized H₂O in a clean bottle. The solution was shaken thoroughly until all the solutes were dissolved. The pH was adjusted to 7.0 using pH monitor with 5 M NaOH. The bacto agar for plates was made by adding 15 g agar with the LB medium solutes in another bottle to make up 1 litre deionized H₂O (agar was added 7.5 g for 500 ml LB solution). Both LB medium and bacto agar were autoclaved before the addition of antibiotics (ampicillin: the stock concentration 100 mg/ml, the working concentration 100 µg/ml; kanamycin: the stock concentration 50 mg/ml, the working concentration 50 µg/ml, recommended by Addgene).

The LB medium and the bacto agar were allowed to cool on the bench at room temperature to about ~50-55 °C. Both of the LB medium and the bacto agar were split into 500 ml bottles; the LB medium or the bacto agar bottles were added with ampicillin and kanamycin respectively after they were cooled. The bacto agar was poured into the culture medium plates labelled with corresponding antibiotics (ampicillin or kanamycin) near to a hot flame for sterility. The plates were allowed to cool at room temperature. Once cooled, the plates were sealed with parafilm and stored at 4 °C before use and kept up to 3 weeks.

2.5. 2 The Selection of the Antibiotics-resistant DNA Plasmids and the Growth of the Bacterial Broth

DNA/RNA free eppendorf tubes were labelled with each plasmid name and negative control (Table 1). The competent E.coli I cells (Mach 10, Promega) were taken from -80°C and thawed on ice for 20 minutes. For each plasmid tube and the negative control tube, 400 µl LB medium with 50 µl of competent cells were added using the sterile pipette tips near to the hot flame, respectively. The negative control tube only contained the competent cells in LB medium. 1 sterile pipette tip of the bacteria was streaked from the corresponding bacterial stab glass bottles and mixed into the labelled plasmid eppendorf tubes. All the tubes were shaken at 80 rpm at 37°C in the water bath for 1 hour initially.

| | | | | |
|--------|-----------------------|---------------------------|-------------------------|--------------------------------|
| Tube 1 | - | Negative control | + 400 µl LB medium only | + 50 µl E.coli competent cells |
| Tube 2 | Kanamycin resistance | mEmerald-Vinculin plasmid | + 400 µl LB medium only | + 50 µl E.coli competent cells |
| Tube 3 | Kanamycin resistance | GFP-Vinculin plasmid | + 400 µl LB medium only | + 50 µl E.coli competent cells |
| Tube 4 | Kanamycin resistance | GFP-Talin 1 plasmid | + 400 µl LB medium only | + 50 µl E.coli competent cells |
| Tube 5 | Ampicillin resistance | HA SUMO-2 plasmid | + 400 µl LB medium only | + 50 µl E.coli competent cells |

Table 1. Transfection: 1 tip of the bacteria from streaking contained the plasmid of interest, which was added with the competent cells and the LB medium for incubation

The agar plates were taken out from 4°C and warmed up at room temperature. 250 µl liquid from each plasmid eppendorf tube was dropped onto the centre of the antibiotics-resistant agar plate (with ampicillin or kanamycin) and spread evenly across the whole surface area of the plate using a sterile VWR® polypropylene cell spreader. All these steps were done near to the hot flame. mEmerald-vinculin, GFP-Vinculin or GFP-Talin 1 plasmid/competent cells liquid mixture was spread and grown on the kanamycin-resistant agar plate; the HA SUMO-2 liquid mixture was spread on the ampicillin-resistant agar plate. For the negative control, 200 µl of the mixture was spread onto the '+ Amp negative control' plate for HA SUMO-2; 200 µl of the mixture was spread onto the '+ Kana negative control' plate for mEmerald-Vinculin, GFP-Vinculin and GFP-Talin 1.

All the plates were incubated overnight (12-16 hours) at 37°C. This was enough time for the bacteria to grow and form colonies, only if the competent cells had taken up the antibiotic-resistant plasmids. After overnight incubation, in all the plasmid agar plates, they had formed colonies of bacteria; in the negative control plates, there were no colonies formed. For each plasmid extraction, a single bacterial colony was picked using the sterile tip near to the hot flame, which would minimize the chances of obtaining a mixture of plasmids during the preparation. The single colony was mixed completely in 10 ml LB medium containing the antibiotics in a 15 ml Falcon tube. There were 4 tubes prepared and they were put in the shaking incubator at 200 rpm for up to 8 hours at 37 °C. A cloudy mixture was observed for each tube, which was then poured into conical flasks (4 flasks were autoclaved with the sponges on top previously) containing 200-250 ml LB medium with antibiotics. All the 4 conical flasks were incubated overnight up to 16 hours optimally with vigorous shaking to obtain a high yield of bacteria containing the plasmid of interest.

The next day, for each flask, the broth was split into 50 ml Falcon tubes. The bacteria pellet was obtained using the cooling centrifuge (MULTIFUGE X3R, Thermo Scientific) at 4814 g for 15 minutes at 4°C. For efficient pellet lysis, lysate filtration, DNA binding, washing and

eluting, the QIAGEN HiSpeed Plasmid Maxiprep Kit was used to extract, purify and collect the ultrapure DNA plasmid.

2.5. 3 Maxiprep Kit

After centrifugation, the supernatant was removed from each 50 ml Falcon tube and the tube was drained. (The cell pellet could be stored at -20°C). The bacterial pellet was resuspended in 10 ml P1 (50mM Tris-Cl, 10mM EDTA, pH 8.0) resuspension buffer containing RNase A (final concentration 100 µg/ml, 1:1000). Each tube was vortexed until no pellet clump was seen. 10 ml lysis buffer P2 (200mM NaOH, 1% SDS) was added and mixed thoroughly and incubated for 5 min. No vortexing was needed.

The QIAfilter cartridges were prepared. The caps were screwed onto the outlet nozzle of each cartridge and left to stand. 10 ml chilled neutralization buffer P3 (3M potassium acetate, pH 5.5) was added into each tube. A fluffy white precipitate containing genomic DNA, proteins and cell debris etc became visible. The mixture was mixed completely with the buffer.

The cell lysate from each 50 ml tube was poured directly into each cartridge and incubated at room temperature for 10 min. The cartridges were left still on the stand. A precipitate containing proteins, genomic DNA and detergent was floated and formed a layer on top of the solution.

The HiSpeed Maxi Tips were prepared. 10 ml equilibration buffer, QBT was poured into each Tip and allowed to empty by gravity flow. The cap was removed from each cartridge and the plunger was gently inserted into each cartridge. The cell lysate was filtered into each equilibrated Tip until all the lysate was passed through the cartridge. The cleared lysate was allowed to enter the resin by gravity flow in the Tip. The Tip was washed with 60 ml wash buffer, QC. The buffer was allowed to move through the Tip by gravity flow. The DNA was eluted from the column with 15 ml elution buffer, QF. The eluate was collected in each tube.

The DNA was precipitated by adding 10.5 ml room temperature isopropanol (2-propanol) to the eluted DNA. It was mixed and incubated at room temperature for 5 min. The 30 ml syringes were prepared. The QIA precipitator Maxi Modules were attached onto the outlet nozzle of the syringes. The plungers were pulled out first then the modules were inserted.

The eluate/isopropanol mixture was transferred into each 30 ml syringe and the plunger was pushed. The eluate mixture was filtered through each precipitator module using constant

pressure. The flow-through was discarded. The precipitator was removed first then the plunger was pulled out. The precipitator was re-attached and 2 ml 70% ethanol was added to the 30 ml syringe. The DNA was washed by inserting the plunger and pressing the ethanol through the precipitate using constant pressure.

The precipitator was removed first and the plunger was pulled out. The precipitator was added back and the plunger was inserted and pushed quickly and forcefully. This was to dry the membrane by pressing the air and to prevent ethanol carryover.

The precipitator was attached to a new 5 ml syringe and a 1.5 ml collection tube was held over (autoclaved). 1-2 ml TE buffer was added to the 5 ml syringe. The plunger was pushed and the DNA was eluted into the collection tube using constant pressure X2. No excess pressure was used. The ultrapure DNA for each plasmid could be stored at -20°C.

| | |
|-------------------|-------------|
| mEmerald Vinculin | 861.6 µg/ml |
| GFP-Vinculin (1) | 297 µg/ml |
| GFP-Vinculin (2) | 331.8 µg/ml |
| GFP-Talin 1 | 414.5 µg/ml |
| HA SUMO 2 (1) | 294.9 µg/ml |
| HA SUMO 2 (2) | 337.5 µg/ml |

Table 2. The concentration of each plasmid in µg/ml

A NanoDrop spectrophotometer 2000 (Thermo Scientific, Labtech International) was used to measure the DNA plasmid yield; once calibrated with the 'blank', the samples were measured as dsDNA µg/ml. The concentration of each plasmid was summarised in Table 2.

2.6 Drug Treatment: Ginkgolic Acid, Gossypetin and 2-D08

Ginkgolic acid C15:1 was dissolved in DMSO [0.1 %] (molecular mass of GA: 346.5 g/mol, Sigma-Aldrich). 100 mM GA stock was prepared by adding 144.3 µl filtered sterile DMSO to the 5 mg GA. 5 µl GA was aliquoted into sterile eppendorf tubes and stored at - 20°C. For the experiments, 100 µM final concentration of GA was used. A two-step series of dilution was done. To each 5 ul, 45 µl fresh normal media was added (1:10). In the T25 culture flask, 30 µl of this 50 µl GA was mixed in 2.97 ml normal media (1:100), this was added to each treated flask (2-5 x 10⁵ cells plated originally = 60-70% confluence). GA treatment was done for 15 mins, 30 mins, 1 hour, 6 hours, 18 hours or 24 hours depending on the previous experiments. In a 6-well plate, 20 µl GA (of the 50 µl GA [1:10]) in 1.98 ml fresh normal media (1: 100) was added to each treated well for 15, 30 or 60 minutes incubation (1 x 10⁵ cells plated originally) in the IHC experiments.

For the gossypetin (3-B08) and 2-D08, these were also prepared as 100 mM stock concentration. Gossypetin (250 mg, G-500) was bought from INDOFINE Chemical Company, Inc. (ICC) and 2-D08 could be found at Merck Millipore. They were also dissolved in DMSO and aliquots stored at -20°C.

DMSO control was used as the same as the inhibitors, i.e. 5 µl DMSO was added with 45 µl medium. 10 µl diluted DMSO was added in 990 µl medium to make 1 ml total media. The cells were treated with each inhibitor at the desired concentration and time; in the 6-well plate, the total media amount was added as 2 ml and the T25 flask was filled with 4 ml media.

2.7 Focal Adhesion Turnover Assay

2.7. 1 DNA Plasmid Transfection

1 x 10⁵ MDA-MB-231 cells were firstly plated in each well of a 6-well plate 1 day prior to transfection. 1 µg DNA plasmid was added with the 100 µl serum free DMEM media in a sterile eppendorf tube for each FA plasmid separately. 1 µg GFP-FAK (695 µg/ml), 1 µg GFP-talin 1 (414.5 µg/ml, Addgene, #26724) or 1 µg GFP-vinculin (297 µg/ml, Addgene, #30312) was mixed in the 100 µl serum free DMEM media and the eppendorf tube end was tapped gently. 3 µl FuGENE HD transfection reagent (Promega) was added to each eppendorf tube and the tube end was tapped gently again. The FA plasmid mixture was incubated at room temperature for 15 minutes. Then the talin plasmid mixture was added drop by drop to the 2 wells labelled as control talin vs. GA talin; the FAK plasmid mixture was added to control FAK vs. GA FAK; the vinculin plasmid mixture was added to control vinculin vs. GA vinculin. Each plate was swirled gently. The cells were incubated for 8 hours initially in the incubator before they were trypsinized and transferred on collagen.

2.7. 2 Non-Compressed Collagen Coating

The collagen matrices were prepared by mixing 4.41 mg/ml chilled rat tail type I non-pepsinized collagen in acetic acid (final concentration 2 mg/ml, BD Biosciences) with DMEM 1X (100 µl/ml, 10X), 15-20 µl of the 1 M NaOH per diluted 1 ml collagen solution (pH normalized to 7.0, until the mixture colour was just changed from yellow to pink purple) and the chilled culture media to make up to 2 ml collagen mixtures. All the ingredients were mixed thoroughly on ice and care was taken to avoid bubble formation in the mixture solution. 200-400 µl of the collagen mixture was added to the centre of ibidi glass bottom dishes forming a 'ring patch'. The collagen gel was allowed to polymerize and solidify in 5% CO₂/95% v/v humidified air environment at 37°C for 20-30 minutes.

2.7. 3 2.5D Cell Culture

After 8 hours transfection, the MDA-MB-231 cells in each well were trypsinized (200 μ l trypsin/well) and 200 μ l fresh DMEM media was added per well for re-suspension (400 μ l total cell suspension/well). 200 μ l of the cell suspension from each non-transfected control and the GA treated well was pipetted into the matching collagen-coated ibidi glass bottom dishes (control and GA treated dishes). The cells were seeded around the edge of the 'collagen patch' and left in the incubator to attach and settle for another 20-30 minutes. Finally, 1.5 ml fresh DMEM media was added to cover the set collagen matrix. The cells were maintained in this environment overnight prior to GA treatment.

The next day, single MDA-MB-231 cells were aligned 'front-to-rear' along the edge of the collagen ring at the 'interphase / border' moving along the collagen patch edge; some other cells were moving adjacent towards the border and gradually they could form 'clumps' of cells; some cells were already migrated through into the 3D collagen matrix. 100 μ M GA was added to the treated ibidi dishes; the cells were incubated in 2 ml GA-containing fresh media for 1.5-2 hours ('talin', 'FAK' or 'vinculin' GFP plasmid transfected cells) prior to confocal microscopy.

To determine the FA turnover, live-cell timelapse imaging was taken as 1s, 2s or 8s per scanning for each control or GA treated ibidi dish for 5-10 minutes. These movies were analysed later to look at the FA number, size and turnover.

2.8 Immunocytochemistry

2.8. 1 Cell Growth on Coverslips

Glass coverslips were put in the wells of a 6-well plate and were immersed in 100% methanol for 15 minutes in the culture hood for washing. The methanol was then aspirated and the coverslips were left to dry. The coverslips were then coated with a thin layer of 0.2% w/v gelatin and left to dry up to 1 hour. MDA-MB-231 cells were resuspended in culture media from T75 flasks and plated on each coverslip in the 6-well plate as 60-70% confluence. The plate was left in the incubator overnight at 5% CO₂/95% humidified air environment at 37°C.

The next day, MDA-MB-231 cells were treated with GA, Gossypetin and 2-D08 to look at their effects on talin or vinculin containing FAs number and size. 100 μ M GA treatment was done as 15, 30 and 60 minutes. For the other inhibitors 2-D08 and gossypetin, the experimental treatment time was 1 hour and the concentration was also 100 μ M.

U2OS cells were prepared for the IHC experiments to study the effects of GA and the other inhibitors 2-D08 and gossypetin on talin or vinculin containing FAs number and size. For the U2OS cells, the inhibitor treatment time was chosen as 15 minutes or 1 hour and the concentration for each inhibitor used was 100µM.

2.8. 2 Immunocytochemistry Staining

The culture media was aspirated in each well in the 6-well plate and the cells were washed in pre-warmed PBS once at room temperature. The cells were fixed in 4% v/v PFA for 20 minutes at room temperature. The cells were washed with PBS for 10 minutes x3 then incubated with 0.5% v/v Triton-X100 for 10 minutes at room temperature. The cells were then washed in PBS for 10 minutes x3. The cells were blocked with 10% v/v goat serum for 10 minutes. Then the cells were incubated with primary antibodies (1:100 dilution) for 1 hour (1 µl primary antibody, 4 µl GS mixed in 94 µl PBS). This 100 µl solution was spread onto the whole area of the coverslip evenly. After washing with PBS 5 minutes x 3, the cells were incubated with secondary antibodies (1:100 dilution) for 1 hour in the dark (1 µl secondary antibody, 4 µl GS mixed in 94 µl PBS). The cells were washed in PBS for 5 minutes x 3 in the dark. 1 drop of DAPI solution (VECTASHIELD®, Vector Laboratories, Inc.) was added on the glass slides in the dark. A needle tip was used to take out the coverslip from each well carefully. The coverslip side with the cells 'on' was covered onto the glass slide immersed with DAPI in the dark. Nail polish was used to brush the borders of the coverslips to fix them onto the slides. All the glass slide samples could be then stored in slide boxes at 4°C and ready for confocal microscope scanning.

2.8. 3 Experimental Controls

In the preliminary experiments the specificity of labelling was tested using controls in which the staining was performed without the primary antibodies or in the absence of the cells. This gave no significant fluorescent labelling.

2.8. 4 Primary and Secondary Antibodies for IHC Experiments

| | |
|---|---|
| 1 | Mouse anti-talin 1 monoclonal antibody reacting with an N-terminal epitope in human talin between amino acids 139-433, Clone TA205, 1 mg/ml, MAB1676, Merck Millipore (1:100) |
| 2 | Mouse anti-vinculin monoclonal antibody, 1 mg/ml, MAB3574, Merck Millipore (1:100) |
| 3 | Alexa-Fluor 488 conjugated goat anti-mouse antibody, Fisher (1:100) |

2.9 Confocal Microscopy and Live-Cell Imaging

100x OIL lens (1.5 or 150 μm working distance) was used for the observation of FAs turnover. GALVANO mode was chosen, where 'interlock' was removed to ensure safe transmitted light from the lasers and E100 was changed to L100 confocal with the fluorescent lamp shutter box closed. The image was taken in the 1024*1024 format in the xyz plane. To do 3-dimensional planes of an image or look closer at a focal adhesion, fast z-stack slices of an image was scanned indicating a 'top' and a 'bottom' of the image; line averaging 4x-16x was taken according to the level of the noise background; the Z/Y position indicated where the section was taken away from the bottom of the culture dish. Fluorescent filters include DAPI (405), GFP (488), Cherry (630) and Cy5 (640-750). The laser fast mode was on and used as $\frac{1}{2}$ (2 scanning/second). The pinhole size was 1.2 which ensures optimal light capture. Pixel saturation indicator was always turned on to allow maximum 1% saturation.

Timelapse movies for FA turnover were generated to record at 2s, 8s or 10s intervals scanning of the 'control' and 'GA treated' samples for 5 minutes and 10 minutes period. The CO₂ chamber was connected to each culture dish to keep the pH at balance for live-cell imaging. GFP laser channel was used and set with the laser intensity and exposure time to ensure the noise background and the brightness of the image were kept in balance. The images were saved as ND2/Tiff files ready for data analysis.

2.10 Phase-Contrast Live-Cell Timelapse

2.10. 1 Cell Growth in 3D Collagen Matrix

The collagen matrix was made (diluted 2 mg/ml collagen + 1x DMEM + 1 M NaOH: see 2.7. 2) and mixed up with the MDA-MB-231 cells, which was prepared up to 10 ml diluted collagen mixture. 125-200 μl cell suspensions were mixed in 1 ml collagen mixture x 10. 12-well plate was used for the cell migration experiments. For each well in the 12-well plate, 600-800 μl of the mixed collagen containing the cells was pipetted and spread fully across the well area. The 12-well plate was left in the incubator for 30 minutes for the collagen matrix to set. 2 ml DMEM media was added into each well. The cells were grown overnight in the 3D collagen matrix.

2.10. 2 Drug Treatments

The MDA-MB-231 cells were treated with 25 μ M, 50 μ M or 100 μ M of GA. In the 12-well plate, 3 triplicate wells were set up as 1 group treatment. 3 groups of treatment were set up as 25 μ M, 50 μ M or 100 μ M GA treatments. The controls were prepared to each group treatment. MDA-MB-231 cells were also treated with 25 nM scrambled siRNA / Ubc9 siRNA (described in 2.17). The MDA-MB-231 cells were grown in 2 mg/ml 3D collagen matrix in the 6-well plate overnight. 3 wells were set up for the Ubc9 siRNA timelapse experiment. A single concentration 25 nM siRNA / 25 nM scrambled siRNA mixture (in 0.2x Lipofectamine dilution) was used; 1 well was set up as the negative control. 200-400 μ l cell suspension in DMEM media were mixed in the 1 ml collagen mixture and a total volume of 1000-1500 μ l final collagen mixture was added to each well surface. The timelapse experiment was run for a period 24-48 hours. The timelapse movies were taken for 2 separate rounds, i.e. the first 24 hours and the second 24 hours.

2.10. 3 Live-Cell Timelapse Microscopy

After adding GA or Ubc9 siRNA, the plate was sealed with Parafilm and a 'hole' was made in the side of the plate wall; this was to connect with the CO₂ supply needle. The plate was put onto the pre-warmed NikonTie timelapse microscope stage immediately. The plate was checked to make sure that it was fitted onto the stage with care. Live-cell imaging timelapse was initialized, where the microscope, the camera, the lamp, the temperature control unit and the CO₂ chamber were previously switched on. The temperature unit was set up as 37°C. The CO₂ pressure was fixed and controlled as between 70-80 mmHg. The light was adjusted at 1/3 light. NIS Elements software was selected. The exposure on the camera settings was set as 45ms and the background was selected as auto white.

10x Microscope lens was selected on the microscope with perfect focus or the auto-focus (PFS) on. When in focus, the eyepiece E100 was changed to L100, the focus was then only used with the fine focus button. ND timelapse programme was set up, where 24hrs timelapse movie was selected as the total time treatment; x/y point positions were selected in each non-treated and treated wells with 5 or 6 points at different eye fields. The interval time frame was set as 20 minutes. The camera was adjusted as live-fast with normal high quality capture. At the end of the experiment, multi-points were split to extract multiple files and then the movies were saved. The movies were analysed using Image J to study the cell migration compared between the non-treated and the treated conditions.

2.11 Western Blotting

2.11. 1 Bradford Protein Assay

A₁-H₁ in one 96-well plate were plated with 195µl Bradford reagent (Br) (blank). A₂₋₃ – H₂₋₃ were plated with 195 µl Br and 5 µl of bovine serum albumin (BSA) standard at 25, 125, 250, 500, 750, 1000, 1500 or 2000 µg/ml. The plate was stirred at 1000 / min for 30s. A standard protein absorption curve was generated and R² value = 0.95-0.99. Then, 5 µl of samples was plated in triplicate wells mixed with 195 µl Br and the plate was stirred. In the unknown protein concentration table, the mean concentration value was used to calculate an equal amount of protein loading (the protein loading concentration was 20-50 µg used) before electrophoresis and the loading volume per well was 40-45 µl. The equation as:

$$\text{Volume to load / well} = \frac{\text{Sample n protein mean } C_n \times 40\mu\text{l}}{\text{Sample n+1 protein mean } C_{n+1}}$$

2.11. 2 Western Blotting Buffers (Manually Prepared)

5x Tris-glycine electrophoresis running buffer: 15.1 g Tris base (Fisher Scientific), 94 g glycine (Fisher Scientific) were dissolved in 900 ml distilled H₂O, then added with 50 ml 10% v/v SDS. This was made up to 1 L solution. 1x Tris-glycine electrophoresis running buffer: 400 ml 5x Tris-glycine was mixed with 1600 ml ddH₂O to make up 2 L solution. These were stored at room temperature.

10% v/v SDS (sodium dodecyl sulphate): 50 g SDS was dissolved in 450 ml ddH₂O which was made up to 500 ml stock solution. It was stored at room temperature.

Transfer buffer: 2.9 g glycine, 2.8 g Tris base and 200 ml methanol were dissolved in 1 L ddH₂O. It was stored at room temperature.

10x TBS (Tris buffer saline): 80 g NaCl (Fisher Scientific), 2 g KCl (Fisher Scientific) and 30 g Tris base were dissolved in 800 ml ddH₂O initially; the pH was adjusted to 7.4 using concentrated HCl and this was made up to 1 L final solution. 1x TBS: 100 ml 10x TBS was mixed with 900 ml ddH₂O. These were stored at room temperature.

TBST (TBS-Tween-20): 0.1% v/v Tween-20 (Sigma) as 1ml Tween-20 was dissolved in 1 L 1x TBS. It was stored at room temperature.

5x SDS boiling gel-loading buffer stock solution: 312.5 mM Tris base (1.514 g), 10% v/v SDS (4 g), 50% v/v glycerol (20 g) final amount taken as 15.9 ml, 25% v/v mercaptoethanol (10 g) final amount taken as 9 ml and 0.0125% v/v bromophenol blue (5 mg) were dissolved in the final volume 40 ml ddH₂O and stored in -20°C. This was the 5x stock solution.

2.11. 3 Electrophoresis

4-20% Mini-PROTEAN® TGX™ precast 50 µl / 10-well Gels (Bio-Rad) were prepared in the tank. The samples were loaded according to the calculations from Bradford assay; 7 µl protein marker was loaded in lane 1. 1x Tris-glycine running buffer was poured to the mark 4-gel or 2-gel. Electrophoresis was set at 180V, 0.05A (1 gel=0.05A, 2 gels=0.05A x 2 = 0.1 A and so on) initially for protein running separation according to protein size, gel pore size and electrode charge. After the stacking gels, the current was changed to 0.03A for the resolving gel separation (1 gel=0.03A, 2 gels=0.06A and so on).

2.11. 4 Membrane Transfer

The PVDF membranes were cut as 8 cm x 8.5 cm. The semi-dry transfer paper was prepared according to the area of the membrane. The gel area was 6 x 8.5 cm². The current was set as the membrane area x 0.8 x 0.001 mA/cm² and the transfer voltage was at 250V. The PVDF membrane was soaked in methanol for 5 minutes. 6 transfer papers were soaked in transfer buffer for 10 minutes and placed on the transfer blotter. A roller was used to roll the paper gently to get rid of the excess transfer buffer and make it even surface. 3 soaked papers were placed underneath; the membrane was placed on top of the 3 soaked papers; the gel was put on top of the membrane carefully; the other 3 soaker papers were placed on top of the gel. This was the 'sandwich' and the transfer was set running for 1.5 hrs.

2.11. 5 Blocking

5% v/v milk-TBST was prepared for blocking non-specific binding of the proteins for 40 minutes. After blocking, the membrane was washed in 1x TBST, 10 minutes x 3 on a rotator machine.

2.11. 6 Primary and Secondary Antibodies

Primary antibodies were prepared in 2% v/v BSA-TBST (see the antibody dilutions 2.12 Antibodies). The membrane was incubated with the 1° antibody overnight on a rotator machine in the cold room at 4°C. The next day, the membrane was washed in 1x TBST, 10 minutes x 3. The secondary antibodies were prepared in 1% v/v milk-TBST. For HRP-conjugated 2° antibodies, anti-mouse or anti-rabbit were used as 1:3000; anti-goat HRP was

1:5000. The membrane was incubated with the 2° antibodies for 1 hour on a rotator machine. The membrane was then washed in 1x TBST, 10 minutes x 3.

2.11. 7 Band Detection

ECL-prime reagent (GE Healthcare) was used. 0.5 ml solution A mixed with 0.5 ml solution B was spread onto the membrane evenly and left for 1 minute in the dark. The luminescent image analyser ImageQuant LAS 4000 mini (GE Healthcare) was used and detection of the bands was carried out in the dark. Auto-exposure time was selected with super-resolution. ImageQuant software was used to map the digital information to the appropriate pixel location on the monitor, which gave an accurate image of the original membrane.

2.11. 8 Primary and Secondary Antibodies for WB Experiments

| | |
|---|--|
| 1 | Mouse anti-UBC9 monoclonal antibody (C-12) raised against amino acids 1-81 of UBC9 of human origin, 200 µg/ml, sc-271057, Santa Cruz Biotechnology, INC. (WB: 1:250-500) |
| 2 | Rabbit anti-GAPDH antibody, 1 mg/ml, G9545, Sigma (WB: 1:1000) |
| 3 | Donkey anti-goat IgG-HRP: 200 µg/0.5ml, sc-2020, Santa Cruz Biotechnology, INC. (1:5000) |
| 4 | Anti-mouse IgG-HRP, Sigma (1:3000) |
| 5 | Anti-rabbit IgG-HRP, Sigma (1:3000) |

2.12 Ubc9 siRNA Knockdown and Western Blotting

2.12. 1 GAPDH siRNA Knockdown

Previous experiments were done with the Silencer® siRNA Starter Kit (Invitrogen) to knock down GAPDH as the control for the Ubc9 siRNA knockdown experiment. Lipofectamine® RNAiMAX Reagent (Invitrogen) was used for Ubc9 siRNA knockdown experiments.

16 µl of GAPDH siRNA or scrambled siRNA was mixed with 384 µl nuclease-free water to give 2µM stock concentration. 30nM final concentration of GAPDH siRNA or scrambled control was used: 45 µl of the GAPDH siRNA or scrambled control was mixed with 300 µl OPTI-MEM®I reduced serum medium (modified Eagle's MEM medium, Gibco) to use per well in the 6-well plate. 7-well volume was made for the siRNA and the OPTI-MEM medium, mixed together.

MDA-MB-231 breast cancer cells were grown in 6-well plate overnight. The cells were washed with PBS once. Then, the cells were trypsinized with 0.2 ml trypsin, left for 5 minutes, then 0.2 ml normal medium was resuspended the cells in medium. Half (0.2 ml) cell suspension was plated into new well/per plate, 1.8 ml normal medium was added to each well.

NeoFX diluted transfection reagent was prepared. 5 μ l of the NeoFX with 300 μ l OPTI-MEM medium was for each well/per plate, 7-well volume was also made for NeoFX and OPTI-MEM medium, mixed together. Once NeoFX and OPTI-MEM medium was mixed, it was left to stand for 10 minutes. The diluted GAPDH / scrambled siRNA was mixed with the diluted NeoFX respectively and left to stand for 10 minutes. 600 μ l each GAPDH / scrambled siRNA/non-transfected control was added to each well containing 2 ml media. The cells were left in the incubator for 2 days. After 24 hours, the media was changed; after 48 hours, whole cell lysates were made.

2.12. 2 Ubc9 siRNA Knockdown

5 nmole Ubc9 siRNA / scrambled siRNA powder (Invitrogen/Life technologies, 4390824) was prepared to make 20 μ M siRNA stock. 250 μ l nuclease-free H₂O was added to 5 nmol siRNA powder gave 20 μ M stock (=20 pmol/ μ l). The siRNA / scrambled was diluted in OPTI-MEM medium. The experiment was done in T25 flasks, where 2.5 was the conversion factor for the siRNA amount added in T25 flasks. From 20 μ M stock: 7.5 μ l siRNA was added with OPTI-MEM medium to make 750 μ l total diluted siRNA, mixed well. Lipofectamine transfection reagent was diluted as 1x, 0.5x or 0.2x, each was mixed with OPTI-MEM medium. For the Opti-MEM medium, 150 x 2.5 x 2 = 750 μ l was taken for each siRNA / scrambled siRNA. Each calculation was prepared as doubled amount (x2, Table 3).

| 20 μ M siRNA stock | Diluted Ubc9 siRNA/scrambled siRNA [0.2 μ M] | Diluted Lipofectamine reagent 1x | Diluted Lipofectamine reagent 0.5x | Diluted Lipofectamine reagent 0.2x |
|------------------------|--|----------------------------------|------------------------------------|------------------------------------|
| Volume | 3.75 x 2 = 7.5 | 9 x 2.5 x 2 = 45 | 11.25 x 2 = 22.5 | 4.5 x 2 = 9 |
| OPTI-MEM medium | 750-7.5 = 742.5 | 750-45 = 705 | 750-22.5 = 727.5 | 750-9 = 741 |

Table 3. The amount of the Ubc9 siRNA, scrambled siRNA or the Lipofectamine reagent added in each preparation in T25 flask; the total diluted volume was 1500 μ l. 7.5 μ l siRNA in 750 μ l=1:100 dilution [0.2 μ M]; 7.5 μ l siRNA in 1500 μ l=1:200 dilution [0.1 μ M/100nM]

In Table 3, 7.5 μ l Ubc9 siRNA or scrambled siRNA was prepared. 9 μ l x 2.5 = 22.5 μ l of Lipofectamine reagent was used as 1x concentration according to the RNAiMAX transfection protocol online (converted from 6-well plate to T25 flask volume). For 0.5x diluted Lipofectamine concentration, 9 \div 2 x 2.5 = 11.25 μ l was calculated but 22.5 μ l was prepared

practically. Similarly, for 0.2x diluted Lipofectamine concentration, $9 \div 5 \times 2.5 \times 2 = 9 \mu\text{l}$ was prepared. The OPTI-MEM medium volume was calculated for each treatment accordingly. 1×10^5 cells were plated in each T25 flask. Ideally, the cells would be 60-70% confluent on the day of transfection. The cells were maintained in 4 ml normal DMEM media in the incubator 5% CO₂/95% v/v humid air at 37°C overnight.

In practice, initially, the diluted siRNA (750 μl) was mixed with diluted 1x Lipofectamine reagent (750 μl) as a total volume of 1500 μl ; this was left to stand for 5 minutes. After mixing, the siRNA concentration was 100 nM. For the final siRNA 25 nM concentration (1:4), 1.125 ml of the mixed total siRNA [100 nM] was mixed with 3.375 ml of the normal media as a total volume of 4.5 ml, which was 25 nM. Therefore, the cells were washed with PBS once and replaced with 3.375 ml fresh media (3 ml using the sterile pipette, 0.375 ml using the sterile tips); then 1.125 ml of the diluted siRNA or scrambled siRNA was added in each T25 flask accordingly. This was set up as 24hr vs. 48hr transfection experiment. Practically, adjusted methods were also used with lower concentrations of the Lipofectamine reagent as 0.5x or 0.2x, where the Ubc9 siRNA / scrambled siRNA / 0.5x vs. 0.2x Lipofectamine was combined as 4x volume in 15 ml falcon tube. See the calculations in Table 4:

| 20 μM siRNA stock | F Tube 1- Diluted siRNA [0.2 μM] (μl) | F Tube 2- Diluted scrambled siRNA [0.2 μM] (μl) | F Tube 3- Diluted Lipofectamine reagent 0.5x (μl) | F Tube 4- Diluted Lipofectamine reagent 0.2x (μl) |
|--|--|--|--|--|
| Volume | $7.5 \times 4 = 30$ | $7.5 \times 4 = 30$ | $22.5 \times 4 = 90$ | $9 \times 4 = 36$ |
| OPTI-MEM medium | $742.5 \times 4 = 2970$ | $742.5 \times 4 = 2970$ | $727.5 \times 4 = 2910$ | $741 \times 4 = 2964$ |
| Total siRNA/Lipofectamine + OPTI-MEM medium volume | 3000 Add 750 to mix (divided 4) | 3000 Add 750 to mix (divided 4) | 3000 Add 750 to mix (divided 4) | 3000 Add 750 to mix (divided 4) |

Table 4. The calculation for each volume used in the treatment

The diluted Ubc9 siRNA, diluted scrambled siRNA, 0.5x and 0.2x Lipofectamine reagent were prepared and left in the culture hood. Meanwhile, the cells were checked at 60-70% confluent. The media in all the flasks was aspirated off. Initially, 3.375 ml fresh media was added to each flask. The diluted Ubc9 siRNA or the scrambled siRNA was mixed with the diluted Lipofectamine quickly. Each Ubc9 siRNA / scrambled siRNA mixture was set as 24hr or 48hr, i.e. 0.5x Lipofectamine 24hr vs. 48hr or 0.2x Lipofectamine 24hr vs. 48hr. 750 μl siRNA or Lipofectamine was added in each eppendorf tube and all the mixed tubes were incubated for 5 minutes in the hood. 1.125 ml of the prepared mixed diluted siRNA/scrambled siRNA + the diluted Lipofectamine (0.5x or 0.2x) was added to each

labelled T25 flask. In the negative control flasks, 1.125 ml of the OPTI-MEM media was added to each flask. One of the flasks was set as Lipofectamine (LIPO) alone negative control. After this, whole cell lysates were made, which were ready for western blotting.

For the siRNA treatment in 6-well plate, the calculations were stated in Table 5:

| 20 μ M siRNA stock | Diluted siRNA/scrambled [0.2 μ M] | Diluted Lipofectamine reagent 0.5x | Diluted Lipofectamine reagent 0.2x |
|------------------------|---------------------------------------|------------------------------------|------------------------------------|
| Volume | $1.5 \times 2 = 3$ | $4.5 \times 2 = 9$ | $1.8 \times 2 = 3.6$ |
| OPTI-MEM medium | 297 | 291 | 296.4 |

Table 5. The amount of siRNA or the Lipofectamine added in each preparation in 6-well plate. Total diluted volume=600 μ l. 3 μ l siRNA in 600 μ l: 1:200 dilution = [0.1 μ M]; from 0.1 μ M: 100nM \rightarrow 25 nM: 1:4 dilution

In Table 5, 3 μ l (10 μ M) siRNA was used according to the company's online protocol for 6-well plates. 20 μ M stock siRNA was prepared previously. 1.5 μ l was used. Practically, doubled amount was taken (x2, Table 5); similarly for the OPTI-MEM medium as doubled amount of 150 μ l was taken. 9 μ l of Lipofectamine was taken in the 6-well plate as 1x concentration. For doubled amount, 9 μ l for 0.5x Lipofectamine or 3.6 μ l for 0.2x Lipofectamine was used.

The MDA-MB-231 cells were grown on coated coverslips in a 6-well plate overnight. The cells were checked for confluence between 60-70% confluent prior to treatment. Once prepared, the diluted siRNA and Lipofectamine mixtures were incubated for 5 minutes. 2 ml total volume was added to each well. For the final 25 nM diluted siRNA concentration, 0.5 ml mixed total siRNA [100 nM] was added with 1.5 ml fresh medium [25 nM]. After 48hr treatment, the cells were immuno-fixed with the talin-1 antibody.

For the IHC, cell migration and the western blotting experiments in the MDA-MB-231 cells, the siRNA mixture concentrations were adjusted as 1x, 0.5x or 0.2x, finally, 0.2x LIPO was used to prevent off-targeted effects of the siRNA.

2.13 Quantitative Data Analysis: Image J

Image J (1.48v) was used to count the time period of focal adhesion turnover (second). In the 2s, 8s or the 10s timelapse movies, each frame selected with Image J represented one 2s, 8s or 10s interval. In each frame, several focal adhesions were followed through the time period of the movie. The time was noted for one focal adhesion to appear and disappear, i.e. the visualization of the timelapse movie with the 'appearing second' frame and 'disappearing second' frame was based on the FA turnover lifetime. This was done for all the movies to calculate the mean turnover time of a focal adhesion, i.e. GFP-talin, GFP-FAK or GFP-vinculin.

Image J was used to calculate the mean area and size of a focal adhesion in these timelapse movies. Each image threshold was adjusted first from the 'image' button. The upper and lower bar values for the threshold measure were noted and adapted for each image. This was to ensure only focal adhesion 'dots' were selected with a red colour background (within the threshold tail). The image would be black and white once the settings were made. All the FAs 'dots' would be made as areas of 'white colour'. The image was made 'binary' in the 'process' button. This would reverse the FAs colour to 'black' and the background to 'white'. The image was selected from the 'process' with 'binary' to make it 'watershed', where the 'black' colour of FAs area would be drawn boundaries according to the 'original' timelapse image. Then the image was ready to analyse 'particles' from the 'analyze' button. The size of the particle was set at 20 μm – Infinity (pixel units ticked) for the image. Each 'particle' was counted as 'ellipses' shape. The FAs would be processed as 'ellipse shaped' only in the image. The mean number (count) and average size (μm^2) were displayed as 'Summary' results.

Image J was used to measure the mean number or size in the IHC z-stack images. The z-stack image was moved to the level until all the FAs appeared. The image was made 8-bit. The image was adjusted with the 'image' threshold button until only the FAs were seen with the background colour set as 'red'. Then the changes made were 'applied'. The background colour changed to black. The image was made 'binary' from the 'process' button and the background changed to 'white' leaving the 'FAs' set as 'black'. In this step, all the FAs could be measured as a mean total number or mean size. However, in the later IHC experiments, most of the experiments were measured as each 1 single cell manually selected around the cell boundary and the mean FAs number or size were calculated according to 'per cell'. The measurement was chosen from the 'analyze' 'particles'. The pixel unit was ticked and the circularity was set as 0.00-1.00. The FAs shape was set as 'ellipses'.

Image J was used to analyse the speed and the directionality of cell migration using the plugins with the MTrackJ selected. Up to 300 cells were tracked in the non-treated and the treated wells. For 1 new cell movement, the tracking orbit of the cell would be noted as a 'new colour' and once the tracking was finished, each tracking 'colour' would be saved. The results were included as the total length of the cell (μm), the distance for a cell to move from the previous point (D2P) and the D2S (distance to start) which were recorded. The equation was used as:

$$\text{Speed} = \frac{\text{Total cumulative length a cell migrated (to pixel)} / \mu\text{m}}{\text{Total time (hr)}}$$

$$\text{Directionality} = \frac{\text{D2S}}{\text{Total cumulative cell migration length}}$$

Image J was also used to measure the gel band area from western blotting experiments. The gel image was selected using 'analyse' 'gels'. The image was made 32-bit type and a rectangle box was used to draw around the bands of interests. This would give a number '1' in the rectangle box. Then the gels were 'plotted lanes' from the rectangle box drawn. 'A straight line' button was selected to draw the vertical line on each band 'peak' generated down at where the peak tail ended, separating between each band 'peak'. A 'wand tracking tool' was used to select on the separated band 'peak'; each peak area underneath selected would give the band area in the summary table. These data were stored in Excel and each FAs band area i.e. talin was calculated against GAPDH band area as a ratio.

2.14 Statistics

Excel has been used to store the 'summary' data sheets from Image J. Graphpad prism has been used to obtain the graphs and the data was presented as mean \pm SEM. One-way ANOVA with a post Tukey test or two-tailed unpaired student's t-test have been performed for any data significant differences ($p < 0.05$).

Chapter 3 - SUMOylation Plays an Important Role in the Dynamics and Turnover Rate of Focal Adhesions and Cell Migration

3. 1 Introduction and Hypothesis

SUMOylation has been extensively studied in nuclear functions including nuclear body organization, transcriptional regulation, pre-mRNA splicing, chromatin remodelling, cell cycle control, genome maintenance stability etc, but much less is known about its roles outside of the nucleus (Hendriks and Vertegaal, 2016).

Four distinct ways of membrane extensions at the leading edge have been elucidated in cell migration namely as lamellipodia and filopodia, these are involved with the actin polymerization directly pushing the plasma membrane forward; invadopodia, the actin polymerization couples with the ECM-degrading metalloproteases to facilitate cell migration through a clear path; and membrane blebs, these are involved with the actomyosin contractility of the membrane and the reversible detachment of the membrane from the cortical actin cytoskeleton (Ridley, 2011). The highly dynamic lamellipodia has been integrated with a second co-localized structure behind, known as the lamella, where it is coupled with actomyosin contraction and substrate adhesion contributing to protrusion and cell migration (Ponti et al., 2004). The lamellipodia and lamella are very distinct: the lamellipodia has high concentration of Arp 2/3 and ADF / cofilin whereas the lamella has a high levels of myosin II and tropomyosin (Ponti et al., 2004). Collective cell movement requires adhesive cell-cell contacts, front-rear asymmetry with ruffling / lamellipodial structure at the cell leading edge and the trailing edge of the cell (Hegerfeldt et al., 2002). Molecular mechanisms controlling collective cell migration and mesenchymal migration involve the cell-substrate interactions, cell-cell interactions, matrix-degrading enzymes (matrix metalloproteinases and serine proteases), $\beta 1$ integrin-mediated adhesion dynamics, the structure of the actin cytoskeleton producing tracking forces, cell-cell adhesion molecules such as cadherin etc and signalling towards the cytoskeleton (Rho GTPases) (Friedl et al., 2004, Friedl, 2004). As previously mentioned, the EMT type of cell migration represents an important development of cell movement in tumour invasiveness and metastasis (Kalluri and Weinberg, 2009). In most types of mesenchymal and collective cell migration, integrin $\beta 1/\beta 3$ -mediated adhesions are involved in focal contacts, e.g. MDA-MB-231 breast cancer cells are spindle-shaped cells which use integrins and proteases for adhesion and matrix remodelling, respectively (Friedl, 2004). In most studies, 2D glass coverslip, 2D fibronectin or gelatin coated surfaces or 3D collagen matrix lattice have been widely used to study cell migration

and these techniques are used for the determination of focal adhesions (FAs) number and size in cell migration.

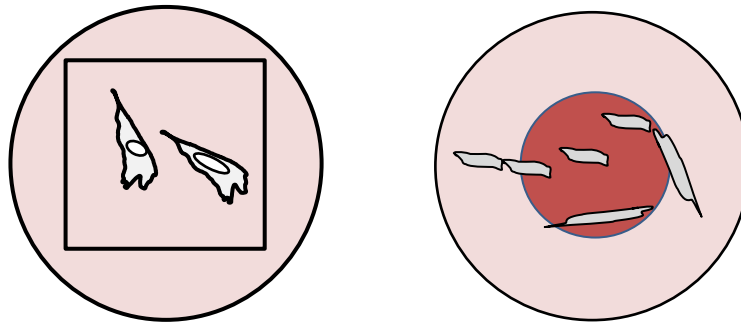


Figure 13. Showing the 2D glass coverslip in a 6-well plate and 2.5D collagen ECM environment set up in a glass bottom ibidi dish. The cells were either placed on top of the glass coverslip or placed at the edge of the collagen or on top (red colour) for them to grow, which has been used in this study to determine the FA dynamics

Figure 13 shows the 2D glass coverslip as the standard method used to detect FA dynamics in cells which have been previously grown on coverslips. The FA expression in these cells plated on coated glass coverslips is different to the cells grown on 2.5D collagen surface. The red ring of collagen has been plated in the centre of a glass bottom dish. The cells were plated and grown either on the glass surface, lined up on the interface of the collagen or on the top surface of the collagen. SUMOylation inhibitors have been used to treat the cells grown in these two environments in order to investigate the effects of the regulatory role of SUMOylation on the FA dynamics and cancer cell migration.

In the two cell lines used, the MDA-MB-231 cell line expresses high level of integrin subunits $\alpha 2$, $\alpha 3$, αv , $\beta 1$, $\alpha 5\beta 1$ and $\alpha v\beta 3$ (Mierke et al., 2011, Morini et al., 2000, Taherian et al., 2011) and the osteosarcoma U2OS cell line expresses $\beta 1$ and $\alpha v\beta 3$, which are directly correlated with the metastatic potential of osteosarcoma (Nguyen et al., 2016, Levinson et al., 2002). Integrins are α/β heterodimeric transmembrane glycoprotein receptors that respond to FA assembly and ECM components signalling i.e. laminin, vitronectin, fibrinogen, fibronectin ($\alpha 5\beta 1$) and collagen I (Pankov et al., 2000, Petit and Thiery, 2000). There are three major groups of proteins which associate with the β integrin cytoplasmic domains: the proteins involved in FA assembly are talin, vinculin, α -actinin, filamin etc, which interact with the intracellular domains of integrin $\beta 1$ and $\beta 3$ and participate in FA assembly (Martel et al., 2000, Petit and Thiery, 2000, Brakebusch and Fässler, 2003). The scaffolding adaptors e.g. kindlin, paxillin and catalytic adaptors e.g. Src, ERK, FAK are also regulatory proteins which associate with the integrin β cytoplasmic tails (Legate and Fässler, 2009). Of these, proteins involved in integrin-FA assembly such as the catalytic adaptor, FAK can be SUMOylated and

the role of SUMOylation in the dynamics and turnover rate of talin, vinculin and FAK is investigated, which are important in cancer cell migration and metastasis.

Hypothesis

Focal adhesion proteins including FAK, talin and vinculin have been the main focus in this study. FAK has been shown to be SUMOylated; this has led to the study of SUMOylation of other FA proteins. Therefore, talin, vinculin and FAK containing FAs have been studied. The hypothesis of this study was that SUMOylation plays a critical role in cancer cell migration. Focal adhesions are known to facilitate cancer cell migration.

In this study, an invasive and metastatic basal-like ER negative breast cancer cell line (carcinoma) MDA-MB-231 was used. The typical MDA-MB-231 cell consists of a lamellipodia structure at its leading edge and is known to form focal adhesions. In this study, this cell line was used initially to study their FA dynamics and the effects of SUMOylation on the FAs in cell migration.

U2OS is a human osteosarcoma cell line, which was used to determine and confirm the effects of the inhibition of SUMOylated FAs in the MDA-MB-231 cells, since the quantitative proteome of this U2OS cell line was studied and the data on the SUMOylation-related proteins were previously shown (Beck et al., 2011b).

Various inhibitors including GA, gossypetin, 2-D08 and the Ubc9 siRNA have been used in MDA-MB-231 cells and U2OS cells to study the effects of inhibition of SUMOylation on the dynamic activities of FAs (i.e. FA number, size and turnover) as altered FA dynamics resulting from the inhibition of SUMOylation could have a big impact on cell migration.

3. 2 Blocking SUMOylation with Ginkgolic Acid Leads to Increased Number of Talin Containing FAs

MDA-MB-231 cells were grown on 0.2% gelatin-coated glass coverslips overnight and the cells were treated with 100 μ M ginkgolic acid at different time intervals. Talin-1 antibody was used in the immunostaining experiments for visualizing the talin containing FAs. The mean talin containing FAs number or size were quantified using Image J. One-way ANOVA with post-hoc Tukey test was performed to analyse the differences between the untreated control and GA treatment at 15, 30 or 60 minutes.

In Figure 14, the cells expressed talin-containing FAs in the representative untreated control panel vs. GA 100 μ M at 15, 30 or 60 minutes panel. The effects of 100 μ M GA on the mean talin containing FAs number or size were summarised in Figure 15.

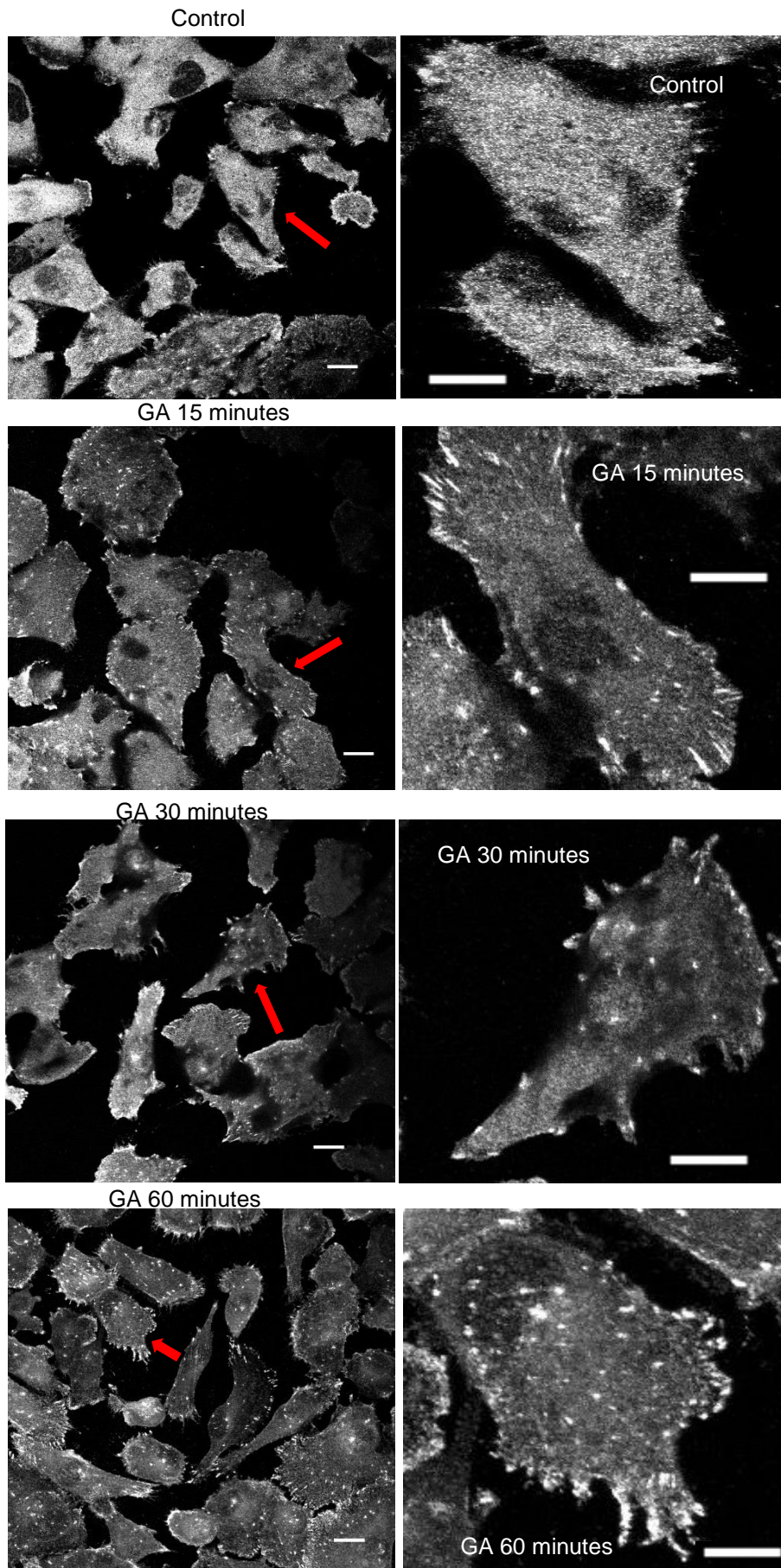
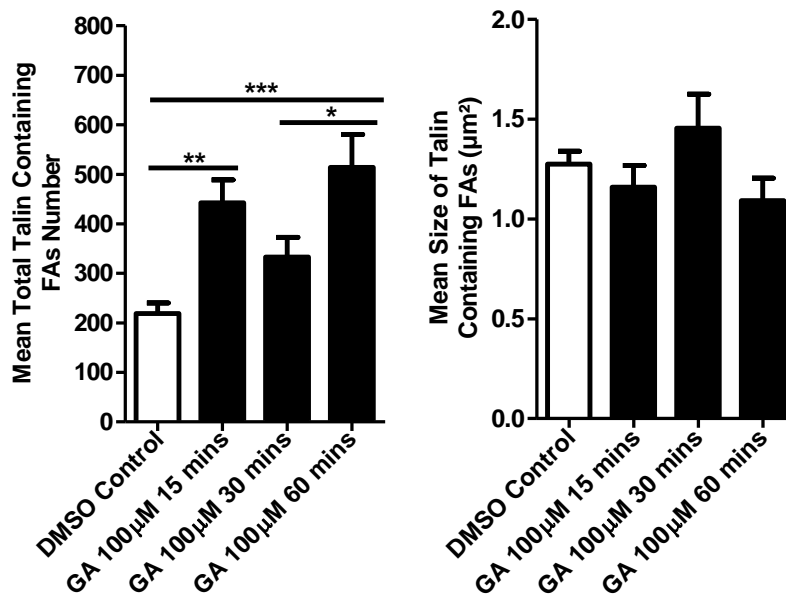


Figure 14. Immunostaining of talin containing FAs in MDA-MB-231 cells for untreated cells in the control vs. 100 μ M GA treatment at 15, 30 or 60 minutes (n=3, representative images of the talin containing FAs in the control vs. GA treated samples. In each control vs. GA treated sample, the red arrow pointing a single cell was zoomed in and presented on the right image showing the expression of talin containing FAs in the cell. Left images scale bar: 20 μ m (right images: zoomed in, Plan Apo λ 100x Oil Lens with 0.2 μ m/pixel)



| Talin n=3 | Mean ± SE Number | Mean ± SE Size µm ² | Number of cells counted |
|------------|------------------|--------------------------------|-------------------------|
| Control | 218.9 ± 21.1 | 1.28 ± 0.065 | 277 |
| GA 15 mins | 442.6 ± 46.0 | 1.16 ± 0.110 | 178 |
| GA 30 mins | 333.2 ± 39.4 | 1.46 ± 0.171 | 201 |
| GA 60 mins | 514.0 ± 66.7 | 1.09 ± 0.113 | 251 |

Figure 15. The mean talin containing FAs number or size measurements in MDA-MB-231 cells analysed from the immunostaining images as a total number of 3 combined experiments for the untreated cells in the control vs. 100µM GA treatment at 15, 30 or 60 minutes (data was presented as mean ± SEM, $p < 0.0001$ ***, $n = 3$, individual replicates)

In Figure 15, the number of the talin containing FAs was counted. The mean total talin containing FAs number was significantly increased from 219 ± 21 for the untreated cells to 443 ± 46 for the 100µM GA 15 minutes treated cells (**). Compared with the control, GA 100µM at 60 minutes treatment significantly increased the mean total talin containing FAs number from 219 ± 21 to 514 ± 67 ($p < 0.0001$ ***).

GA 100µM treatment at 15, 30 or 60 minutes did not cause any effects in the mean talin containing FAs size compared with the untreated control in the cells.

3. 3 Inhibition of SUMOylation with GA in MDA-MB-231 Cells Grown on the Top of 2mg/ml Collagen Causes Increased Number, Size and Turnover of Focal Adhesions

The 2.5D ECM model for studying the turnover of FAs was set up using the 2mg/ml rat-tail collagen I, where MDA-MB-231 cells were seeded around the set patch of the collagen rings and grown on the top of the collagen or at the collagen interphase overnight. The seeded cells were previously transfected with GFP-FA plasmids, including GFP-talin, GFP-vinculin or GFP-FAK for 8 hours before seeding. These cells were grown in the 2.5D ECM environment and then treated with 100 μ M GA for 2 hours. High magnification confocal live-cell imaging timelapse movies were then taken for 5 or 10 minutes period with intervals of every 2s, 8s or 10s; some frame images were selected shortly from a 10s-interval/5 minutes FAs turning over timelapse movie and shown in Figure 16. This was to illustrate the fast dynamic turning over of the talin containing FAs. This model was used to study the effects of 100 μ M GA treatment after 2hrs on the FA number, size or turnover time.

Various time interval timelapse movies were conducted as 2s, 8s or 10s-interval movies; the turnover time of each FA was analyzed manually. The mean turnover time of each GFP-FA type was analysed by combining a total number of 5 experiments in the GFP-talin turnover experiments, 6 for the GFP-FAK turnover experiments or 4 for the GFP-vinculin turnover experiments. The turnover time unit was represented in second.

The mean FA number or size was measured using the Image J particles function and an unpaired student's t-test was conducted to analyse the differences before and after GA treatment in the mean number, size and turnover time of the talin, FAK or vinculin containing FAs.

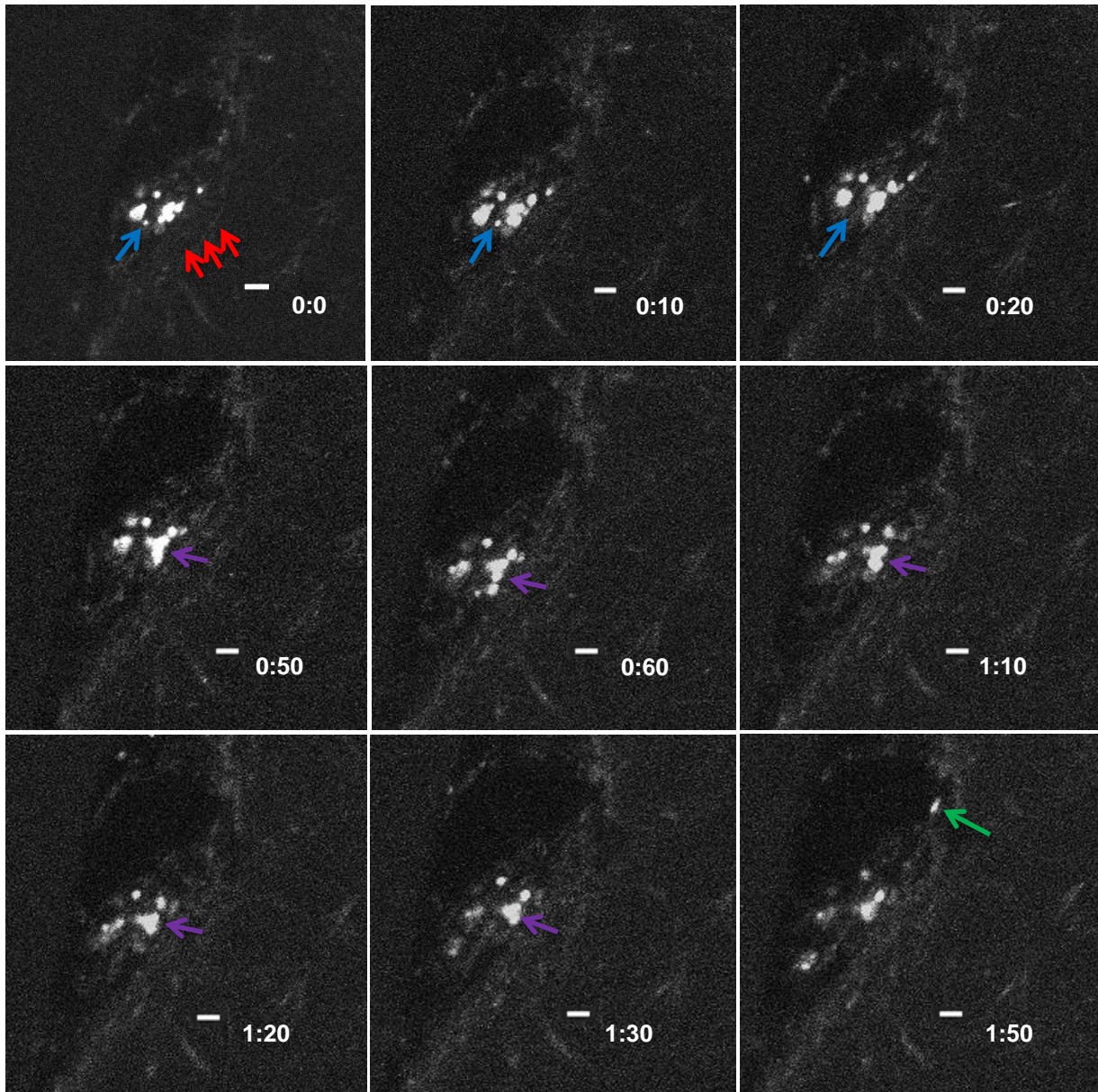
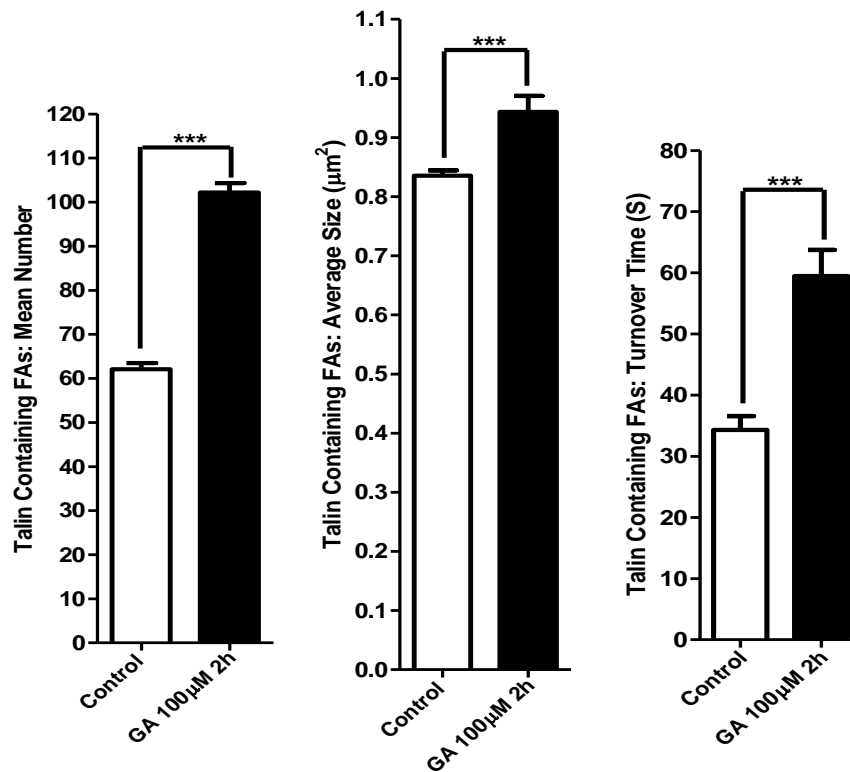


Figure 16. These images were taken from a 5-minute timelapse movie selectively and made black and white by Image J. GFP-talin plasmid transfection in the MDA-MB-231 cells in the untreated control cell showing the dynamic turnover of the talin containing FAs in a ‘appearing’ and disappearing’ fashion during a live-cell imaging timelapse experiment. The three red arrows in the first image showing: the cells were seeded on the top of the collagen mesh; the talin containing FAs in this one particular cell were turning over in seconds: the blue arrow in 10-20s images: the duration turnover time of this one talin containing FA was turning over in 10s, where it was appearing at 0s, continuing to be present for 10s and disappearing at 20s, indicating that the turnover time for this particular talin containing FA was 10s; the green arrow in the 1 min:50s image: this one talin containing FA just appeared at 110s, indicating that it only appeared at this particular time and new talin containing FA formation was continuously taking place; the purple arrow from 50s to 1 min:30s: these talin containing FAs seemed to split and fuse joining closer to each other throughout this time period (scale bar = 10 μ m).

In Figure 16, in the first panel, one talin containing FA appeared at 10s and disappeared at 20s (blue arrow) indicating the duration turning over time of this one particular talin containing FA was 10s. Some other talin containing FAs appeared at different time frames e.g. in the last image at 1 min: 50s, this particular talin containing FA appeared at the cell front edge pointing upwards. Talin containing FAs may also split or fuse closer together at different time frames during the timelapse experiment. In this way, this model was capable of visualizing dynamic FAs expressed by the GFP FA plasmids during the collagen set-up. The MDA-MB-231 cells were then treated with 100 μ M GA for 2 hours in this 2.5D ECM environment.

3. 3. 1. GA Treatment Increases the Mean Talin Containing FAs Number, Size and Turnover Time

The mean number, size and turnover time of talin containing FAs was measured using Image J. Two tailed unpaired t-tests showed significant differences before and after GA 100 μ M 2h treatment; where the mean number of talin containing FAs was increased significantly, the mean size of talin containing FAs was increased significantly and the mean turnover time of talin containing FAs was increased significantly.



| Talin (n=5, p<0.0001***) | Mean \pm SE FA Number | Mean \pm SE Size (μm^2) | Mean \pm SE Turnover time (s) | Adhesion number counted |
|--------------------------|-------------------------|--|---------------------------------|-------------------------|
| Talin: Control | 62.1 \pm 1.41 | 0.835 \pm 0.009 | 34.3 \pm 2.29 | 280 |
| Talin: GA 100 μ M 2h | 102 \pm 2.11 | 0.944 \pm 0.027 | 59.5 \pm 4.24 | 182 |

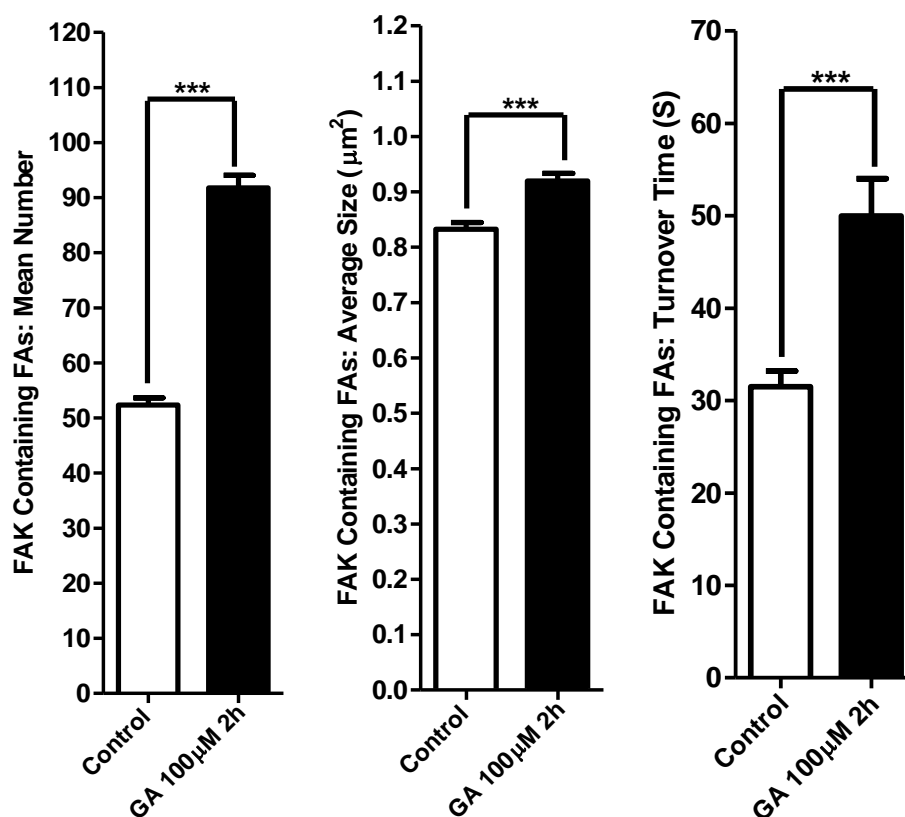
Figure 17. Showing the mean number, size and turnover time of talin containing FAs measurements between the control untreated MDA-MB-231 cells and the 100 μ M GA 2hrs treated cells from the GFP-talin transfection live-cell imaging timelapse movies (n=5, individual replicates, data was presented as mean \pm SEM, p<0.0001***).

In Figure 17, in the GFP-talin turnover assay, the mean number, size or turnover time of the talin containing FAs was increased significantly after 100 μ M GA 2 hours treatment compared with the control. The mean talin containing FAs number was increased significantly from 62 \pm 1 to 102 \pm 2 (p<0.0001 ***); the mean talin containing FAs size was increased significantly from 0.835 \pm 0.009 μm^2 to 0.944 \pm 0.027 μm^2 (p<0.0001 ***); also, the

mean talin containing FAs turnover time was increased significantly from 34.3 ± 2.29 s to 59.5 ± 4.24 s ($p < 0.0001$ ***).

3. 3. 2. GA Treatment Increases the Mean FAK Containing FAs Number, Size and Turnover Time

The mean number, size or turnover time of FAK containing FAs was measured using Image J. Two tailed unpaired t-tests showed significant differences before and after GA 100 μ M 2h treatment; where the mean number of FAK containing FAs was increased significantly, the mean size of FAK containing FAs was increased significantly and the mean turnover time of FAK containing FAs was increased significantly.



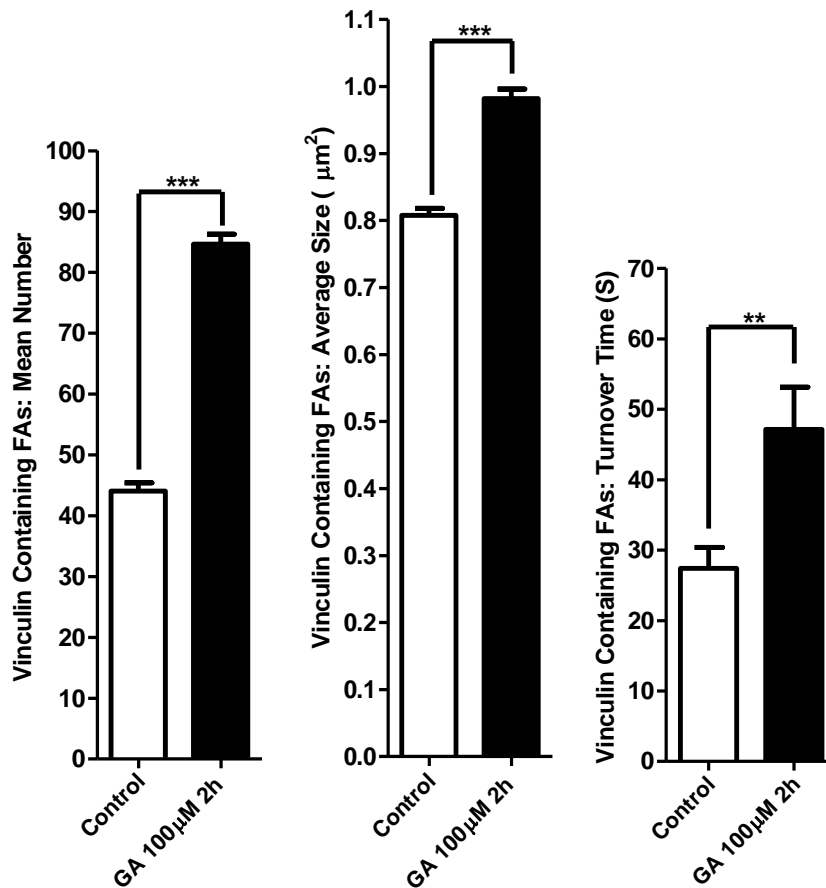
| FAK (n=6, p<0.0001***) | Mean \pm SE FA Number | Mean \pm SE Size (μm^2) | Mean \pm SE Turnover time (s) | Adhesion number counted |
|------------------------|----------------------------|---|---------------------------------------|-------------------------------|
| FAK: Control | 52.4 \pm 1.29 | 0.833 \pm 0.012 | 31.5 \pm 1.70 | 342 |
| FAK: GA 100 μ M 2h | 91.8 \pm 2.31 | 0.920 \pm 0.014 | 50.0 \pm 4.03 | 163 |

Figure 18. Showing the mean number, size and turnover of FAK containing FAs measurements between the control untreated MDA-MB231 cells and the 100 μ M GA 2hrs treated cells from the GFP-FAK transfection live-cell imaging timelapse movies (n=6, individual replicates, data was presented as mean \pm SEM, $p < 0.0001$ ***).

In Figure 18, in the GFP-FAK turnover assay, the mean number, size or turnover time of the FAK containing FAs was increased significantly after 100 μ M GA 2 hours treatment compared with the control. The mean FAK containing FAs number was increased significantly from 52 ± 1 to 92 ± 2 ($p < 0.0001$ ***); the mean FAK containing FAs size was increased significantly from $0.833 \pm 0.012 \mu\text{m}^2$ to $0.920 \pm 0.014 \mu\text{m}^2$ ($p < 0.0001$ ***); also, the mean FAK containing FAs turnover time was increased significantly from 31.5 ± 1.70 s to 50.0 ± 4.03 s ($p < 0.0001$ ***).

3. 3. 3. GA Treatment Increases the Mean Vinculin Containing FAs Number, Size and Turnover Time

The mean number, size or turnover time of vinculin containing FAs was measured using Image J. Two tailed unpaired t-tests revealed significant differences before and after GA 100 μ M 2h treatment; where the mean number of vinculin containing FAs was increased significantly, the mean size of vinculin containing FAs was increased significantly and the mean turnover time of vinculin containing FAs was increased significantly.



| Vinculin (n=4, p<0.0001***, turnover time p=0.0014) | Mean \pm SE FA Number | Mean \pm SE Size μm^2 | Mean \pm SE Turnover time (s) | Adhesion number counted |
|---|-------------------------|------------------------------------|---------------------------------|-------------------------|
| Vinculin: Control | 44.0 \pm 1.38 | 0.808 \pm 0.011 | 27.4 \pm 3.00 | 128 |
| Vinculin: GA 100 μ M 2h | 84.7 \pm 1.62 | 0.982 \pm 0.014 | 47.2 \pm 6.00 | 83 |

Figure 19. Showing the mean number, size and turnover of vinculin containing FAs measurements between the control untreated MDA-MB-231 cells and the 100 μ M GA 2hrs treated cells from the GFP-vinculin transfection live-cell imaging timelapse movies (n=4, individual replicates, data was presented as mean \pm SEM, p < 0.0001***, vinculin turnover time p=0.0014**).

In Figure 19, in the GFP-vinculin turnover assay, the mean number, size or turnover time of the vinculin containing FAs was increased significantly after 100 μ M GA 2 hours treatment compared with the control. The mean vinculin containing FAs number was increased significantly from 44 ± 1 to 85 ± 2 ($p < 0.0001$ ***); the mean vinculin containing FAs size was increased significantly from $0.808 \pm 0.011 \mu\text{m}^2$ to $0.982 \pm 0.014 \mu\text{m}^2$ ($p < 0.0001$ ***); also, the mean vinculin containing FAs turnover time was increased significantly from 27.4 ± 3.00 s to 47.2 ± 6.00 s ($p = 0.0014$ **).

The mean number, size or turnover time were increased significantly in all the three GFP-tagged FAs after 100 μ M GA 2hrs treatment compared to the control, which could predict slower cell migration. To determine if inhibiting SUMOylation could lead to changes in cell migration speed and total cell movement length, 24 hours timelapse experiment was conducted where single cell movement was tracked using MTrack J in Image J.

3. 4 GA at 25, 50 or 100 μ M Leads to Decreased Speed of Cell Migration and Reduced Total Cell Migration Length

To determine the effects of GA on cell migration, phase-contrast timelapse was performed. The MDA-MB-231 cells were seeded in 2mg/ml rat-tail collagen I and grown overnight prior to GA treatments. The next day, at time point 0, the cells were treated with GA at 25, 50 or 100 μ M in the triplicate wells/12-well plate for each treatment. The cells in the control wells were treated with 0.1% DMSO in DMEM media. The cells were then followed for a period of 18-24hrs on the timelapse microscope with 10x lens used for cell migration.

The tracking of each cell was shown in Figure 20. Each cell was denoted with a coloured number and manual tracking starts from time 0 until the last time interval of the movie finishes. The speed of cell migration, total length of each cell travelled and the directionality could be analysed using MTrackJ.

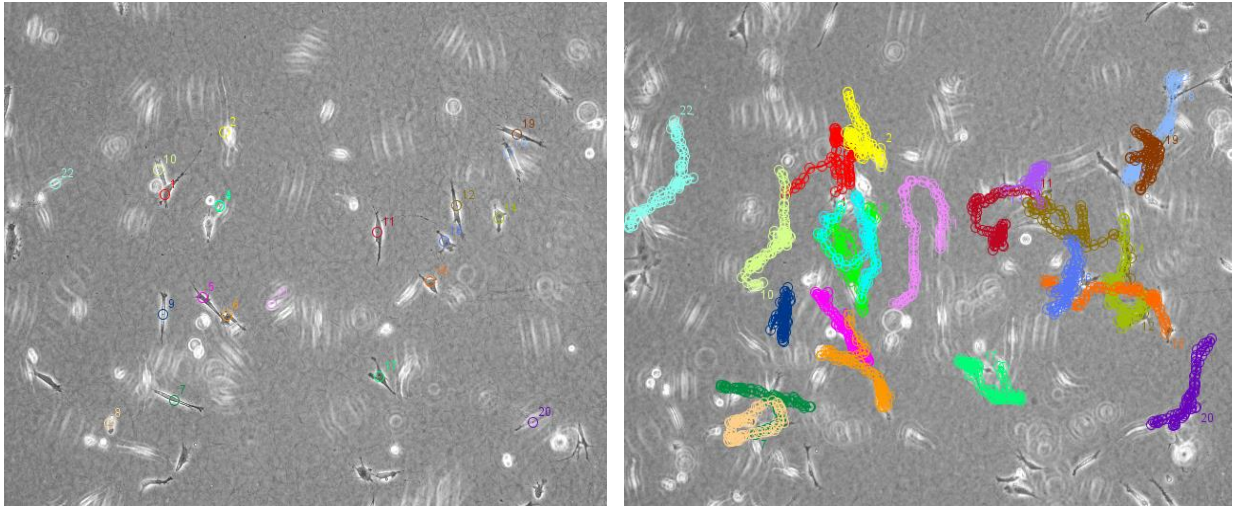
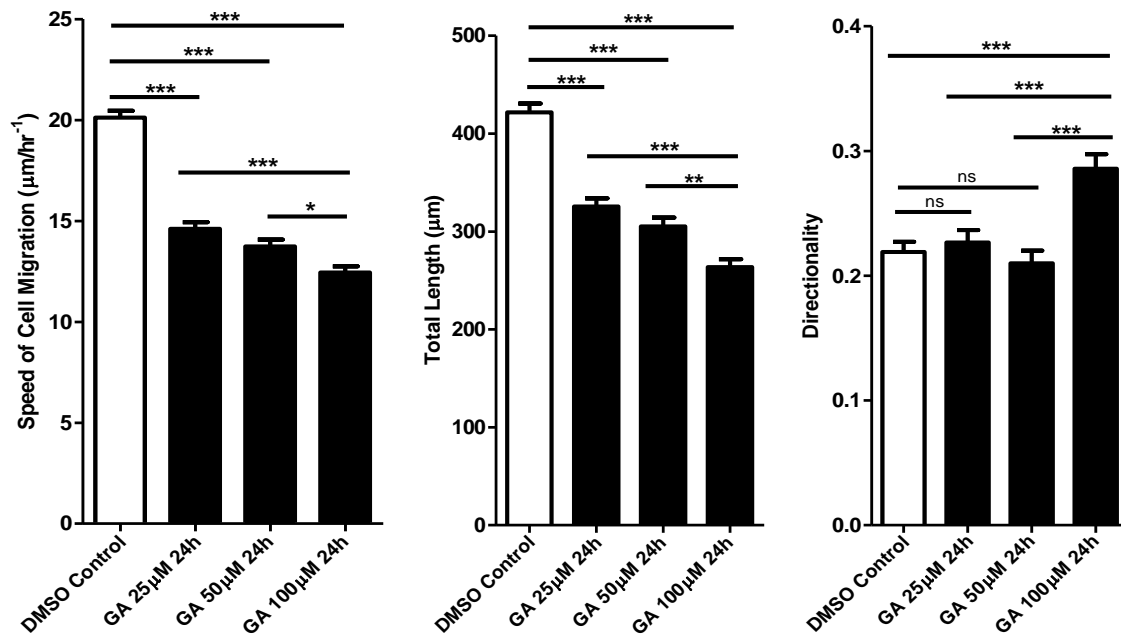


Figure 20. Manual tracking of each cell in a control experiment using MDA-MB-231 cells, representative images were shown. Single cell was denoted with a coloured number and the tracking was finished till the movie finished. The path of each cell travelled from start to end and the total travel distance could be recorded using MTrackJ.



| 24h, n=3 | Mean \pm SE Speed ($\mu\text{m/hr}^{-1}$) | Mean \pm SE Total Length (μm) | Mean \pm SE Directionality | Cell tracking number |
|----------------------|---|--|------------------------------|----------------------|
| Control | 20.1 \pm 0.341 | 421.7 \pm 9.14 | 0.219 \pm 0.008 | 361 |
| GA 25 μM | 14.6 \pm 0.330 | 325.5 \pm 8.50 | 0.227 \pm 0.010 | 255 |
| GA 50 μM | 13.7 \pm 0.337 | 305.2 \pm 9.10 | 0.210 \pm 0.010 | 248 |
| GA 100 μM | 12.4 \pm 0.306 | 263.7 \pm 8.06 | 0.286 \pm 0.012 | 273 |

Figure 21. Showing the mean speed of cell migration, the mean total cell migration length and the mean directionality measurements from the timelapse experiments; GA at 25, 50 or 100 μM after 24hr period reduced the mean speed of cell migration and the mean total migration distance significantly compared with the control in the MDA-MB-231 cells; GA at 100 μM only increased the directionality in the MDA-MB-231 cells (n=3, individual replicates, data was presented as mean \pm SEM, $p < 0.0001$ ***).

In the 24 hours timelapse experiment, single cells were tracked shown in Figure 20. Each time interval was 20 minutes for a period of 24 hours. The speed of cell migration was represented as the total cell migration length divided by the time of experiment, shown in $\mu\text{m} / \text{hr}^{-1}$. The directionality was represented as the 'distance to start (D2S)' divided by the total cell migration length (D2S / μm). The results were summarised as a total number of 3 combined experiments in Figure 21.

In Figure 21, after 24hrs cell tracking, compared with the control, the mean speed of cell migration was decreased significantly after 25 μM GA treatment from $20.1 \pm 0.341 \mu\text{m}/\text{hr}^{-1}$ to $14.6 \pm 0.330 \mu\text{m}/\text{hr}^{-1}$ ($p < 0.0001$ ***). Similarly, the mean speed of cell migration was decreased significantly after 50 μM GA treatment from $20.1 \pm 0.341 \mu\text{m}/\text{hr}^{-1}$ to $13.7 \pm 0.337 \mu\text{m}/\text{hr}^{-1}$ ($p < 0.0001$ ***); the mean speed of cell migration was decreased significantly after 100 μM GA treatment from $20.1 \pm 0.341 \mu\text{m}/\text{hr}^{-1}$ to $12.4 \pm 0.306 \mu\text{m}/\text{hr}^{-1}$ ($p < 0.0001$ ***).

Similarly, compared with the control, the mean total cell migration length was decreased significantly after 25 μM GA treatment from $421.7 \pm 9.14 \mu\text{m}$ to $325.5 \pm 8.50 \mu\text{m}$ ($p < 0.0001$ ***); the mean total cell migration distance was decreased significantly after 50 μM GA treatment from $421.7 \pm 9.14 \mu\text{m}$ to $305.2 \pm 9.10 \mu\text{m}$ ($p < 0.0001$ ***); the mean total cell migration length was decreased significantly after 100 μM GA treatment from $421.7 \pm 9.14 \mu\text{m}$ to $263.7 \pm 8.06 \mu\text{m}$ ($p < 0.0001$ ***).

The mean directionality was only increased significantly after 100 μM GA treatment from 0.219 ± 0.008 to 0.286 ± 0.012 ($p < 0.0001$ ***). GA at 25 μM or 50 μM was not significant at increasing the mean cell movement directionality (ns). However, even in the control, 0.219 indicated random movement of the cells as the value was much smaller than 1; the more the value is close to 1 the cells would move along in a more straight and directed tracking line. Although GA at 100 μM caused a little bit more directional than random cell migration, 0.286 was not very close to 1, therefore directionality of the cells was not affected.

3. 5 Ubc9 siRNA Knockdown Reduces the Ubc9 Expression

MDA-MB-231 cells were transfected with the Ubc9 siRNA or the scrambled siRNA (prepared in 0.2x diluted Lipofectamine[®] RNAiMAX reagent, 25nM) for 48 hours. The results were summarised in Figure 21 as a total number of 4 combined experiments. In Figure 22, compared with the negative control, after 48 hours, the Ubc9 E2 enzyme expression was decreased significantly from $99.2 \pm 5.51\%$ (Ubc9/GAPDH ratio *100%) to $49.6 \pm 4.19\%$ ($p < 0.0001$ ***); also, compared with the scrambled siRNA, the Ubc9 expression was decreased significantly from $101.0 \pm 4.65\%$ to $49.6 \pm 4.19\%$ ($p < 0.0001$ ***); whereas the

scrambled siRNA control working as a control did not cause the knockdown effect in the Ubc9 expression. Therefore, Ubc9 siRNA transfection at this transfection concentration was used in the IHC and western blotting experiments to determine the mean number, size and the half-life of the FAs. GAPDH was not found to have any amino acid motifs that could be SUMOylated, therefore, it was chosen as the control for the Ubc9 siRNA experiment.

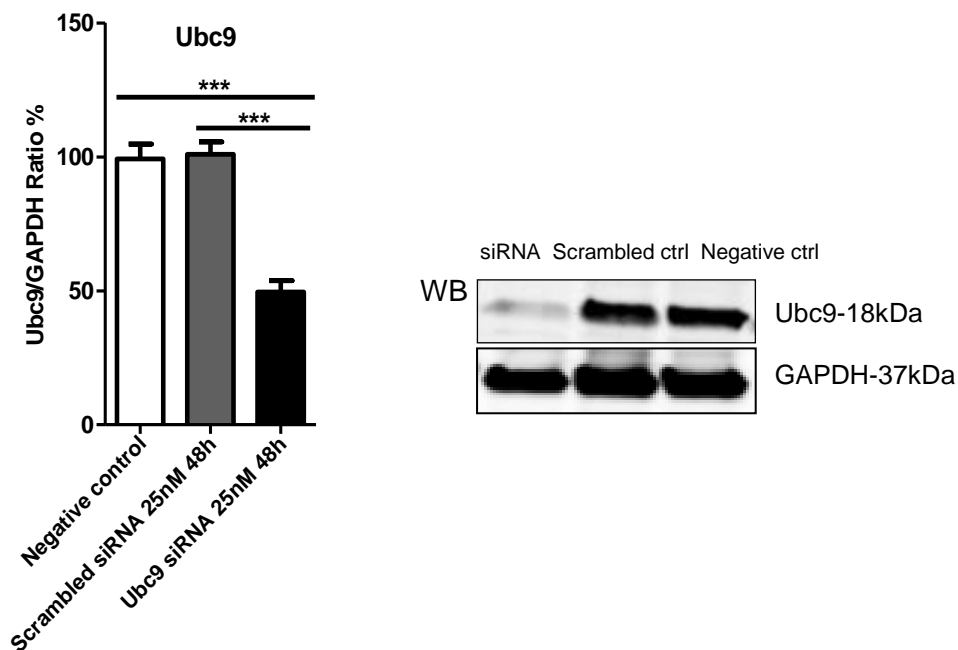


Figure 22. Ubc9 siRNA and scrambled siRNA treatments for 48hrs (25nM final concentration); Ubc9 siRNA treatment in the MDA-MB-231 cells caused knockdown of Ubc9 E2 enzyme, the bar chart was presented as Ubc9 vs. GAPDH ratio (n=4, data was presented as mean \pm SEM, $p < 0.0001$ ***).

The concentrations of the Lipofectamine[®] RNAiMAX reagent used to mix with the Ubc9 siRNA or the scrambled siRNA was ranged from 0.2x, 0.5x to 1x (diluted siRNA transfection reagent Lipofectamine[®] RNAiMAX used, see method: 2.12). The diluted 0.2x concentration of Lipofectamine[®] RNAiMAX was used, indicating that mixing 0.2x Lipofectamine[®] RNAiMAX reagent with the Ubc9 siRNA or the scrambled siRNA for 48 hour transfection represented a significant knockdown in the Ubc9 E2 enzyme, leaving the scrambled siRNA control unaffected.

3. 6 Ubc9 siRNA 48hrs Treatment Leads to Increased FA Number and Size Similarly to the GA 100 μ M Treatment; However, Ubc9 siRNA Treatment Also Causes Cell Membrane Ruffling

MDA-MB-231 cells were treated with the 0.2x diluted Lipo mixture with Ubc9 siRNA, scrambled siRNA or negative control for 48 hours. The talin containing FAs number or size were measured using Image J. The effects of Ubc9 siRNA 48h treatment in the cells caused membrane ruffling, which were shown in Figure 23.

MDA-MB-231 cells were immunostained with the talin-1 antibody and the selective images are shown for the Ubc9 siRNA treated cells expressing talin containing FAs, shown in Figure 23. Image A was presented as one of the z-stack frame images showing at the depth where talin containing FAs could be observed in the z-stack; by adjusting the focal plane, the cell membrane structure was shown in image B. In the Ubc9 siRNA treated cells, it seemed that Ubc9 siRNA caused small membrane ruffling with the red arrows indicating the plasma membrane area in Fig 23 B.

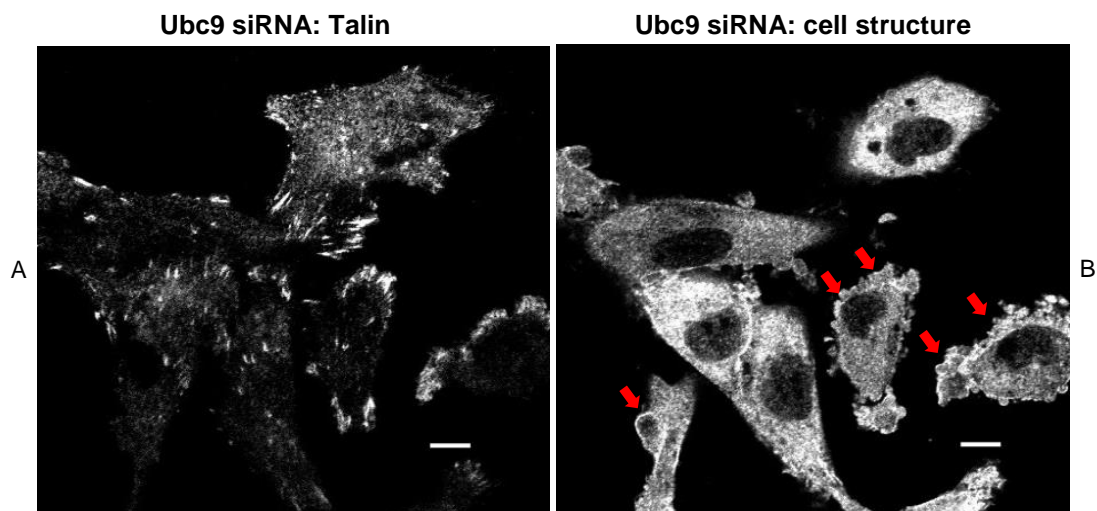
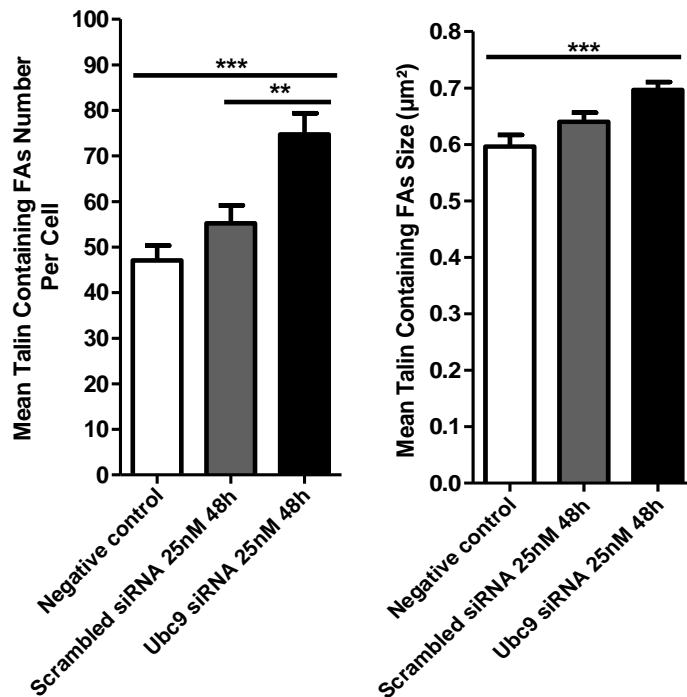


Figure 23. Showing the observation changes of the cell morphology in the Ubc9 siRNA treated MDA-MB-231 cells causing Ubc9 knockdown effects. The cells were stained with the anti talin-1 antibody. Images A+B represented the same image at different z-stack plane: A showed the expression of talin at the bottom of the cells; B showed the confocal plane near to the cell membrane; the red arrows indicated the cell membrane ruffling after 48 hours of Ubc9 siRNA treatment (scale bar = 20 μ m)

After 25nM Ubc9 siRNA or scrambled siRNA treatment for 48 hours, the mean FA number or size was measured and the data was shown in Figure 24.



| Talin n=4 | Mean ± SE Number | Mean ± SE Size µm ² | number of cells counted |
|------------------|------------------|--------------------------------|-------------------------|
| Negative control | 47.1 ± 3.27 | 0.596 ± 0.021 | 255 |
| Scrambled siRNA | 55.2 ± 3.99 | 0.640 ± 0.016 | 173 |
| Ubc9 siRNA | 74.8 ± 4.59 | 0.697 ± 0.014 | 240 |

Figure 24. Showing that the mean talin containing FAs number or size measurements after 25nM Ubc9 siRNA or scrambled siRNA 48hrs treatments in the MDA-MB-231 cells (n=4, individual replicates, data was presented as mean ± SEM, p<0.0001***)

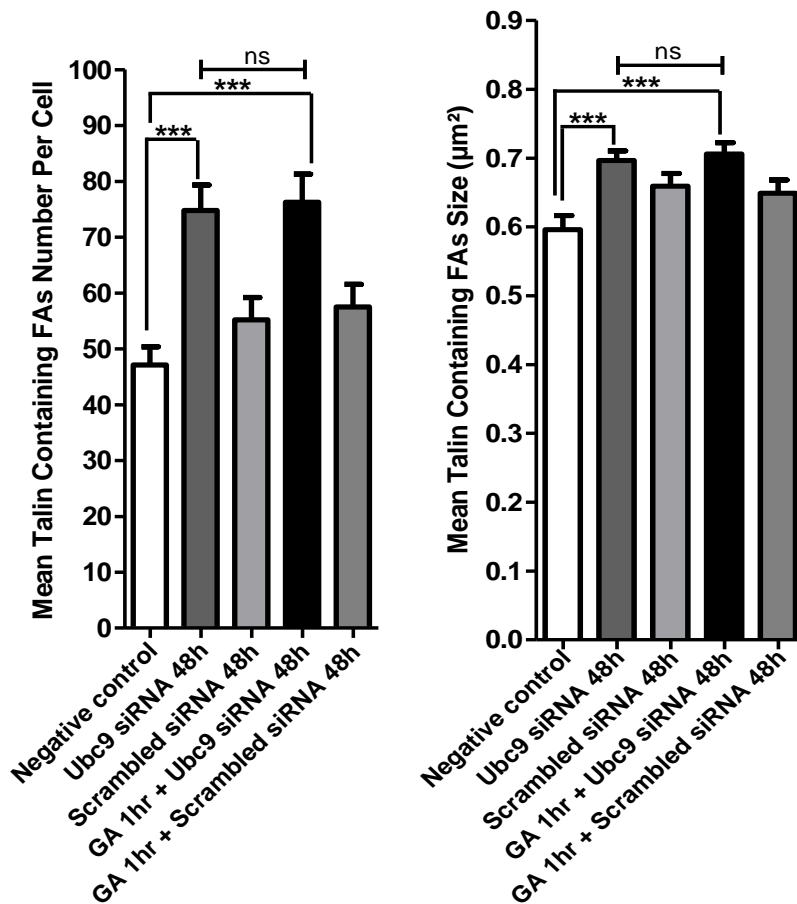
Each single cell was selected manually per image and the mean talin containing FAs number or size was measured using Image J: counting particles function and was represented as mean talin containing FAs number / per cell in Figure 24.

Compared with the untreated control, the mean talin containing FA number increased significantly after 25nM Ubc9 siRNA treatment from 47 ± 3 to 75 ± 5 ($p < 0.0001$ ***). Similarly, compared with the 25nM scrambled siRNA, the mean talin containing FAs number was increased significantly after 25nM Ubc9 siRNA 48hrs treatment from 55 ± 4 to 75 ± 5 (**). Compared with the untreated control, the mean size of talin containing FAs was also increased significantly after 25nM Ubc9 siRNA 48hrs treatment from $0.596 \pm 0.021 \mu\text{m}^2$ to $0.697 \pm 0.014 \mu\text{m}^2$ ($p < 0.0001$ ***).

3. 7 Combining 100µM GA and 25nM Ubc9 siRNA Treatment does not further Increase the FAs Number or Size

The use of GA together with Ubc9 siRNA could increase the mean number or size of the talin containing FAs, compared to untreated cells. However, the combinations of GA and Ubc9 siRNA did not produce additional increase in the mean number or size of the FAs compared to each treatment on its own. MDA-MB-231 cells were treated with 100µM GA first for 1 hour (GA was not removed) then treated with 25nM Ubc9 siRNA or 25nM scrambled siRNA for 48 hours. The cells were then immunostained with the anti talin-1 antibody and the mean number or size of the FAs were measured using Image J both in the Ubc9 siRNA only samples and in the combination samples.

The results were summarised in Figure 25 as a total number of 4 combined experiments.



| Talin n=4 | Mean ± SE Number | Mean ± SE Size µm ² |
|-------------------------|---------------------|-----------------------------------|
| Negative control | 47.1 ± 3.27 | 0.596 ± 0.021 |
| Scrambled siRNA | 55.2 ± 3.99 | 0.659 ± 0.018 |
| GA 1h + scrambled siRNA | 57.5 ± 4.02 | 0.649 ± 0.019 |
| Ubc9 siRNA | 74.8 ± 4.59 | 0.697 ± 0.014 |
| GA 1h + Ubc9 siRNA | 76.2 ± 5.05 | 0.706 ± 0.016 |

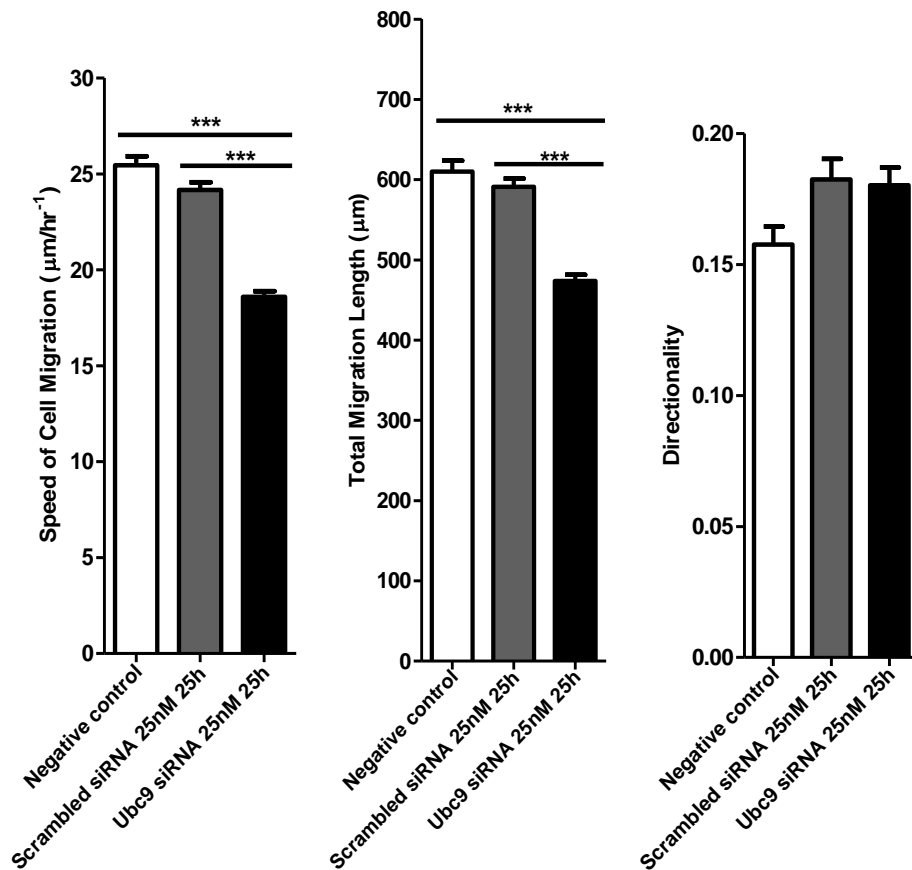
Figure 25. Ubc9 siRNA alone (25nM) or the combination of GA (100µM) with the Ubc9 siRNA (25nM) give significant increases in the mean talin containing FA number or size, though the combination gives similar effects compared to the Ubc9 siRNA alone, there is no further increase in the mean talin number or size (n=4, individual replicates, data presented as mean ± SEM, p<0.0001***)

In Figure 25, compared with the negative control, the mean talin containing FAs number was increased significantly after the combinations of 100µM GA 1h with 25nM Ubc9 siRNA 48hr treatment from 47 ± 3 to 76 ± 5 ($p < 0.0001$ ***); the mean talin containing FAs number was increased significantly after 25nM Ubc9 siRNA 48hrs treatment alone from 47 ± 3 to 75 ± 5 ($p < 0.0001$ ***). However, the combinations of 100µM GA 1hr with 25nM Ubc9 siRNA 48hrs did not cause further increase in the mean talin containing FAs number compared with 25nM Ubc9 siRNA 48hrs treatment alone (ns, $p = 0.83$).

The mean talin containing FAs size was increased significantly after the combinations of 100 μ M GA 1h with 25nM Ubc9 siRNA 48hr treatment from $0.596 \pm 0.021 \mu\text{m}^2$ to $0.706 \pm 0.016 \mu\text{m}^2$ ($p < 0.0001^{***}$). The mean talin containing FAs size was increased significantly after 25nM Ubc9 siRNA 48hrs treatment alone from $0.596 \pm 0.021 \mu\text{m}^2$ to $0.697 \pm 0.014 \mu\text{m}^2$ ($p < 0.0001^{***}$). However, the combinations of 100 μ M GA 1hr and 25nM Ubc9 siRNA 48hrs treatment did not cause further increase in the mean talin containing FAs size (ns, $p = 0.66$).

3. 8 Ubc9 siRNA Knockdown Leads to Reduced Speed of Cell Migration for Both 25h and 48h Timelapse

MDA-MB-231 cells were treated with 25nM Ubc9 siRNA or scrambled siRNA for 25 hours first and for another 23 hours. The mean speed of cell migration, the mean total cell migration length and the mean directionality were measured as a total number of 3 experiments shown in Figure 26.



| 25h, n=3 | Mean ± SE Speed (µm/hr ⁻¹) | Mean ± SE Total Length (µm) | Mean ± SE Directionality | Cell tracking number |
|------------------|--|-----------------------------|--------------------------|----------------------|
| Negative control | 25.5 ± 0.465 | 610.0 ± 13.6 | 0.158 ± 0.007 | 289 |
| Scrambled siRNA | 24.2 ± 0.404 | 591.1 ± 10.2 | 0.183 ± 0.008 | 335 |
| Ubc9 siRNA | 18.6 ± 0.297 | 473.7 ± 7.78 | 0.180 ± 0.007 | 375 |

Figure 26. Showing that the mean speed of cell migration, mean total migration length and mean directionality measurements after 25nM Ubc9 siRNA or scrambled siRNA treatments for 25hrs period in the MDA-MB-231 cells (n=3, individual replicates, data was presented as mean ± SEM, p<0.0001***)

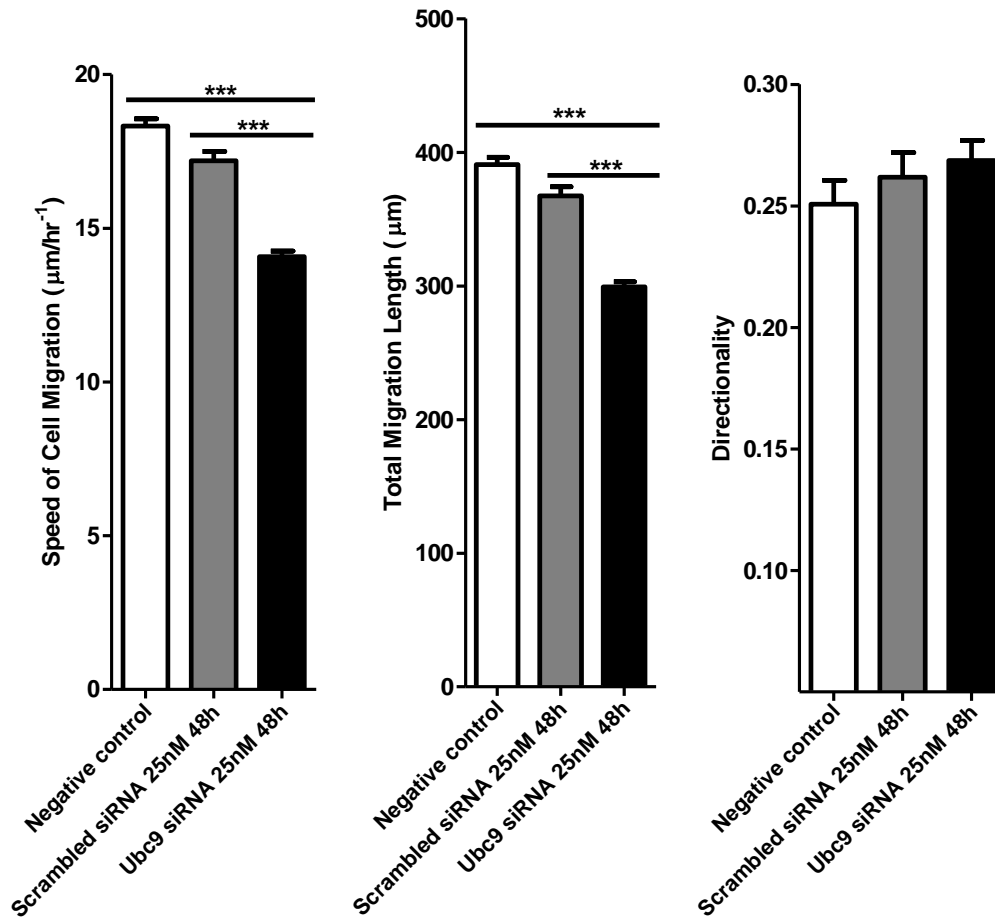
MDA-MB-231 cells were grown in 2mg/ml collagen overnight then treated with 25nM Ubc9 siRNA and the timelapse experiment was recorded for a period of 25 hours.

In Figure 26, compared with the negative control, the mean speed of cell migration was decreased significantly after 25nM Ubc9 siRNA 25hrs treatment from $25.5 \pm 0.465 \mu\text{m/hr}^{-1}$ to $18.6 \pm 0.297 \mu\text{m/hr}^{-1}$ ($p < 0.0001^{***}$). Similarly, compared with the scrambled siRNA, the mean speed of cell migration was decreased significantly after 25nM Ubc9 siRNA 25hrs treatment from $24.2 \pm 0.404 \mu\text{m/hr}^{-1}$ to $18.6 \pm 0.297 \mu\text{m/hr}^{-1}$ ($p < 0.0001^{***}$).

Compared with the negative control, the mean total cell migration distance was also significantly decreased after 25nM Ubc9 siRNA 25hrs treatment from $610.0 \pm 13.6 \mu\text{m}$ to $473.7 \pm 7.78 \mu\text{m}$ ($p < 0.0001^{***}$); compared with the scrambled siRNA, the mean total cell migration distance was significantly decreased after 25nM Ubc9 siRNA 25hrs treatment from $591.1 \pm 10.2 \mu\text{m}$ to $473.7 \pm 7.78 \mu\text{m}$ ($p < 0.0001^{***}$).

The mean directionality of the cell migration was not significantly affected compared between the negative control and the Ubc9 siRNA or the scrambled siRNA and the Ubc9 siRNA.

The MDA-MB-231 cells were also grown in 2mg/ml collagen then treated with 25nM Ubc9 siRNA for 24 hours first in the incubator, then at the post-24h time point, the migration of the cells were recorded in the timelapse experiment for a 48 hours treatment. The results were summarised as a total number of 4 combined experiments in Figure 27.



| 48h, n=4 | Mean ± SE Speed (µm/hr ⁻¹) | Mean ± SE Total Length (µm) | Mean ± SE Directionality | Cell tracking number |
|------------------|--|-----------------------------|--------------------------|----------------------|
| Negative control | 18.3 ± 0.236 | 390.9 ± 5.46 | 0.251 ± 0.010 | 292 |
| Scrambled siRNA | 17.2 ± 0.308 | 367.3 ± 6.94 | 0.262 ± 0.010 | 290 |
| Ubc9 siRNA | 14.1 ± 0.189 | 299.3 ± 3.88 | 0.269 ± 0.008 | 350 |

Figure 27. Showing that the mean speed of cell migration, mean total migration length and mean directionality measurements after 25nM Ubc9 siRNA or scrambled siRNA treatments for 48hrs period in the MDA-MB-231 cells (n=4, individual replicates, data was presented as mean ± SEM, p<0.0001***)

In Figure 27, compared with the negative control, the mean speed of cell migration was decreased significantly after 25nM Ubc9 siRNA 48hrs treatment from $18.3 \pm 0.236 \mu\text{m/hr}^{-1}$ to $14.1 \pm 0.189 \mu\text{m/hr}^{-1}$ ($p < 0.0001^{***}$). Similarly, compared with the scrambled siRNA, the mean speed of cell migration was decreased significantly after 25nM Ubc9 siRNA 48hrs treatment from $17.2 \pm 0.308 \mu\text{m/hr}^{-1}$ to $14.1 \pm 0.189 \mu\text{m/hr}^{-1}$ ($p < 0.0001^{***}$).

Compared with the negative control, the mean total cell migration distance of the cells was decreased significantly after 25nM Ubc9 siRNA 48hrs treatment from $390.9 \pm 5.46 \mu\text{m}$ to $299.3 \pm 3.88 \mu\text{m}$ ($p < 0.0001^{***}$). Compared with the scrambled siRNA, the mean total cell migration distance of the cells was decreased significantly after 25nM Ubc9 siRNA 48hrs treatment from $367.3 \pm 6.94 \mu\text{m}$ to $299.3 \pm 3.88 \mu\text{m}$ ($p < 0.0001^{***}$).

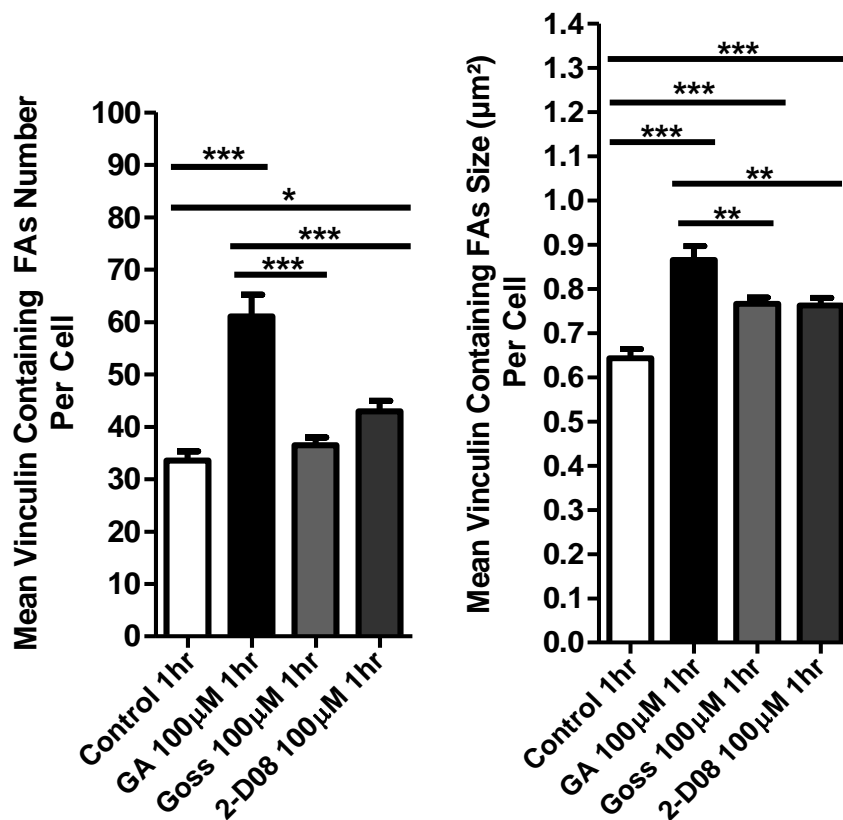
The mean directionality of the cells after 48hrs was not significantly changed between the negative control and the Ubc9 siRNA treatment or the scrambled siRNA and the Ubc9 siRNA treatment.

3. 9 Other SUMOylation Inhibitors Also Cause an Increase in the Mean FAs Number or Size

3. 9. 1. GA, Gossypetin or 2-D08 1hour Treatments Cause an Increase in the Mean Number or Size of Vinculin Containing FAs

MDA-MB-231 cells were grown on 0.2% v/v gelatin coated coverslips overnight and then treated with GA, Gossypetin or 2-D08 at $100\mu\text{M}$ for 1 hour. The cells were then immunostained with a vinculin antibody and the mean number or the size of vinculin containing FAs were measured after each inhibitor treatment.

In Figure 28, the results were summarised as a total number of 4 combined experiments.



| Vinculin n=4 | Mean ± SE Number | Mean ± SE Size µm ² | Number of cells counted |
|----------------|------------------|--------------------------------|-------------------------|
| Control 1hr | 33.5 ± 1.78 | 0.643 ± 0.021 | 159 |
| GA 1hr | 61.0 ± 4.18 | 0.866 ± 0.031 | 118 |
| Gossypetin 1hr | 36.5 ± 1.49 | 0.766 ± 0.014 | 230 |
| 2-D08 1hr | 43.0 ± 1.96 | 0.763 ± 0.017 | 231 |

Figure 28. The mean vinculin containing FAs number or size measurements per cell after 100µM GA, Gossypetin or 2-D08 1hr treatment in the MDA-MB-231 cells (n=4, individual replicates, data was presented as mean ± SEM, p<0.0001***)

In Figure 28, compared with the control, the mean vinculin containing FAs number was increased significantly after 100µM GA 1hr treatment from 34 ± 2 to 61 ± 4 (p<0.0001***) . Compared with the control, the mean vinculin containing FAs number was increased significantly after 100µM 2-D08 1hr treatment from 34 ± 2 to 43 ± 2 (*). Gossypetin had no significant effects in the mean number of the vinculin containing FAs (p=0.21).

100µM GA 1 hour treatment was more effective in increasing the mean vinculin FAs number than 100µM 2-D08 1 hour treatment (p<0.0001***) .

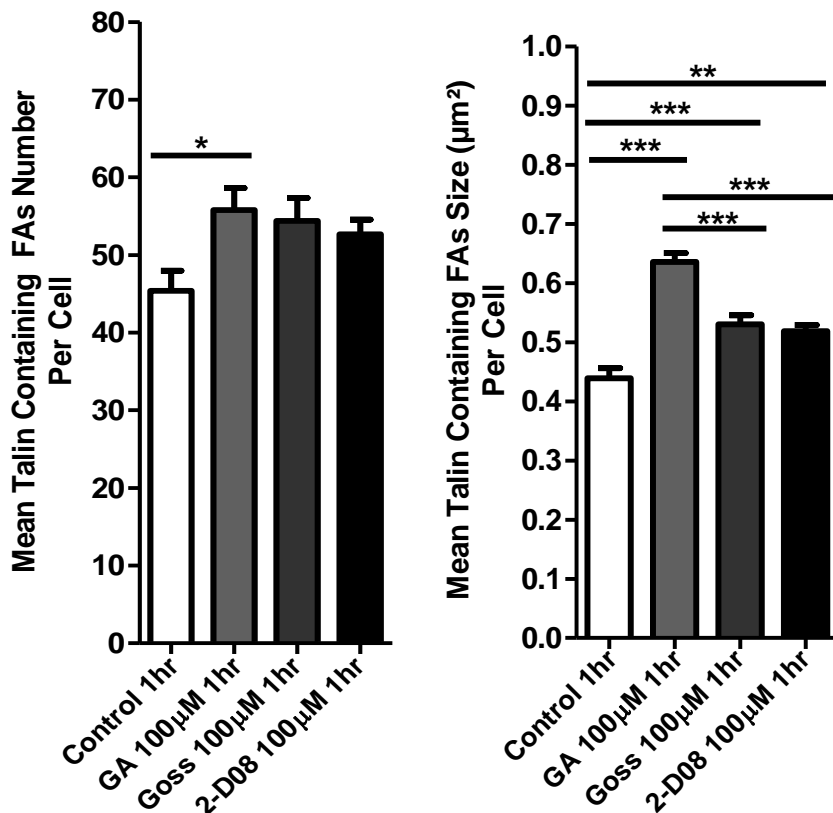
All of the three inhibitors GA, Gossypetin or 2-D08 at 100µM for 1hr treatment increased the mean size of the vinculin containing FAs significantly compared with the control.

The mean vinculin containing FAs size was increased significantly after 100µM GA 1hr treatment from $0.643 \pm 0.021 \mu\text{m}^2$ to $0.866 \pm 0.031 \mu\text{m}^2$ ($p < 0.0001^{***}$). The mean vinculin containing FAs size was increased significantly after 100µM Gossypetin 1hr treatment from $0.643 \pm 0.021 \mu\text{m}^2$ to $0.766 \pm 0.014 \mu\text{m}^2$ ($p < 0.0001^{***}$). The mean vinculin containing FAs size was increased significantly after 100µM 2-D08 1hr treatment from $0.643 \pm 0.021 \mu\text{m}^2$ to $0.763 \pm 0.017 \mu\text{m}^2$ ($p < 0.0001^{***}$).

100µM GA 1hr treatment was more effective in increasing the mean vinculin containing FAs size than 100µM Gossypetin or 2-D08 at 1hr treatment (**).

3. 9. 2. GA, Gossypetin or 2-D08 1 hour Treatments Cause an Increase in the Mean Number or Size of Talin Containing FAs

MDA-MB-231 cells were grown on 0.2% v/v gelatin coated coverslips overnight and then treated with GA, Gossypetin or 2-D08 at 100µM for 1 hour. The cells were then immunostained with the anti talin-1 antibody and the mean number or size of the talin containing FAs were measured after each inhibitor treatment. The results were summarised as a total number of 4 combined experiments in Figure 29.



| Talin n=4 | Mean ± SE Number | Mean ± SE Size µm ² | Number of cells counted |
|----------------|------------------|--------------------------------|-------------------------|
| Control 1hr | 45.4 ± 2.60 | 0.439 ± 0.017 | 138 |
| GA 1hr | 55.8 ± 2.87 | 0.636 ± 0.015 | 226 |
| Gossypetin 1hr | 54.4 ± 2.96 | 0.531 ± 0.016 | 169 |
| 2-D08 1hr | 52.7 ± 1.87 | 0.519 ± 0.010 | 226 |

Figure 29. Mean talin containing FAs number or size measurements per cell after 100µM GA, Gossypetin or 2-D08 at 1hr treatment in the MDA-MB-231 cells (n=4, individual replicates, data presented as mean ± SEM, p<0.0001****)

In Figure 29, compared with the control, the mean talin containing FAs number increased significantly after 100µM GA 1hr treatment from 45 ± 3 to 56 ± 3 (*). Gossypetin or 2-D08 at 1hr treatment did not have any significant effects in the mean talin containing FAs number compared with the control.

All of the three inhibitors GA, Gossypetin or 2-D08 at 1hr treatment significantly increased the mean talin containing FAs size compared with the control. The mean talin containing FAs size was increased significantly after 100µM GA 1hr treatment from 0.439 ± 0.017 µm² to 0.636 ± 0.015 µm² (p<0.0001 ***); the mean talin containing FAs size was increased significantly after 100µM Gossypetin 1hr treatment from 0.439 ± 0.017 µm² to 0.531 ± 0.016

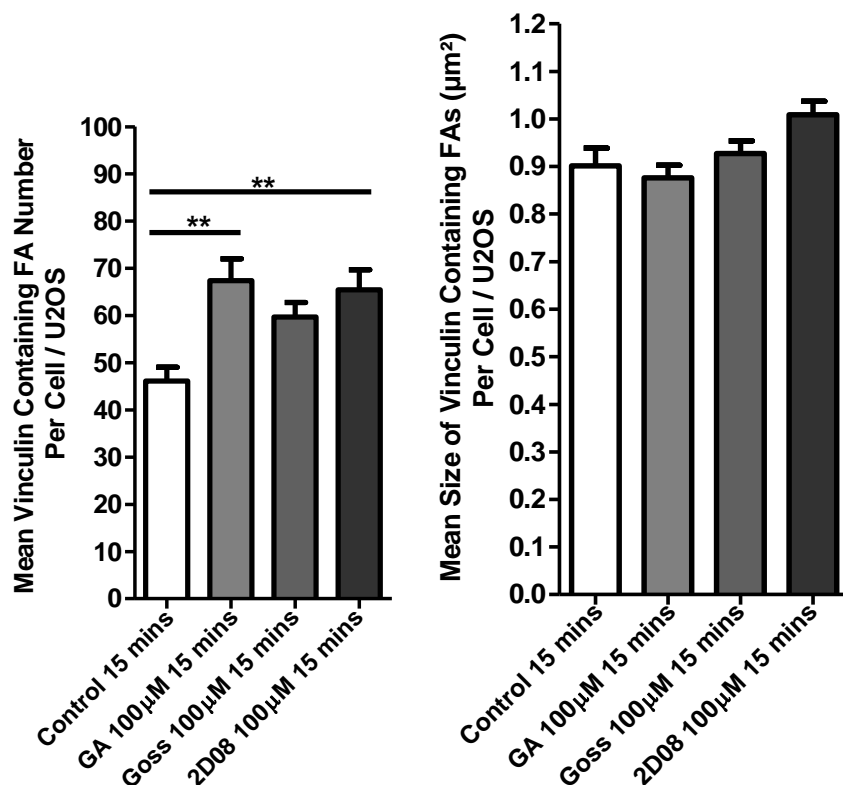
μm^2 ($p < 0.0001$ ***); The mean talin containing FAs size was increased significantly after 100 μM 2-D08 1hr treatment from $0.439 \pm 0.017 \mu\text{m}^2$ to $0.519 \pm 0.010 \mu\text{m}^2$ (**).

100 μM GA 1hr treatment was more effective in increasing the mean talin containing FAs size than the 100 μM Gossypetin or 2-D08 1hr treatment ($p < 0.0001$ ***).

U2OS Cells

3. 9. 3. GA or 2-D08 Treatments Caused an Increase in the Mean Number of Vinculin Containing FAs

U2OS cells were used to determine the mean vinculin containing FA number or size. U2OS cells were grown on 0.2% v/v gelatin coated coverslips overnight and then treated with 100 μM GA, Gossypetin or 2-D08 for 15 minutes. The cells were then immunostained with an anti-vinculin antibody and the mean number or size of the vinculin containing FAs were measured after each inhibitor treatment. The results were summarised as a total number of 3 combined experiments in Figure 30.



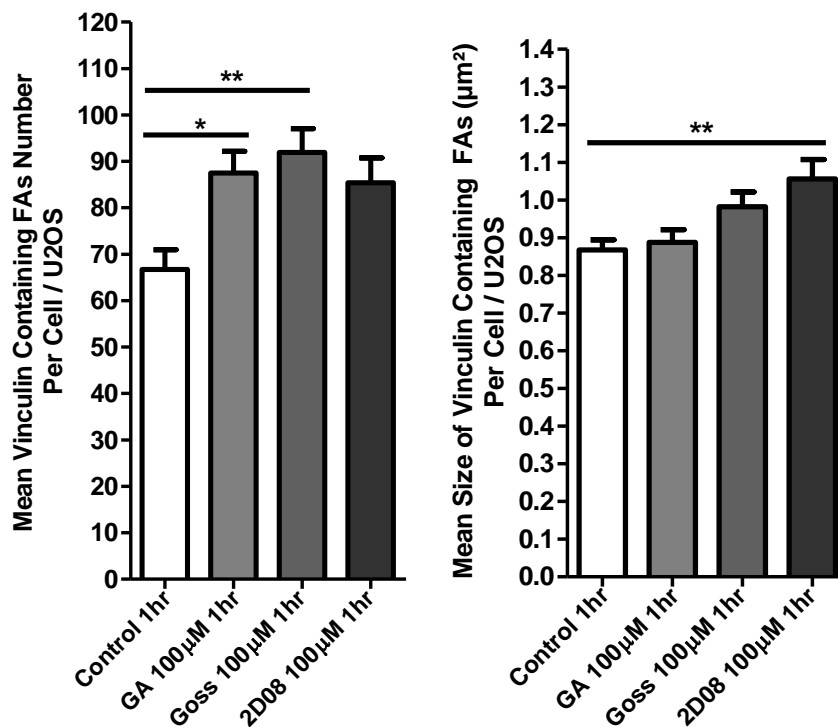
| Vinculin n=3 | Mean ± SE Number | Mean ± SE Size µm ² | Number of cells counted |
|--------------------|------------------|--------------------------------|-------------------------|
| Control 15 mins | 46.1 ± 2.96 | 0.901 ± 0.038 | 90 |
| GA 15 mins | 67.4 ± 4.65 | 0.876 ± 0.027 | 107 |
| Gossypetin 15 mins | 59.7 ± 3.07 | 0.927 ± 0.027 | 109 |
| 2-D08 15 mins | 65.4 ± 4.29 | 1.01 ± 0.028 | 103 |

Figure 30. Mean vinculin containing FAs number or size measurements per cell after 15 minutes of 100µM GA, Gossypetin or 2-D08 treatments in U2OS cells (n=3, individual replicates, data presented as mean ± SEM, p=0.0008 **)

In Figure 30, compared with the control, the mean vinculin containing FA number was increased significantly after 100µM GA 15 minutes treatment from 46 ± 3 to 67 ± 5 (p=0.0008 **). Compared to the control, 100µM 2-D08 after 15 minutes treatment also significantly increased the mean vinculin containing FAs number from 46 ± 3 to 65 ± 4 (p=0.0008 **). The mean vinculin containing FAs size was not affected.

3. 9. 4. GA or Gossypetin Treatments Caused an Increase in the Mean Number of Vinculin Containing FAs; 2-D08 Caused an Increase in the Mean Size of Vinculin Containing FAs

The U2OS cells were grown on 0.2% v/v gelatin coated coverslips overnight and then treated with 100µM GA, Gossypetin or 2-D08 for 1 hour. The cells were then immunostained with the anti-vinculin antibody and the mean number or size of the vinculin containing FAs were measured after each inhibitor treatment. The results were summarised as a total number of 3 combined experiments in Figure 31.



| Vinculin n=3 | Mean ± SE Number | Mean ± SE Size µm ² | Number of cells counted |
|----------------|---------------------|-----------------------------------|----------------------------|
| Control 1hr | 66.7 ± 4.22 | 0.868 ± 0.027 | 95 |
| GA 1hr | 87.5 ± 4.68 | 0.888 ± 0.034 | 94 |
| Gossypetin 1hr | 91.9 ± 5.08 | 0.982 ± 0.039 | 97 |
| 2-D08 1hr | 85.4 ± 5.37 | 1.06 ± 0.052 | 77 |

Figure 31. Mean vinculin containing FAs number or size measurements per cell after 1 hour of 100µM GA, Gossypetin or 2-D08 treatments in the U2OS cells (n=3, individual replicates, data presented as mean ± SEM, p=0.0021 **)

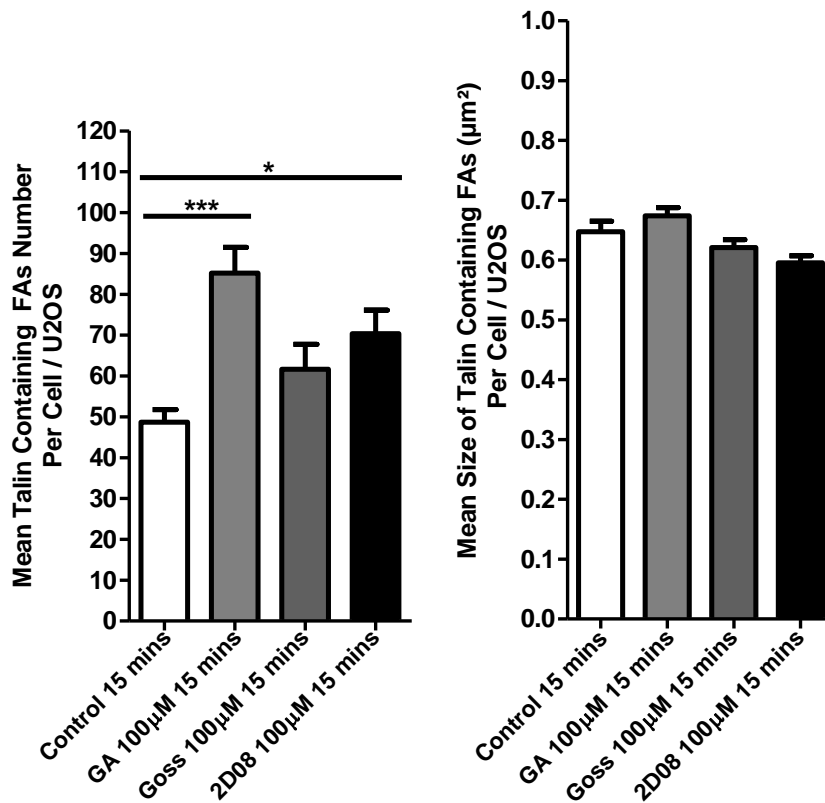
In Figure 31, compared with the control, the mean vinculin containing FA number was increased significantly after 100µM GA 1 hour treatment from 67 ± 4 to 88 ± 5 (*).

Compared with the control, 100µM Gossypetin after 1 hour treatment significantly increased the mean number of the vinculin containing FAs from 67 ± 4 to 92 ± 5 ($p=0.0021$ **).

Compared to the untreated cells, 100µM 2-D08 after 1 hour treatment significantly increased the mean size of the vinculin containing FAs from $0.868 \pm 0.027 \mu\text{m}^2$ to $1.06 \pm 0.052 \mu\text{m}^2$ ($p=0.0020$ **).

3. 9. 5. GA or 2-D08 Treatments Caused an Increase in the Mean Number of Talin Containing FAs

U2OS cells were grown on 0.2% v/v gelatin coated coverslips overnight and then treated with 100µM GA, Gossypetin or 2-D08 for 15 minutes. The cells were then immunostained with the anti-talin-1 antibody and the mean number or size of the talin containing FAs were measured after each inhibitor treatment. The results were summarised as a total number of 3 combined experiments in Figure 32.



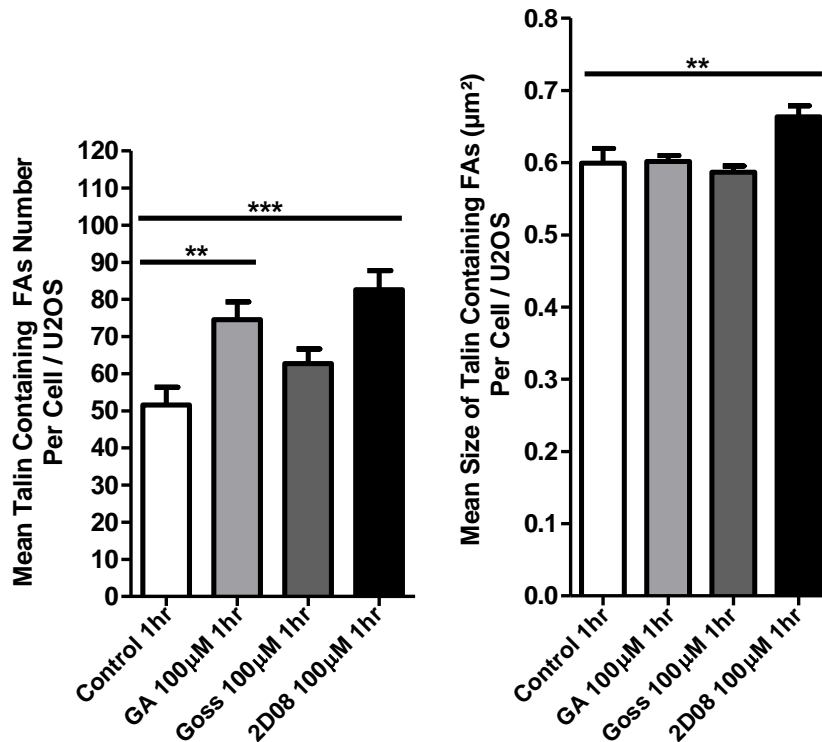
| Talin n=3 | Mean ± SE Number | Mean ± SE Size µm ² | Number of cells counted |
|--------------------|------------------|--------------------------------|-------------------------|
| Control 15 mins | 48.7 ± 3.11 | 0.648 ± 0.017 | 92 |
| GA 15 mins | 85.2 ± 6.27 | 0.674 ± 0.014 | 71 |
| Gossypetin 15 mins | 61.6 ± 6.14 | 0.621 ± 0.013 | 52 |
| 2-D08 15 mins | 70.4 ± 5.77 | 0.596 ± 0.012 | 61 |

Figure 32. Mean talin containing FAs number or size measurements per cell after 15 minutes of 100µM GA, Gossypetin or 2-D08 treatments in the U2OS cells (n=3, individual replicates, data presented as mean ± SEM, p<0.0001***)

In Figure 32, compared with the control, the mean talin containing FA number was increased significantly after 100µM GA 15 minutes treatment from 49 ± 3 to 85 ± 6 ($p < 0.0001^{***}$). Compared with the control, 100µM 2-D08 after 15 minutes treatment significantly increased the mean talin containing FAs number from 49 ± 3 to 70 ± 6 (*).

3. 9. 6. GA or 2-D08 Treatments Caused an Increase in the Mean Number of Talin Containing FAs; 2-D08 Caused an Increase in the Mean Size of Talin Containing FAs

U2OS cells were grown on 0.2% v/v gelatin coated coverslips overnight and then treated with 100µM GA, Gossypetin or 2-D08 for 1 hour. The cells were then immunostained with the anti-talin-1 antibody and the mean number or size of the talin containing FAs were measured after each inhibitor treatment. The results were summarised as a total number of 3 combined experiments in Figure 33.



| Talin n=3 | Mean ± SE Number | Mean ± SE Size µm ² | Number of cells counted |
|----------------|------------------|--------------------------------|-------------------------|
| Control 1hr | 51.6 ± 4.75 | 0.599 ± 0.021 | 68 |
| GA 1hr | 74.6 ± 4.82 | 0.602 ± 0.008 | 91 |
| Gossypetin 1hr | 62.8 ± 3.88 | 0.587 ± 0.008 | 65 |
| 2-D08 1hr | 82.6 ± 5.21 | 0.663 ± 0.015 | 68 |

Figure 33. Mean talin containing FA number or size measurements per cell after 1 hour of 100µM GA, Gossypetin or 2-D08 treatments in the U2OS cells (n=3, individual replicates, data presented as mean ± SEM, p=0.0003 ***)

In Figure 33, compared with the control, the mean talin containing FAs number was increased significantly after 100 μ M GA 1 hour treatment from 52 ± 5 to 75 ± 5 (**). Compared to the control, 100 μ M 2-D08 after 1 hour treatment significantly increased the mean talin containing FAs number from 52 ± 5 to 83 ± 5 ($p=0.0003$ ***).

Compared to the control, 100 μ M 2-D08 after 1 hour treatment significantly increased the mean talin containing FAs size from $0.599 \pm 0.021 \mu\text{m}^2$ to $0.663 \pm 0.015 \mu\text{m}^2$ (**).

| Summary of This Study: Inhibition of SUMOylated Focal Adhesions | | | |
|---|--|---|--|
| Inhibitors | Immunostaining: fixed cell Mean number of focal adhesions increased significantly (numbers/per cell) | Immunostaining: fixed cell Mean size of focal adhesions increased significantly (μm^2 /per cell) | GFP-tag FAs turnover assay: live cell Mean number (numbers/per cell), size (μm^2 /per cell) and turnover time (s) of focal adhesions increased significantly |
| GA (E1) (Fukuda et al., 2009a) | MDA-MB-231+ <u>1 hour:</u> Talin: 45 vs. 56 Vinculin: 34 vs. 61 U2OS+ <u>15 minutes:</u> Talin: 49. vs. 85 Vinculin: 46 vs. 67 <u>1 hour:</u> Talin: 52 vs. 75 Vinculin: 67 vs. 88 | MDA-MB-231+ <u>1 hour:</u> Talin: 0.44 vs. 0.64 Vinculin: 0.64 vs. 0.87 | MDA-MB-231+ <u>2 hours:</u> Talin: Number: 62 vs. 102; Size: 0.84 vs. 0.94 Turnover: 34.3 vs. 59.5 Vinculin: Number: 44 vs. 85 Size: 0.81 vs. 0.98 Turnover: 27.4 vs. 47.2 FAK: Number: 52 vs. 92 Size: 0.83 vs. 0.92 Turnover: 31.5 vs. 50.0 |
| 2-D08 (Kim et al., 2013) | MDA-MB-231+ <u>1 hour:</u> Vinculin:34 vs. 43 U2OS+ <u>15 minutes:</u> Talin: 49 vs. 70 Vinculin:46 vs. 65 <u>1 hour:</u> Talin: 52 vs. 83 | MDA-MB-231+ <u>1 hour:</u> Talin: 0.44 vs. 0.52 Vinculin: 0.64 vs. 0.76 U2OS+ <u>1 hour:</u> Talin: 0.60 vs. 0.66 Vinculin: 0.87 vs. 1.1 | n/a |
| Gossypetin (Chen et al., 2013, Lin, 2015) | U2OS+ <u>1 hour:</u> Vinculin: 67 vs. 92 | MDA-MB-231+ <u>1 hour:</u> Talin: 0.44 vs. 0.53 Vinculin: 0.64 vs. 0.77 | n/a |
| Ubc9 siRNA (E2) 48hrs treatment | MDA-MB-231+ Talin: 47 vs. 75 | MDA-MB-231+ Talin: 0.60 vs. 0.70 | n/a |
| GA+Ubc9 siRNA 49hrs treatment | MDA-MB-231+ Talin: 47 vs. 76 | MDA-MB-231+ Talin: 0.60 vs. 0.71 | n/a |
| The speed of cell migration decreased significantly ($\mu\text{m}/\text{hr}^{-1}$) after the Inhibition of SUMOylated focal adhesions: 3D collagen matrix | | | |
| GA (E1) MDA-MB-231 <u>24 hours:</u> 20.1 < 14.6 < 13.7 < 12.4 | | Ubc9 siRNA (E2) MDA-MB-231 <u>25 hours:</u> 25.5 < 18.6 <u>48 hours:</u> 18.3 < 14.1 | |

Table 6. Summarising the changes in the mean number, size and turnover of FAs in two different cell lines used: the MDA-MB-231 cells and the U2OS cells and in two different microenvironments: the immunostaining fixed-cell cell culture environments and the 2.5D 2 mg/ml collagen type I microenvironments; the summary of the effects after the inhibition of SUMOylation on cell migration

Discussion

GA increased the mean number and size of FAs in MDA-MB-231 cells and U2OS cells. In live-cell experiments, GA increased the mean number, size and turnover time of talin, vinculin or FAK containing FAs in MDA-MB-231 cells. 2-D08 and gossypetin increased the mean number and size of FAs in MDA-MB-231 cells and U2OS cells. Ubc9 siRNA increased the mean number and size of the talin containing FAs in MDA-MB-231 cells. GA and siRNA treatments decreased the speed of cell migration in MDA-MB-231 cells.

The dose used in this study (100 μ M GA) was also used in the inhibition of SUMOylated RanGAP1-C2 and p53; other concentrations were used as 1 μ M and 10 μ M for RanGAP1-C2 and 10 μ M and 100 μ M of GA completely inhibited the SUMOylation of RanGAP1-C2 *in vitro*; 10, 25 and 50 μ M of GA were used for p53 and 100 μ M GA inhibited the SUMOylation of p53 *in vivo*; GA at 10, 25, 50 and 100 μ M did not affect ubiquitination *in vivo* for 4 hours treatment (Fukuda et al., 2009a). 25, 50 and 100 μ M of GA were used in the cell migration study, which reduced the speed of cell migration. 100 μ M GA treatment in HEK293 cells for 6 hours resulted in significant decrease in SUMO-1 and SUMO 2/3 conjugation and in global protein tyrosine phosphorylation; a specific example of tyrosine kinases, FAK, was shown that 100 μ M GA treatment for 6 hours showed a decrease in tyrosine phosphorylation of Tyr-397 in the SUMOylated form of FAK (Yao et al., 2011).

The effects of 2-D08 are discussed in some examples. 2-D08 at 10 μ M and 30 μ M inhibited SUMOylated I κ B α with SUMO-1 modification; 2-D08 at 30 μ M inhibited SUMOylated I κ B α with SUMO-2 and SUMO-3 modification; 30 μ M 2-D08 inhibited SUMOylated topoisomerase I in ZR-75-1 and BT-474 breast cancer cells (Kim et al., 2013). GA, but not 2-D08, inhibits E1 (SAE)-SUMO-1 thioester formation; GA, but not 2-D08 inhibits Ubc9-SUMO-1 thioester formation; whereas 2-D08 inhibits the transfer of SUMO-1 from the E2 thioester to the SUMO substrate with no disruption in other biochemical steps (Kim et al., 2013). 3-B08 or gossypetin has also been selectively screened as an inhibitor for SUMOylation reaction (Kim et al., 2013). These studies have shown that GA is an E1 (SAE) inhibitor and can inhibit E1 activation (Fukuda et al., 2009a); 2-D08 is a pathway-selective inhibitor, 100 μ M 2-D08 does not affect global ubiquitination (Kim et al., 2013); GA and 2-D08 are specific inhibitors for SUMOylation and not ubiquitination inhibitors, however, it does not rule out their activities in cellular pathways other than SUMOylation and ubiquitination.

Inhibition of SUMOylation is not the only activity of these inhibitors. It was reported that more than 100 μ M GA was necessary for activating protein phosphatase type 2C α (PP2C α) *in*

vitro: incubation with GA at 600 μ M for 24 hours could increase the activity of cytosolic PP2C α by 14-fold, which was responsible for the neurotoxic effects in chicken embryo neurons (Ahlemeyer et al., 2001). 2-D08 is a synthetic flavone which has radical scavenging property (Seyoum et al., 2006). Gossypetin could inhibit PMA induced activation of nuclear factor-kB (NF-kB) signalling in MDA-MB-231 cells and it caused a slight increase in the MMP-9 matrix metalloproteinase-9 and COX-2 cyclooxygenase-2 mRNA transcript levels (Amrutha et al., 2014). Gossypetin was shown to possess potent neuraminidases inhibitory effects and *in vitro* anti-influenza viral activities (Jeong et al., 2009). GA, 2-D08 and gossypetin have antioxidant and antimutagenic effects (Zhou et al., 2004, DeFeudis et al., 2003, Francis et al., 1989, Mahadevan and Park, 2008).

Protein substrate modification with SUMO relies on a single E2 enzyme, Ubc9 in the SUMOylation pathway, where Ubc9 is unique among E2 enzymes in its capability to specifically recognize and conjugate SUMO1 or SUMO 2/3 to their substrates (Gareau and Lima, 2010, Tatham et al., 2001, Sampson et al., 2001). In the absence of specific inhibitors, Ubc9 siRNA was used to knock down the expression of Ubc9. Some studies on Ubc9 siRNA knockdown have been shown. Ubc9 siRNA knockdown could inhibit *in vivo* p53 SUMOylation and β -estradiol-induced cell proliferation in MCF7 cells (Hirohama et al., 2013). Ubc9 siRNA transfection caused impaired melanoma cell proliferation and melanoma cell apoptosis; moreover, incubation of Ubc9 siRNA (100nM) in the presence of the cytotoxic drug cisplatin (20 μ M) increased its sensitivity from 35% to 70% in metastatic growth phase (MGP) melanomas; Ubc9 siRNA treatment (100nM) with paclitaxel (20 μ M) also achieved 70% cell apoptosis in MGP melanomas (Moschos et al., 2007). Ubc9 siRNA (25nM) was used and it reduced cell migration significantly in this study.

There are advantages and disadvantages to using siRNA. Generally, the small interfering RNA can be easily introduced into the target cells with high efficiency, but the resources are non-renewable and the transfection effect is only transient (Campeau and Gobeil, 2011, Mocellin and Provenzano, 2004). The siRNA is designed to ensure that it targets specifically to the protein mRNA of interest without off-targeted effects, this is its specificity; meanwhile, the siRNA is expected to have a desirable effect in the knockdown efficiency, which is its potency (Shan, 2010). The disadvantage of siRNA is its unwanted off-targeted effects. To obtain highest knockdown efficiency and minimal off-targeted effects, nanomolar or even lower concentrations have to be determined specifically for each cell type used.

The combinatorial use of GA and Ubc9 siRNA in MDA-MB-231 cells had similar results and from the two treatments together compared to individual treatments did not produce a further

increase in the mean FAs number and size. This suggests that GA and Ubc9 siRNA are pathway selective inhibitors, shown in Figure 34.

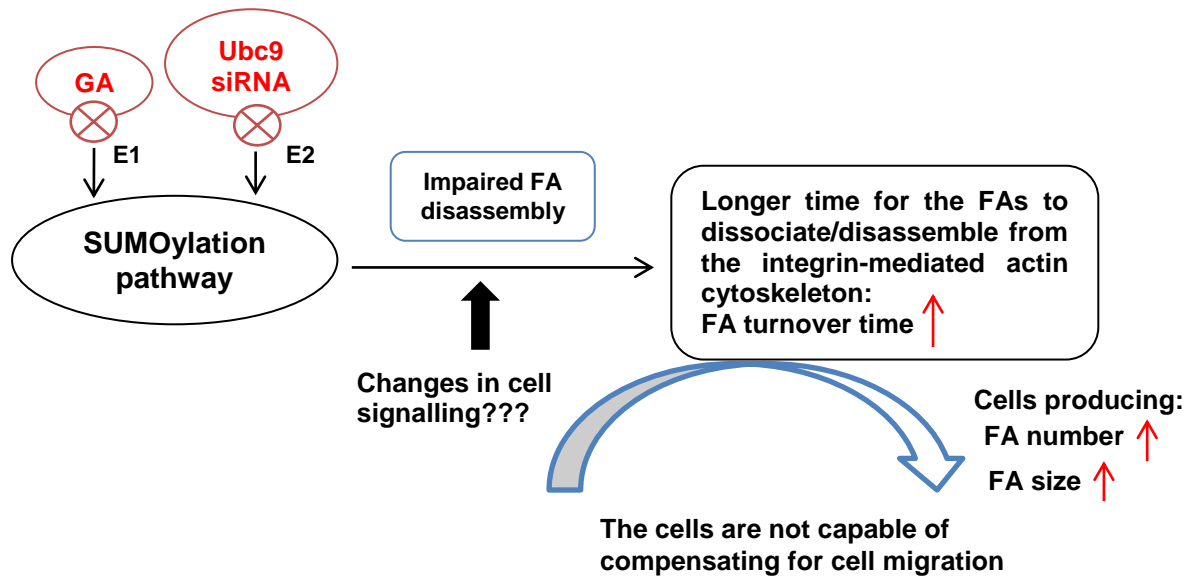


Figure 34. Summarising in the regulatory role of SUMOylation in the focal adhesions; the inhibition of SUMOylation prolongs the time of FA disassembly leading to increased time of FA turnover, which may have also affected cell signalling downstream of the integrin mediated FA to actin; the cells could be initiated with other compensatory mechanisms from slower turnover and impaired dynamics of FA, which the cells were produced with more FAs and larger FAs. SUMOylation may be upregulated in persistent FA turnover and FA disassembly.

Figure 34 summarises the proposed regulatory role of SUMOylation in focal adhesions. After blocking protein SUMOylation, the number, size and turnover of FAs increased, suggesting SUMOylation may be important in regulating FAs. This leads to the idea that SUMOylation could be playing a critical role in the dynamic activities and turnover of FAs. The inhibition of protein SUMOylation leads to the stability of FAs; the mature FAs cannot break down or disassemble and therefore accumulate and increase in size. The larger FA accumulation leads to increased FA turnover time and results in reduced cell migration. Any newly synthesized FA proteins will be prevented from SUMO conjugation. Therefore, SUMOylation may have a critical regulatory role in FA disassembly. Integrin mediated FAs are important in cell migration (Huttenlocher, 2011, Zaidel-Bar and Geiger, 2010). Proper dynamics of FAs are essential as the trailing adhesions or the adhesions at the cell rear are periodically released to allow rapid movement (Broussard et al., 2008). SUMOylation may regulate FAs specifically during their rapid disassembly.

However, the inhibitory effects cannot be ruled out of changes in other cell signalling pathways. Inhibition of FA disassembly decreases cell migration. The effects of slowed down cell migration may also indicate the interruption of SUMOylated FAs in the inside-out integrin signalling. Further studies will be needed to determine the inhibitory effects on cell migration

are reversible or not. FA disassembly is precisely controlled by signalling pathways and the regulation of actin-myosin tensile forces; the specific regulatory or adaptor proteins associated need to be investigated in future experimental work.

Ubc9 siRNA treatment caused some effects in cells during the cell migration study. Ubc9 siRNA knockdown showed membrane ruffling on the frontal surface of the cells in some MDA-MB-231 cells, whilst the FAs were still able to be observed around the cell membrane. This observation of membrane ruffling represents a question if the Ubc9 siRNA treatment was able to affect cell plasticity. The inhibition of SUMOylation may have interrupted the lamellipodia formation resulting in misshapen membrane polarisation. One study has shown that the membrane ruffles in cell migration could be resulted from inefficient lamellipodia adhesion and actin filament compartment reorganization; suboptimal cell-substrate adhesion e.g. inefficient integrin-ligand interaction led to significant reduced lamellipodia persistence and inefficient cell migration resulted in a dramatic increase in ruffle frequency (Borm et al., 2005). Membrane protrusion and cell adhesion process are highly and physically coupled; failed lamellipodia to establish stable adhesions are detached from the substrate and retracted centripetally toward the cell body (DeMali and Burridge, 2003).

Another aspect from this effect is that tumour cells have been shown to be capable of remarkable plasticity and can move in a proteolysis-independent manner using membrane blebs (Ram, 2005, Wolf, 2003). The membrane blebs are formed either from the transient detachment of the cell membrane from the actin cortex or the localized rupture of the actin cortex, where the amoeboid blebbing cells migrate due to actomyosin contraction (Charras, 2008b, Lorentzen, 2011, Frackler, 2008). Tumour cells can use blebs as an alternative to the lamellipodia-driven migration in 3D environments switching between bleb mode and filopodia-lamellipodia mode (Charras, 2008a, Yoshida and Soldati, 2006). The transitions between mesenchymal and amoeboid migration modes are associated with actin protrusivity and actomyosin contractility independent of the cell morphology, polarity and adhesions, which the contractile actin cortex is crucial in driving bleb retraction (Bergert et al., 2012, Charras et al., 2006). The morphology of mesenchymal migrating cells and amoeboid cells are different, the mesenchymal migrating cells have adherent, long and extended tail from the cytoplasmic cell body, which leaves a trailing path behind when they move; whereas in amoeboid cells the tail is almost disappeared and rounded, which de-adhesion and tail retraction is much more efficient and migration is faster (Mitchison and Cramer, 1996, Charras, 2008a, Lammermann, 2009). Currently, the effect of inhibition of SUMOylation on cell plasticity is unknown but it may be important in cancer metastasis.

Ubc9 has other effects in the cells. Ubc9 was shown to promote breast cancer cell invasion and metastasis in a SUMOylation-independent manner, which was distinct from its role in conjugating SUMO to protein substrates (Zhu et al., 2010). A case-control study in 181 breast cancer cases and 277 controls has shown that the variability of the polymorphism of the Ubc9 gene is associated with an increased risk of ductal breast cancer occurrence (Wozniak et al., 2014). Ubc9 expression levels were much higher in ovarian tumours (Mo et al., 2005) and up-regulated in breast, head and neck and lung cancer (Wu et al., 2009).

Directionality is an important indicator in cell motility; directional persistent cell movement is accomplished by the formation and stabilization of actin-rich membrane protrusions, lamellipodia maintenance determining the orientation of the cell leading edge, actin-myosin contraction convergence on the regulation of Rho family GTPases, topography of the ECM, cell polarity and cell adhesion (Petrie et al., 2009). In the presence of GA, some of the cells become less retractile, i.e. the leading edge of the cells were less extensive with spiky protrusion activities and some cells were almost stuck in one point; compared to the control, MDA-MB-231 cells were spindle-shaped and their lamellipodial structures were constantly protruded and retracted, this occurred less frequently in the GA treated cells.

During cell migration, there are other factors involved in SUMOylated such as Rac 1 and the cytoskeleton. Rac 1 (Rho GTPase family) has been discovered to conjugate with SUMO-1 and Rac 1 interacts with a SUMO E3 ligase, PIAS3; this controls Rac 1-GTP levels and is required to increase Rac 1 activation, stimulate optimal cell migration and invasion in relation to hepatocyte growth factor (HGF) signalling (Castillo-Lluva et al., 2010). Rac 1 or Cdc42 activation is required for Arp 2/3-dependent actin polymerisation (Bergert et al., 2012). Cell membrane protrusions/lamellipodial ruffling and spreading at the leading edge in migrating cells requires Rac1, Cdc42 and actin cytoskeleton mediated by integrin $\alpha\beta3$ (Petrie and Yamada, 2012, Parsons et al., 2010, Huveneres and Danen, 2009). The inhibition of SUMOylation caused impaired FA disassembly resulting in decreased speed of cell migration; however, the effects accounted for the decrease in cell migration cannot be excluded for Rac1 SUMOylation.

LC-MALDI/MS/MS analysis of TAP-purified proteins have identified actin as a putative SUMO-1 and SUMO-3 substrate (Rosas-Acosta et al., 2005). Several other studies have also applied proteome-wide approaches to identify SUMOylated substrate proteins and shown actin is a substrate (Panse et al., 2004, Vertegaal et al., 2004, Wohlschlegel et al., 2004). Emerging evidence has shown several SUMOylated targets in the cytoskeleton including the microtubules, i.e. α/β tubulin; microfilaments, i.e. actin and Rac 1 and

intermediate filaments i.e. vimentin (Alonso et al., 2015). Vimentin (vimentin₃₅₄) was shown to be modified by SUMO-1 in the nucleus in invasive glioblastoma multiforme cells; the SUMOylated vimentin₃₅₄ was stimulated by PIAS3, which played an important role in the inhibition of glioma cell migration (Wang et al., 2010). Actin cytoskeleton-myosin linkage to FAs exert tension and contractile forces which leads to cell motility (Hu et al., 2007, Giannone et al., 2007). Nuclear actin has been firstly shown to be modified by SUMO 2 and SUMO 3 *in vitro* and *in vivo*; computational modelling and site-directed mutagenesis have identified K68 and K284 are critical SUMO binding sites for the SUMOylation of actin (Hofmann et al., 2009).

Similarly, inhibiting protein SUMOylation in cells could affect the cytoskeleton e.g. actin, as FA associates with actin, however, these potential SUMOylation substrates need to be determined individually to see whether they can be SUMOylated firstly. Antibodies against cytoskeleton e.g. microtubule and actin can be used in the IHC studies to visualize the effects of these SUMOylation inhibitors on cytoskeleton, count for the number or size of microtubules or actin to determine whether any changes on cytoskeleton could be resulted from the inhibition of SUMOylation.

The microenvironments are important for the cells. Non-compressed rat tail collagen type I matrix has been used in the FA turnover (live cell) experiments to enable the observation of FAs in 2.5D experimental conditions, as the tumour microenvironment is important, the differences in matrix type and the composition of the matrix could affect the formation of FAs. The ECM softness can significantly influence cell-matrix adhesions (Zaman et al., 2006). An increase in matrix stiffness can increase the number and size of focal adhesions (Gu et al., 2014). 3D migration assays have been used for the analysis of cell migration process, as breast carcinoma cells move within a 3D collagen matrix network (Entschladen et al., 2005).

In this study, a 2.5D collagen matrix system was used, where MDA-MB-231 cells were grown on the collagen border forming a tracking path aligned with the collagen interphase or the cells were seeded on top of the collagen. MDA-MB-231 cells were previously transfected with GFP-talin-1, GFP-vinculin or GFP-FAK plasmids. The cells seeded in this 2.5D collagen matrix model expressed GFP-tagged FA proteins dynamically over a short period of time (optimal transfection window was within 24 hours from the transfection point), which was useful to apply and study the effects of the inhibitor GA caused in the changes of the dynamic FAs activities. These GFP-tagged FA transfected cells could also be imaged using

Reflection imaging on the confocal microscope, which reflects away the light making the collagen matrix visible and the FA proteins expressed by the cells could be seen.

In this experiment, FAs were difficult to detect in the 3D collagen matrix when the cells were fully embedded, which could make the analysis difficult and inaccurate. From the literature, FAs were not easily detectable in cells embedded deeply in 3D matrix, several explanations have been proposed for the lower expressions of FAs in 3D: their turnover time was too fast, their occupied size was uncertain or the down-regulation of FAs was mediated through post-transcriptional mechanism (Kubow and Horwitz, 2011, Fraley et al., 2011, Wang, 2003). In Kubow and Horwitz's study using rat tail collagen with the mesenchymal cell line U2OS osteosarcoma and HT1080 fibrosarcoma cells transfected with the EGFP-paxillin construct under the 'crippled' CMV (cytomegalovirus) promoter control showed reduced fluorescence background, which revealed adhesions in 3D collagen matrix; as over-expression of fluorescently-labelled proteins such as GFP-tag FA proteins could accumulate and cause molecular diffusion in the cytoplasm, which resulted in diffused fluorescence background and masked the actual observation of the adhesion 'dots' in 3D cellular compartments (Kubow and Horwitz, 2011, Fraley et al., 2010). The truncated CMV promoter could reduce protein expression from the EGFP paxillin plasmid resulting in lowered plasmid copy number than EGFP-paxillin and enhanced visualisation of paxillin in U2OS and HT-1080 cells (Kubow and Horwitz, 2011).

Another study showed that using GFP-talin encoding baculovirus, discrete adhesions and their dynamics were visualized and analysed during cell migration in a 3D environment (Deakin and Turner, 2011). Using intravital imaging from cancer cells injected into the deep dermis of mice, the existence of adhesion aggregates (GFP-paxillin and GFP-vinculin) were able to be shown for the first time *in vivo* and these adhesion aggregates seemed to share similarities with the ones found in 3D collagen matrices (Geraldo et al., 2012).

Fraley et al. suggested that when the distance of the cells expressing FAs from the matrix substrate was 200 μm or more suggesting the cells were fully embedded in the matrix, the FAs were hardly seen; in their experiment, the number and size of FAs (paxillin or zyxin) in HT1080 cells were automatically measured using a thresholding technique in NIS-Elements software, which also showed that the number of FAs was decreased from 20/per cell in 2D environment to 14/per cell in 2.5D environment to 4/per cell in 3D (<200 μm) and it was no longer detected in 3D (>200 μm); similarly, the size of FAs was decreased from 1 μm^2 /per cell in 2D environment to 0.4 μm^2 /per cell in 2.5D environment and further down to 0.25 μm^2 /per cell in 3D (<200 μm) until no longer seen in 3D (>200 μm) (Fraley et al., 2011).

The formations of the FAs are different in 2.5D collagen matrix and 2D fixed gelatin coated coverslips (Table 6). In the 2D cell culture microenvironments, the cells were grown on hard surfaces and the cells responded to the changes in the stiffness of the substrate they were surrounded in (Discher et al., 2005). The dimensionality of the cells in connective tissues or organs are embedded deeply whereas the cells are adhered and flattened on 2D standard tissue culture ECM-coated coverslips or surfaces (Geiger, 2011). The mechano-sensing FA formation is different in different surfaces, which this could affect adhesion, spreading and the tension forces generated at the cell protrusions (Goldmann and Ingber, 2002). In tissues cells are in contact with multiple layers of ECM components and consequently, several types of integrin may be activated creating multiple signalling cascades *in vivo* (Wozniak et al., 2004). The microenvironments *in vivo* are very heterogeneous and complex, however, it has been suggested that 2D FAs are an exaggerated version of FAs in 3D (Wozniak et al., 2004). Given the complexities of the environment *in vivo* which makes imaging FAs extremely challenging, the role of SUMOylation in FA turnover *in vivo* will require significant further study.

The FA number, size and turnover time in MDA-MB-231 cells have been compared with the other types of cells in the literature. The dynamics of vinculin to its recruitment to FA is tension-dependent; higher tension/force applied across vinculin is associated with adhesion assembly and increase in size (Grashoff et al., 2010). The rate of assembly of adhesion is increased upon force increases (Hákonardóttir et al., 2015). Fibronectin-mediated FAK activation was tension-dependent to integrin $\alpha 5\beta 1$ in HT1080 cells (Seong et al., 2013). Vinculin itself is important in FA turnover; vinculin^{-/-} mouse embryo fibroblasts MEFs showed smaller, much less abundant but a higher turnover rate FAs compared to wild type MEFs (Saunders et al., 2006). The mean vinculin containing FA number was 100 and the mean vinculin containing FA size was $0.8 \mu\text{m}^2$ in NIH3T3 mouse fibroblast cells (Humphries et al., 2007), compared to 34 and $0.64 \mu\text{m}^2$ in 2D experimental conditions in MDA-MB-231 cells, the mean vinculin containing FAs number was nearly halved and the mean vinculin containing FAs size was smaller in MDA-MB-231 cells compared to NIH3T3 cells (Humphries et al., 2007). The lifetime of FAs in embryonic fibroblast cells on FN coated coverslips was less than 2 minutes (Ren et al., 2000), compared to MDA-MB-231 cells in this study, the mean turnover time of FAs was 34.3s (talin), 31.5s (FAK) or 27.4s (vinculin), which was much faster, indicating the different substrate surfaces the cells were grown on (collagen I was used in the FA turnover study) and the different cell phenotype. In wild type keratinocytes on coated FN coverslips, the mean vinculin containing FAs size was $1.6 \mu\text{m}^2$ and the turnover time was 30 minutes (Schober et al., 2007), which was doubled the mean size of vinculin containing FAs in MDA-MB-231 cells and the turnover time was much longer

in the keratinocytes. The vinculin FA number was 102 in MCF10a human breast epithelial cells (Bays et al., 2014). The vinculin FA size was about $0.4 \mu\text{m}^2$ in MDA-MB-231 cells, perhaps they were under different experimental conditions as these cells were transfected with a control siRNA, subcloned or coinfecting with retroviruses (Yang et al., 2009). Fast cell migration is correlated with intermediate FAs lifetime and rapid renewal of the FA proteins; moreover, the FA lifetime is inversely correlated with FAs strength, where the epithelial cells on FN coated coverslips showed that at high FN (30 $\mu\text{g}/\text{ml}$) with high adhesion strength, the FAs did not disassemble within 45 minutes, at intermediate FN (10 $\mu\text{g}/\text{ml}$) or low FN (5 $\mu\text{g}/\text{ml}$), FAs average lifetime was 17 and 9 minutes (Gupton and Waterman-Storer, 2006). Therefore, the FAs number, size and turnover time was dependent on the cell line studied and the ECM matrix used. MDA-MB-231 cells were known to be motile and invasive, which accounts for the fast turnover time of their FAs.

The inhibition of SUMOylation using various inhibitors have increased the mean FA number and size significantly in MDA-MB-231 cells and U2OS cells. This implies that SUMOylation plays an important role in the dynamic activities of FA in cell migration. This leads to the next step to identify whether talin and vinculin are protein substrates for SUMOylation and can be SUMOylated.

Chapter 4 – SUMOylation of Talin and Vinculin

4. 1 Introduction and Hypothesis

Talin Turnover in FAs and Cell Migration

Talin has two isoforms, talin 1 and talin 2, talin 1 is essential for integrin-mediated cell adhesion (Debrand et al., 2009). Talin contains the globular N-terminal FERM (band 4.1, ezrin, radixin and moesin) domain (F0-F3 domains), which binds to the proximal Asn-Pro-x-Tyr (NPxY) motif in β -integrin cytoplasmic regions; the C-terminal tail domain of talin contains actin binding sites (ABS) (Ziegler et al., 2006). The FERM domains F3 binds to integrin β tails whilst F1 and F2 are required for membrane association and integrin activation, cell spreading and FA assembly (Elliott et al., 2010). The rod domain of talin contains multiple vinculin binding sites (VBSs) (Gingras et al., 2005). Talin is autoinhibited by an intramolecular interaction between the FERM and the rod domains, which are highly conserved sequences in human and flies and talin autoinhibition is required for morphogenesis (Ellis et al., 2013). Talin autoinhibition is essential and a key process in the mechanism of controlling integrin activation and cell adhesion, where the C-terminal rod domain of talin specifically masks a region involved in the interaction of the phosphotyrosine binding domain (PTB) of the N-terminal talin head, allosterically locking up talin in a closed conformation whilst this PTB domain of talin is competitive for integrin β membrane proximal cytoplasmic tail binding (Goksoy et al., 2008).

The talin head consists of amino acids 1-400 and the talin head is linked via the linker residues between 401-481 and at the linker regions it contains calpain-2 mediated cleavage sites between Q433 and Q434, followed by the C-terminus long flexible talin rod domain consisting of the amino acids from 482-2541 (13 helical bundles, R1-R13) (Bate et al., 2012). It has been shown that the talin, FAK, Src, p130CAS, paxillin, myosin light-chain kinase (MLCK) and the ECM signalling regulated-kinases engaged with the integrin are critical in FA turnover (Lebart and Benyamin, 2006).

The small GTPase Rap1 and its effector RIAM bind directly to talin leading to talin-dependent integrin activation and recruitment of talin to the plasma membrane (Goult et al., 2013a). Talin and RIAM focal complexes can activate integrin at the cell leading edge, where FA maturation is required of talin and vinculin FA complexes (Goult et al., 2013b). The binding of vinculin and RIAM to talin R2R3 domain is mutually exclusive: the binding of vinculin to talin requires both protein partners domain unfolding (Gingras et al., 2006) and

talin and vinculin binding is found in mature FA; whereas RIAM can bind to talin R2R3 folded domain directly and is found in nascent FA (Goult et al., 2013b).

The binding of talin to β integrin and the interactions between talin, vinculin and actin are also strengthened and regulated by Phosphatidylinositol-4,5-bisphosphate (PtdIns(4,5)P₂) indicating this lipid mediator is involved in focal adhesion assembly (Ling et al., 2002). The recruitment of talin to the plasma membrane and its localization to the integrin-mediated FAs in spreading cells is facilitated by the phosphorylation of type I phosphatidylinositol phosphate kinase isoform- γ 661 (PIPKI γ 661, an enzyme that makes PtdIns(4,5)P₂), PIPKI γ 661 is phosphorylated by c-Src and phosphorylation is regulated by FAK; PIPKI γ 661 tyrosine phosphorylation increases its binding affinity of PIP₂ to talin head and talin binding between PIPKI γ 661 and β 1 integrin may regulate dynamic FA turnover (Ling et al., 2003, Ling et al., 2002).

Talin is one of the first FA proteins that recruits to integrin binding and triggers FA assembly to activate downstream signalling, which the cells can respond to (Shattil et al., 2010). Talin-1 can regulate cell migration and metastasis in 3D, and it has been reported that overexpression of talin-1 enhanced prostate cancer cell adhesion, migration and invasion by activating survival signals through phosphorylation of FAK and Src and mediating anoikis resistance *in vitro* (Sakamoto et al., 2010); shRNA talin-1 knockdown resulted in significant suppression of prostate cancer cell migration and invasion *in vitro* and significant inhibition of metastasis *in vivo* (Sakamoto et al., 2010). Talin-1 was reported as a valuable marker for diagnosis and prognosis of hepatocellular carcinomas (Zhang, 2011). p130Cas, Src and talin regulate oral carcinoma invasion and cisplatin-resistance (Sansing et al., 2011). Cell adhesions and remodelling of the ECM requires bidirectional integrin signalling and linkages between ECM, integrin and cytoskeleton; cells lacking both talin 1 and 2 could abolish ECM-integrin-cytoskeleton linkage, particularly, downstream FAK signalling was severely affected and the cells form unstable lamellipodial spreading on substrates, where the traction force generation was also diminished (Zhang et al., 2008b).

The calcium-dependent protease, calpain, is able to regulate the focal adhesion complex disassembly (Bhatt et al., 2002). A list of calpain substrates including the focal adhesions, focal complexes, podosomes or integrin-containing clusters that can be cleaved by calpain include: α -actinin, filamins, talin, vinculin, paxillin, FAK, integrin β 1, β 3, zyxin, cortactin, spectrin, P130CAS, PKC, RhoA and tubulin etc (Lebart and Benyamin, 2006, Glading et al., 2002). Calpain mediated proteolysis of talin is critical for FA disassembly and the cleavage of the other FAs such as vinculin etc are also dependent on the ability of calpain to cleave

talin, therefore this is important in the regulation of FA turnover (Liu and Schnellmann, 2003, Franco et al., 2004). The talin head and rod liberated by the calpain-2 cleavage has been shown to be important in FA turnover (Bate et al., 2012). The cleavage of talin separates the N-terminal 47kDa talin head domain from the C-terminal rod domains and this cleaved talin head was found to have a 6-fold higher binding affinity for the integrin β 3 tail than the intact talin (Yan et al., 2001). This mechanism of action of talin cleavage may contribute to the clustering and activation of these integrin receptors (Yan et al., 2001).

Vinculin Turnover in FAs and Cell Migration

Vinculin contains the 90-kDa globular head N-terminus domain and the 30-kDa tail C-terminus domain connected by a proline-rich hinge region (Miller et al., 2001). The C-terminal tail region of vinculin contains conserved region for direct paxillin binding associated with the focal contacts (Bendori et al., 1989, Wood et al., 1994). Vinculin is also autoinhibited by a head-tail Vh-Vt intramolecular interaction, which mask the binding sites for talin in the Vh D1 domain and actin, paxillin and phosphatidylinositol (4, 5)-biphosphate (PIP2) binding sites to the Vt domain (Cohen et al., 2005, Janssen et al., 2006). The vinculin head Vh contains D1-D4 domains and the vinculin tail Vt consists D5 (Bakolitsa et al., 2004). Vinculin is activated through talin and α -actinin high-affinity vinculin binding sites (VBSs) buried in talin rod domain and these VBSs are sufficient to disrupt the Vh-Vt intramolecular interactions of vinculin, which induces conformational change allowing talin and α -actinin binding to Vh and for the vinculin to bind to F-actin in its Vt domain (Bois et al., 2006, Borgon et al., 2004).

The formation of tumour metastases are associated with the phenotypic changes in reduced cell adhesion and increased cell motility, which are related with the loss of vinculin (Carisey and Ballestrem, 2011). The cells lacking vinculin or with much reduced vinculin level were usually less spreading, less adhesive i.e. containing smaller and fewer adhesion plaques and became much more motile (Xu et al., 1998, Rodríguez Fernández et al., 1993, Coll et al., 1995). Upregulated expression of vinculin could alter locomotion properties of the cells, which were severely suppressed (Fernández et al., 1992). So far, 19 binding partners of vinculin have been identified including talin-1, α -actinin, catenin α/β , vinexin α/β , VASP, Arp2/3, paxillin, F-actin, calpain, PIP2 and so on (Carisey and Ballestrem, 2011).

Hypothesis

The previous chapter has shown that the inhibition of protein SUMOylation using GA, 2-D08, gossypetin and Ubc9 siRNA produces more numerous FAs, larger FAs and prolonged FA turnover time. Moreover, inhibiting protein SUMOylation decreases the speed of cell migration in MDA-MB-231 cells. This suggests that SUMOylation plays a critical regulatory role in the dynamic activities of the FAs, particularly in the disassembly of FA turnover. Talin and vinculin are focal adhesion proteins, which are important in their recruitment to integrin and in focal adhesions disassembly. Therefore, in this study, talin and vinculin have been studied to determine whether talin or vinculin can be SUMOylated.

Three different immunoprecipitation methods have been used in two cell lines: MDA-MB-231 cells and U2OS cells. The first IP experiments were conducted using whole cell lysates to investigate whether endogenous talin or vinculin could be SUMOylated. Then, a HA-tagged SUMO-2 plasmid was used. This would introduce the HA-tagged SUMO plasmids into the cells for them to overexpress SUMO-2 level transiently. This IP method would generate consistently precipitated SUMOylated proteins. A third IP method was to use a SUMO VIVA™ Binding Assay system to investigate whether talin or vinculin could be SUMOylated within isolated concentrated focal adhesions.

A possible consequence of SUMOylation is its potential role in FA protein-protein interactions. Co-immunoprecipitations in the presence of inhibitors GA, 2-D08, gossypetin and Ubc9 siRNA would be used to investigate the role of SUMOylation in protein-protein interactions in both cell lines.

4.2 Method Development

In order to immunoprecipitate the individual talin or vinculin proteins in the MDA-MB-231 cells or the U2OS cells, specified IP methods were developed and modified. The cells were initially immunoprecipitated only with the endogenous talin, vinculin or SUMO 2/3 to determine in the western blotting whether they could be SUMOylated. Later, the cells were transfected with the HA-tagged SUMO-2 plasmids to overexpress SUMO-2. A third method was to use a SUMO binding column kit and a SUMO binding assay was developed.

The methods were developed as: IP and WB detection of the SUMOylated talin or vinculin in the whole cell lysates only or reverse IP and WB; IP SUMO-2 and WB detection: transfection of the cells with the HA-tagged SUMO-2 plasmid; SUMO VIVA™ binding assay – detection of the SUMOylated talin or vinculin and its use in the isolation of the FAs; more concentrated FA collection – investigation on the cleavage of talin.

4.2. 1 Antibodies for IP and WB Experiments

The antibodies used in the IP experiments were the N-terminus and the C-terminus antibodies which could detect the N or C terminal ends of the molecules. For example, the antibodies from Santa Cruz (c-9 or H-300) could detect N-terminal of talin at 230kDa; the antibody from Merck Millipore could detect N-terminal of talin at 250kDa.

Primary antibodies

| | |
|----|--|
| 1 | Purified mouse anti-HA.11 epitope tag monoclonal antibody, 1 mg/ml, 16B12, Biologend (IP: 1:100-150) |
| 2 | Anti-GFP mouse monoclonal antibody [9F9.F9] ab1218, abcam (IP: 1:150-200) |
| 3 | Mouse anti-talin 1 monoclonal antibody reacting with an N-terminal epitope in human talin between amino acids 139-433, Clone TA205, 1 mg/ml, MAB1676, Merck Millipore (IP: 1:100, WB: 1:1000) |
| 4 | Mouse anti-talin monoclonal antibody (C-9) raised against amino acids 1-300 mapping at the N-terminus of talin of human origin, 200 µg/ml, sc-365875, Santa Cruz Biotechnology, INC. (WB: 1:200) |
| 5 | Rabbit anti-talin polyclonal antibody (H-300) raised against amino acids 1-300 mapping at the N-terminus of talin of human origin, 200 µg/ml, sc-15336, Santa Cruz Biotechnology, INC. (WB: 1:200) |
| 6 | Rabbit anti-vinculin polyclonal antibody (H-300) raised against amino acids 1-300 mapping at the N-terminus of vinculin of human origin, 200 µg/ml, sc-5573, Santa Cruz Biotechnology, INC. (WB: 1:200) |
| 7 | Rabbit anti-filamin 1 polyclonal antibody (H-300) raised against amino acids 2348-2647 mapping at the C-terminus of filamin 1 of human origin, 200 µg/ml, sc-28284, Santa Cruz Biotechnology, INC. (WB: 1:200) |
| 8 | Goat anti-filamin 1 polyclonal antibody (N-19) mapping near the N-terminus of filamin 1 of human origin, 200 µg/ml, sc-7565, Santa Cruz Biotechnology, INC. (WB: 1:200) |
| 9 | Goat anti-SUMO 2/3 polyclonal antibody (N-18) mapping at the N-terminus of SUMO-2 of human origin, 200 µg/ml, sc-26969, Santa Cruz Biotechnology, INC. (WB: 1:250-500) |
| 10 | Rabbit anti-SUMO 2/3 polyclonal antibody detecting at the N-terminus, 0.5 mg/ml, P61956, Millipore (WB: 1:1000) |
| 11 | Rabbit anti-SUMO-2 (Sentrin-2) polyclonal antibody, 519100, Invitrogen (WB: 1:1000) |
| 12 | Mouse anti-UBC9 monoclonal antibody (C-12) raised against amino acids 1-81 of UBC9 of human origin, 200 µg/ml, sc-271057, Santa Cruz Biotechnology, INC. (WB: 1:250-500) |
| 13 | Rabbit anti-GAPDH antibody, 1 mg/ml, G9545, Sigma (WB: 1:1000) |

Secondary Antibodies

| | |
|---|--|
| 1 | Alexa-Fluor 546 conjugated donkey anti-rabbit antibody, Fisher (Cy3, 1:1000) |
| 2 | Alexa-Fluor 647 conjugated donkey anti-goat antibody, Fisher (Cy5, 1:1000) |

4.2. 2 Immunoprecipitation and Western Blotting (IP and WB)

IP Preparation with Whole Cell Lysates: 6-well Plates for GA 15, 30 or 60 Minutes

MDA-MB-231 cells were grown on 0.2% gelatin coated coverslips. After GA 15, 30, 60 minutes, the media was aspirated and the cells were washed in cold PBS once. In each time point, 1 ml cold RIPA buffer (25 mM Tris HCl pH 7.6, 150 mM NaCl, 1% v/v NP-40, 1% v/v sodium deoxycholate, 0.1% v/v SDS, Thermo Fisher Scientific) with 1x protease inhibitor cocktail (10 μ l, 1:100, PIC, Calbiochem[®]) was added to the cells for each well at the time point. The 1 ml whole cell lysates sample was split as 500 μ l x 2 for each well. For the immunoprecipitation sample preparations (IPs), 500 μ l lysed cell solution for each well was collected in an eppendorf tube and kept on ice; for the whole cell lysates samples, 500 μ l lysed cell solution was transferred in another eppendorf tube and 80 μ l 6x RSTB buffer was added to the whole cell lysates, vortexed and kept on ice or stored at -20°C.

IP Preparation with Whole Cell Lysates: T25 Flasks

MDA-MB-231 cells were grown on T25 flasks overnight. After drug treatment i.e. GA 6 hours, the media was aspirated in the T25 flasks (control and treated) and the cells were washed in cold PBS once. 3 ml cold PBS was added to each T25 flask. A sterile disposable cell scraper (Fisher scientific) was used to get the cells detached. The cells were re-suspended in 3 ml cold PBS and transferred into cold 15 ml Falcon tubes on ice. The cells were then centrifuged at 1500 rpm for 10 minutes at 4°C. The cell pellet was formed in the tube and the PBS was drained. 297 μ l cold RIPA buffer mixed with 3 μ l PIC was added to the cell pellet in the tube. A needle was used to re-suspend and shear the pellet with forces. Each Falcon tube was stood on ice for 30 minutes. The cell suspension from each Falcon tube was then transferred into a cold eppendorf tube and centrifuged at 13, 000 rpm for 15 minutes at 4°C. The supernatant was transferred into a new cold eppendorf tube and kept on ice; the pellet was discarded. 15 μ l of the prepared cell supernatant in each eppendorf tube ('control' and 'treated') was used for Bradford assay. The rest of the supernatant samples were added with 5x RSTB buffer, vortexed and stored at -20°C.

IP and Reverse IP with the Whole Cell Lysates

2-5 x 10⁵ cells were plated in each T25 flask initially. The IP talin or vinculin samples (Western blotting: IB with SUMO 2/3 ab) and the reverse IP SUMO 2/3 samples (IB: with talin or vinculin ab) were prepared as shown in Table 7. After whole cell lysates preparations, each endogenous IP sample was added with the FA antibody (talin or vinculin, single antibody used). Western blotting was done with the SUMO 2/3 (N-18) goat polyclonal antibody (Santa Cruz). The reverse endogenous IP sample was added with the SUMO 2/3 antibody and the reverse WB would be done with the FA antibodies (talin or vinculin ab). For the whole cell lysates prepared in the 6-well plates, the samples (500 µl control or treated) were centrifuged at 10.000 rcf for 10 minutes at 4°C. The supernatant was transferred into a new eppendorf tube for each sample.

| | | | | |
|--|------------------------|------------------------|------------------------|------------------------|
| Endogenous IP: Talin | Control | GA 15 minutes | GA 30 minutes | GA 60 minutes |
| 6-well plate | 500µl wcl + talin ab |
| T25 flask | 300µl wcl + talin ab |
| Western Blotting | IB: SUMO 2/3 | IB: SUMO 2/3 | IB: SUMO 2/3 | IB: SUMO 2/3 |
| Endogenous IP: SUMO 2/3 (reverse) | Control | GA 15 minutes | GA 30 minutes | GA 60 minutes |
| 6-well plate | 500µl wcl + SUMO2/3 ab |
| T25 flask | 300µl wcl + SUMO2/3 ab |
| Western Blotting | IB: Talin | IB: Talin | IB: Talin | IB: Talin |

Table 7. The endogenous IP experiments were only done with the whole cell lysates prepared from either 6-well plate or T25 flask. For each IP sample i.e. control vs. GA treated, only 1 antibody was added into each sample. This experiment was repeated for the vinculin antibody used, i.e. all the samples were prepared and each of the endogenous IP samples were added with vinculin ab only and the reverse SUMO 2/3 IP remained the same

Normally, for a T25 flask whole cell lysate, the concentration of the cell lysate i.e. the total protein concentration calculated from Bradford assay was around 1~1.5 mg/ml=1000~1500µg/1000µl. For example, for 1500µg/1000µl, in around 300 µl there was 500 µg total protein concentration. For the talin/vinculin antibody (1mg/ml=1000µg/1000µl, Millipore), 2 µg of the antibody was needed per 100-500 µg of the total protein. Therefore, 2 µl of the talin/vinculin antibody was added to the sample. In practice, 1.2-1.5 µl was added per 300 µl sample. For the talin-1 (H-300, c-9) or the filamin-1 (H-300) antibodies (200µg/1ml, Santa Cruz) used, in practice, 10-15 µl was used for doing the IP (2-3 µg antibody used) and 25 µl was used for doing western blotting. 10 µl SUMO 2/3 goat polyclonal antibody (200 µg/ml, 2 µg final concentration) was added per 500 µl or 6 µl per 300 µl sample and rotated in the cold room at 4°C overnight.

200 µl of the protein A/G plus-agarose beads was taken into an eppendorf tube and span at 2000 rcf for 1min at 4°C; then the beads were washed in 0.3 ml cold RIPA buffer x 3 and

spun at 2000 rcf for 1 minute at 4°C after each wash. The beads were re-suspended in 1.3 ml of cold RIPA buffer (13 samples aliquots); then 100 µl of the re-suspended beads in RIPA buffer was added to each sample tube. The samples were then incubated with the beads in RIPA buffer at 4°C for 2 hours on the rotating machine. After rotating, the samples in the eppendorf tubes were spun at 2000 rcf for 1 minute at 4°C. The first supernatant was removed and obtained into a new eppendorf tube for each sample tube. They were labelled as 1st supernatant and added with the 1x loading buffer directly. All the sample tubes were then washed in 0.3 ml cold RIPA buffer x3. A pellet was obtained in each sample tube after each washing pulling down the beads bound with the antibody attaching to the protein of interest. The pellet was kept and the RIPA washing buffer was discarded. After washing, 100 µl 1x loading buffer was added to each beads-containing sample tube and vortexed. All the 1st supernatant and the eluted IP samples were then boiled at 95°C for 5 minutes.

The samples tubes were spun for 1 minute at 2000 rcf at 4°C, leaving the beads in the pellet at the bottom of the tube (the pulled down talin/vinculin or the SUMO protein were separated in the supernatant). The supernatant in 1x loading buffer for each sample tube was transferred into a new eppendorf tube ready for western blot or stored at -20°C. The pellet beads were discarded.

4.2. 3 pcDNA3 HA SUMO-2 WT Plasmid Transfection, Immunoprecipitation and Western Blotting

HA SUMO-2 Plasmid Transfection / 6-well Plates and IHC

1 x 10⁵ MDA-MB-231 cells were firstly plated and grown on 0.2% v/v gelatin coated coverslips in a 6-well plate 1 day prior to transfection.

| HA-SUMO 2 transfection 6-well plate | Control | GA 1hr |
|-------------------------------------|---|---|
| Per well/volume | 2 ml | 2ml |
| Mixing for 15 minutes | 100µl serum-free media: HA+PEI 1:3 3.4µl+6.8-10.2µl (range) | 100µl serum-free media: HA+PEI 1:3 3.4µl+6.8-10.2µl (range) |
| 24hr transfection incubation | + mixture | + mixture |
| GA treatment at 100µM | Media change only | Media change + GA |
| STOP time | IHC | IHC |

Table 8. The HA SUMO-2 plasmid transfection time for MDA-MB-231 cells for 6-well plates

In Table 8, MDA-MB-231 cells were grown in the 6-well plate and transfected with the HA SUMO-2 plasmid first (in 100 µl serum free DMEM media: 3.4 µl HA SUMO-2 plasmid was added first and a range of 6.8-10.2 µl PEI Polyethylenimine was added the last). The cells were left for incubation for 24 hours. Then, for both control and GA 1hr wells, the cells were

washed with PBS once and fixed in 4% v/v PFA immediately for 20 minutes. Immunostaining was processed and the cells were stained with the mouse HA antibody and Alexa 488 anti-mouse secondary antibody.

HA SUMO-2 Plasmid Transfection / T25 Flasks

The MDAMB231 cells were plated out and grown in T25 flasks as 70-80% confluence overnight. 216-234 μ l serum free DMEM media (total volume 250 μ l) was added with 8.5 μ l HA SUMO-2 plasmid to a sterile eppendorf tube shown in Table 9, the tube end was tapped gently several times. 7.5-25.5 μ l PEI (Polyethylenimine, 1 mg/ml) transfection reagent was added to the mixture the last and the tube end was tapped gently to mix the content well.

| HA-SUMO 2 transfection T25 flask (2.5x factor) | Control 1 flask | GA 15 mins 1 flask | Control 1 flask | GA 30 mins 1 flask | Control 1 flask | GA 60 mins 1 flask |
|--|--|--|--|--|--|--|
| Per flask/volume | 5 ml |
| Mixing for 15 minutes | 250 μ l serum-free media: HA+PEI 1:3 8.5 μ l+ 7.5-25.5 μ l | 250 μ l serum-free media: HA+PEI 1:3 8.5 μ l+ 7.5-25.5 μ l | 250 μ l serum-free media: HA+PEI 1:3 8.5 μ l+ 7.5-25.5 μ l | 250 μ l serum-free media: HA+PEI 1:3 8.5 μ l+ 7.5-25.5 μ l | 250 μ l serum-free media: HA+PEI 1:3 8.5 μ l+ 7.5-25.5 μ l | 250 μ l serum-free media: HA+PEI 1:3 8.5 μ l+ 7.5-25.5 μ l |
| 24hr incubation | + mixture |
| 3 rd day: GA treatment at 100 μ M | Media change only | Media change + GA | Media change only | Media change + GA | Media change only | Media change + GA |
| STOP time | Wash in PBS |

Table 9. The HA SUMO-2 plasmid transfection in the MDA-MB-231 cells for T25 flasks; this was used in the IP experiments.

Table 9 shows the outlines of the T25 flasks prepared and the time for this experiment. The amount of HA SUMO-2 plasmid mixtures were prepared in the eppendorf tubes according to the number of the T25 flasks needed i.e. control flasks vs. GA flasks. The optimal plasmid DNA and the PEI was prepared as 1:3 ratio, however, PEI was also used as much as up to 25.5 μ l and the range was used between 7.5-25.5 μ l. The amount for the serum free media, HA SUMO-2 plasmid or the PEI prepared was also accounted for the 2.5x bigger surface area than 1 well/6-well plate. The Eppendorf tubes were stood in the culture hood for incubation at room temperature for 15 minutes.

After 15 minutes, the HA SUMO-2 plasmid mixture was added into each T25 flask containing 5 ml fresh DMEM media and the transfection time was left for 24 hours. After 24 hours, 100 μ M GA was added into the treatment flasks accordingly and the incubation time was 15, 30 or 60 minutes. In the control flasks, the media was changed only. Antibodies for GAPDH and total Akt were also used for these samples in the western blot experiments to determine

whether GAPDH or Akt could be SUMOylated, therefore they could be used as experimental controls for these HA-tagged SUMO-2 IP experiments.

Immunoprecipitation Using the HA SUMO-2 Plasmid

All the T25 flasks were washed with PBS once. All the buffers and steps were prepared on ice. The lysis buffer was prepared as 300 µl Pierce RIPA lysis and extraction buffer (Thermo Fisher scientific), 3 µl protease inhibitor cocktail (PIC 1x, 1:100, Calbiochem) and 50 µM N-Ethylmaleimide (NEM, stock concentration 100mM: 50mg NEM dissolved in 4ml double distilled H₂O, reagent for the covalent modification of cysteine residues in proteins, Sigma) were added into an eppendorf tube and mixed well. The lysis buffer was prepared enough according to the number of T25 flasks needed. The PBS was removed completely from the T25 flask and the 300µl lysis buffer was added into each T25 flask directly. A sterile disposable cell scraper (Fisher scientific) was used to scrape all the cells in the lysis buffer attached on the bottom of the T25 flask. The whole cell lysate from the T25 flask was collected into a new eppendorf tube immediately and all the whole cell lysate tubes collected from each T25 flask were left on ice. No centrifugation steps were used.

In practice, 1.5-3 µl of the mouse IgG1 anti-HA.11 epitope tag antibody (1 mg/ml, Biolegend, for IP used as 1:100-200) was added into each labelled 300µl cell lysate tube as control or treated. All the sample tubes were rotated with continuous mixing overnight at 4°C. The Pierce™ protein A/G magnetic beads solution (10mg/ml in H₂O containing 0.05% NaN₃, 1ml, Thermo scientific) was gently mixed until all of the beads were uniformly resuspended. 16 µl of the A/G magnetic beads was added into each corresponding eppendorf tube and placed into the magnetic stand (Millipore) to capture the beads. The beads were washed with 500 µl TBST (1x) once in each tube. The beads were captured using the magnetic stand in each tube, the TBST solution was discarded. Each 300 µl wcl sample tube was added with the 16 µl washed magnetic beads correspondingly and mixed well. All the tubes were rotated for 1h at 4°C with continuous mixing.

The sample tubes were re-engaged with the magnet to capture the beads. The first supernatant was removed into a new corresponding eppendorf tube and stored for each sample tube labelled as supernatant control or supernatant treated. The sample tubes were dis-engaged from the magnet and the beads were washed with 500 µl TBST x 3; with each washing, the beads were re-engaged with the magnet and the TBST solution was discarded. 110 µl of the 1x RSTB buffer was added to each IP sample tube (prepared from 1 T25 flask). In practice, 110 µl was appropriate for doing 2 4-20% Mini-PROTEAN® TGX™ precast polyacrylamide gels (10-well, 50 µl, Bio-Rad). For the supernatant samples, each tube was

added with 1x RSTB. The IP beads sample tubes and the supernatant samples containing 1x RSTB buffer were boiled at 95°C for 5 minutes. Then, the IP tubes were put on the magnetic stands to isolate the RSTB solution liberating the precipitated antigens of proteins from the insoluble protein A/G magnetic beads. These were labelled as IP control or IP treated samples.

Western Blotting with Fluorescence

For western blots, 3.5 µl precision plus protein™ dual colour standards was added at the stacking well lane 1 of the 4-20% gel. 50 µl from each prepared IP sample was loaded into the corresponding stacking well. 1x running buffer was prepared from 10x Tris/Glycine/SDS electrophoresis buffer (Bio-Rad) and filled to the mark indicated on the gel tank. The proteins were run through the resolving gel at constant voltage 150V for 45 minutes by SDS-PAGE.

The electrophoresis was stopped until the protein tracking dye migrated just over the black mark gel end. The trans-blot® semi-dry transfer cell (Bio-Rad) was used for protein transfer. 1 gel size was 8.6 x 6.7 cm; all the papers cut were taken for the size of 1 gel. 6 blotting chromatography papers (GE Healthcare, Whatman™) were soaked in the anode buffer (final volume 500 ml: 18.165g 300mM Tris, 100ml 20% methanol prepared in 400ml Nano pure H₂O, dissolved and pH=10.4) for 3-5 minutes and put on the transfer cell. 1 hydrophobic Immobilon®-FL PVDF transfer membrane at pore size 0.45 µm (Millipore, best use for fluorescence scanning) was soaked in 100% methanol for 5 minutes; then the membrane was put on top of the 6 anode buffer soaked papers. The gel was then covered on top of the membrane evenly with no bubbles. 6 blotting papers were soaked in the cathode buffer (final volume 500 ml: 1.514g Tris, 2.624g amino caproic acid, 100ml methanol prepared in 400ml Nano pure H₂O, dissolved and pH=9.2) for 3-5 minutes and put on top of the gel. The excess buffer was removed from the edge of the transfer 'sandwich'. The transfer was set at 15V for 1.5 hrs.

The membrane was blocked in 5% v/v BSA in TBST solution (BSA, Bovine Serum Albumin, First Link, Ltd) for 20 minutes. Then the membrane was blotted with the primary antibody. For example, talin H-300 detecting at the N-terminus of human talin (rabbit polyclonal, Santa Cruz biotechnology) or vinculin H-300 detecting at the N-terminus of human vinculin (rabbit polyclonal, Santa Cruz biotechnology), in practice, these 2 primary antibodies were prepared as 25µl added with 5ml of 2% BSA-TBST solution (1:200). Depending on the size of the membrane used, the primary antibody used was between 20-25µl. The membrane was incubated with the primary antibody overnight at 4°C with continuous rotation.

The membrane was washed with 1x TBST 3 times, each time was 10-15 minutes washing. Then the membrane was added with the secondary antibody. The secondary antibodies used were Alexa Fluor® 546 donkey anti-rabbit IgG (H+L) (red colour, life technologies) or Alexa Fluor® 647 donkey anti-goat IgG (H+L) (blue colour, life technologies). Alexa 546 is equivalent to Cy3, which would be scanned by the green laser on the Typhoon at 532nm; Alexa 647 is Cy5, which would be scanned by the red laser at 635nm. The antibody was prepared in 5ml 2% BSA-TBST solution. The membrane was incubated with the secondary antibody solution for 1hr at 4°C with continuous rotation. After secondary antibody incubation, the membrane was washed with 1x TBST for 3 times, each time 10-15 minutes.

Fluorescent Scanning

The membranes were ready for fluorescent scanning and imaging using the Typhoon FLA 9500 (GE Healthcare). The Typhoon machine has multiple imaging modes which can produce digital images from chemiluminescent, fluorescent or radioactive samples. It scanned the membrane with 2 lasers: green as Cy3, Channel 1 or red as Cy5, Channel 2, which led to the fluorescent dye (secondary antibodies) on the samples emitting light. The secondary antibodies were the Alexa 546 donkey anti-rabbit (pink) Cy3 (which could detect GAPDH, SUMO etc) or the Alexa 647 donkey anti-mouse (blue) Cy5 (talin, Ubc9 etc), which could detect the proteins of interest for separate channels. The membrane was placed onto the glass platen of the Typhoon instrument. The scanner control software was selected with 550-600 scanning parameters; the dye colours were appropriately selected, which the green laser (532 nm) or the red laser (633 nm) could illuminate and produce fluorochrome, which would emit light with a characteristic spectrum. The optical system directs the light through the emission filters, which passes the emitted light to the PMT (photomultiplier tube) only within the filter's bandwidth. The signal can then be converted into digital images. The level of signal is proportional to the amount of fluorescence in the membrane. ImageQuant was used to quantify the variations in the signal and the bands area.

4.2. 4 VIVA Bind™-SUMO Kit and Western Blotting

Whole Cell Lysates Preparations for Non-Flushed Cells with Fibronectin Coating

The T25 flasks were coated with the human fibronectin (hFN) previously before cell plating. 0.4ml of thawed 2mg/ml hFN solution was mixed with 4.6ml cold PBS to make up 150µg/ml working stock solution. For coating each T25 flask, 15µg/ml final concentration was used. 2.5ml of the diluted hFN was added to each T25 flask to coat the base. The hFN solution

was left for 1 hour incubation at room temperature in the culture hood. Then the hFN solution was aspirated off and the flasks were washed with PBS gently.

For the non-flushed MDA-MB-231 cells preparation, the cells were plated into the required number of hFN coated T25 flasks and grown on coated hFN for 2 days in the incubator. The next day, the cells were treated with 100 μ M GA for 1 hour and also the control flasks were prepared. For the T25 flasks, 250-300 μ l lysis buffer supplemented with 50mM NEM (the lysis buffer was included in the SUMO Kit containing 50mM Tris-Cl, pH 7.5, 150mM NaCl, 1% NP40, 0.5% deoxycholate, 200mM iodoacetamide, 0.1% v/v protease inhibitor cocktail III, Roche) was added to each flask immediately and the cells were scraped off. 1 T25 flask wcl collected as 250-300 μ l was enough to add 1 SUMO matrix volume as 40 μ l or up to 75 μ l. All the samples collected in eppendorf tubes were kept on ice. Sonication for the samples was done on ice for about 10s.

VIVA Bind™-SUMO Matrix Preparation

All the preparations were done on ice. The VIVAbind™ SUMO matrix (viva bioscience) was resuspended by inverting the tube gently several times. 40 μ l VIVAbind™ SUMO matrix suspension was aliquoted into required number of capped VIVA biospin™ columns. 250 μ l equilibration buffer (made with 50mM Tris-Cl at pH 7.5, 150mM NaCl and 1% NP40) was added into each capped column and mixed with the SUMO matrix for 1 minute. The base cap was then removed and the columns placed in clean eppendorf tubes and centrifuged at 5000g for 1 minute to collect the matrix. The flow through was discarded. The matrix wash and collection was repeated at least 2 times.

VIVA Bind™-SUMO Assay

200-300 μ l cell lysate was added to each capped VIVAbind™ SUMO matrix column and mixed by inversion. The cell lysate with the matrix for each capped column was incubated at 4°C overnight with continuous rotation. Input samples were also prepared as the whole cell lysates only for the control vs. GA 1 hour. The next day, the column base was uncapped and the column was placed in a VIVA biospin™ collection tube. The collection tubes were centrifuged at 5000g for 1 minute to collect the matrix. The first flow through was removed and retained as 1st supernatant unbound fraction. These unbound samples were later added with 1x RSTB buffer and noted as control unbound vs. GA unbound. The input and the unbound samples were calculated for the protein loading control using the Bradford assay. The columns were replaced in the corresponding collection tubes and the materials were washed with 250 μ l wash buffer (made with 50mM Tris at pH 7.5, 250mM NaCl and 1%

NP40). The collection tubes were centrifuged at 5000g for 1 minute to collect the matrix and the flow through was discarded. The materials were washed 3 times.

Elution of Captured SUMOylated Proteins

The columns were capped again and 100µl 1x RSTB SDS-PAGE sample loading buffer was added to each capped column and mixed by inversion. The columns were placed in heat-protected clean microfuge tubes. The tubes were heated to 95°C for 5 minutes. The base caps were removed and the columns were centrifuged at 5000g for 1 minute to collect the eluted materials. These were ready to run on the gels. The input, unbound and eluted samples were run on 4-20% gradient gels. The eluted samples were run twice on the gels. The IP eluted samples were blotted with talin or vinculin antibody and GAPDH antibody for each membrane.

4.2. 5 Isolation of Focal Adhesions with the VIVA Bind™-SUMO Kit and Western Blotting

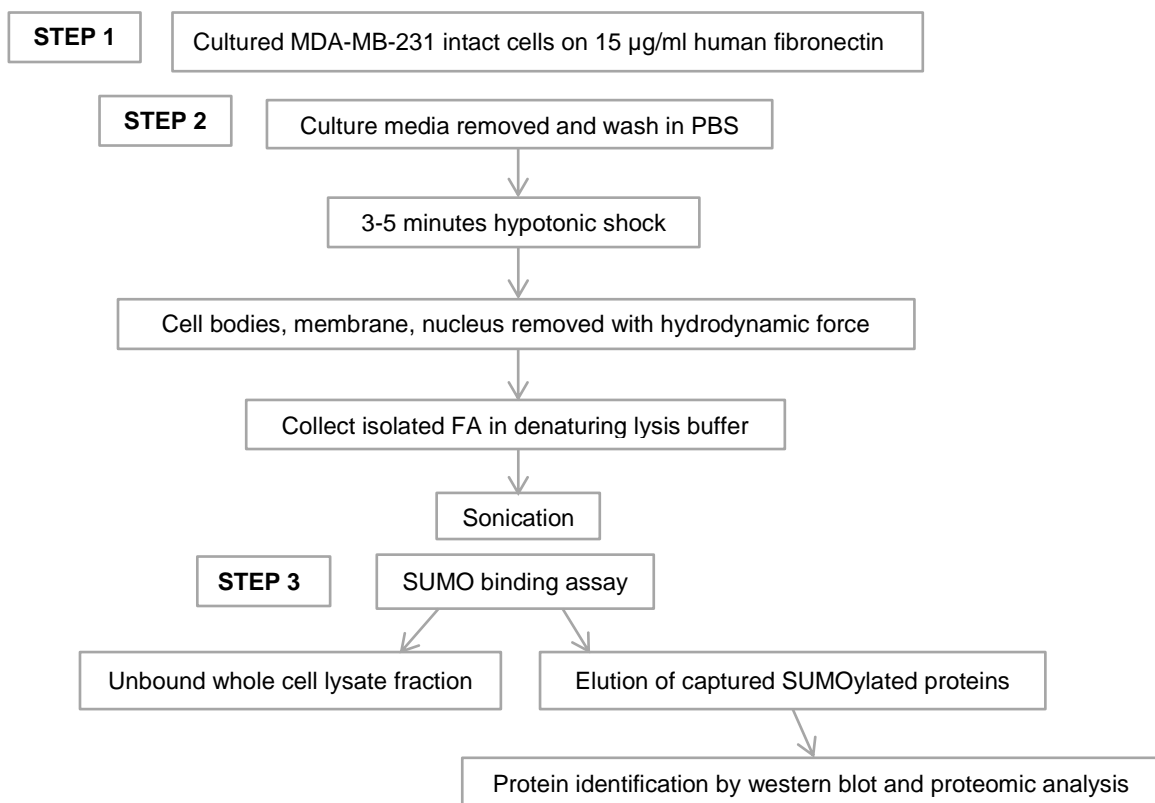


Figure 35. The isolation of FA outlined method shown in three steps

The focal adhesion isolation protocol was modified from Waterman C.M. 2011 (Integrin and cell adhesion molecules, methods and protocols, chapter 19) in Figure 35. MDA-MB-231 cells were grown on fibronectin (15µg/ml) coated T25 flasks or petri dishes and left in the incubator at 37°C/5% CO₂ for 1-2 days. The dishes were prepared as control petri dishes x3 and GA 1h dishes x3. A higher concentrated isolated FA whole cell lysates were also prepared as control petri dishes x6 and GA 1h dishes x6. The culture media was removed and the cells were washed in 1x PBS once. The osmotic shock and the trituration steps were optimized for the MDA-MB-231 cells. The cells were incubated in 2.5mM low ionic strength TEA buffer (Triethanolamine, Sigma, 7.5mg TEA was dissolved in 20ml ddH₂O, pH 7.0) for 3-5 minutes at room temperature. This would give the cells a hypotonic shock, which gave osmotic pressure inside the cells, as the cells were observed a little bit swelling in the cell body and around the cell plasma membrane indicating the membrane integrity was weakened. At this time, the cells were given strong trituration quickly to remove the nuclei, soluble proteins and materials of the cytoplasm. An Ultra Waterpik® Waterflosser® Jet water flush was used, which the tank was filled with 1x flushing buffer containing 20ml of 1x PBS mixed with 200µl 1x PIC and 50mM NEM. The trituration pressure was set between '0' and '1' and the nozzle of the waterflosser was held at about 150° angle with a slight tilt towards the neck of the T25 flask or the edge of the petri dish. It was sprayed evenly and carefully across the entire dish/flask area with the nozzle back and forth. The spraying lasted for about 8~10s. This gives hydrodynamic force on the cells to flush out cell bodies, nuclei, cell plasma membranes leaving only focal adhesions adhered on the bottom of the T25 flasks or the petri dishes. The excess buffer was removed and the cells were washed with fresh PBS once. The flushing buffer was collected after each spraying and recycled for use in trituration of the next dish. The isolated FAs were collected in denaturing lysis buffer. 100µl RIPA containing 1µl PIC and 20µl 20mM NEM was added to each dish and a cell scraper was used to remove and collect the rest remaining cell contents. Sonication was supplied to the collected FA samples for about 10s on ice.

The flushed FA samples were then run through the SUMO binding kit column containing 40µl SUMO matrix to obtain 'unbound' and 'eluted' samples. 'Input' samples were also run through for the samples which were probed for GAPDH. Some eluted samples were stored at -20°C for proteomic analysis later. The protein amount of the isolated FAs was compared between the non-flushed and the first flushed unbound samples. Antibodies used were talin, vinculin, FAK, paxillin, α-actinin, α-tubulin, phosphor-Rac1/Cdc42 and actin which are known FA or FA associated proteins. Antibodies including total Akt, phospho-Akt, phospho-p44/42 MAPK (Erk1/2), E-cadherin, cleaved caspase 3 and RhoA were also used to detect these proteins in the flushed wcl samples. In the higher concentration of FA isolation experiment,

the eluted samples were split in eppendorf tubes x3 and loaded onto separate gels x3. For western blot, the samples were run with 50µl loaded on the 4-20% precast gel. Talin and vinculin primary antibodies were used.

Stripping and Re-blotting with the Isolated FA Samples

The membranes were washed in TBST x3. 1x stripping buffer (Millipore) made from 0.5ml+4.5ml ddH₂O was added to each membrane sealed in the plastic bag and rotated for 20 minutes at room temperature. The stripping buffer was removed and the membrane was washed in TBST x3. The membranes were re-blocked in 5% v/v BSA-TBST for 20 minutes. Then the membranes were blotted with the vinculin primary antibody and incubated overnight.

4.2. 6 Co-Immunoprecipitation

MDA-MB-231 cells or U2OS cells were grown in T25 flasks overnight. 1 set of 4 T25 flasks of cells were transfected with the GFP-Talin 1 plasmid (414.5µg/ml) as IP talin and 2 sets of 4 T25 flasks of cells were transfected with the mEmerald-vinculin plasmid (861.6µg/ml) as IP vinculin (Table 10). In total 12 T25 flasks were prepared. The transfection ratio was 1:3. Then IP whole cell lysates were made by using the mouse GFP antibody for these IP talin or IP vinculin samples, pulling down all the talin or vinculin proteins for each cell line used. Western blotting was done; in the IP talin and WB experiments, these samples were blotted with filamin-1 or actin antibodies; in the IP vinculin WB experiments, these samples were blotted with talin-1 antibodies.

| HA-SUMO 2 transfection T25 flask | Control 1hour 1 flask | GA 1hour 1 flask | Goss 1hour 1 flask | 2D08 1hour 1 flask |
|---|-------------------------------|-------------------------------|-------------------------------|-------------------------------|
| Per flask/volume | 5 ml | 5 ml | 5 ml | 5 ml |
| Mixing for 15 minutes | 250µl serum-free media: 1:3 |
| IP talin | GFP-talin 1+PEI 6µl+7.5µl | GFP-talin 1+PEI 6µl+7.5µl | GFP-talin 1+PEI 6µl+7.5µl | GFP-talin 1+PEI 6µl+7.5µl |
| IP vinculin | mE-vinculin+PEI 3 µl+7.5µl | mE-vinculin+PEI 3 µl+7.5µl | mE-vinculin+PEI 3 µl+7.5µl | mE-vinculin+PEI 3 µl+7.5µl |
| 24hr incubation | + mixture | + mixture | + mixture | + mixture |
| 3 rd day: drug treatment at 100µM | Media change only | Media change + GA | Media change + Gossypetin | Media change + 2D08 |
| STOP time | Wash in PBS | Wash in PBS | Wash in PBS | Wash in PBS |

Table 10. Showing the transfection time and different drug treatments for each T25 flask

In Table 10, 6µl GFP-talin 1 or 3µl mE-vinculin plasmid (1 µg plasmid DNA used and applied for 2.5x surface area in T25 flask) was mixed with 7.5µl PEI; the mixture was added into the corresponding T25 flask for 24 hours incubation. Then the cells were treated with GA, Goss

or 2-D08 for 1 hour at 100 μ M final concentration. Whole cell lysates were made. 1.5 μ l of the anti-GFP antibody was added into each IP whole cell lysates samples. All the samples were incubated at 4°C for continuous rotatory mixing overnight; 16 μ l of the washed protein A/G magnetic beads were added into each IP samples for immunoprecipitation and the steps were described in the IP methods previously; these samples were ready for WB experiments.

4.2. 7 Co-Transfection with siRNA and HA SUMO-2 Plasmid

MDA-MB-231 cells were grown on T25 flasks overnight. The cells were transfected with 25nM Ubc9 siRNA the next day for 24 hrs. Then at the 24 hrs point, the cells were transfected with the HA-SUMO-2 plasmid for 24 hrs. This would be within the time as the Ubc9 siRNA transfection time was for 48 hrs. Then the cells were made whole cell lysates and IP samples were prepared. Western blotting was done and talin primary antibody was used.

Results

4. 3. 1 IP and WB Reveals Talin is SUMOylated

IP samples were prepared from MDA-MB-231 whole cell lysates. In Figure 36, for the IP SUMO 2/3 samples, any proteins that were bound with SUMO were precipitated, western blotting was done to probe with the talin antibody (two antibodies were used in various repeated experiments: talin-1 Millipore, c-9 Santa Cruz); the talin antibody used was able to detect the N-terminus of the talin molecule. On the membrane, talin at 250kDa was seen in both of the untreated control samples and the GA treated 15, 30 or 60 minutes samples. For the IP talin samples, all the talin proteins in the whole cell lysates were precipitated and WB was done to probe with the SUMO 2/3 antibody, which detected the SUMOylated talin band at 250kDa in both of the untreated control samples and the GA treated 15, 30 or 60 minutes samples on the WB membrane. All the antibodies used were made in different species.

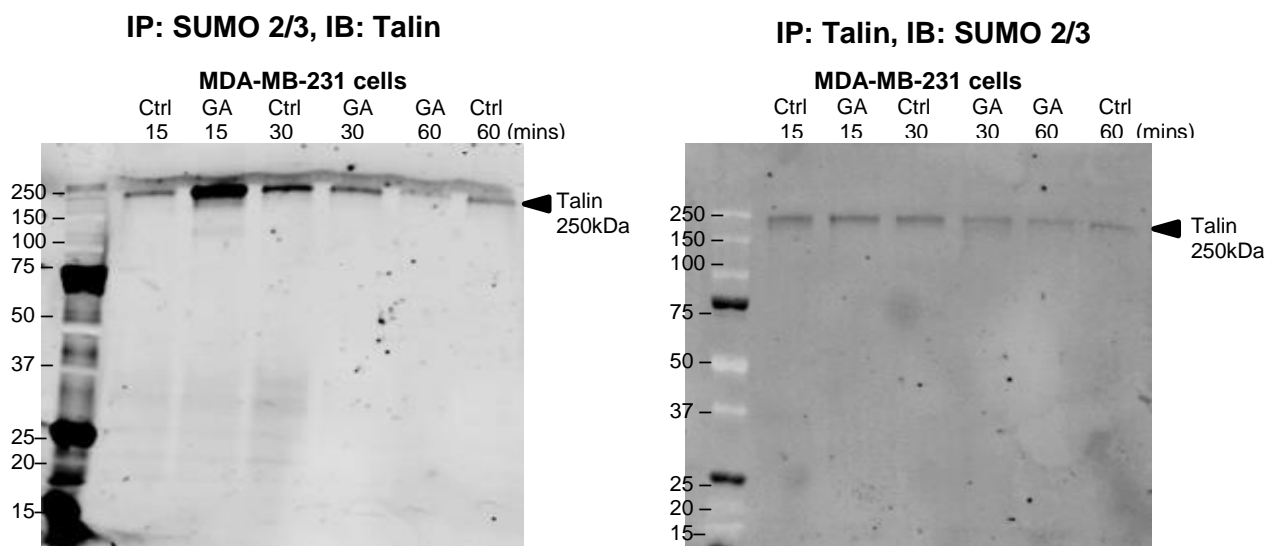


Figure 36. IP SUMO 2/3 and WB probing for talin detected the SUMOylated talin at 250kDa in the untreated control 15, 30 or 60 minutes and in the 100μM GA 15, 30 or 60 minutes treated cells; for the IP talin and WB probing for SUMO 2/3 also detected the SUMOylated talin at 250kDa in the untreated control 15, 30 or 60 minutes and in the GA 15, 30 or 60 minutes treated cells. Both IPs were shown from the whole cell lysates preparations only in the MDA-MB-231 cells, n>3 repeated more than 3 replicate experiments (representative immunoblots are shown)

In the IP SUMO 2/3 experiment, after 60 minutes of 100μM GA treatment, much less SUMOylated talin was detected compared to GA at 15 and 30 minutes treatment. Similarly, in the IP talin experiment, less SUMOylated talin was obtained in the GA 60 minutes treatment. In these experiments, the IPs and immunoblots have shown the intact full-length of talin band at 250kDa from the whole cell lysates preparations only.

4. 3. 2 IP and WB Reveals Vinculin is SUMOylated

The IP SUMO 2/3 experiments (samples prepared from whole cell lysates only) have shown SUMOylated vinculin in MDA-MB-231 cells in Figure 37. Similarly, after 100 μ M GA 1 hour treatment, it has shown a lower amount of SUMOylated vinculin in the cells compared to the untreated controls or GA 2h treatment.

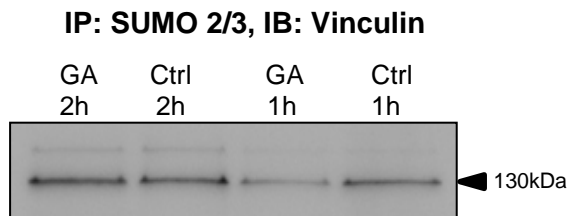


Figure 37. IP SUMO 2/3 and WB probing for vinculin showing the SUMOylated vinculin at 130kDa in both of the untreated control and 100 μ M GA treatment at 1hr or 2hrs samples in the MDA-MB-231 cells, n>3 repeated more than 3 replicate experiments (representative immunoblots are shown)

4. 3. 3 HA-tag SUMO-2 Plasmid Transfection Shows the Expression of SUMO-2 in the Cytoplasm and in the Nucleus of the MDA-MB-231 Cells

MDA-MB-231 cells were transfected with the HA-tagged SUMO-2 plasmid and left for 24 hours incubation. The anti-HA tag primary antibody was used in the IHC experiment to stain SUMO-2 in the cells. The cells were also stained with DAPI (blue staining for the nucleus).

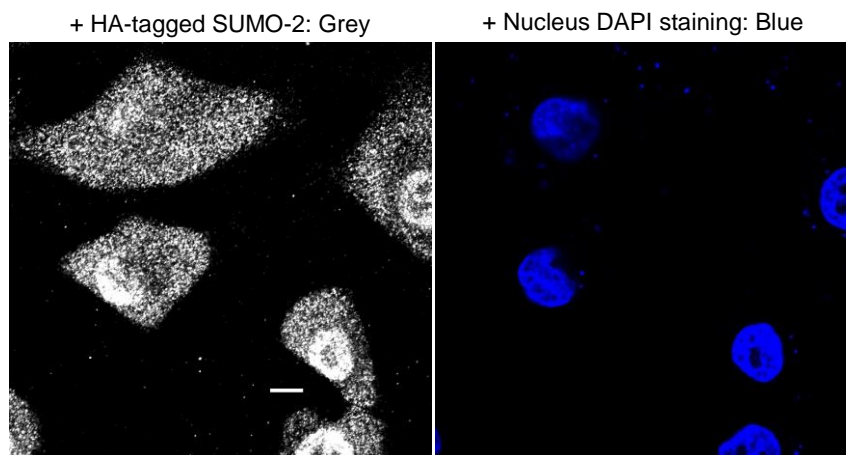


Figure 38. The HA-tagged SUMO-2 plasmid transfection in MDA-MB-231 cells showing SUMO-2 expression in grey; DAPI was shown as blue on the right picture. The transfection efficiency was optimized to express SUMO-2 in the cells. SUMO-2 was expressed in the nucleus and in the cytoplasm (scale bar =20 μ m)

In Figure 38, SUMO-2 was expressed in the nucleus and in the cytoplasm of the MDA-MB-231 cells. In this experiment, the transfection with the HA-tag SUMO-2 plasmid in the cells would increase the expression of SUMO-2 level in the cells, which were used in the IP experiments. This method would also increase the chance of capturing SUMOylated proteins in the cells for the IP experiments.

4. 3. 4 GAPDH or Akt are not SUMOylated

In the HA-tagged IP experiments, 100 μ M GA was used to treat the cells at 30 and 60 minutes. GAPDH and Akt antibodies were used to determine whether GAPDH or Akt could be SUMOylated in MDA-MB-231 cells, as there is no evidence that they can be SUMOylated. They were used as a negative control.

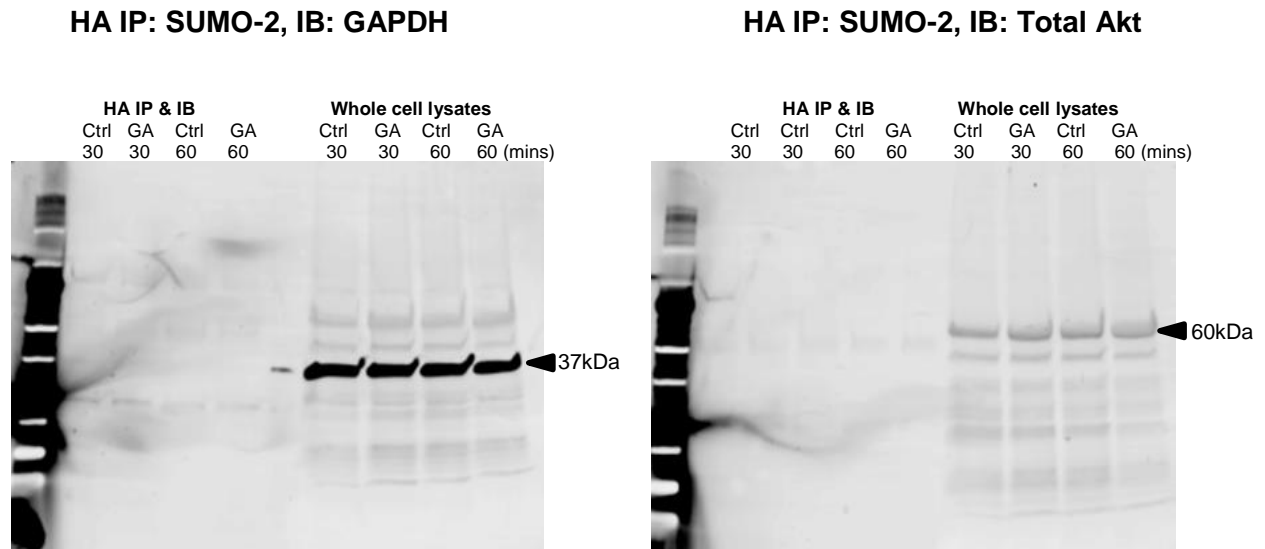


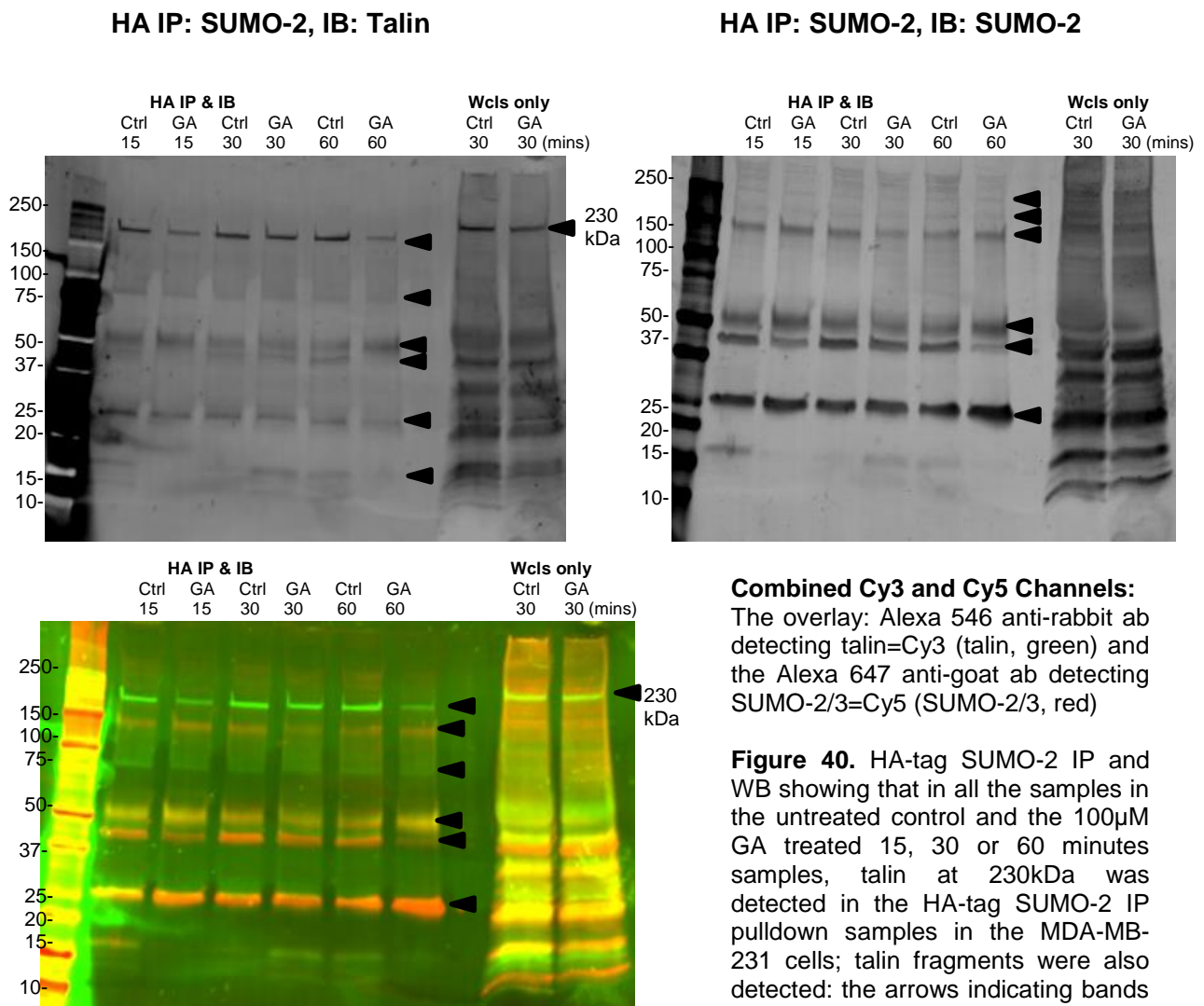
Figure 39. HA-tagged SUMO-2 IP and WB showing that GAPDH and Akt were only in the WB whole cell lysates but not in the HA IP pull-down SUMO-2 samples in the MDA-MB-231 cells

In Figure 39, the HA-tagged SUMO-2 IP samples were on the left half of the IB membrane, the first supernatant whole cell lysates samples were on the right half of the IB membrane as a control for the experiments. GAPDH at 37kDa was found in the cells only in the whole cell lysates prepared samples; total Akt was found in the cells only in the whole cell lysates. In the HA IP SUMO-2 pulldown samples, GAPDH was not seen at 37kDa in any of the samples; similarly, total Akt was not seen at 60kDa in any of the samples. This suggests that the GAPDH or the total Akt were present in the cells, but they may not be SUMOylated.

4. 3. 5 HA-tag SUMO-2 IP Detects both Full-length SUMOylated Talin and Fragments of Talin

MDA-MB-231 cells were prepared for the HA-tagged IP SUMO-2 samples. The cells were treated with 100 μ M GA for 15, 30 or 60 minutes. Anti-HA tag mouse primary antibody was added to all samples and incubated at 4°C overnight; the HA IP samples were then added with the protein A/G magnetic beads to immunoprecipitate the SUMO binding proteins. Western blotting was done to probe for talin using the talin primary antibody (H300, Santa Cruz). The membranes were also probed for SUMO 2/3 using the SUMO 2/3 primary

antibody. All the antibodies used were made in different species to avoid cross-reaction of the antibodies.



Combined Cy3 and Cy5 Channels:

The overlay: Alexa 546 anti-rabbit ab detecting talin=Cy3 (talín, green) and the Alexa 647 anti-goat ab detecting SUMO-2/3=Cy5 (SUMO-2/3, red)

Figure 40. HA-tag SUMO-2 IP and WB showing that in all the samples in the untreated control and the 100µM GA treated 15, 30 or 60 minutes samples, talin at 230kDa was detected in the HA-tag SUMO-2 IP pulldown samples in the MDA-MB-231 cells; talin fragments were also detected: the arrows indicating bands between 75-100kDa, 37-50kDa; the bands at 230kDa and 37-50kDa were overlaid on the overlay immunoblot. Bands at 50kDa and 25kDa were also shown. The total talin was present in the whole cell lysates in both of the control and GA at 30 minutes as a control of the IP experiments. n=5 (representative experiment immunoblots are shown)

In Figure 40, 5 experiments were done to demonstrate the SUMOylation of talin. In these HA-SUMO 2 IP pulldown experiments, all the SUMO modified proteins were precipitated. On the immunoblots, SUMOylated talin were shown as full-length protein at 230kDa in all the samples (depending on the antibody used). After GA 60 minutes treatment, a lesser amount of SUMOylated talin was detected compared to the control 60 minutes.

In both of the control and the GA treated samples, other fragments of the talin bands were seen (shown pointed with the black arrows). There were four other fragmented bands of talin

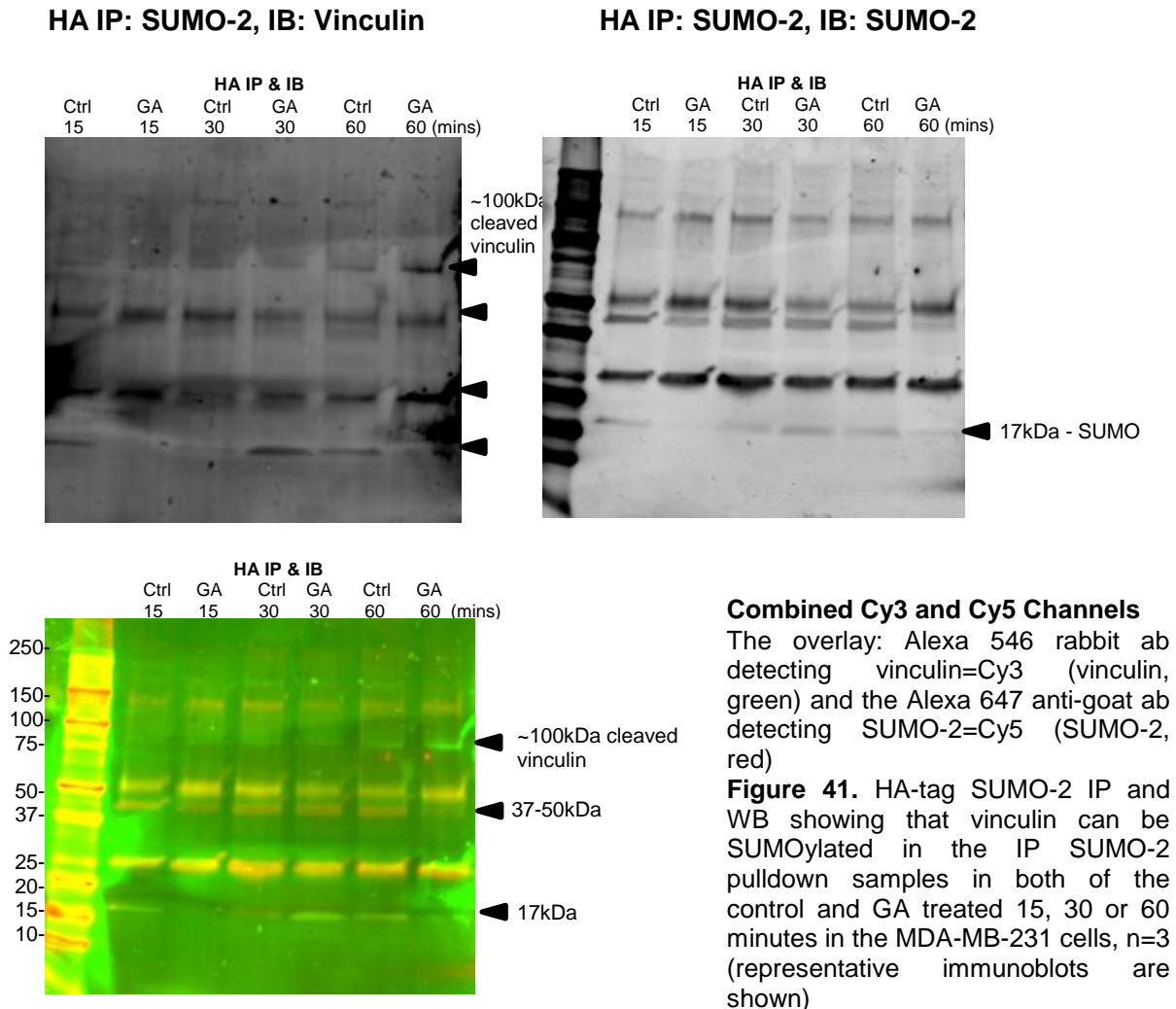
detected. The fragmented bands were ranged as: one fragment band was between 75-100kDa in all of the samples including the untreated control samples and the GA treated samples; one band was at 50kDa in all of the samples; one fragment was between 37-50kDa and this band was most likely at 47kDa detected as the head of talin, which was in the control samples and in the GA 30 minutes sample, however, this band was less detected in the GA 15 minutes and GA 60 minutes treatment samples; one band was shown at 25kDa in all of the samples.

On the SUMO-2 membrane, there were two very faint bands ranged above 230-250kDa in all of the samples; there were also four prominent bands showing ranged as: one band was detected at 150kDa in all of the samples; one band was at 50kDa in all of the samples; one band was detected between 37-50kDa and was likely to be at 47kDa in all of the samples; however, this band was less shown in the GA 15 minutes and GA 60 minutes treatment; one band was at 25kDa in all of the samples.

On the overlay membrane, the bands at 50kDa and 25kDa were overlaid together in both of the separate membranes; the bands at 230kDa and 47kDa were also overlaid, as the overlaid bands at 47kDa were less detected in the GA 15 minutes and the GA 60 minutes samples. From these overlaid bands, it suggests that these fragmented bands of talin must also be SUMOylated. Looking closely, the fragments between 37-50kDa (and more likely to be the 47kDa head of talin) were gone on the Talin membrane after 100 μ M GA 15 and 60 minutes treatments, on the SUMO-2 membrane, these bands were also less shown; on the overlay membrane after 100 μ M GA 15 and 60 minutes treatments they were less detected. The evidence of the cleaved products of talin molecules after 100 μ M GA 15 minutes treatment were confirmed in platelets (discussed in Chapter 6).

4. 3. 6 HA-tag SUMO-2 IP Detects SUMOylated Vinculin

HA-tagged IP samples were prepared from MDA-MB-231 cells and western blotting was done to probe for vinculin and SUMO-2/3 on the membrane.



In Figure 41, cleaved vinculin seemed to be immunoprecipitated in the IP SUMO-2 pulldown in all controls and GA treated 15, 30 and 60 minutes samples.

4.3. 7 SUMO VIVA™ Binding Assay and IP SUMOylated Talin or SUMOylated Vinculin in Isolated FAs

This isolation of FAs method was used and modified from Waterman C.M. 2011 (Integrin and cell adhesion molecules, methods and protocols, chapter 19). The purpose of FA isolation from cultured cells was to maintain the native FA protein structure and composition leaving them bound to culture flask/dish substratum, whilst removing substantial cytoplasmic membrane-bound organelles, nuclei and most cell plasma membrane with careful hydrodynamic force. As this method unavoidably preserved a significant amount of the cytoskeletons including the F-actin, tubulin etc, it was modified in practice to maintain FA structure and composition as the FA and actin cytoskeleton are interdependent structures.

In Figure 42, MDA-MB-231 cells were prepared as whole cell lysates without flushing to detect their FA proteins. Talin, vinculin, FAK and actin were present in the cells. This serves as a control for the 'flushing method'. In Figure 43, the cells were also prepared as flushed unbound whole cell lysates samples and the first run-through whole cell lysates from the SUMO binding columns were kept to detect their main FA proteins. Talin, vinculin, FAK, α -actinin, α -tubulin and actin were present in the flushed unbound whole cell lysates. Surprisingly, phospho-Rac1/cdc42 (Ser71) was also found in the flushed unbound whole cell lysate samples. The cytoplasmic proteins and the others that are not directly associated with the FAs including total Akt, phospho-Akt, Phospho-p44/42 MAPK (Erk1/2), E-cadherin, cleaved caspase 3 and RhoA were absent in the collected flushed whole cell lysate samples indicating the cell bodies were removed.

'Non-flushed' Unbound Whole Cell Lysates

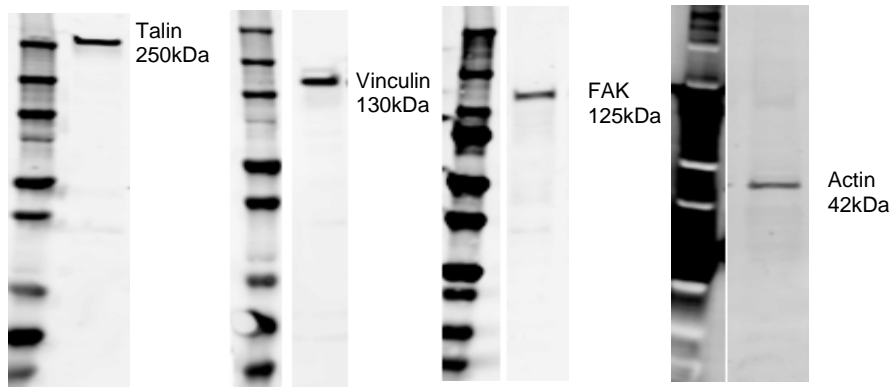


Figure 42. MDA-MB-231 cells were grown on fibronectin-coated T25 flasks and whole cell lysates were prepared without 'flushing' to detect their focal adhesions in the cells. The samples were run through the SUMO binding columns and kept as the first run-through unbound supernatant. Talin, vinculin, FAK and actin were present in the cells using the antibodies correspondingly.

In the non-flushed unbound whole cell lysates samples in Figure 42, talin, vinculin, FAK and actin were present, which were used as a control to compare with the flushed unbound whole cell lysates samples.

'Flushed' Unbound Whole Cell Lysates

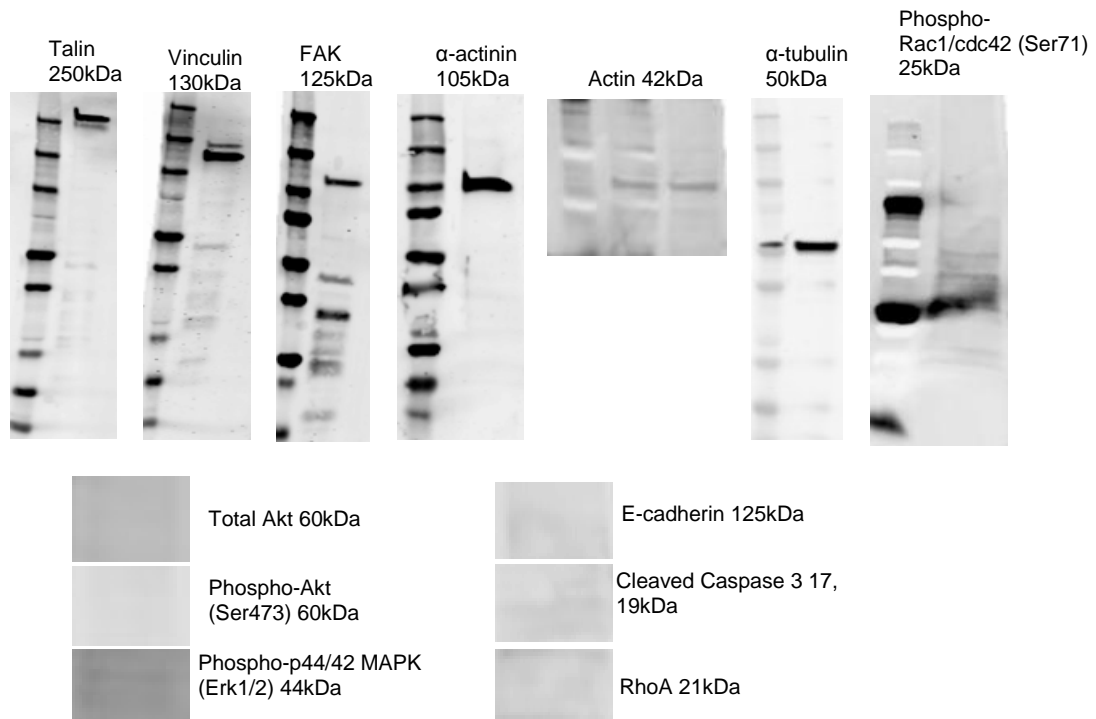


Figure 43. MDA-MB-231 cells were grown on fibronectin-coated T25 flasks and the cells were given 'flushing' using the water flosser. The flushed cells were collected from the flasks, whole cell lysates were made and the samples were run through the SUMO binding columns and kept as the first run-through unbound supernatant. Talin, vinculin, FAK, α-actinin, actin, α-tubulin and phospho-Rac1/cdc42 were present in the flushed unbound whole cell lysates, indicating that the 'flushing' method could still keep the FA proteins in the preparations. The cytoplasmic proteins were absent in the flushed unbound whole cell lysates including the total Akt, phospho-Akt, phospho-p44/42 MAPK (Erk1/2), E-cadherin, cleaved caspase 3 and RhoA.

In Figure 43, the cells were flushed using the water flosser. The main FA proteins including talin, vinculin, FAK, α -actinin, actin, α -tubulin and phospho-Rac1/cdc42 were present in the flushed unbound whole cell lysates, indicating that the 'flushing' method was able to keep the FA proteins in the preparations. The cytoplasmic proteins were absent in the flushed unbound whole cell lysates including the total Akt, phospho-Akt, phospho-p44/42 MAPK (Erk1/2), E-cadherin, cleaved caspase 3 and RhoA, indicating that the flushing method could remove the cell body.

The flushed isolation of FA protein samples were prepared for MDA-MB-231 cells (3x petri dishes for the control and 3x petri dishes for the GA 1hr treated). In the flushed isolated FA 'eluted' samples, GAPDH was probed on the WB membranes in Figure 44. GAPDH was found in the 'input' and 'unbound' samples but not found in the 'eluted' samples. In Figures 45 and 46, talin and vinculin were found to be bound with SUMO and eluted down through the columns, indicating that talin or vinculin could be SUMOylated.

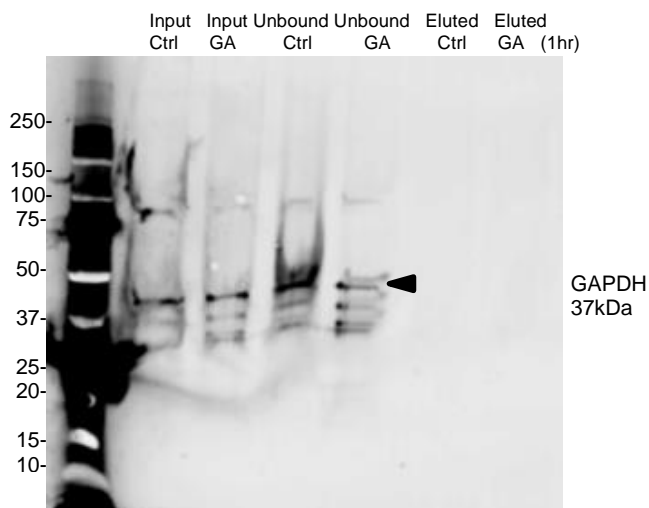


Figure 44. SUMO binding assay using the SUMO matrix and binding columns in the IP SUMO and WB experiments has shown that GAPDH was present in the 'unbound whole cell lysates' control or GA1hr treatment samples or in the 'input whole cell lysates' control or GA 1hr treatment samples, but GAPDH was not found in the eluted IP control or GA 1hr treated samples, suggesting that GAPDH was not SUMOylated in the MDA-MB-231 cells. This was shown as a negative control for the SUMO binding assay experiments. n=3 (representative immunoblots were shown)

In Figure 44, GAPDH was not SUMOylated in MDA-MB-231 cells as GAPDH was not found to be SUMO-bound and not shown after the elution during the SUMO columns binding process.

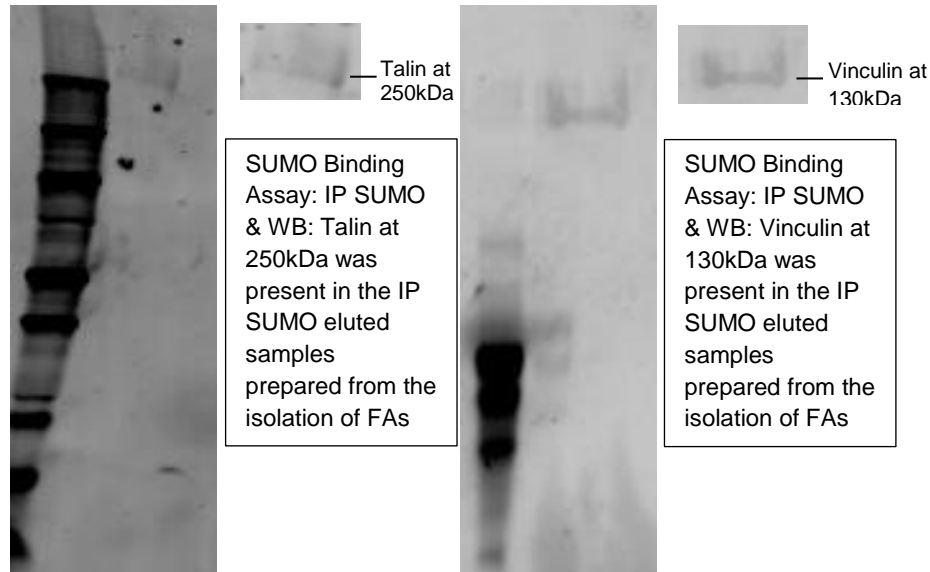


Figure 45. SUMO binding assay using the SUMO matrix and binding columns in the IP SUMO and WB experiments has shown that talin or vinculin could be SUMOylated in the isolated focal adhesions in the MDA-MB-231 cancer cells; this was done as 'control' experiments with no GA treatments

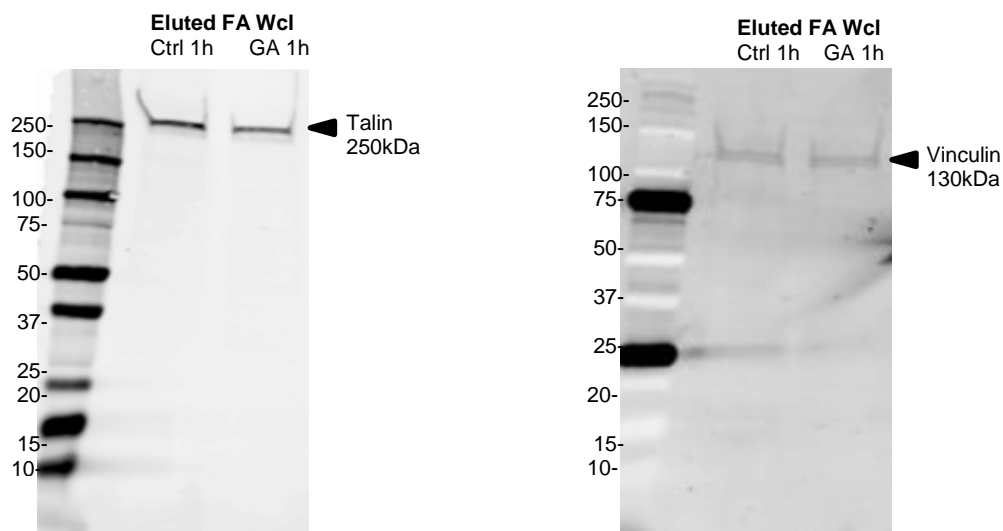


Figure 46. SUMO binding assay using the SUMO matrix and binding columns in the IP SUMO and WB experiments probing for talin or vinculin has shown that talin was found in the flushed isolated eluted FAs indicating talin could be SUMOylated in the FAs; after 100 μ M GA 1hr treatment, less talin that were SUMOylated were detected compared with the non-treated control; vinculin was also SUMOylated in the FAs. These experiments have shown that only the full-length of talin or vinculin were SUMO-bound, n=3 (representative immunoblots were shown)

In Figure 45 and 46, talin or vinculin could be SUMOylated in the FAs. These also have shown that only intact full-length of talin or vinculin that were SUMOylated were bound with SUMO in the columns and pulled down. In Figure 46, in the GA 1 hour treated sample for talin, there was less SUMOylated full-length talin detected than in the control 1 hour samples.

SUMO VIVA™ Binding Assay with the More Concentrated Isolated FAs Detects SUMOylated Talin and SUMOylated Vinculin, but with Fragmented Products

MDA-MB-231 cells were grown on the fibronectin-coated petri dishes and grown for 2 days. The cells were then treated with 100µM GA for 1 hour. The cells were flushed and the FAs were collected. The FAs were collected from six dishes for the control and 6 dishes for the GA 1 hour treated. These samples were transferred into the SUMO binding columns and incubated at 4°C overnight. The eluted samples were prepared and used in the WB experiments to determine whether talin or vinculin could be SUMOylated.

SUMO-Bound Assay IP: SUMO, IB: Talin SUMO-Bound Assay IP: SUMO, IB: Vinculin

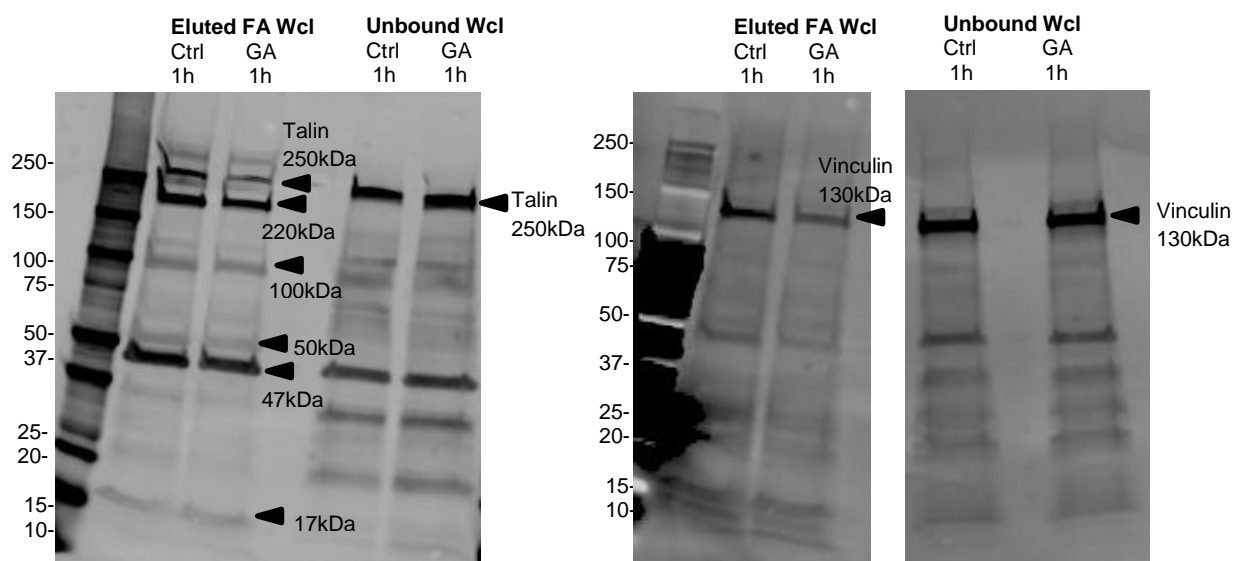


Figure 47. SUMO binding assay using the SUMO matrix and binding columns in the IP SUMO and WB experiments probing for talin showing that talin was present in the IP SUMO pulldown in both of the control and the GA 1hr treatment suggesting that talin could be SUMOylated in the focal adhesions in MDA-MB-231 cells; similarly, vinculin was also found in the SUMO binding eluted IP control and GA 1hr treatment samples suggesting that vinculin could be SUMOylated. These experiments were done to collect more concentrated flushed cells as the focal adhesions were collected from 6 petri dishes for the controls and 6 petri dishes were collected for the GA treatment at 1hr, n=3 (representative WB immunoblots were shown)

In Figure 47, the full-length intact talin at 250kDa was present in the eluted IP SUMO binding samples including the control and GA 1 hour treatment samples; similarly, intact vinculin at 130kDa was found to be in the eluted IP SUMO binding samples in both of the control and GA 1 hour treatment. These experiments suggest that intact talin or intact vinculin can be SUMOylated. However, more bands of talin were seen in the IP SUMO pulldown on the WB membrane shown with the black arrow, where these bands were ranged as: a band at 250kDa were found in both of the control and 100µM GA 1 hour treatment; a band was at 220kDa in both of the control and GA 1 hour treatment and this was likely to be the rod

domain of talin; a band was at 100kDa in both of the control and GA 1 hour treatment representing further cleavage in the rod domain of talin; a band was found at 50kDa in both of the control and GA 1 hour treatment; a band was found at 47kDa in both of the control and GA 1 hour treatment; there was also a band at about 15kDa in both of the control and GA 1 hour treatment. The most prominent talin bands in the eluted IP SUMO binding samples were the bands at 250kDa, 220kDa, 100kDa and 47kDa. All of these bands suggest that these must be products of talin that were binding with SUMO during the SUMO binding assay, suggesting that these fragmented products of talin must also be SUMOylated.

GA 1hr treatment reduced the amount of the eluted intact talin at 250kDa; similarly, vinculin at 130kDa was less shown after GA 1 hr treatment.

These results suggest that as more of the MDA-MB-231 cells were used in the isolation of FAs experiments, the cleaved products of FAs were able to be detected, however, they were not able to be detected or obtained during the endogenous IP experiments where SUMO-2 was not overexpressed and the IP experiments were done only using the whole cell lysates.

One of the effects of GA was also shown in the unbound whole cell lysates, where these samples were prepared as the first run-through supernatant and run on the WB membrane and kept as a 'control' for the IP eluted samples. It seemed that more products of the FAs i.e. talin in the unbound whole cell lysates were shown after GA 1 hour treatment and these effects was quite frequently seen in the experiments, also in the HA-tag SUMO-2 IP experiments.

4.3. 8 Ubc9 siRNA Transfection with HA-tag SUMO-2 plasmid Transfection

MDA-MB-231 cells were grown in the T25 flasks overnight and then transfected with the Ubc9 siRNA for 24 hours first then the cells were added with the HA-tag SUMO-2 plasmid for another 24 hours transfection. IP samples were prepared and the samples were run on the PAGE gels.

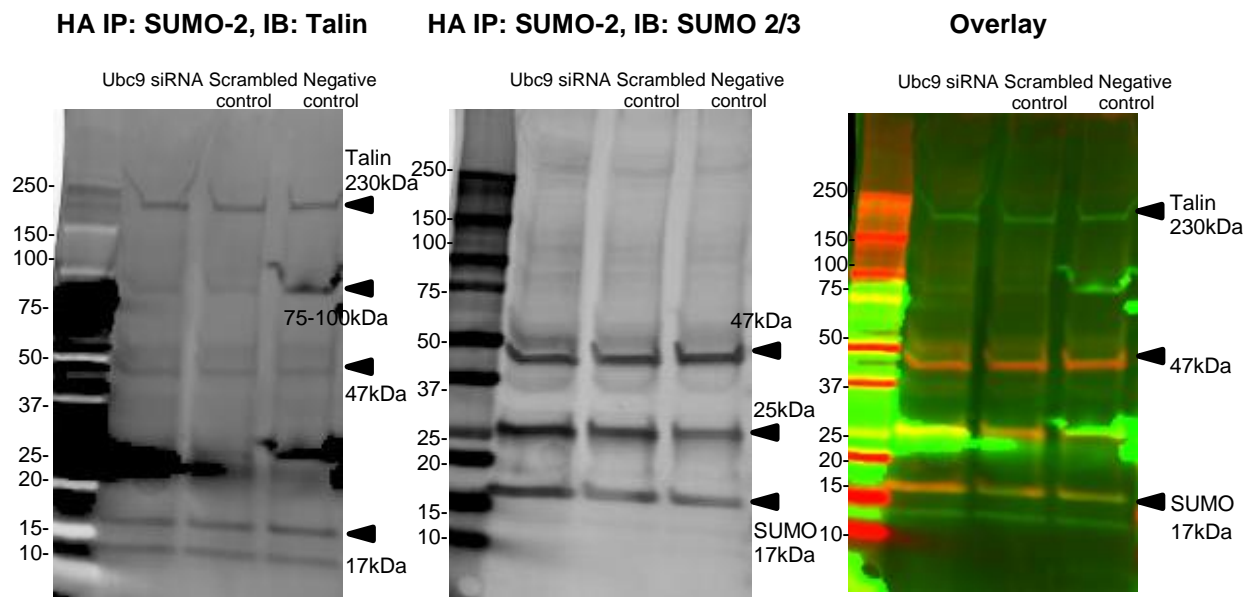
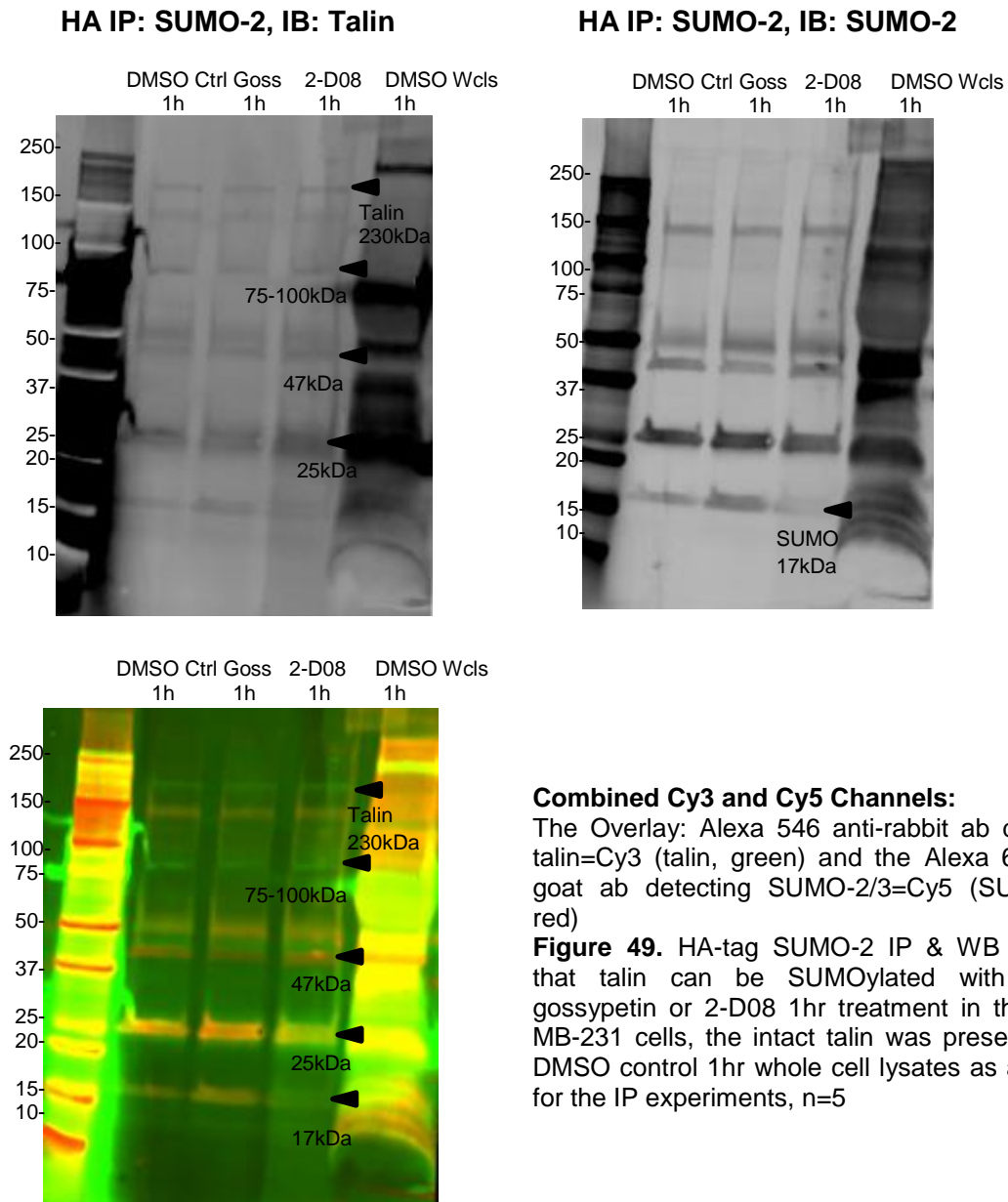


Figure 48. Ubc9 siRNA transfection in the MDA-MB-231 cells for 48 hours treatment with the HA IP SUMO-2 and WB showing that talin at 230kDa was SUMOylated in the Ubc9 siRNA, scrambled siRNA and negative control samples (the talin antibody used was the H300, Santa Cruz). The Overlay: Alexa 546 rabbit ab detecting talin=Cy3 (talin, green) and the Alexa 647 anti-goat ab detecting SUMO-2=Cy5 (SUMO-2, red), n=3

In Figure 48, the cells were treated with the Ubc9 siRNA and also transfected with the HA-tag SUMO-2 plasmid. Talin was shown in the IP SUMO-2 samples at 230kDa suggesting that talin was SUMOylated in the Ubc9 siRNA, scrambled siRNA and negative control samples. However, even after 48 hours Ubc9 siRNA treatment, SUMOylated talin was still able to be detected at the time where Ubc9 siRNA treatment was finished at 48 hours, suggesting that even after knocking down the Ubc9 siRNA for 48 hours, there were still enough Ubc9 enzyme to accompany talin to interact with the SUMO-2 proteins, since the inhibition may have reduced the newly formed expression of Ubc9 enzyme but the Ubc9 enzyme that were already produced and present in the cells before the inhibition may still be available for attaching SUMO-2 to the talin containing FAs. In the overlay, the bands between 37-50kDa most likely to be 47kDa as the head of talin and 15kDa were overlaid, suggesting that these must be SUMOylated products, since any bands detected must be SUMOylated proteins that could be immunoprecipitated.

4.3.9 Effect of Gossypetin and 2-D08 Treatments on Talin SUMOylation

MDA-MB-231 cells were grown in the T25 flasks overnight and then treated with 100 μ M gossypetin and 2-D08 for 1 hour. HA-tag SUMO-2 IP samples were prepared and the samples were run on PAGE gels.



In Figure 49, talin was SUMOylated at 230kDa in both of the DMSO control and the gossypetin or 2-D08 treatment on the HA IP: SUMO-2, IB: Talin membrane. Talin was seen with many products and these products of talin must also be SUMOylated to be immunoprecipitated with SUMO-2.

4.3. 10 Focal Adhesion Expression was not Affected after GA or Ubc9 siRNA Treatment

MDA-MB-231 cells were grown in T25 flasks overnight and then treated with 100 μ M GA for 6 hours. Whole cell lysates were made after 6 hours treatment. FA antibodies were used in WB experiments to detect talin, FAK or vinculin level in the whole cell lysates.

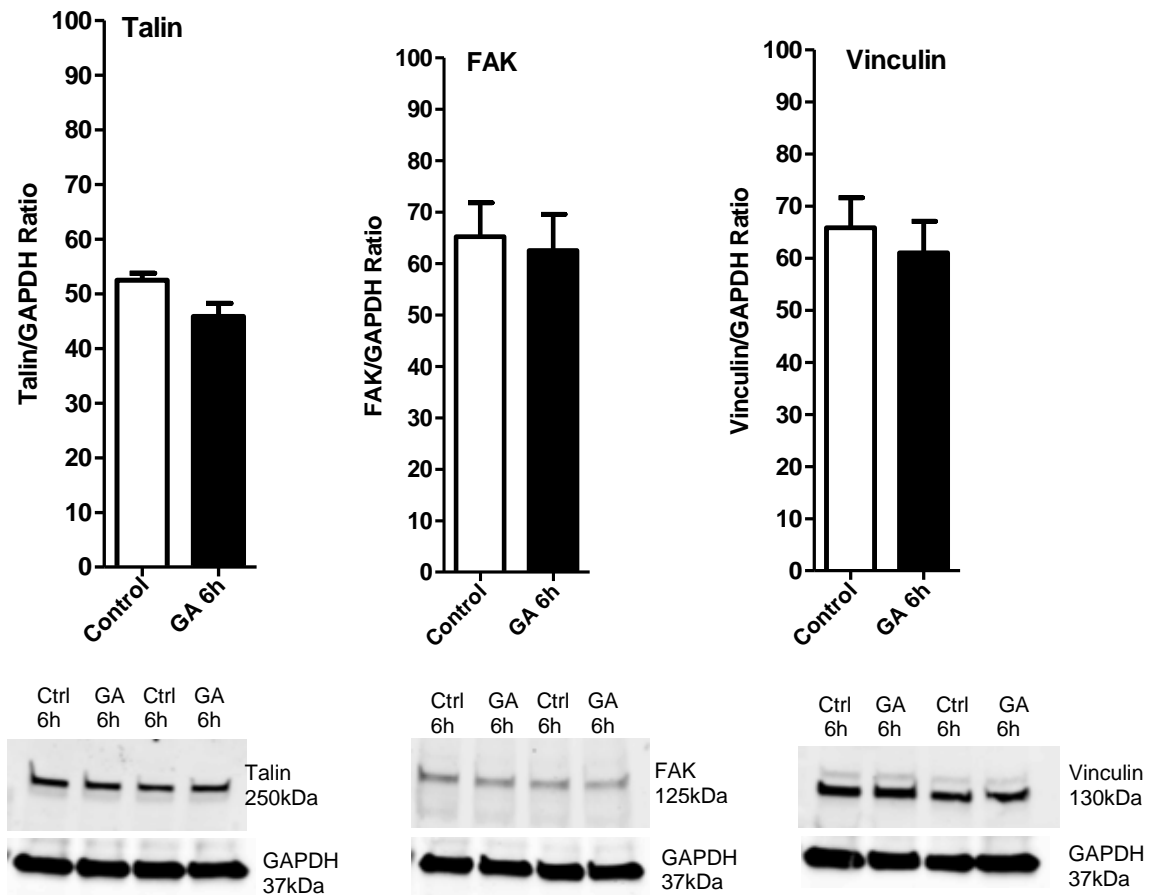


Figure 50. 100 μ M GA after 6 hours treatment in the MDA-MB-231 cells does not change the FAs talin, FAK or vinculin expression compared with the control (n=3).

In Figure 50, the expression of the total amount of talin containing FAs in the MDA-MB-231 cells was not significantly affected after 100 μ M GA 6 hours treatment compared with the control; similarly, the expression of FAK or vinculin containing FAs in the MDA-MB-231 cells was not significantly affected after treatment. This suggests that after the inhibition of SUMOylation, the FA proteins level in the cells was not changed.

MDA-MB-231 cells were treated with Ubc9 siRNA for 48 hours. Whole cell lysates were made after 48 hours treatment. FA antibodies were used in WB experiments to detect talin, FAK or vinculin protein level in the whole cell lysates. Ubc9 siRNA treatment after 48 hours treatment did not affect the degradation of FA proteins.

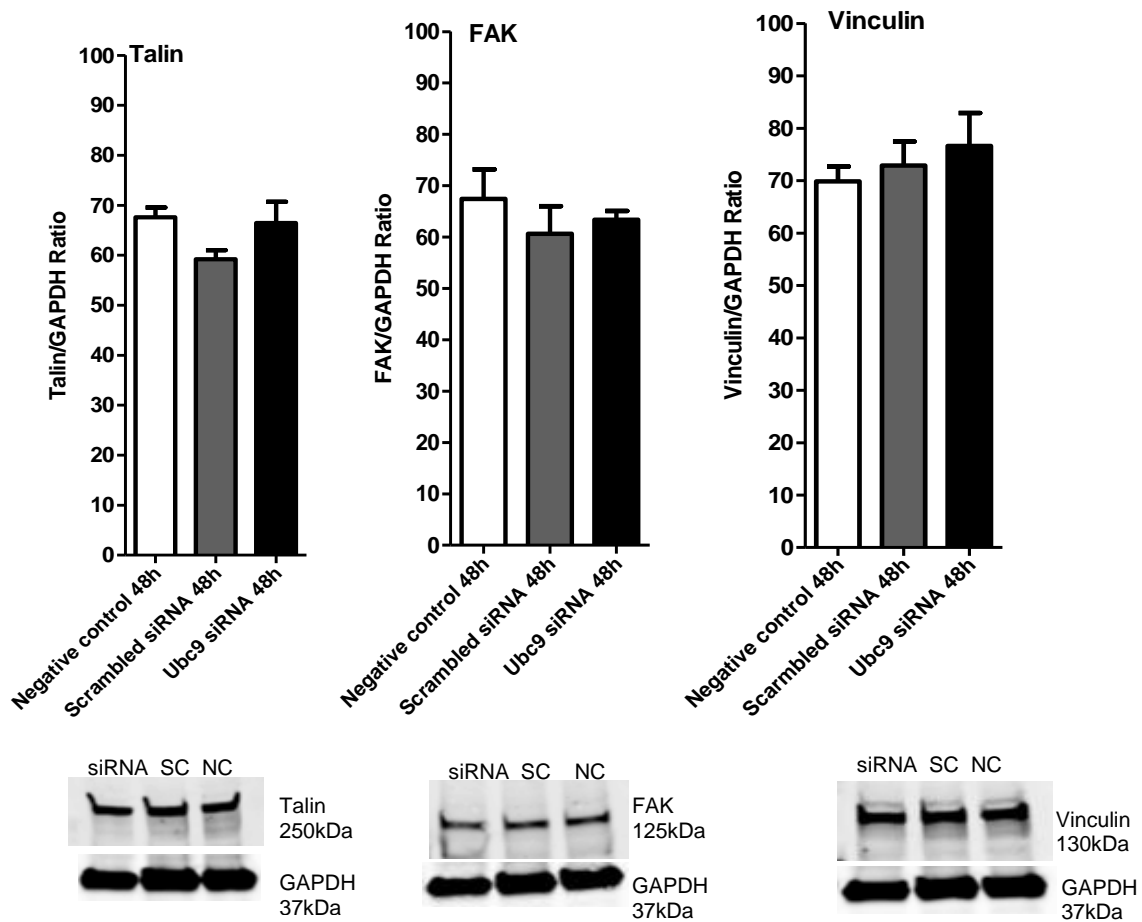


Figure 51. 25nM Ubc9 siRNA after 48 hours treatment in the MDA-MB-231 cells does not change the FAs talin, FAK or vinculin expression compared with the control (n=3).

In Figure 51, Ubc9 siRNA treatment did not affect the total amount of the FA proteins including talin, FAK or vinculin compared with the control.

4.3. 11 Talin is SUMOylated in U2OS Cells

U2OS cells were grown in T25 flasks overnight and then treated with 100 μ M GA. The IP samples were prepared with the whole cell lysates only and the primary talin-1 antibody was added to these samples.

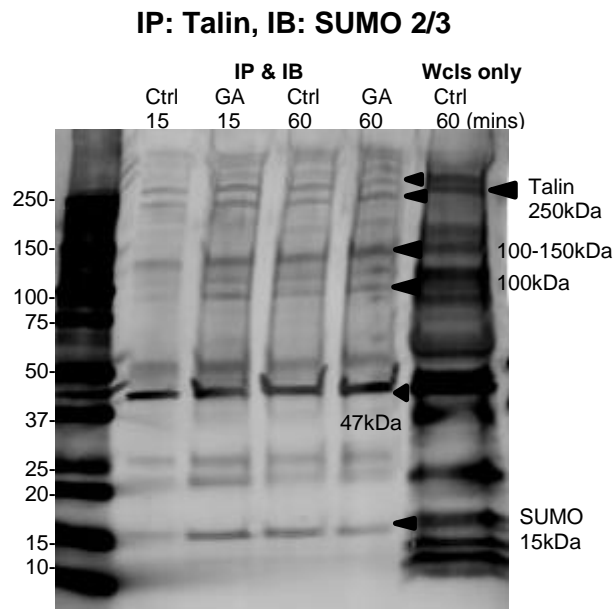


Figure 52. IP talin-1 and WB showing that in all the IP talin samples in the untreated control and the 100 μ M GA 15 or 60 minutes treated samples, talin at 250kDa was detected when SUMO 2/3 was probed for in the U2OS cells; the total talin was present in the whole cell lysates in the control 60 minutes as a control of the IP experiments. n=4 (representative experiment immunoblots are shown)

In Figure 52, SUMOylated talin at 250kDa was able to be detected in the untreated control and 100 μ M GA treated samples in U2OS cells, confirming the SUMOylation of talin in these cells. The intact talin was SUMOylated at 250kDa; however, there are also other products present suggesting that these may also be SUMOylated talin products. The bands were ranged as: two bands were present near at 250kDa in all of the samples; one prominent band was between 100-150kDa in all of the samples; one band was between 37-50kDa and this was probably the enriched head of talin at 47kDa; SUMO bands at 15kDa were present. These band patterns in the U2OS cells were quite similar compared to the MDA-MB-231 cells.

4.3. 12 HA-tag SUMO-2 IP Detects SUMOylated Full-Length Talin and Fragments of Talin

U2OS cells were transfected with the HA-tag SUMO-2 plasmid overnight. The cells were treated with 100 μ M GA for 15 or 60 minutes. The IP samples were prepared with magnetic beads and the IP samples were run on the WB gels probed with talin (N-terminus antibody).

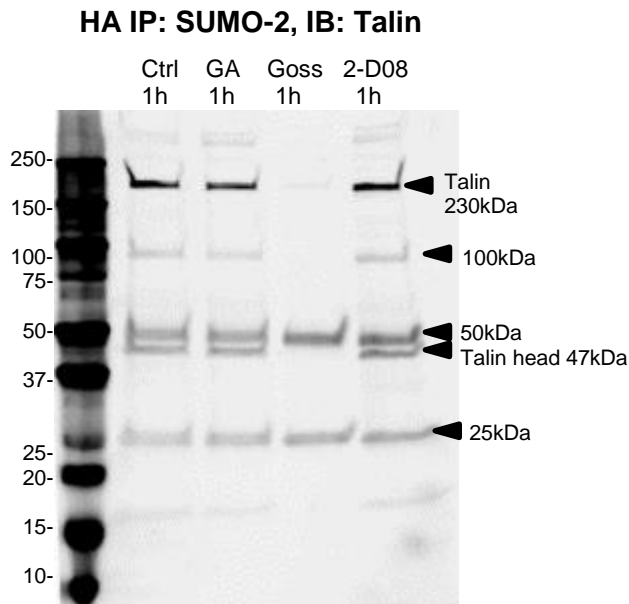


Figure 53. HA-tag SUMO-2 IP and WB showing that in all the IP SUMO-2 samples in the untreated control and the 100 μ M GA, Gossypetin or 2-D08 1hr treated samples, full-length talin at 230kDa was detected when talin was probed for in the U2OS cells, however, the fragments of the SUMOylated talin were clearly seen n=3 (the representative experiment immunoblots were shown here)

In Figure 53, the full-length intact talin at 230kDa was SUMOylated in the control and treated samples, but it was much reduced in the gossypetin 1 hour treated sample. The fragments of the SUMOylated talin were: the bands between 75-100kDa was present in the control 1 hour or GA 1 hour and 2-D08 1 hour treated samples, but it was absent in the gossypetin 1 hour treated sample. The bands between 37-50kDa (talin head at 47kDa) was present in the control 1 hour or GA 1 hour and 2-D08 1 hour treated samples, but it was absent in the gossypetin 1 hour treated sample.

4.3. 13 SUMOylation may Cause an Interruption of the FA Proteins Complex

MDA-MB-231 cells were grown in T25 flasks overnight and then the cells were transfected with the GFP-Talin plasmid overnight. The cells were treated with 100 μ M GA, gossypetin or 2-D08 for 1 hour. The GFP Talin IP samples were prepared by adding the primary GFP antibody overnight and then adding the magnetic beads for 2 hours to pull down all the talin proteins in the cells. The samples were then run on the WB gels to probe for filamin-1 (N-

terminus H300, Santa Cruz). All the antibodies used were made in different species to avoid antibody cross reactions.

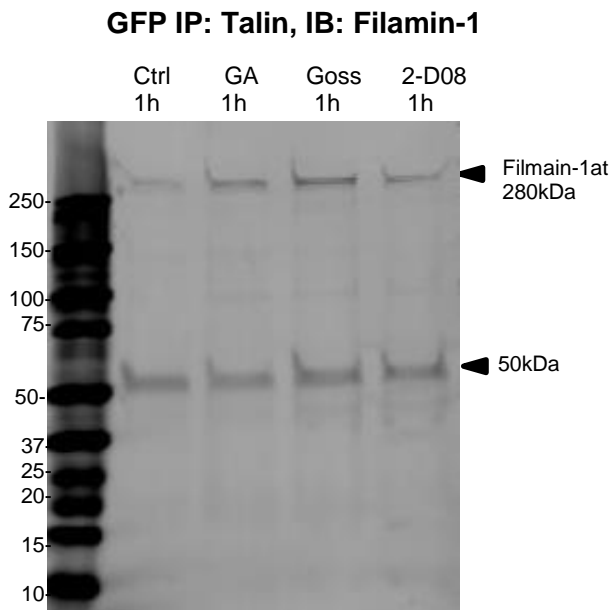


Figure 54. GFP IP and WB showing that in all the IP GFP samples in the untreated control and the 100 μ M GA, gossypetin or 2-D08 1hr treated samples, full-length talin was bound with filamin-1 detected in the MDA-MB-231 cells when probing for filamin-1 on the WB membrane, however, there was less filamin-1 detected in the control 1hr than in the 100 μ M GA, gossypetin or 2-D08 1hr treated samples n=3 (the representative experiment immunoblots were shown here)

In Figure 54, the full-length talin was present in a complex with filamin-1 in the MDA-MB-231 cells, as filamin-1 was detected following IP of talin. Filamin-1 was present in all samples. It seems that SUMOylated FAs may cause the interruption of the talin-filamin-1 complex in the cells, as the GA, gossypetin or 2-D08 treated samples, compared with the control, seemed to have immunoprecipitated more filamin-1 after inhibitor treatments, suggesting that SUMOylation of FAs may affect the FA protein-protein interactions.

MDA-MB-231 cells were grown in T25 flasks overnight and then the cells were transfected with the mEmerald-Vinculin plasmid overnight. The cells were treated with 100 μ M GA, gossypetin or 2-D08 for 1 hour. The GFP Vinculin IP samples were prepared by adding the primary GFP antibody overnight and then adding the magnetic beads for 2 hours to pull down all the vinculin proteins in the cells. The GFP IP vinculin samples were run on the WB gels to probe for talin (N-terminus, H300 ab, Santa Cruz). All the antibodies used were made in different species to avoid antibody cross reactions.

GFP IP: Vinculin, IB: Talin

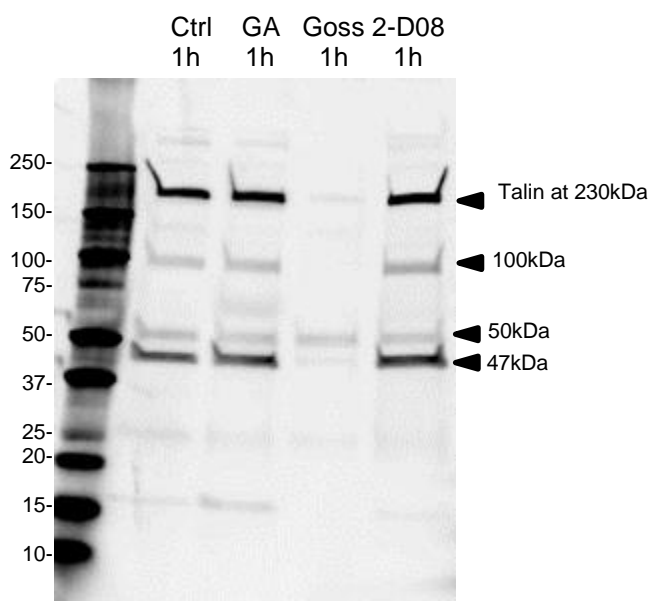


Figure 55. GFP IP and WB showing that in all the IP GFP samples in the untreated control and the 100 μ M GA, gossypetin or 2-D08 1hr treated samples, full-length talin was bound with vinculin detected in the MDA-MB-231 cells when probing for vinculin on the WB membrane, however, there was less talin detected in the gossypetin 1hr than in the control 1hr or the 100 μ M GA and 2-D08 1hr treated samples n=3 (the representative experiment immunoblots were shown here)

In Figure 55, the full-length talin was present in the complex with vinculin in the MDA-MB-231 cells, as the talin was detected following IP of vinculin. Full length talin was detected at 230kDa in the control or GA and 2-D08 treated samples, but it was much less detected in gossypetin treated sample. The bands at 100kDa were present in the control or GA and 2-D08 treated samples, but it was absent in the gossypetin treated sample. Similarly, the bands between 37-50kDa (47kDa more likely to be talin head) was present in the control or GA and 2-D08 treated samples, but it was gone in the gossypetin treated sample. It seems that the inhibition of SUMOylated FAs has caused the interruption of the talin-vinculin complex in the cells, suggesting that the inhibition of SUMOylation may affect the FA protein-protein interactions.

MDA-MB-231 cells were transfected with the GFP-Talin plasmid overnight. The cells were treated with 100 μ M GA, gossypetin or 2-D08 for 1 hour. The GFP Talin IP samples were prepared by adding the primary GFP antibody overnight and then adding the magnetic beads for 2 hours to pull down all the talin proteins in the cells. The GFP IP talin samples were run on the WB gels to probe for actin. All the antibodies used were made in different species to avoid antibody cross reactions.

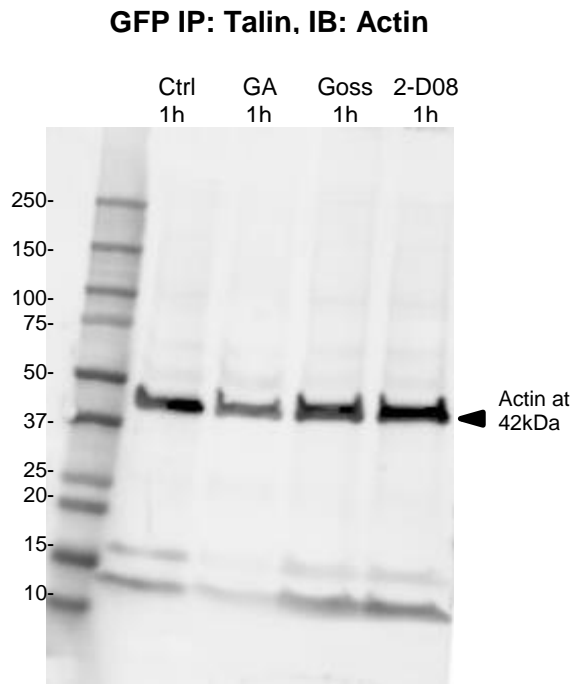


Figure 56. GFP IP and WB showing that in all the IP GFP samples in the untreated control and the 100 μ M GA, gossypetin or 2-D08 1hr treated samples, actin was bound with talin detected at the 42kDa in the MDA-MB-231 cells when probing for actin on the WB membrane, however, there was less actin detected in GA 1hr than in the control, gossypetin or 2-D08 1hr treated samples n=3 (the representative experiment immunoblots were shown here)

In Figure 56, the actin was present in the complex with talin in the MDA-MB-231 cells, as the actin was detected following IP of talin. Actin was present in the control or GA, gossypetin and 2-D08 treated samples. Actin was found to be SUMOylated in the mass spectrometry results (Chapter 5) and it was found to be bound with talin together in the cells.

4.3. 14 Determination of Inhibition of SUMOylated FAs on FA Protein-Protein Interaction in U2OS Cells

U2OS cells were grown in T25 flasks overnight and then the cells were transfected with the GFP-Talin plasmid overnight. The cells were treated with 100 μ M GA, gossypetin or 2-D08 for 1 hour. The GFP Talin IP samples were prepared by adding the primary GFP antibody overnight and then adding the magnetic beads for 2 hours to pull down all the talin proteins in the cells. The GFP IP talin samples were run on the WB gels to probe for filamin-1. All the antibodies used were made in different species to avoid antibody cross reactions.

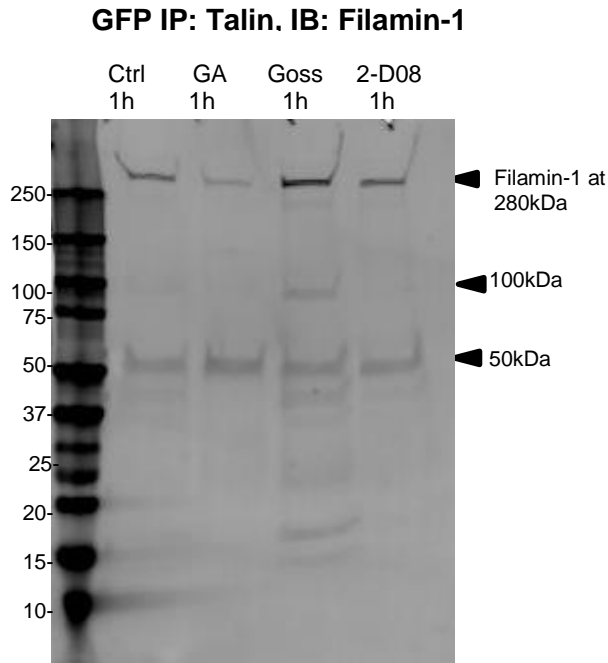


Figure 57. GFP IP and WB showing that in all the IP GFP samples in the untreated control and the 100 μ M GA, gossypetin or 2-D08 1hr treated samples, full-length talin was bound with filamin-1 detected in the U2OS cells following IP of talin, however, there was less filamin-1 detected in the GA 1hr than in the control 1hr, gossypetin or 2-D08 1hr treated samples n=3 (the representative experiment immunoblots were shown here)

In Figure 57, full-length talin was present in the complex with filamin-1 in the U2OS cells. Filamin-1 at 280kDa was less shown in the GA treated sample than in the control or the gossypetin and 2-D08 treated samples. The band at ~100kDa was only shown in gossypetin treated sample.

U2OS cells were transfected with the mEmerald-Vinculin plasmid overnight. The cells were treated with 100 μ M GA, gossypetin or 2-D08 for 1 hour. The GFP Vinculin IP samples were prepared by adding the primary GFP antibody overnight and then adding the magnetic beads for 2 hours to pull down all the vinculin proteins in the cells. The GFP IP vinculin samples were run on the WB gels to probe for talin (N-terminus, H300 ab, Santa Cruz). All the antibodies used were made in different species to avoid antibody cross reactions.

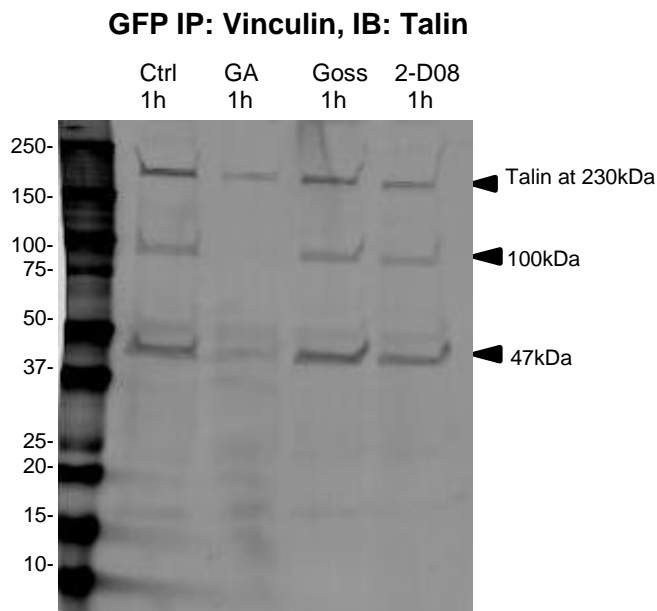


Figure 58. GFP IP and WB showing that in all the IP GFP samples in the untreated control and the 100 μ M GA, gossypetin or 2-D08 1hr treated samples, full-length talin was bound with vinculin detected in the U2OS cells following IP of vinculin, however, less talin was detected in the GA 1hr than in the control 1hr or the 100 μ M gossypetin and 2-D08 1hr treated samples n=3 (representative experiment immunoblots were shown)

In Figure 58, full-length of talin was present in the complex with vinculin in the U2OS cells. Full length talin was detected at 230kDa in the control or 100 μ M GA, gossypetin and 2-D08 treated samples; however, talin at 230kDa was less detected in the GA treated sample. The bands at 100kDa were present in the control or gossypetin and 2-D08 treated samples, but it was absent in the GA treated sample. Similarly, the bands between 37-50kDa (47kDa more likely to be talin head) was present in the control or gossypetin and 2-D08 treated samples, but it was gone in the GA treated sample. It seems that the inhibition of SUMOylated FAs caused the interruption of the talin-vinculin complex suggesting the inhibition of SUMOylation of FAs may affect FA protein-protein interactions.

Discussion

In this study, three different IP methods, the endogenous IP, the HA-tag SUMO-2 IP and the SUMO binding assay have shown that the intact talin was SUMOylated consistently in MDA-MB-231 cells and U2OS cells. This has also been shown with vinculin. The endogenous IP and the SUMO binding assay have shown that the intact vinculin was SUMOylated consistently. Inhibiting SUMOylation probably leads to more cleavage of talin. SUMOylation may also have a potential role in FA protein-protein interactions.

SUMO 1, SUMO 2/3 proteins work closely with the SUMO proteases in the cycle as a steady-state regulatory system (Makhnevych et al., 2009), inhibiting the E1 enzyme inhibits the SUMO conjugating process, which means that SUMO 2/3 could not be conjugated to protein substrates by SAE1/SAE2 and Ubc9 (Tatham et al., 2001). 100 μ M GA targets the E1 enzyme in the SUMOylation pathway; 2-D08 and gossypetin have also been shown to be potent inhibitors for protein SUMOylation; 25nM Ubc9 siRNA targets the E2 Ubc9 enzyme in the SUMOylation pathway; these inhibitors have been discussed previously. These inhibitors were used to prevent FA proteins from modified through SUMO 2/3 covalent binding, therefore blocking SUMO 2/3 attachment to these FA substrate proteins consensus motifs and resulting in inhibition of protein SUMOylation. SUMO 2/3 is mostly expressed in the cytoplasm and in the nucleus, the inhibitors may also have inhibitory effects in the SUMO 2/3 free pool (Hay, 2005). The HA-tag SUMO-2 plasmid transfection showed that SUMO-2 was expressed prominently in the nucleus and in the cytoplasm of cells. SUMO 1 has not been determined in these experiments as SUMO-1 is mostly expressed in the nucleus but these inhibitors could also affect SUMOylated proteins through SUMO-1 conjugations.

For talin SUMOylation, one effect of the inhibitors was that compared to the untreated cells, it seemed to decrease the SUMOylated intact talin, which obtained much less consistently in the endogenous IP, HA-tag SUMO-2 IP and the SUMO binding assay after 1 hour of 100 μ M GA treatment. This effect with the inhibitor may be transient within the first 1 hour of treatment, however, the treatment time can be critical since SUMOylation is a dynamic process, given at any time *in vivo*, only less than 1% of the proteome can be SUMOylated (Johnson, 2004), which makes it crucial to grasp the slight changes caused during the treatment time and the effects on the SUMOylated proteins in FA turnover.

The full-length of talin consists of an N-terminal FERM domain linked to a flexible rod comprised of R1-R13 amphipathic helical bundles, which ends with the dimerization domain (DD), which forms the anti-parallel coil-coil dimer (Goult et al., 2013a). The F3 head domain

of talin has higher affinity for binding to the $\beta 3$ integrin tail leading to integrin activation (Calderwood et al., 2002). Normally, the interactions between integrin, talin and vinculin binding are crucial in FA assembling; SUMO modification to these adhesion proteins may be a new mechanism to regulate FA disassembly, the binding of vinculin to talin in the focal adhesion, hence its regulatory role in adhesion turnover.

To better understand how SUMOylation regulates talin and vinculin in the focal adhesion, the method used to isolate and collect focal adhesions was modified from Waterman, 2011's protocols (Kuo et al., 2012). In this study, they developed and validated the isolation of focal adhesions method. They isolated human foreskin fibroblasts (HFF1) focal adhesions, followed by protein identification analysis of peptides using multidimensional protein identification technology mass spectrometry (MudPIT MS) and protein identification with SEQUEST (Kuo et al., 2011). The focal adhesions including talin, vinculin, paxillin, actin, pFAK³⁹⁷ etc were present in the isolated FA fractions before actin and fibrin immunodepletion (Kuo et al., 2011). This method was adopted for this study. In this study, the intact talin or the intact vinculin was shown to be SUMOylated within the isolated FA, making the role of SUMOylation in the FA more dynamic and diverse, which serves as a useful tool to study the individual protein SUMOylation in the FA adhesion.

Full-length talin was SUMOylated. There were also fragments of talin which were shown to be SUMOylated. Numerous motility related adhesion proteins have been found to be calpain proteolytic substrates, where the MAP kinase kinase (MEKK1) associated with FAK acting upstream of ERK works in the regulation of phosphorylating and activating calpain-2, thereby it mediates talin cleavage, resulting in adhesion disassembly, transformation and cell migration (Franco and Huttenlocher, 2005). These FAs have been consistently produced with cleaved products, which were SUMOylated. In MDA-MB-231 cells, the results with the more concentrated isolated FA lysates used has shown more clearly the cleaved fragments of talin: they consisted of the rod domain at 220kDa, cleaved product at 100kDa and the cleaved head domain of talin at 47kDa and these were observed in both control and GA 1 hour treated samples. In contrast, in the whole cell lysates unbound samples: no rod domain of talin being cleaved at 220kDa was seen in both control and GA 1 hour treated samples, confirming the eluted samples were pulled down with the SUMO matrix and these cleaved products must be SUMOylated fragments of talin. Furthermore, looking more closely in the HA-tag IP SUMO-2 experiments, the effects of the inhibitor 100 μ M GA treatment at 15 minutes and 60 minutes have abolished the 47kDa cleaved head of talin, compared to the controls and GA 30 minutes; full-length of talin was less obtained in the SUMO binding assay after GA 1 hour treatment.

Talin has been described in two conformational states in the literature as the inactive and active states. Probably, talin was in its activated state in the cancer cells, where SUMO-2 modification has been persistently required for talin, under the conditions when SUMO-2 was stably overexpressed, as the endogenous SUMOylated talin has not always been stably expressed and obtained. These results suggest that the talin containing FAs in the cancer cells were consistently cleaved, probably by calpain-2 and the intact talin was consistently conjugated with SUMO-2; the SUMOylated intact talin and the consistent talin proteolysis resulting in cleaved SUMOylated head and rod domain of talin are required for talin turnover.

The increased turnover time of the FAs may result from the loss of the cleaved SUMOylated head domain or the SUMOylated rod domain of talin after the first 1 hour of inhibitor treatments, which indicates that inhibiting SUMOylation could disrupt the talin turnover and FA disassembly. In all the three IP methods used, the IP was pulling down talin that was in FAs, but perhaps it was a cytoplasmic pool of talin that was pulled down, where these cytoplasmic SUMOylated talin were sufficient to contribute to fast and dynamic FA turnover. This was interesting (as it was also observed in the Co-IPs): the effects of the inhibitors have caused the loss of the cleaved products of talin, i.e. the loss of SUMOylated head domain and rod domain of talin could lead to the loss of the F3 head domain of talin binding to integrin β 3 tail, therefore affecting talin turnover. Similarly, the talin rod domain contains a second lower-affinity integrin binding site (Ziegler et al., 2008), inhibiting SUMOylation could result in the loss of the rod domain of talin binding to integrin. SUMO modification site can also be in the extended loops: the talin head F1 domain has an unstructured loop at the same positions of its respective F1 domains between amino acid 132-170 and the loop residues does not interact with the other regions of the FERM domain (Goult et al., 2010, Elliott et al., 2010, Bouaouina et al., 2012).

The stability of the helical bundles which make up the talin rod is critical in determining the activity of individual vinculin binding sites (VBSs), where these VBSs are defined by the hydrophobic residues in the amphipathic helices that are buried within the helical bundles of the talin rod (Patel et al., 2006). The C-terminal of talin rod (220kDa) consists of the R1-R13 13 helical bundles, where the N-terminal region of talin rod R2 and R3, each contains two VBSs atypically (Yao et al., 2014). Talin (residues 482-889) binds to vinculin head domain Vd1 with high affinity, indicating that one or more of the four VBSs are active which likely represents the vinculin binding domain in intact talin (Patel et al., 2006). Vinculin has been found to have a stabilizing role in the focal adhesion; vinculin can exist in an open conformational state in focal adhesions in the actin-binding conformation in spreading cells (Chen et al., 2005). The first evidence of the cleaved vinculin into 95kDa head domain and

30kDa tail fragment was produced by the sepharose-immobilized protease V8 in a specific, dose-dependent manner and this intramolecular interactions of vinculin was important to the modulation of talin binding in the focal adhesion i.e. talin rod domain could compete for binding to the vinculin head domain and this 95kDa cleaved head of vinculin had higher affinity in binding to talin than the intact vinculin molecule (Johnson and Craig, 1994). Talin, rather than α -actinin, is the major protein involved in the activation of vinculin, since talin colocalizes with vinculin in the focal complexes and with the majority of FA proteins including β 3-integrin, talin, vinculin, FAK, paxillin, α -actinin, VASP and zyxin, except tensin have shown 80-90% very high degrees of colocalization with phosphotyrosine at the large, elongated FAs of the regions further from the cell edge in endothelial cells (Zaidel-Bar et al., 2003). The cleaved vinculin at ~100kDa in the HA-IP overexpression with SUMO-2 in both MDA-MB-231 cells and U2OS cells probably showed that this head domain of vinculin had higher affinity for binding to talin.

SUMOylation may play a general role in protein-protein interactions, where SUMO modification could probably provide a new binding site for interactions with the other proteins (Song et al., 2004). In the Co-IPs, talin was immunoprecipitated in the MDA-MB-231 cells and looked for its interaction partners, filamin-1 and actin. Talin was able to be co-immunoprecipitated with filamin-1 or actin in MDA-MB-231 cells suggesting that talin was associated with filamin-1 or actin in the same adhesion complex. Similarly, talin was associated with filamin-1 in U2OS cells. Vinculin was also co-immunoprecipitated with talin in both MDA-MB-231 cells and U2OS cells, suggesting that since talin has multiple vinculin binding sites (VBSs), they were coupled together in the same adhesion complex. Talin and filamin-1 can crosscompete for integrin binding; the structurally defined talin binding and filamin binding regions of β integrin tails overlap (Kiema et al., 2006). In the Co-IPs, SUMOylation may have its role in talin and filamin interactions in the regulation of FA turnover.

The association between vinculin and talin is force-dependent and therefore, their interactions are critical in FA turnover. The N-terminal region of RIAM contains two talin binding sites, which bind synergistically to R2-R3 rod domain of talin; at the same time, the vinculin head domain Vd1 can bind to the R2-R3 region of talin therefore displacing RIAM from association with talin, this suggests that RIAM and vinculin binding to talin is mutually exclusive (Calderwood et al., 2013). This has further made the interaction of talin and vinculin more dynamic and also the FA turnover is spatially and temporally controlled. The vinculin tail Vt competes with the talin rod domain for the binding to the vinculin head Vh D1

domain (amino acid residues 1-258) hence inducing the activation of vinculin from its auto-inhibited conformation, which also requires the Vh D4 domain (residues 710-836) interface (Cohen et al., 2005). Therefore, SUMOylation may be required for the interaction of vinculin with talin, inhibiting protein SUMOylation caused a reduction in their interactions. Treatment with 100 μ M gossypetin for the first 1 hour in MDA-MB-231 cells or 100 μ M GA 1 hour in U2OS cells in Co-IP experiments showed the reduction in the intact SUMOylated talin at 230kDa, 100kDa talin rod fragmented product and the 47kDa talin head. All the fragmented products must be SUMOylated since they were immunoprecipitated. Talin association with vinculin is required for fast FA turnover. Talin rod domain has up to 11 vinculin binding sites (VBSs). Inhibition of SUMOylation caused the depletion in the rod domain of talin which inhibited vinculin binding. The talin head was also lost which could abolish its binding to the integrin. These suggest that SUMOylation is important in talin and vinculin protein interactions.

Talin has been shown to have the C-terminal actin binding domain, where this core actin-binding domain as a region of highly conserved residues is a five-helix bundle linked to the C-terminal helix and is responsible for talin dimerization; specifically, this dimerization helix itself (residues shown 2494-2541) is essential for F-actin binding (Gingras et al., 2008). The single mutation of K2445 results in significant reduction in the F-actin binding to the talin C-terminal domain (Gingras et al., 2008). Interestingly, this K2445 residue has been predicted with high probability for SUMO modification in both of the SUMOplot and GPS SUMO programmes. The co-IP of talin and actin in MDA-MB-231 cells showed that after 1 hour of 100 μ M GA treatment, actin band at 42kDa was less obtained, suggesting that the inhibition of SUMOylation may have diminished talin and actin binding interactions, indicating SUMOylation may be important in talin and actin association.

The Proposed Simplified Model for the Role of SUMOylation in the Regulation of FA Turnover and the Protein Interactions of Integrin, Talin, Vinculin and Actin: SUMO may be required for the FA Disassembly

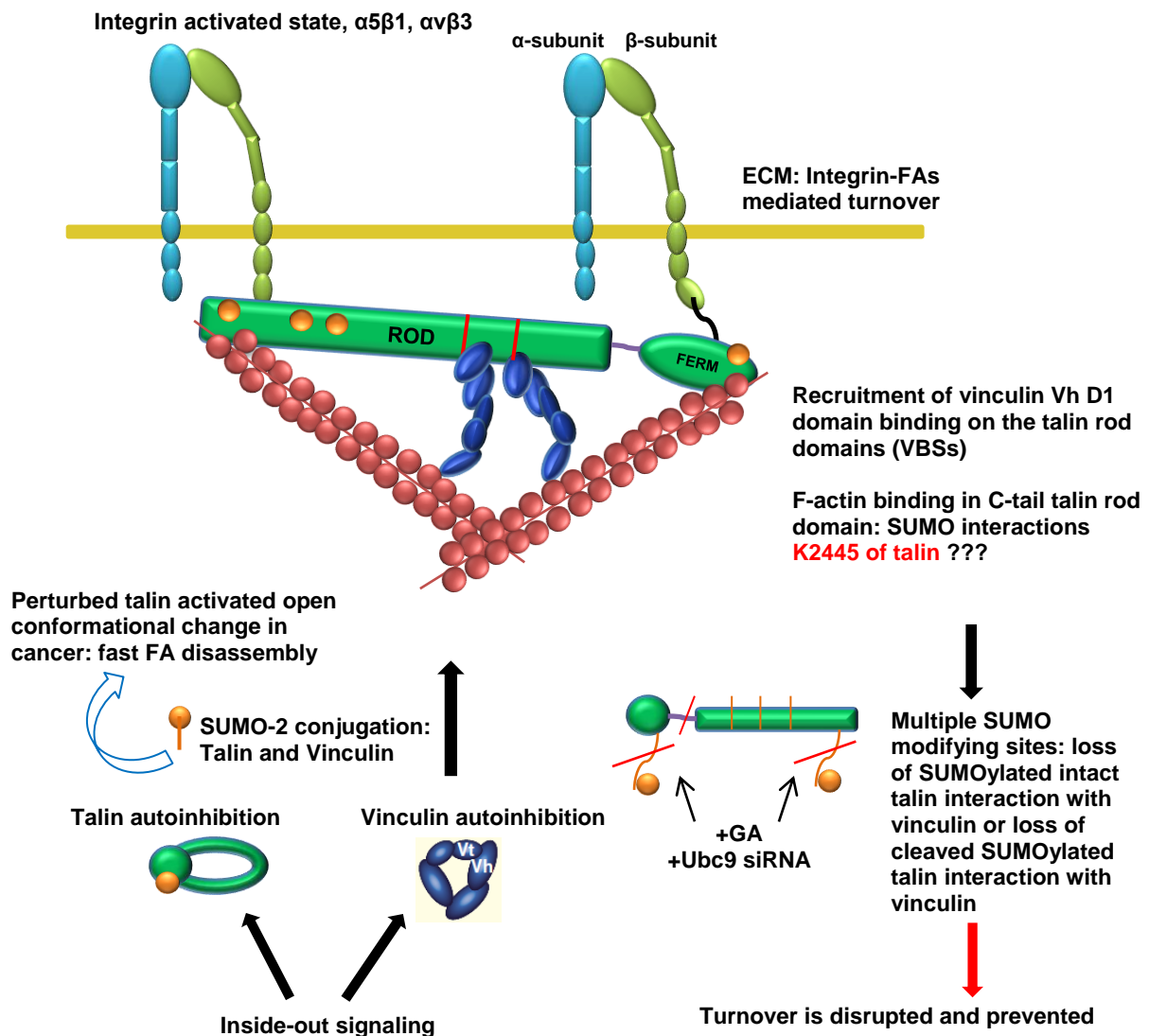


Figure 59. A simplified illustration of the interactions between β_3 integrin, talin, vinculin and actin binding in the adhesion complex: talin or vinculin are in their steady-state equilibrium in the cells; talin is activated through integrin inside-out signalling: this makes the talin rod domain competing with the vinculin Vh D1 domain and activates the vinculin from its auto-inhibited conformation. The recruitment of vinculin Vh binding to talin rod through the VBSs continues to incorporate F-actin binding to FERM domain or C-terminal THATCH domain of talin and onto the Vt domain. SUMO-2 conjugation is required consistently for talin or vinculin modifications and this process happens very dynamically within the FA adhesion complex; K2445 is a predicted lysine with a high probability for SUMO binding as well as actin binding in the talin C-terminal rod; once SUMOylation was inhibited, the newly synthesized SUMO-2 proteins were inhibited from modifying newly produced talin or vinculin probably. The talin containing FAs that were SUMOylated previously and the cleaved SUMOylated fragments of talin associated with the vinculin interactions in the cells were also inhibited and lost, this effect was accounted for inhibition of FA disassembly.

Recently, proteomics has been used to analyse the total protein extracts in U2OS cell line: the total protein extracts were separated by 2D gel electrophoresis and analysed by matrix-assisted laser desorption ionisation-mass spectrometry (MALDI-MS) and MALDI-MS-MS following protein identification and 237 different gene products were identified (Niforou et al., 2008). They have found that the tumour suppressive genes p53 and pRb were functional in the U2OS cells. Later, a global analysis of both mRNA and protein levels using sequence-based transcriptome analysis (RNA-seq) and SILAC-based mass spectrometry analysis was conducted in three different human cell lines, the U2OS, the A-431 an epidermoid squamous cell carcinoma and the U-251 brain glioblastoma; where 5399 proteins were identified in U2OS by MS and 5333 proteins were common in all three cell lines (Lundberg et al., 2010). Another study has shown a new method with filter-aided sample preparation (FASP) and identified 2750 proteins in Hela cells (Wisniewski et al., 2009). The large-scale absolute cellular protein abundance that constitutes a cell is very important in understanding their function and evolution (Beck et al., 2011a). In Beck et al.'s study, they quantified the copy number of focal adhesion proteins and SUMO, Ubc9 etc per cell in the human tissue culture U2OS cell line in Table S1, where the U2OS cells expressed ~10,000 proteins at least (Beck et al., 2011a), this was one of the first studies with the most comprehensive proteome map in a U2OS cell line by far, which is very useful to compare the data obtained with this study and to predict the quantity of the SUMOylated focal adhesions related functions in the cancer cells used, as Beck et al. also have found and predicted that the regulatory functions of proteins i.e. cell adhesion were often correlated with large variable protein families however in very low abundance principally in a cell. This leads to the idea that the FA proteins involved in post-translational modifications i.e. SUMOylation will be mostly conducted with very low abundance proteins.

| Bone osteosarcoma U2OS cell line: Quantitative proteome of focal adhesions and SUMOylation related protein copy number / per cell | | | | | |
|---|--------|---------------------|--------|--|--------|
| Talin-1 | 456000 | Integrin $\beta 5$ | 30000 | SUMO-conjugating enzyme Ubc9 | 392000 |
| Vinculin | 276000 | Integrin $\beta 1$ | 113000 | SUMO activating enzyme subunit 1 SAE1 | 198000 |
| FAK | 3290 | Integrin $\alpha 5$ | 2970 | SUMO activating enzyme subunit 2 UBA2/SAE2 | 152000 |
| Filamin A | 824000 | Integrin $\alpha 3$ | 44500 | Small ubiquitin-related modifier 1 SUMO-1 | 22800 |
| Calpain-2 | 344000 | Integrin αV | 27200 | E3 SUMO-protein ligase RanBP2 | 17400 |
| SUMO-2 | 889000 | Integrin $\alpha 2$ | 13400 | E3 SUMO-protein ligase PIAS1 | 1530 |

Table 11. The complete quantitative proteome of U2OS cell line: the copy number of the cell adhesion related proteins and the SUMOylation proteins per cell are included here from Beck et al.'s study.

From Beck's study (Beck et al., 2011a) in Table 11, the copy number of SUMO-2 was nearly doubled the copy number of talin-1, whereas the copy number of Ubc9 was relatively at a comparable level to the copy number of talin-1 and vinculin. Filamin A was similar to the number of SUMO-2. This has suggested that in a U2OS cell, the copy number of the SUMOylated talin, vinculin, FAK or filamin A all depends on the ratio of the E1 enzyme SAE1/UBA2, SUMO-conjugating E2 enzyme Ubc9 and SUMO-2 conjugation through the ligation E3 enzyme in each step of the SUMOylation cycle and this process is highly regulated and dynamic in equilibrium balance with the cytoplasmic SUMO pool. Relatively, only a small fraction of the protein substrate, often less than 1% that is SUMOylated at any given time (Johnson, 2004). For talin, 1% of talin can get SUMOylated which is 1% of 456000 to be 4560 copy number of SUMOylated talin molecule. For vinculin that gets SUMO-2 modification would be 2760 copy number of SUMOylated vinculin. This could suggest that with the IP experiments shown, the endogenous individual FA protein would be expressed stably with a HA tag of SUMO-2 to obtain the SUMOylated FA before and after the inhibitors treatments. Also with the Ubc9 siRNA knockdown, there would be time required before the SUMOylated individual FA and the free SUMO pool to be diminished.

The expression of FA WB experiments have shown that the total FA protein levels were not affected long-term after 6 hours of 100 μ M GA treatments or 48 hours of 25nM Ubc9 siRNA treatments; the expression of FA total protein level was not significantly changed even after the inhibition of protein SUMOylation globally. The inhibition of SUMOylated FAs did not necessarily decrease the pool of the FAs. This may suggest that inhibiting protein SUMOylation does not induce protein ubiquitination at the same time necessarily. The balance of SUMOylation pathway for the FAs is highly regulated and controlled; the reactions for the SUMOylation of FAs can be competitive for the other post-translational

modifications PTMs, such as phosphorylation, acetylation, ubiquitination, this increases the complexity of the SUMO role in the assembly and disassembly of FAs.

In the SUMO binding assays, where concentrated isolated FA lysates were used, there was also a nice comparison between the SUMOylated intact talin and the total talin level in the cells after 100µM GA 1 hour treatment: the eluted SUMOylated intact talin obtained less compared to its control, whereas for the total talin level, the unbound talin fraction in the whole cell lysate seemed to increase more in the GA treated sample than the control. When after the inhibitor treatment, it increased the total FA levels in the whole cell lysates, which was observed quite consistently in the cells, similarly, this effect was seen in the IP filamin-1 experiments, too. This has suggested that after the GA 1 hour treatment, there was a transient disruption and imbalance in the SUMOylation cycle, which could affect the fractions of the talin protein being SUMOylated.

The talin head domain binding can be competitive between ubiquitination and phosphorylation: the talin head can bind to Smurf 1, which is an E3 ubiquitin ligase involved in cell migration; the calpain-2 mediated cleavage of the talin head can be degraded via the binding of talin head to Smurf 1 mediated ubiquitination; the talin neck can also be phosphorylated by Cdk5 at Ser₄₂₅ within the talin amino acid sequence 393-433, where Cdk5 is a regulator of cell migration and cancer metastasis and this results in the inhibition of the talin head binding to Smurf 1 therefore it prevents talin head from ubiquitination and degradation (Huang et al., 2009). In order to investigate the effects between talin ubiquitination and SUMOylation, the cells would be treated with the inhibitors and immunoprecipitated and blotted with ubiquitin antibodies to determine if the inhibition of SUMOylation could affect ubiquitylation of FAs. It has shown that inhibition of SUMOylation did not induce ubiquitylation of FAs, i.e. talin, which was done in the platelets (data not shown, references to Dr. Diana Barker).

In the double transfection IP experiments, where MDA-MB-231 cells were transfected with the Ubc9 siRNA first then with the HA-tag SUMO-2 plasmid for a total time of 48 hours, SUMOylated intact talin was still detectable. This has indicated that after 48 hours of Ubc9 siRNA treatment, there was still time to achieve the depletion in the pool of SUMOylated FAs, but the first transient effects of the inhibitors were important and critical to determine the effects in the FA turnover after the inhibition of protein SUMOylation.

The reversible post-translational modifications of proteins including acetylation, phosphorylation or ubiquitylation is governed by the recognition of specific interaction domains, which regulates the plasticity of protein-protein interactions (Ullmann et al., 2012). The lysine-directed modifications can be positively or negatively regulated between ubiquitylation and SUMOylation; for example, I κ B α can be mono-SUMOylated or poly-ubiquitinated on K21; phosphorylation could also inhibit or enhance protein SUMOylation (Bossis and Melchior, 2006). The attachment of SUMO paralogues to target substrate proteins is not only through the covalent binding but can also be through a noncovalent binding to the SUMO-interaction motifs (SIMs), which either SIM N terminal or C terminal binding to SUMO is mediated by hydrophobic and electrostatic interactions and the binding could be weakened with increasing ionic strength (Escobar-Cabrera et al., 2011). These SIMs bind to the SUMO moiety that is conjugated to Ubc9, thereby these SUMO substrate can promote their own conjugation (Wang and Dasso, 2009). The site-specific acetylation of SUMO-1 at K37 or SUMO-2 at K33 have revealed a central regulatory mechanism in the selective modulation of SUMO-SIM interactions, where K37/K33 acetylation abolished the binding of SUMO to SIMs in PML protein, Daxx and PIAS family members, thereby affecting the dynamics of PML nuclear bodies and attenuating SUMO and PIAS-mediated gene silencing; this acetyl-dependent switch expands the regulatory functions of SUMO signalling (Ullmann et al., 2012). Daxx, a transcriptional co-regulator, also contained a bona fide SIM that could bind to SUMO-1 in a parallel orientation: this Daxx-SIM can be phosphorylated by CK2 kinase at residues S737 and S739, where this Daxx-SIM phosphorylation causes Daxx binding preference towards SUMO-1 conjugation and enhances Daxx to sensitize stress-induced cell apoptosis via anti-apoptotic gene repression (Chang et al., 2011). These indicate that not only consensus motif in protein are modified by SUMO, other interaction domains can also be important in protein SUMO modification and these are determined in the next step in the Mass Spectrometry and bioinformatics studies.

The total Akt has been used in the HA-tagged SUMO-2 IP experiments as a negative control. The proto-oncogene Akt can be SUMOylated, which has been identified as a novel mechanism for activating Akt function, mediating cell proliferation, cell migration and tumorigenesis; however, Akt could be modified by SUMO-1 and enhanced by SUMO E3 ligase PIAS1 and reversed by the SUMO protease SENP1 and K276 was identified to be a major SUMO-1 acceptor lysine site (Li et al., 2013b). Compared to this study, total Akt was used as a substrate to probe for SUMO-2/3 modification and there were hardly any bands seen in the IP-HA-SUMO-2 samples in the negative control experiments, as Akt SUMO-1 modification shifted up with bands at higher molecular weights. It can be seen that some of the proteins could be modified by SUMO-1 and Akt is an example.

Three IP methods have shown that talin and vinculin were identified to be SUMOylated for the first time. SUMOylation also plays a role in the protein-protein interactions of the FAs. Once protein SUMOylation was inhibited globally, the SUMOylated FA proteins were less obtained. There have been other FA proteins that were predicted to be SUMOylated using the SUMOplot and GPS SUMO bioinformatics software i.e. FAK, actin and filamin-1. This leads to the next step to confirm that the FAs that were previously SUMOylated in the cells could be identified in the mass spectrometry analysis hence increasing the chance of identifying SUMOylated proteins in the FAs and other FA related proteins/adaptors and IP & western blotting will be conducted to confirm the SUMO modified substrates from the mass spectrometry data, i.e. filamin-1.

Chapter 5 – The Identification of Focal Adhesion Proteins Which Can be SUMOylated

5.1 Introduction and Hypothesis

Mass spectrometry analysis have revealed more than 1000 SUMOylated lysines in 539 proteins (Tammsalu et al., 2014). Several approaches have been developed to discover the putative SUMO substrates, using the yeast *Saccharomyces cerevisiae* system, human HEK293 cells, the non-covalent SUMO interacting motifs (SIMs), SUMO fusion technology, LC-MALDI-MS/MS etc to selectively enrich and identify SUMOylated proteins, as for any given protein, the amount of post-translational modified protein is only a small fraction of the total cellular pool (Rosas-Acosta et al., 2005, Galisson et al., 2011, Da Silva-Ferrada et al., 2013, Butt et al., 2005). The most successful studies providing novel SUMO substrates for identifying the SUMOylation proteome has been in the yeast *S. cerevisiae*, as SUMO was independently discovered during yeast two-hybrid screens; this system has supplied with unlimited amounts of starting material, can be easily scaled-up and manipulation accompanied with high accuracy and stringency of the LC-MS/MS analysis instrument (Wykoff and O'Shea, 2005, Wohlschlegel et al., 2004, Rosas-Acosta et al., 2005, Denison et al., 2005). The new strategies for investigating SUMO conjugation, recognition or de-conjugation have become more important to recognize SUMO modification motifs that are not only common to the SUMO-GG signature peptides but to the uncommon motifs (Da Silva-Ferrada et al., 2012).

Computational programmes have been developed to identify potential SUMOylation sites in proteins to match the motif B-K-x-D/E, i.e. using the SUMOplot programme. However, there could be other SUMOylation sites which cannot be identified due to their low abundance in peptide trypsinolysis used for mass spectrometry. There are other motifs that were identified recently: a SUMO-binding motif (SBM) denoted as V/I-X-V/I-V/I (defined as an amino acid sequence motif) was identified by NMR spectroscopic characterization of interactions among SUMO-1 and SUMOylated protein peptides that were known to bind to SUMO and this motif was able to bind to all SUMO paralogues SUMO 1-3 and this newly identified SBM was responsible for the interactions within RanBP2/Nup358 and SUMOylated RanGAP1 (Song et al., 2004). The SUMO interaction motifs (SIMs) motifs interact non-covalently with SUMO and their recognition still seems limited (Kerscher, 2007). SIM domains have been found in the E3 ubiquitin ligase RNF4 (RING finger protein 4), where these repeated four tandem SIMs were for selective interactions with the poly SUMO-modified proteins leading to their degradation (Kung et al., 2014). The previously identified B-K-x-D/E i.e. Ψ -K-X-E binds to

E2 enzyme for covalent modification by SUMO but it cannot bind to SUMO noncovalently (Song et al., 2004).

Tandem mass spectrometry amino acid sequencing is a direct, unbiased and sensitive approach to determine post-translational modification sites, where the tandem mass spectrometry analysis involves the proteolysis of protein conjugates by trypsin to the identification of these modification sites; the successful identification of SUMOylation sites depends heavily on the sensitivity of the mass spectrometer and the retrieval of the low abundance SUMOylated peptides for fragmentation (Knuesel et al., 2005). Other approaches to identify SUMO substrates include overexpressing the SUMO isoforms which each contains an N-terminal histidine tag and a tryptic cleavage site at the C terminus, they can be stably expressed in human cells such as HEK293 cells to selectively enrich and identify SUMOylated peptides from human cells by affinity enrichment and mass spectrometry (Osula et al., 2012, Galisson et al., 2011).

Several programmes have been used for the bioinformatic identification and prediction of protein SUMOylation. Two of them have been used in this study. The SUMOplot™ analysis program predicts the probability of the SUMO consensus sequence associated in the protein-SUMO attachment; the SUMOplot™ score system has two criteria: direct amino acid match to the SUMO consensus sequence and the substituted amino acid residues exhibiting similar hydrophobicity to the consensus amino acid residues (SUMOplot™ analysis programme, Abgent).

A new generation group-based prediction system (GPS) algorithm GPS SUMO was firstly used as a prediction tool for both protein SUMOylation sites and SUMO interaction motifs SIMs (Zhao et al., 2014). In their study, they stated that approximately 40% of SUMOylation sites do not conform to the canonical consensus motif of B-K-x-D/E i.e. Ψ -K-X-E and recently nearly ten types of SIMs were experimentally identified but only representing a small proportion of the SIMs, therefore GPS SUMO was developed as a reliable tool to construct the SIMs data sets (Zhao et al., 2014). Many other programmes have been developed such as SUMOsp, seeSUMO web server, SUMOpre etc with many performance measure evaluations such as accuracy, sensitivity, specificity, strength and MCC (Matthews correlation coefficient) (Teng et al., 2012, Xu et al., 2008).

The two prediction tools for SUMOylation in this study can be found at <http://sumosp.biocuckoo.org/> and <http://www.abgent.com/sumoplot>

In this study, human cell lines have been used to identify and confirm potential SUMO targets. The validity of the LS/MS proteomics approach have been confirmed by performing subsequent western blotting experiments for filamin-1 and determining the predicted SUMOylation sites on the protein amino acid sequences. The simplified filamin-1 structure is shown in Figure 60.

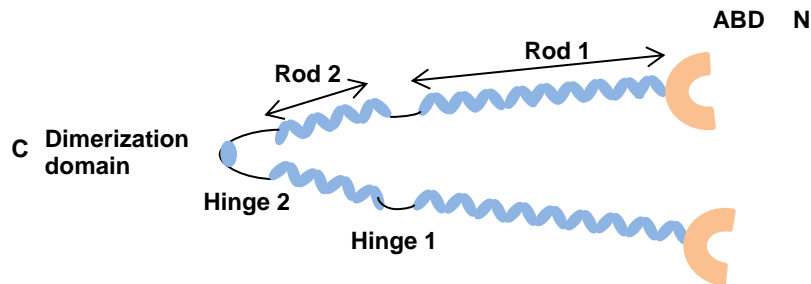


Figure 60. Simplified diagram of the structure of filamin-A (filamin-1): filamin-1 has C-terminal dimerization domain and N-terminal ABD domain (actin binding domain), it also has Rod 1 and Rod 2 domain which are the major protein partner interaction domains, Modified from (Popowicz et al., 2006)

Filamin-A (filamin-1) is a large actin-binding protein and filamins link the actin network to cellular membrane to integrate with cellular signalling for cell locomotion; filamins are located both at the cell leading edge and the rear of motile cells where they can directly regulate actin cytoskeleton remodelling important for cell protrusions and retractions (Zhou et al., 2009). Filamin-1 can bind to the cytoplasmic tail of β integrin to prevent integrin activation in cells, where they could undergo intramolecular auto-inhibition of integrin binding; this is important for controlling cell adhesion and migration (Pentikäinen and Yläne, 2009).

Hypothesis

Chapter 3 and 4 have shown that the focal adhesion proteins, talin and vinculin can be SUMOylated and that SUMOylation plays a critical regulatory role in the dynamic activities of the FAs in cancer cells, where inhibiting protein SUMOylation caused increased numbers of FAs and enlarged FAs. SUMOylation may have a diverse role in the regulation of cell migration. The FA proteins assemble and form FA adhesion complex at the membrane fractions. Therefore, in this Chapter, it was hypothesized that not just one FA protein could be SUMOylated, but SUMOylation may be implicated in the regulation of FA adhesion complex and FA protein-protein interactions. In this study, MDA-MB-231 cells, platelets, and a human megakaryocyte-like cell line, CMK11-5 cells, have been used to investigate, identify and confirm whether talin, vinculin and other FA proteins in the adhesion complex and any proteins associated in the inside-out integrin-FA signalling can be SUMOylated.

Methods

5.2 Mass Spectrometry

A two-step process has been done to obtain the mass spectrometry samples. The MDA-MB-231 cells, platelets and the CMK11-5 cells were prepared for the SUMO VIVA™ Binding Assay system. Next, these samples were followed through for the mass spectrometry preparations. Firstly, MDA-MB-231 cells and the CMK11-5 cells were treated and prepared as control 1 hour vs. GA 1 hour; the platelets samples were prepared as control 30 minutes vs. GA 30 minutes. Whole cell lysates were made using the lysis buffer from the VIVAbind™ SUMO Kit (see previous method 4.2). The lysis buffer was added with 50mM NEM additionally and prepared for the number of sample tubes needed. For CMK11-5 cells, the cell suspensions were centrifuged at 1500 rpm for 5 minutes. The media was removed and the cell pellets were kept. For each cell pellet, 300µl lysis buffer was added and mixed well in the tube. The cell lysates were transferred into the eppendorf tubes and kept on ice. For the platelets, blood was taken from the donors directly and the platelets were extracted from the blood by centrifugation, isolation and purification. Fresh platelets were prepared and used immediately. 1×10^9 platelets / 6ml were used, which the protein concentration was around 0.6mg / 2ml. The platelets were also centrifuged to get the pellets. For each control and GA treated samples was added with 200µl lysis buffer and mixed well.

0.1% v/v formic acid was prepared and filtered (pH=4.0). All the sample reactions were done on ice. Each sample tube was added with the 40µl VIVAbind™ SUMO matrix suspension. Once the sample capped columns were washed with the wash buffer x3 and the unbound fractions were transferred into separate eppendorf tubes for each sample, the capped column was added with 200µl 0.1% v/v filtered formic acid. All the sample columns were mixed and rotated on the rotary machine for 5-10 minutes at room temperature. Then the column base was uncapped and placed into a new eppendorf tube for each sample. All the sample tubes were centrifuged at 5000g for 1 minute to collect eluted materials. The elution fractions could then be stored at -20°C and ready to be sent out for mass spectrometry analysis of Birmingham University, the functional genomics and proteomics laboratories, School of Biosciences, the University of Birmingham. LC-MS/MS analysis has been applied in these samples' analysis.

LC-MS/MS (University of Birmingham)

Trypsin digestion: this step was performed using 10µl of samples (~1-100µg of protein) and added 40µl of 100mM ammonium bicarbonate (pH=8). Then the sample was added 50µl of 10 mM dithiothreitol (DTT) and the samples were incubated at 56 °C for 30 minutes. The samples were then cooled to room temperature and cysteines alkylated by the addition of 50µl of 50mM iodoacetamide, mixed and incubated at room temperature in the dark for 30 minutes. 25 µl of trypsin gold (Promega, Southampton, Hampshire, UK, 6ng/µl) was subsequently added to the samples, which were then incubated at 37 °C overnight.

LC-MS/MS experiment: UltiMate[®] 3000 HPLC series (Dionex, Sunnyvale, CA USA) was used for peptide concentration and separation. The samples were trapped on uPrecolumn Cartridge, Acclaim PepMap 100 C18, 5 µm, 100A 300µm i.d. x 5mm (Dionex, Sunnyvale, CA USA) and separated in Nano Series™ Standard Columns 75 µm i.d. x 15 cm, packed with C18 PepMap100, 3 µm, 100Å (Dionex, Sunnyvale, CA USA). The gradient used was from 3.2% to 44% solvent B (0.1% formic acid in acetonitrile) for 30 minutes. Peptides were eluted directly (~ 300 nL min⁻¹) via a Triversa Nanomate nanospray source (Advion Biosciences, NY) into a LTQ Orbitrap Elite mass spectrometer (ThermoFisher Scientific, Germany). The data-dependent scanning acquisition was controlled by Xcalibur 2.1 software. The mass spectrometer alternated between a full FT-MS scan (m/z 380 – 1800) and subsequent collision-induced dissociation (CID) MS/MS scans of the 7 most abundant ions. Survey scans were acquired in the Orbitrap with a resolution of 120 000 at m/z 400 and automatic gain control (AGC) 1x10⁶. Precursor ions were isolated and subjected to CID in the linear ion trap with AGC 1x10⁵. Collision activation for the experiment was performed in the linear trap using helium gas at normalized collision energy to precursor m/z of 35% and activation Q 0.25. The width of the precursor isolation window was 2 m/z and only multiply-charged precursor ions were selected for MS/MS.

The MS was run to obtain the spectra of digested peptides from the samples and the MS and MS/MS scans were searched against Uniprot database (or supplied by customer) using SEQUEST algorithm (Thermo Fisher PD 1.4), where the database could provide theoretical spectra / computational calculated masses of peptides from the theoretical trypsin digested protein peptides. The protein peptide sequence would be identified by the searching software: the data-dependent scanning acquisition was controlled by Xcalibur 2.1 software and the survey scans were acquired in the Orbitrap. Variable modifications were deamidation (N and Q), oxidation (M) and phosphorylation (S, T and Y). Carbamidomethyl (C) modification was for fixed modification. The precursor mass tolerance was 10 ppm and

the MS/MS mass tolerance was 0.8Da. Two missed cleavage was allowed and were accepted as a real hit protein with at least two high confidence peptides.

If the experimental mass matched the computational calculated mass, the peptide sequence would be identified by the searching software and the software has validated the peptide sequences identified statistically and these peptide sequences were used to confer which proteins were in the samples. The software could only find the peptides which the peptide sequences were present in the database. For the Orbitrap the Birmingham proteomics unit has used which could identify the length of amino acids between 6 and 14.

Results

5.3 The Predictions of SUMOylated Talin Using SUMO-plot and GPS SUMO Programmes

The amino acid sequence in the head, linker and rod domain of human talin-1



Figure 61. The amino acid sequence of human talin-1, its head, linker domain and the dimerization domain have been highlighted in the structure of the molecule, where the rod domain of talin consists the major part of the amino acid sequence; any lysine residues that were predicted previously to be SUMO modified have been highlighted in either red or blue colour: the red lysine residues were the motifs with probability score above 0.5 using the SUMOplot; the blue lysine residues were the motifs with probability score just under 0.5

In Figure 61, talin-1 molecule has been highlighted in three regions: the head domain (1-400 amino acids), the linker domain where a calpain-2 cleavage site is located and the rod

domain which consists of the talin dimerization domain and it also contains a calpain-2 cleavage site. In all the three regions of talin: the head, linker and the rod domains, there have been predictions of SUMO conjugation sites in the talin-1 molecule and these residues were highlighted in red and blue according to the SUMOplot programme predictions.

SUMOplot™ Analysis Programme (Abgent) Predictions on the SUMOylation Sites in Talin (Protein ID: Q9Y490): Motif B-K-x-D/E

Motifs with probability score > 0.5

Motifs with probability score < 0.5

| No. | Lysine Position | Peptide Sequence | Probability Score |
|-----|-----------------|-------------------------|-------------------|
| 1 | K841 | DLVNA IKAD AEGES | 0.94 |
| 2 | K2445 | LVACK VKAD QDSEA | 0.93 |
| 3 | K2063 | RLADV VKLG AASLG | 0.76 |
| 4 | K441 | QYNRV GKVE HGSVA | 0.67 |
| 5 | K1415 | GISQN AKNG NLPEF | 0.62 |
| 6 | K263 | AGFLD LKDF LPKEY | 0.56 |
| 7 | K274 | KEYVK QKGE RKIFQ | 0.50 |
| 8 | K2375 | ELVAQ GKVG AIPAN | 0.50 |
| 9 | K2104 | TKAAA GKVG DDPAN | 0.50 |
| 10 | K137 | RELME EKKE EITGT | 0.50 |
| 11 | K157 | LLRDE KKME KLKQK | 0.48 |
| 12 | K138 | ELMEE KKEE ITGTL | 0.48 |
| 13 | K2322 | IEAAA KKLE QLKPR | 0.48 |

GPS SUMO Programme Predictions on the Talin-1 Protein Peptide Sequence

| Position | Peptides | Score | Cut-off | Type |
|-------------|-------------------------------|--------|---------|------------------|
| 2445 | LLVACK V KADQDSEA | 44.828 | 36.625 | Sumoylation |
| 841 | SDLVNA I KADAEGES | 38.22 | 36.625 | Sumoylation |
| 300 | EAKVRY V KLARSLKT | 36.667 | 36.625 | Sumoylation |
| 1599 -1603 | GRAAMEP I VISA KTMLESA | 62.07 | 59.29 | SUMO Interaction |
| 2078 - 2082 | AEDPETQ V VLIN AVKDVAK | 61.629 | 59.29 | SUMO Interaction |
| 965 -969 | AVAEQIP L LVQG VRGSQAQ | 60.904 | 59.29 | SUMO Interaction |
| 396 - 400 | AQLIAGY I DIIL KKKKSKD | 60.757 | 59.29 | SUMO Interaction |
| 388 - 392 | QTTEGEQ I AQLI AGYIDII | 59.806 | 59.29 | SUMO Interaction |

Table 12. SUMOplot predictions on the talin SUMOylation sites, lysine positions with score above 0.5 were highlighted in red and the position scores below 0.5 were highlighted in blue. Another software GPS SUMO programme shows the SUMOylation predictions as well as the SUMO interactions SIMs of talin-1 SUMOylation, where the FASTA sequence of talin-1 was inputted and the medium threshold was used: the modified positions, modified peptides, score for the modification, cut-off and the type of SUMO modifications were presented

In Table 12, talin was predicted to be a protein substrate for SUMOylation using both SUMOplot and GPS SUMO programmes. The SUMOplot analysis programme predicts the probability of the direct match of the SUMO consensus motif B-K-x-D/E associated in the

talín-SUMO conjugation and the adjacent lysine residues that could substitute the amino acid residues exhibiting similar hydrophobicity to the consensus amino acid residues. The probability score of the prediction of the SUMO consensus motif: the lysine residues were coloured red with a high probability score above 0.5; the lysine residues were coloured blue with a probability score below 0.5. The lysine positions predicted as the SUMO conjugation sites were highlighted in red as K841 and K2445 from the SUMOplot programme, which were also predicted as the same lysine residues using the GPS SUMO programme, indicating these two lysine residues are highly likely to be SUMOylated in talin.

5.4 The Predictions of SUMOylated Vinculin Using SUMO-plot and GPS SUMO Programmes

The amino acid sequence in the head, neck region and tail domain of human vinculin

1 MPVFHTRTIE SILEPVAQKI SHLVIMHEEG EVDGKAIPDL TAPVAAVQAA VSNLVRVGKE
61 TVQTTEDQIL **KRD**MPPAFIK **VEN**ACTKLVQ AAQMLQSDPY SVPARDYLID GSRGILSGTS
121 DLLLTFDEAE VRKIIRVCKG ILEYLTVAEV VETMEDLVTY TKNLGPGMTK MAKMIDERQQ
181 **ELTHQ**EHVRVM **LVNSM**NTVKE **LLPVL**ISAMK **IFVTT**KNSKN **QGIEE**ALKNR NFTVEKMSAE
241 INEIRVLQL TSWDEDAWAS KDTEAMKRAL ASIDSKLNQA KGWLRDPSAS PGDAGEQAIR
301 QILDEA**GKVG** ELCAGKERRE ILGTCKMLGQ MTDQVADLRA RGQGSSPVAM QKAQQVSQGL
361 DVLT**AKV**ENA ARKLEAMTNS KQSIKKIDA AQNWLADPNG GPEGEEQIRG ALAEARKIAE
421 LCDDPKERDD ILRSLGEISA LTSKLADLRR **QKG**DSPEAR ALAKQVATAL QNLQTKTNRA
481 VANSRPAKAA VHLE**GKIE**QA QRWIDNPTVD DRGVGQAAIR GLVAEGHRLA NVMMGPYRQD
541 **LLAKC**DRVDQ LTAQLADLAA RGEGESQAR ALASQLQDSL KDLKARMQEA MTQEVSDVFS
601 DTTTPIKLLA VAATAPPDAP NREEVFDERA ANFENHS**GKL** GATAEKAAAV GTANKSTVEG
661 IQASVKTARE LTPQVVSAAAR ILLRNPQNQA AYEHFETMKN QWIDNVEKMT GLVDEAIDTK
721 SLLDASEEAI **KKD**LDKCKVA MANIQPQMLV AGATSIARRA NRILL**VAKRE** VENSEDPKFR
781 EAVKAASDEL SKTISPMVMD AKAVAGNISD PGLQKSFLDS GYRILGAVAK VREAFQPQEP
841 DFPPPPPDLE QLRLTDELAP **PKPPL**PEGEV PPRPPPP**PEE** **KDEE**FPEQKA GEVINQPMMM H1
901 AARQLHDEAR KVS**SKG**NDI AAKRMALLM AEMSRLVYRG SGT**KRAL**IQG AKDIKASDE H2
961 **VTRLA**KEVAK **QCTD**KRIRTN **LLQV**CERIPT **ISTQL**KILST **VKATML**GRTN ISDEESEQAT H3 H4
1021 **EMLVH**NAQNL **MQSVK**ETVRE **AEAAS**IKIRT **DAGFT**LRWVR **KTPWY**Q H5

Vh (D1, D2, D3, D4, amino acids 1-835)

An intramolecular binding site for the vinculin tail (181-226)

V proline-rich neck region (836-877): binding of VASP, ponsin, vinexin

Vt (877-1066): binding of PIP2, paxillin, actin

Figure 62. The amino acid sequence of the human vinculin: the vinculin molecule has been highlighted in three regions: the vinculin head Vh, the intramolecular binding site for the vinculin tail and the vinculin tail Vt; there have been many predictions in the SUMO conjugation sites of the vinculin molecule; SUMO modified residues were highlighted in red with probability above 0.5 using SUMOplot

In Figure 62, the vinculin molecule has been highlighted in four regions: the vinculin head domain (1-835 amino acids), an intramolecular binding site for the vinculin tail (181-226), the proline-rich neck region (836-877) and the vinculin tail domain (877-1066). In the three regions of vinculin: the head, the neck region and the tail domains, there have been predictions of SUMO conjugation sites in the vinculin molecule and these residues were highlighted in red according to the SUMOplot programme predictions.

SUMOplot™ Analysis Programme (Abgent) Predictions on the SUMOylation Sites in Vinculin (Protein ID: P18206-2, Isoform 1): Motif B-K-x-D/E

Motifs with probability score > 0.5

| No. | Lysine Position | Peptide Sequence | Probability Score |
|-----|-----------------|--------------------------|-------------------|
| 1 | K731 | ASEEA IKKD LDKCK | 0.94 |
| 2 | K80 | MPPAF IKVE NACTK | 0.94 |
| 3 | K71 | TEDQI LKRD MPPAF | 0.91 |
| 4 | K768 | RILLV AKRE VENSE | 0.79 |
| 5 | K544 | RQDLL AKCD RVDQL | 0.79 |
| 6 | K366 | LDVLT AKVE NAARK | 0.79 |
| 7 | K496 | AVHLE GKIE QAQRW | 0.67 |
| 8 | K453 | DLRRQ GKGD SPEAR | 0.67 |
| 9 | K881 | PPPPE EKDE EFPEQ | 0.5 |
| 10 | K862 | DELAP PKPP LPEGE | 0.5 |
| 11 | K639 | FENHS GKLG ATA EK | 0.5 |
| 12 | K308 | ILDEA GKVG ELCAG | 0.5 |

GPS SUMO Programme Predictions on the Vinculin Protein Peptide Sequence

| Position | Peptides | Score | Cut-off | Type |
|------------|------------------------------|--------|---------|------------------|
| 80 | DMPPAF IK VENACTK | 50.727 | 16 | Sumoylation |
| 71 | TTEDQIL KRD MPPAF | 41.438 | 36.625 | Sumoylation |
| 731 | DASEEA IKD LDKCK | 39.463 | 36.625 | Sumoylation |
| 366 | GLDVLT AK VENAARK | 19.444 | 16 | Sumoylation |
| 768 | NRILLV AK REVERSE | 18.608 | 16 | Sumoylation |
| 245 -249 | SAEINEI IRVLQ LTSWDED | 65.014 | 59.29 | SUMO Interaction |
| 20 - 24 | LEPVAQQ ISHLV IMHEEGE | 61.265 | 59.29 | SUMO Interaction |

Table 13. SUMOplot predictions on the vinculin SUMOylation sites, lysine positions with score above 0.5 were highlighted in red indicating high probabilities. GPS SUMO programme shows the SUMOylation predictions as well as the SUMO interactions SIMs of vinculin SUMOylation, where the FASTA sequence of vinculin was inputted and the medium threshold was used: the modified positions, modified peptides, score for the modification, cut-off and the type of SUMO modifications were presented

In Table 13, vinculin was also predicted to be a protein substrate for SUMOylation using both SUMOplot and GPS SUMO programmes. The highlighted lysine residues in black K731, K80 and K71 have been predicted as the SUMOylation sites using both programmes, indicating that these lysine residues could be SUMOylated with a high probability. K768 and K366 are also predicted to be the SUMOylation sites in vinculin with lower probability compared to these top three lysine residues.

5.5 Mass Spectrometry Analysis Identifies Focal Adhesions can be SUMOylated

Protein Score

The protein score is the sum of the scores of the individual peptides. SEQUEST search algorithm was used (Thermo Fisher PD 1.4), for which the software was used to search the peptides that were matched with the protein peptides directly; the percolator statistical software with FDR (false discovery rate) setting at 0.01 was applied to validate how good the matches were for the found peptides: the score is the sum of all the peptide XCorr values above the specified score threshold and this XCorr score for each matched peptide was validated. With FDR 0.01, a set of threshold values were generated for the ions at different charge states and only the peptides found above the specified threshold was considered high confidence peptides and they were only sent by the Birmingham Proteomics Unit. The analysis from the Birmingham Proteomics Unit has listed the high confidence peptide according to the threshold: +1: 0.05, +2: 2.215, +3: 2.46, +4: 3.705, +5: 3.715, +6: 3.72, \geq +7: 3.725. Only the highest peptide score in each searching above the set threshold was kept, all the other peptides under that threshold were filtered out. Only the highest scored peptide was used with the Proteome Discoverer application. Whilst a search was performed using dynamic modifications, one spectrum might have multiple matches because of permutations of the modification site. The higher the score the better it is.

Coverage

The percent coverage was calculated by dividing the number of amino acids in all found peptides by the total number of amino acids in the entire protein sequence. The higher the coverage value the better it is for a peptide.

The Mass Spectrometry Identification of SUMOylated Proteins:

As for the three different cell lines, each cell line was prepared as control and GA treated whole cell lysate samples before they were put through the SUMO binding kit columns. All the samples sent were set as control and GA treated samples that were obtained with SUMOylated proteins as prepared previously. Most of the focal adhesions were completely gone after the 1 hour of 100 μ M GA treatment.

MDA-MB-231 cells control 1 hour

| Accession | Protein Description | Score | Coverage |
|-----------------|--|--------------|--------------|
| Q9Y490 | Talin-1 | 73.77 | 13.58 |
| B4DW52 | cDNA FLJ55253, highly similar to Actin, cytoplasmic 1 | 48.18 | 55.62 |
| A6NDY9 | Filamin A | 24.81 | 6.18 |
| B3KTS5 | Voltage-dependent anion-selective channel protein 1 | 18.20 | 33.57 |
| P68366-2 | Isoform 2 of Tubulin alpha-4A chain | 17.55 | 18.71 |
| Q8WU19 | Tubulin alpha-1B chain | 17.15 | 24.18 |
| P07355 | Annexin A2 | 15.43 | 25.66 |
| Q86XU5 | MYH9 protein | 14.23 | 3.71 |
| Q96B49 | Mitochondrial import receptor subunit TOM6 homolog | 13.62 | 22.97 |
| P63104 | 14-3-3 protein zeta/delta | 13.42 | 26.12 |
| E9PLJ3 | Cofilin-1 | 11.21 | 35.44 |
| P61224-2 | Isoform 2 of Ras-related protein Rap-1b | 10.67 | 21.17 |
| D6REL8 | Fibrinogen beta chain | 9.98 | 15.81 |
| MOR111 | Tubulin beta-4A chain | 9.00 | 35.14 |
| P01834 | Ig kappa chain C region | 8.72 | 51.89 |
| B4DKM5 | Voltage-dependent anion-selective channel protein 2 | 8.10 | 13.73 |
| B0QYP8 | Beta-parvin | 7.19 | 7.22 |
| K7EJ44 | Profilin 1 | 7.08 | 26.92 |
| P18206-2 | Isoform 1 of Vinculin | 5.06 | 3.38 |

Table 14. Summarising the identification of SUMOylated proteins in MDA-MB-231 cells for the control sample in the MS data analysis (Birmingham Proteomics Unit); these cells were previously prepared as whole cell lysates, mixed and incubated with the SUMO matrix-containing columns to obtain eluted SUMOylated proteins and reserved in 0.1% formic acid previously

MDA-MB-231 cells GA 100µM treatment 1 hour

| Accession | Protein Description | Score | Coverage |
|-----------|---|-------|----------|
| P21796 | Voltage-dependent anion-selective channel protein 1 | 30.98 | 45.58 |
| P07355 | Annexin A2 | 29.05 | 39.23 |
| P01834 | Ig kappa chain C region | 12.13 | 66.98 |
| B4DKM5 | Voltage-dependent anion-selective channel protein 2 | 9.62 | 21.96 |
| B4DNG6 | Annexin | 8.75 | 13.68 |
| Q96B49 | Mitochondrial import receptor subunit TOM6 homolog | 8.22 | 22.97 |
| H0YFX9 | Histone H2A | 6.17 | 20.65 |
| S6BGE0 | IgG H chain | 5.89 | 11.00 |

Table 15. Summarising the identification of SUMOylated proteins in MDA-MB-231 cells for the 100µM GA 1 hour treated sample in the MS data analysis (Birmingham Proteomics Unit). These cells were previously prepared as whole cell lysates, mixed and incubated with the SUMO matrix-containing columns to obtain eluted SUMOylated proteins and reserved in 0.1% formic acid previously

In Table 14, the FA proteins including talin-1 (with high protein score and relatively high coverage), actin-1 (with high protein score and high coverage), filamin A (with high protein score), tubulin α4A chain, tubulin α1B chain, myosin 9, vinculin, cofilin-1, profilin-1 etc have been identified in the MDA-MB-231 cells in the control sample in the MS data analysis. In table 15, after 100µM of GA 1 hour treatment, all of them were gone in the sample.

CMK11-5 cells control 1 hour

| Accession | Protein Description | Score | Coverage |
|-----------------|--|---------------|--------------|
| Q9Y490 | Talin-1 | 269.47 | 39.87 |
| Q60FE6 | Filamin A | 158.23 | 34.04 |
| P35579 | Myosin-9 | 94.96 | 18.52 |
| B4DW52 | cDNA FLJ55253, highly similar to Actin, cytoplasmic 1 | 72.31 | 49.57 |
| P08514-3 | Isoform 3 of Integrin alpha-IIb | 52.82 | 25.92 |
| P12814-2 | Isoform 2 of Alpha-actinin-1 | 40.49 | 16.12 |
| P61224-3 | Isoform 3 of Ras-related protein Rap-1b | 34.11 | 49.70 |
| B7Z4U6 | Gelsolin | 32.10 | 24.24 |
| P18206-2 | Isoform 1 of Vinculin | 31.78 | 9.10 |
| X6RJP6 | Transgelin-2 | 28.49 | 52.41 |
| B4DQN9 | Tubulin beta-7 chain | 28.30 | 22.85 |
| P08567 | Pleckstrin | 28.22 | 32.86 |
| Q53GA7 | Tubulin alpha 6 variant | 28.01 | 26.06 |
| B4DVY2 | cDNA FLJ54184, highly similar to Tropomyosin alpha-4 chain | 24.00 | 36.68 |
| A0A024R9Q1 | Thrombospondin 1 | 23.88 | 12.05 |
| D3JV41 | Thrombocidin-2 antimicrobial variant | 22.41 | 41.27 |
| G3V1A4 | Cofilin 1 (Non-muscle) | 21.53 | 44.97 |
| Q9H4B7 | Tubulin beta-1 chain | 20.93 | 23.50 |
| P02675 | Fibrinogen beta chain | 20.06 | 22.61 |
| P68366-2 | Isoform 2 of Tubulin alpha-4A chain | 18.44 | 22.40 |
| P02679-2 | Isoform Gamma-A of Fibrinogen gamma chain | 17.43 | 23.34 |
| B4E2L8 | Coagulation factor XIII A chain (EC 2.3.2.13) | 16.95 | 6.55 |
| P07737 | Profilin 1 | 15.39 | 50.00 |
| P68871 | Hemoglobin subunit beta | 14.63 | 53.74 |
| E9M4D4 | Hemoglobin alpha-1 globin chain | 13.10 | 69.00 |
| F5H1C6 | Fermitin family homolog 3 | 13.09 | 23.78 |
| P02671-2 | Isoform 2 of Fibrinogen alpha chain | 12.62 | 9.47 |
| L7UUZ7 | Integrin beta | 12.21 | 6.22 |
| Q9H299 | SH3 domain-binding glutamic acid-rich-like protein 3 | 10.12 | 55.91 |
| B0QYP8 | Beta-parvin | 8.25 | 14.43 |
| P19105 | Myosin regulatory light chain 12A | 7.36 | 17.54 |
| B4DQX7 | Zyxin | 7.04 | 12.53 |
| H3BQ34 | Pyruvate kinase | 6.73 | 17.44 |
| S6BGE0 | IgG H chain | 6.68 | 11.00 |
| B4DNG6 | Annexin | 6.51 | 23.93 |
| P04075 | Fructose-bisphosphate aldolase A | 6.00 | 11.54 |
| E9PI65 | Heat shock cognate 71 kDa protein | 5.75 | 13.69 |
| E5RGE1 | 14-3-3 protein zeta/delta | 5.39 | 43.14 |

Table 16. Summarising the identification of SUMOylated proteins in CMK11-5 cells for the control sample in the MS data analysis (Birmingham Proteomics Unit); these cells were previously prepared as whole cell lysates, mixed and incubated with the SUMO matrix-containing columns to obtain eluted SUMOylated proteins and reserved in 0.1% formic acid previously

CMK11-5 cells GA 100µM treatment 1 hour

| Accession | Protein Description | Score | Coverage |
|-----------|---|-------|----------|
| B4DKM5 | Voltage-dependent anion-selective channel protein 2 | 25.31 | 46.67 |
| P21796 | Voltage-dependent anion-selective channel protein 1 | 24.62 | 38.16 |
| B4DVQ0 | Actin, cytoplasmic 2 | 24.04 | 30.33 |
| Q8IUUK7 | ALB protein | 13.61 | 9.09 |
| Q8WU19 | TUBA1B protein | 12.88 | 18.81 |
| B4DNH8 | Annexin | 12.24 | 26.29 |
| Q9Y277 | Voltage-dependent anion-selective channel protein 3 | 10.94 | 11.31 |
| P01834 | Ig kappa chain C region | 7.10 | 49.06 |
| P07737 | Profilin 1 | 6.27 | 21.43 |
| E9PI65 | Heat shock cognate 71 kDa protein (Fragment) | 4.42 | 14.88 |
| Q5TCU6 | Talin-1 | 4.23 | 0.58 |
| O96008 | Mitochondrial import receptor subunit TOM40 homolog | 3.84 | 4.16 |
| M0QZN2 | 40S ribosomal protein S5 | 3.73 | 11.19 |
| F8VV32 | Lysozyme C | 3.46 | 11.54 |
| H0YFX9 | Histone H2A (Fragment) | 3.40 | 20.65 |
| A6NDY9 | Filamin A | 3.22 | 0.65 |
| Q6B823 | Histone H4 (Fragment) | 2.83 | 23.26 |
| P02776 | Platelet factor 4 | 2.81 | 14.85 |
| G3V1A4 | Cofilin 1 (Non-muscle) | 2.80 | 9.40 |
| Q0MVN7 | Integrin subunit α IIb (Fragment) | 2.38 | 6.36 |

Table 17. Summarising the identification of SUMOylated proteins in CMK11-5 cells after 100µM GA 1 hour treatment in the MS data analysis (Birmingham Proteomics Unit); these cells were previously prepared as whole cell lysates, mixed and incubated with the SUMO matrix-containing columns to obtain eluted SUMOylated proteins and reserved in 0.1% formic acid previously

In Table 16, the FA proteins including talin-1 (with high protein score and high coverage), filamin A (with high protein score and high coverage), myosin-9 (with high protein score and high coverage), actin-1 (with high protein score and high coverage), integrin α IIb β 3 (with high protein score and high coverage), α -actinin-1, isoform 2 (with high protein score and high coverage), vinculin (with high protein score and relatively high coverage), tubulin β 7 chain, tubulin α 6, tubulin β 1, tubulin α 4A chain, cofilin-1, profilin-1 etc have been identified in the CMK11-5 cells in the control sample in the MS data analysis. In table 17, after 100µM of GA 1 hour treatment, most of the FA proteins were gone in the GA treated sample, i.e. talin-1 protein score was 4.23 with only 0.58 protein coverage score; filamin-A protein score was 3.22 with only 0.65 protein coverage score.

Platelets Control 30 minutes

| Accession | Protein Description | Score | Coverage |
|---------------|--|--------------|--------------|
| B4DW52 | cDNA FLJ55253, highly similar to Actin, cytoplasmic 1 | 43.39 | 42.94 |
| X6RJP6 | Transgelin-2 | 22.34 | 46.52 |
| P61224-2 | Isoform 2 of Ras-related protein Rap-1b | 14.35 | 21.17 |
| G3V1A4 | Cofilin 1 (Non-muscle) | 13.27 | 28.19 |
| P01834 | Ig kappa chain C region | 12.25 | 66.98 |
| P08514-3 | Isoform 3 of Integrin alpha-IIb | 12.23 | 6.40 |
| MOQZN2 | 40S ribosomal protein S5 | 8.18 | 11.19 |
| D3DX71 | LIM and senescent cell antigen-like domains 1 | 8.17 | 25.86 |
| F8VVB9 | Tubulin alpha-1B chain | 6.66 | 11.79 |
| K7EPB9 | Tropomyosin alpha-4 chain (Fragment) | 6.64 | 18.18 |
| B7Z4U6 | Gelsolin | 6.63 | 5.81 |
| S6BGE0 | IgG H chain | 6.21 | 11.00 |
| D3DP16 | Fibrinogen gamma chain | 5.84 | 5.99 |
| P11142-2 | Isoform 2 of Heat shock cognate 71 kDa protein | 5.78 | 10.55 |
| Q5TCU6 | Talin 1 | 5.58 | 1.03 |

Table 18. Summarising the identification of SUMOylated proteins in platelets for the control sample in the MS data analysis (Birmingham Proteomics Unit); these cells were previously prepared as whole cell lysates, mixed and incubated with the SUMO matrix-containing columns to obtain eluted SUMOylated proteins and reserved in 0.1% formic acid previously

Platelets GA 100µM treatment 30 minutes

| Accession | Protein Description | Score | Coverage |
|-----------|-----------------------------------|-------|----------|
| P01834 | Ig kappa chain C region | 6.93 | 33.96 |
| C9JKR2 | Albumin | 6.79 | 6.71 |
| C9JDS9 | Tubulin alpha-4A chain (Fragment) | 3.94 | 8.97 |

Table 19. Summarising the identification of SUMOylated proteins in platelets after 100µM GA 30 minutes treatment in the MS data analysis (Birmingham Proteomics Unit). These cells were previously prepared as whole cell lysates, mixed and incubated with the SUMO matrix-containing columns to obtain eluted SUMOylated proteins and reserved in 0.1% formic acid previously

In Table 18, some of the FA proteins that have been identified in the MDA-MB-231 cells and the CMK11-5 cells have also been identified in the platelets in the control sample including: actin-1 (with high protein score and high coverage), talin-1, integrin α IIb β 3, tubulin α 1B chain, cofilin-1 etc have been identified in the MS data analysis. In table 19, after 100µM of GA 30 minutes treatment, all of the FA proteins were gone in the GA treated sample.

The proteins identified at least in 2 cell lines or in all 3 cell lines were summarised in the table below:

| | |
|------------------------|-----------------------------------|
| All 3 cell lines | Talin 1 |
| All 3 cell lines | Actin, cytoplasmic 1 |
| All 3 cell lines | Cofilin 1 |
| MDA-MB-231 & CMK11-5 | Filamin A (Filamin 1) |
| MDA-MB-231 & CMK11-5 | Vinculin isoform 1 |
| MDA-MB-231 & CMK11-5 | Myosin-9 |
| MDA-MB-231 & CMK11-5 | Tubulin alpha-4A chain, isoform 2 |
| MDA-MB-231 & Platelets | Tubulin alpha-1B chain |
| MDA-MB-231 & CMK11-5 | Profilin 1 |
| MDA-MB-231 & CMK11-5 | Fibrinogen beta chain |
| CMK11-5 & Platelets | Fibrinogen gamma chain |

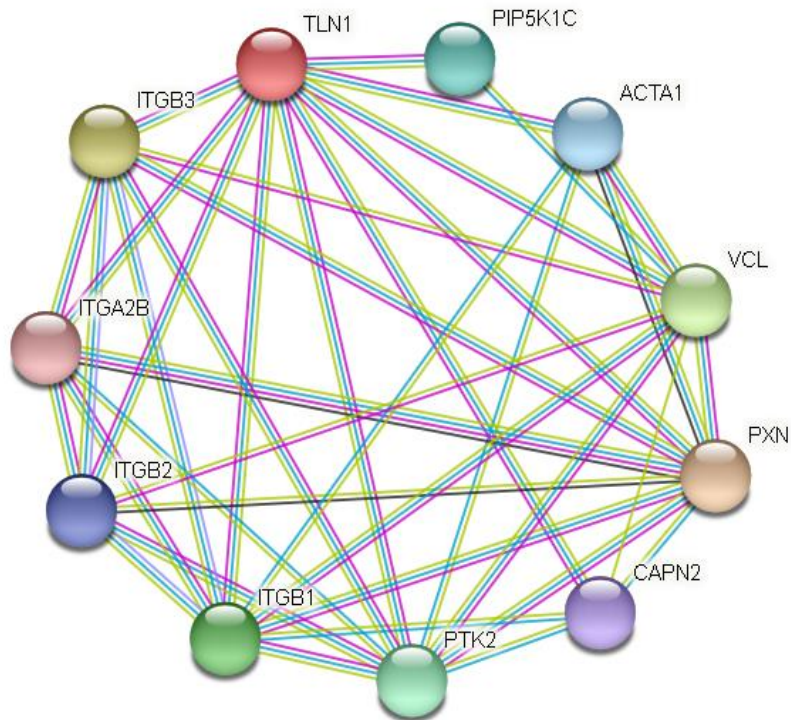
Table 20. Summarising some of the FAs appeared in at least 2 cell lines or in all the 3 cell lines after the samples were analysed in the MS. These were the whole cell lysates & SUMO binding samples of each cell line that obtained the previously SUMOylated proteins and identified in the MS.

In Table 20, the FA proteins have been identified in all three cell lines or in at least two cells lines, are: talin-1, actin cytoplasmic 1, filamin A, vinculin, myosin 9, tubulin α 4A chain, tubulin α -1B chain, cofilin 1 (Non-muscle), profilin-1, fibrinogen beta chain, fibrinogen gamma chain. Among these proteins, talin-1, filamin A and vinculin have been done in the IP & WB experiments in both of the MDA-MB-231 cells and the U2OS cells. Talin 1 was also looked at in platelets.

5.6 STRING Data Analysis Shows the Protein-Protein Interactions in Focal Adhesions

STRING protein network analysis has been used to obtain talin, vinculin and filamin-A protein network analysis. The network nodes represent proteins and post-translational modifications and each node in the protein network represents all the proteins produced by a single encoding gene locus. The edges in the network represent protein-protein associations, which are specific, i.e. the proteins co-interact and contribute to a shared function jointly but this co-interaction does not represent their physical binding to each other necessarily. The red coloured node represents the query protein and first shell of interactors: talin-1, vinculin or filamin-A.

Human Talin-1 and Its Interaction Partners: Integrin, Vinculin, Actin, Paxillin, Calpain-2 etc

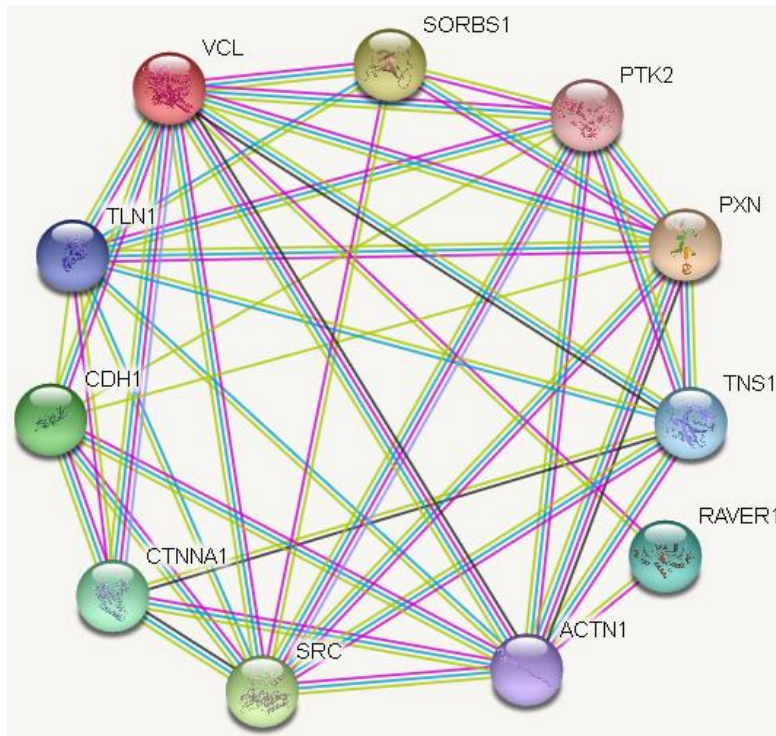


| Protein node | Predicted functional partners: | Score |
|--------------|--|-------|
| PXN | Paxillin | 0.998 |
| ITGB3 | Integrin, beta 3 (platelet glycoprotein IIIa, antigen CD61) | 0.998 |
| VCL | Vinculin | 0.996 |
| ITGB1 | Integrin, β 1 | 0.993 |
| PTK2 | Protein tyrosine kinase 2 | 0.993 |
| PIP5K1C | Phosphatidylinositol-4-phosphate 5-kinase, type I, gamma | 0.985 |
| ACTA1 | Actin, alpha 1 | 0.981 |
| ITGB2 | Integrin, β 2 | 0.981 |
| CAPN2 | Calpain 2 | 0.971 |
| ITGA2B | Integrin, alpha 2b (platelet glycoprotein IIb of IIb/IIIa complex, antigen CD41) | 0.970 |

Figure 63. Schematic representation of the various contacts of the protein-protein interactions in the talin network established by the string analysis in the focal adhesion contacts: the blue edge was represented as the database for the known interactions (e.g. nearly all protein nodes were connected with blue edge); the known interactions from experimentally determined were linked by purple edge (e.g. talin-1 – paxillin, talin-1 – integrin β 1, talin-1 – calpain 2); the black edge represented the co-expression (e.g. integrin β 2 – paxillin, integrin α 2b – paxillin; actin-1 – paxillin); the yellow edge represented as the text data mining (in nearly all the protein-protein interactions); the light purple (e.g. integrin β 3-integrin β 2-integrin β 1) were protein homology

In Figure 63, talin-1 has been in the network associated with vinculin, paxillin, actin α 1, integrin β 1, β 3, α 2b, calpain-2, protein tyrosine kinase 2 and PIP5K1C Phosphatidylinositol-4-phosphate 5-kinase, type I, gamma.

Human Vinculin and Its Interaction Partners: Talin, Actin 1, Paxillin and etc



| Protein node | Predicted functional partners: | Score |
|--------------|--|-------|
| PXN | Paxillin | 0.999 |
| SORBS1 | Sorbin and SH3 domain containing 1 | 0.999 |
| SRC | Src | 0.998 |
| CDH1 | Cadherin 1, type 1, E-cadherin (epithelial) | 0.998 |
| CTNNA1 | Catenin (cadherin-associated protein), alpha 1 | 0.998 |
| RAVER1 | Ribonucleoprotein, PTB-binding 1 | 0.997 |
| TNS1 | Tensin 1 | 0.997 |
| TLN1 | Talin 1 | 0.996 |
| ACTN1 | Actinin, alpha 1 | 0.995 |
| PTK2 | Protein tyrosine kinase 2 | 0.995 |

Figure 64. Schematic representation of the various contacts of the protein-protein interactions in the vinculin network established by the string analysis in the focal adhesion contacts: the blue edge was represented as the database for the known interactions (e.g. nearly all protein nodes were connected with blue edge); the known interactions from experimentally determined were linked by purple edge (e.g. vinculin – talin-1, vinculin – src, vinculin – actinin α 1, vinculin – paxillin); the black edge represented the co-expression (e.g. vinculin – actinin α 1, vinculin – tensin 1, catenin α 1- tensin 1, paxillin- actinin α 1); the yellow edge represented as the text data mining (in nearly all the protein-protein interactions); the light purple (e.g. vinculin – catenin α 1, PTK2 – Src) were protein homology

The protein-protein interaction map of the vinculin network in Figure 64 has shown that vinculin is associated with paxillin, sorbin and SH3 domain containing 1, src, cadherin 1, type 1, E-cadherin (epithelial), catenin (cadherin-associated protein), alpha 1, ribonucleoprotein, PTB-binding 1, tensin 1, talin 1, actinin, alpha 1 and protein tyrosine kinase 2.

From the talin or the vinculin protein-protein network and the mass spectrometry identification of the previously SUMOylated proteins in the MDA-MB-231 cells, CMK11-5 cells and the platelets, alterations in one protein in the network such as talin SUMOylation could affect a number of signalling proteins in the protein-protein interactions.

5.7 Validation of Filamin-A (Filamin-1) as a SUMOylation Substrate

Filamin A is also known as filamin 1 and it was shown as a SUMOylation substrate in the mass spectrometry analysis in the MDA-MB-231 cells and in the CMK11-5 cells. Analysis of filamin-1 was done using the SUMOplot and GPS SUMO software to investigate whether filamin-1 was predicted to be SUMOylated and if so to obtain the positions at which lysines they may be SUMOylated. The highlighted lysine residues in red were predicted as the SUMOylation or SUMO interaction sites from the SUMOplot and the GPS SUMO programme.

SUMOplot™ Analysis Programme (Abgent) Predictions on the SUMOylation Sites in Filamin (Protein ID: P21333, Isoform A): Motif B-K-x-D/E

Motifs with probability score > 0.5

| No. | Lysine Position | Peptide Sequence | Probability Score |
|-----|-----------------|----------------------------------|-------------------|
| 1 | K2473 | DGPSK V <u>K</u> MDCQECP | 0.93 |
| 2 | K876 | HDASK V <u>K</u> AEGPGLS | 0.93 |
| 3 | K865 | TSPiR V <u>K</u> VEPSHDA | 0.93 |
| 4 | K520 | ELKVT V <u>K</u> GPKGEER | 0.82 |
| 5 | K2165 | HCDLS L <u>K</u> IP EISIQ | 0.8 |
| 6 | K620 | EGPSQ A <u>K</u> IECDDKG | 0.79 |
| 7 | K2500 | SYLIS I <u>K</u> YGPYHI | 0.77 |
| 8 | K1800 | VIPFT I <u>K</u> KGEITGE | 0.77 |
| 9 | K1621 | RYTIL I <u>K</u> YGEDEIP | 0.77 |
| 10 | K1234 | AYTVT I <u>K</u> YGGQPVP | 0.77 |
| 11 | K2631 | EYTLV V <u>K</u> WGDHHP | 0.76 |
| 12 | K569 | RSPFE V <u>K</u> VGTECGN | 0.76 |
| 13 | K1439 | VPGSP F <u>K</u> VPVHDVT | 0.74 |
| 14 | K1964 | MRMSH L <u>K</u> VGSAADI | 0.73 |
| 15 | K270 | FPKAK L <u>K</u> PGAPLRP | 0.73 |
| 16 | K367 | AGQHI A <u>K</u> SPFEVYV | 0.69 |
| 17 | K906 | KAAGK G <u>K</u> LDVQFSG | 0.67 |
| 18 | K781 | YGPV A <u>K</u> TGLKAHE | 0.62 |
| 19 | K700 | EFTVD A <u>K</u> HGGKAPL | 0.62 |
| 20 | K523 | VTVKG P <u>K</u> GERVKQ | 0.61 |
| 21 | K1071 | TKPSK V <u>K</u> AGPGLQ | 0.58 |
| 22 | K704 | DAKHG G <u>K</u> APLRVQV | 0.57 |
| 23 | K2623 | SYLLK D <u>K</u> GEYTLVV | 0.5 |
| 24 | K982 | VSGLG E <u>K</u> VDVGKDQ | 0.5 |
| 25 | K958 | GGDPI P <u>K</u> SPFSVAV | 0.5 |
| 26 | K626 | KIECD D <u>K</u> GDGSCDV | 0.5 |

GPS SUMO Programme Predictions on the Filamin-1 Protein Peptide Sequence

| Position | Peptides | Score | Cut-off | Type |
|-------------|-------------------------------|--------|---------|------------------|
| 865 | PTSPIRV K VEPSHDA | 47.746 | 16 | Sumoylation |
| 876 | SHDASKV K AEGPGLS | 45.301 | 16 | Sumoylation |
| 1486 | GVAPLQV K VQGPKGL | 39.881 | 36.625 | Sumoylation |
| 299 | EPTGNMV K KRAEFTV | 39.383 | 36.625 | Sumoylation |
| 2631 | GEYTLVV K WGDEHIP | 39.261 | 36.625 | Sumoylation |
| 2473 | IDGPSKV K MDCQECF | 37.737 | 36.625 | Sumoylation |
| 676 | DFHPDRV K ARGPGL | 37.622 | 36.625 | Sumoylation |
| 523 | KVTVKGP K GEERVKQ | 19.972 | 16 | Sumoylation |
| 620 | VEGPSQA K IECDDKG | 17.91 | 16 | Sumoylation |
| 923 - 927 | KGDAVRD V DIID HHNTYT | 64.791 | 59.29 | SUMO Interaction |
| 2035 - 2039 | QHVASSP I PVVI SQSEIGD | 64.04 | 59.29 | SUMO Interaction |
| 316 - 320 | RSAGQGE V LVYV EDPAGHQ | 63.818 | 59.29 | SUMO Interaction |
| 144 - 148 | ILGLIWT L LHY SISMPMW | 63.24 | 59.29 | SUMO Interaction |
| 1136 - 1140 | TEPGDYN I NILF ADTHIPG | 62.415 | 59.29 | SUMO Interaction |
| 1696 - 1700 | CTPDGSE V DVDV VENEDGT | 61.103 | 59.29 | SUMO Interaction |
| 416 - 420 | AGAGTGE V EVVI QDPMGQK | 60.671 | 59.29 | SUMO Interaction |
| 1497 - 1501 | PKGLVEP V DVVD NADGTQT | 60.321 | 59.29 | SUMO Interaction |

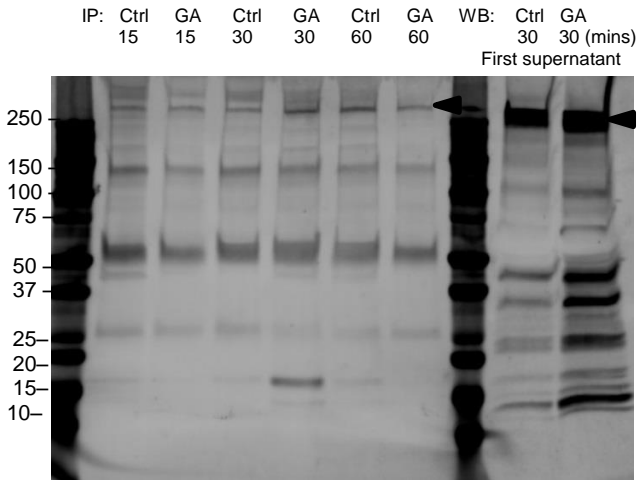
Table 21. SUMOplot predictions on the filamin-A (filamin-1) SUMOylation sites, lysine positions with score above 0.5 were highlighted in red indicating high probabilities. GPS SUMO programme shows the SUMOylation predictions as well as the SUMO interactions SIMs of filamin-1 SUMOylation, where the FASTA sequence of filamin-1 was inputted and the medium threshold was used: the modified positions, modified peptides, score for the modification, cut-off and the type of SUMO modifications were presented

In Table 21, the highlighted black SUMOylated lysine positions from the SUMOplot prediction programme were also predicted using the GPS SUMO programme for the SUMOylation of filamin-1. K876 and K865 have been predicted as the top lysine positions being SUMOylated using both programmes. In Table 21, filamin-1 has been predicted with multiple modified lysine positions using both programmes.

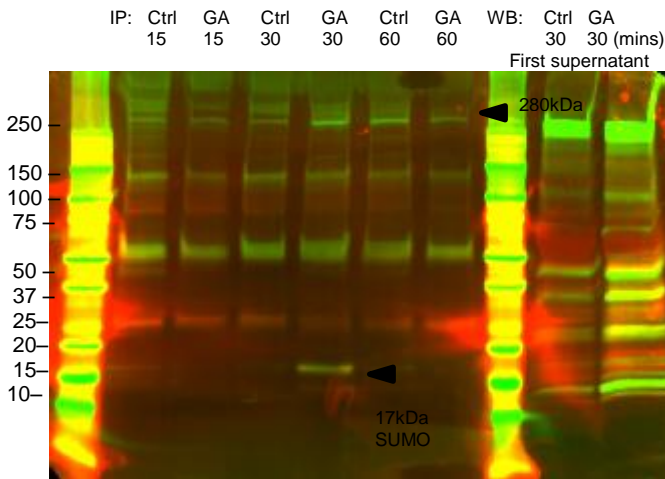
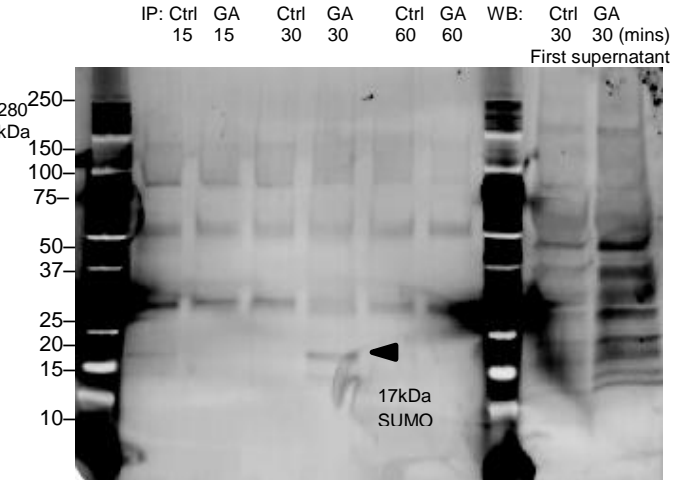
Filamin-1 was a SUMOylation protein substrate from the mass spectrometry analysis and filamin 1 was predicted with many SUMOylated lysine positions and with high probability. To confirm whether filamin-1 can be SUMOylated, IP was conducted in the MDA-MB-231 cells using the HA-tag SUMO-2 plasmid and the cells were transfected and incubated for 24 hours. The cells were then treated with 100µM GA for 15, 30 or 60 minutes. IP and western blotting was done. Filamin-1 can be detected in the MDA-MB-231 cells using 2 different antibodies against the N-terminus and the C-terminus to detect the protein. Interestingly, filamin-1 was able to be cleaved after the inhibition of SUMOylation at 1 hour treatment.

HA IP: SUMO-2, IB: Filamin-1

(N-19 ab, detecting N-terminus of filamin-1)



HA IP: SUMO-2, IB: SUMO-2



Combined Cy3 and Cy5 Channels:

The overlay: the Alexa 546 anti-goat ab detecting filamin-1=Cy3 (filamin-1, green) and the Alexa 647 anti-rabbit ab detecting SUMO-2 Cy5 (SUMO-2, red), n=3

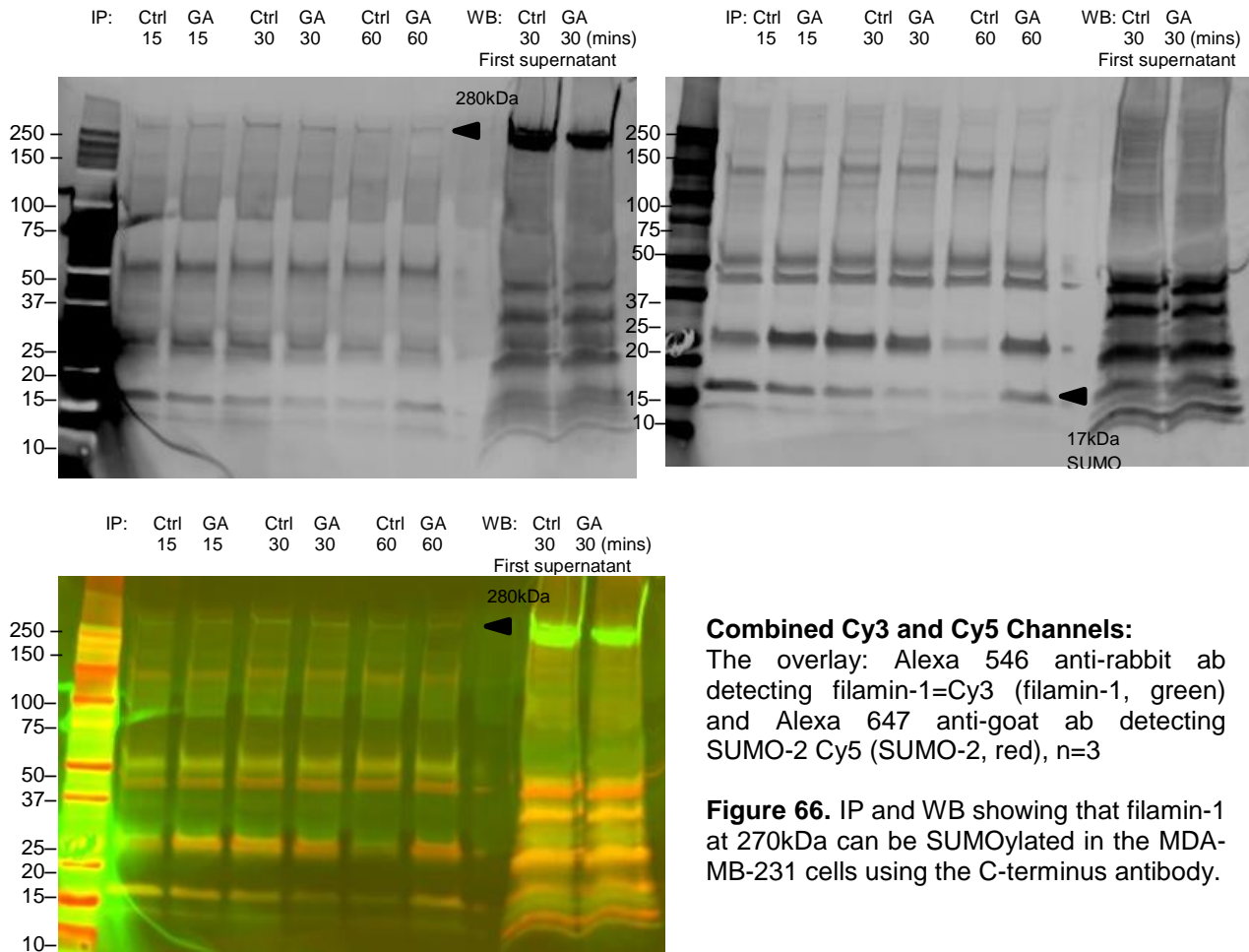
Figure 65. IP and WB showing that filamin-1 at 270kDa can be SUMOylated in the MDA-MB-231 cells in both control and GA 15, 30, 60 minutes treated samples using the N-terminus antibody.

In Figure 65, in the control and GA treated 15, 30 and 60 minutes samples of the IP: SUMO-2, IB: Filamin-1 membrane, filamin-1 was found to be SUMOylated at 280kDa using the N-terminus antibody. Bands at ~150kDa and 50kDa were also detected.

HA IP: SUMO-2, IB: Filamin-1

(H-300 ab, detecting C-terminus of filamin-1)

HA IP: SUMO-2, IB: SUMO-2



In Figure 66, in the control and GA treated 15, 30 and 60 minutes samples of the IP: SUMO-2, IB: Filamin-1 membrane, filamin-1 was found to be SUMOylated at 280kDa using the C-terminus antibody.

5.8 The Predicted SUMO Modified Sites in Known SUMOylated Substrates: p53, Rac1, FAK and Actin, Cytoplasmic 1 Using SUMOplot and GPS SUMO Programmes

As validation of software prediction for SUMOylation sites, SUMOplot and GPS SUMO have been used to predict the SUMO modification sites or SUMO interactions in already identified and known SUMOylated substrates, p53, Rac1 and actin-1 to determine how stringent these programmes are in order to compare the results with the predictions of talin and vinculin.

SUMOplot™ Analysis Programme (Abgent) Predictions on the SUMOylation Sites in FAK (Protein ID: Q05397): Motif B-K-x-D/E

Motifs with probability score > 0.8

| No. | Lysine Position | Peptide Sequence | Probability Score |
|-----|-----------------|-------------------------|-------------------|
| 1 | K152 | FFYQQ VKSD YMLEI | 0.93 |
| 2 | K834 | KEERF LKPD VRLSR | 0.91 |

GPS SUMO Programme Predictions on the FAK Protein FASTA Sequence

| Position | Peptides | Score | Cut-off | Type |
|------------|------------------------------|--------|---------|------------------|
| 152 | NFFYQQV KSD YMLEI | 40.097 | 36.625 | Sumoylation |
| 903 | DSYNEGV KL QPQEIS | 39.886 | 36.625 | Sumoylation |
| 561 | VSSNDCV KL GDFGLS | 37.265 | 36.625 | Sumoylation |
| 834 | EKEERFL KPD VRLSR | 36.977 | 36.625 | Sumoylation |
| 121 | AHPPEEW KY ELRIRY | 19.022 | 16 | Sumoylation |
| 267 - 271 | CALGSSW IISVE LAIGPEE | 73.562 | 59.29 | SUMO Interaction |
| 972 - 976 | LATVDET IPLLP ASTHREI | 67.784 | 59.29 | SUMO Interaction |
| 495 - 499 | GVITENP VWIIM ELCTLGE | 65.627 | 59.29 | SUMO Interaction |
| 487 - 491 | HPHIVKL IGVIT ENPVWII | 62.573 | 59.29 | SUMO Interaction |

Table 22. SUMOplot predictions on the FAK SUMOylation sites, lysine positions with score above 0.5 were highlighted in red using SUMOplot. GPS SUMO programme shows the SUMOylation predictions as well as the SUMO interactions SIMs of FAK SUMOylation, where the FASTA sequence of FAK was inputted and the medium threshold was used: the modified positions, modified peptides, score for the modification, cut-off and the type of SUMO modifications were presented

In Table 22, K152 of FAK is a SUMO modification site which has been validated in experimental conditions (Kadaré et al., 2003) and this has been discussed in the discussion section. K152 appears both in the first top of the predicting list of positions in the SUMOplot and in the GPS SUMO. K834 has also been predicted to be SUMOylated lysine sites using both programmes.

SUMOplot™ Analysis Programme (Abgent) Predictions on the SUMOylation Sites in p53 (Protein ID: P04637): Motif B-K-x-D/E

Motifs with probability score > 0.8

| No. | Lysine Position | Peptide Sequence | Probability Score |
|-----|-----------------|-------------------------|-------------------|
| 1 | K386 | HKKLM FKTE GPDSD | 0.85 |

GPS SUMO Programme Predictions on the p53 Protein FASTA Sequence

| Position | Peptides | Score | Cut-off | Type |
|------------|------------------------------|--------|---------|------------------|
| 386 | RHKKLM F KTEGPDSD | 17.901 | 16 | Sumoylation |
| 143 - 147 | QLAKTCP VQLWV DSTPPPG | 63.665 | 59.29 | SUMO Interaction |

Table 23. SUMOplot predictions on the p53 SUMOylation sites, lysine positions with score above 0.5 were highlighted in red using SUMOplot. GPS SUMO programme shows the SUMOylation predictions as well as the SUMO interactions SIMs of p53 SUMOylation, where the FASTA sequence of p53 was inputted and the medium threshold was used: the modified positions, modified peptides, score for the modification, cut-off and the type of SUMO modifications were presented

In Table 23, K386 has been both predicted to be the single SUMOylated site in p53, the oncogene as the guardian gene in cancer. K386 has been validated to be the SUMOylated site in p53 experimentally (Kwek et al., 2001) and this is discussed in the discussion.

SUMOplot™ Analysis Programme (Abgent) Predictions on the SUMOylation Sites in Rac1 (Protein ID: P63000): Motif B-K-x-D/E

| Position | Peptides | Score | Cut-off | Type |
|----------|-------------------------------|--------|---------|------------------|
| 7-11 | *MQAIKC VVVG D GAVGKTC | 59.593 | 59.29 | SUMO Interaction |

Table 24. No motifs has been found for Rac1 consensus SUMO modified motifs; GPS SUMO shows the SUMO interactions SIMs of Rac1 SUMOylation, where the FASTA sequence of Rac1 was inputted and the medium threshold was used: the modified positions, modified peptides, score for the modification, cut-off and the type of SUMO modifications were presented

In Table 24, Rac1 has not been shown with any consensus SUMO modified motifs using both SUMOplot and GPS SUMO. Castillo-Lluva et al has shown that in Rac1 the non-consensus sites within the polybasic region (PBR) of Rac1 as the main location for SUMO conjugation: almost 95% of the SUMO-1 modified Rac1 was conjugated at lysine 188, 183 and 184 or 186 present within the C-terminal PBR of Rac1 (Castillo-Lluva et al., 2010).

SUMOplot™ Analysis Programme (Abgent) Predictions on the SUMOylation Sites in actin, cytoplasmic 1 (Protein ID: P60709): Motif B-K-x-D/E

Motifs with probability score > 0.8

| No. | Pos. | Group | Score |
|-----|------|-------------------------|-------|
| 1 | K284 | TFNSI MKCD VDIRK | 0.8 |
| 2 | K68 | RGILT LKYP IEHGI | 0.8 |

GPS SUMO Programme Predictions on the Actin Protein FASTA Sequence

| Position | Peptides | Score | Cut-off | Type |
|-----------|------------------------------|--------|---------|------------------|
| 284 | TTFNSIM KCD VDIRK | 42.92 | 36.625 | Sumoylation |
| 103 - 107 | VAPEEHP VLLTE APLNPKA | 63.606 | 59.29 | SUMO Interaction |

Table 25. SUMOplot prediction on the actin SUMOylation sites, lysine positions with score above 0.5 were highlighted in red using SUMOplot. GPS SUMO programme shows the SUMOylation prediction as well as the SUMO interaction SIM of actin SUMOylation, where the FASTA sequence of actin was inputted and the medium threshold was used: the modified positions, modified peptides, score for the modification, cut-off and the type of SUMO modifications were presented

In Table 25, K284 and K68 have been predicted to be the SUMOylation sites for actin; computational modelling and site-directed mutagenesis have identified K284 and K68 as critical sites for SUMOylating actin experimentally (Hofmann et al., 2009). Here, SUMOplot and GPS SUMO have both predicted K284 to be the SUMOylation site in actin; SUMOplot also predicted K68 in actin as the SUMOylation site.

The reliability and stringency of the two bioinformatics software have been discussed in the discussion section for the prediction of talin, vinculin and filamin-1 SUMOylation.

Discussion

The identification and confirmation of SUMOylated focal adhesion proteins have been investigated and validated for the first time in these studies. The discussion for this study covers several aspects: the up-to-date list of all the novel SUMOylated proteins discovered and identified; the proposed SUMO modified sites in the SUMOylated proteins, some proteomics methods have been discussed; the SUMOylation of focal adhesion proteins have been identified and validated for the first time, however, the most up-to-date proteomics studies still underappreciate the novel identification of these SUMOylated focal adhesion proteins; in the future work, focal adhesion mutagenesis will be the next approach.

5.9 The Identification and Validation of SUMOylated FA Proteins

From the most up-to-date list of all the SUMOylated proteins identified by any of 22 published proteomic studies or low-throughput studies, only talin-1 and filamin-1 have been identified although there was no experimental validation. There has been no vinculin SUMOylation identification in any published studies.

In Hendriks and Vertegaal's study (summarised in Table 26), talin-1, filamin-A, cofilin-1 (non-muscle), profilin-1, myosin-9 / myosin regulatory light chain 12A, tubulin beta-4A chain, tubulin alpha-4A chain, tubulin alpha-1B chain, fibrinogen gamma chain and fibrinogen alpha chain have all been identified to be SUMO target protein substrates without additional validation e.g. through IP & WB experimental determination. These FA related proteins have been identified in this current study and furthermore, talin-1, vinculin and filamin-1 SUMOylation has been experimentally validated for the first time. Additionally, Hendriks and Vertegaal's most updated study has not yet identified vinculin and actin as SUMOylation substrates. This suggests that the MS methods used to identify SUMOylated proteins and the MS data analysis in this current study have been in the agreement with the most comprehensive study (Hendriks and Vertegaal, 2016), although vinculin SUMOylation was not identified suggesting very low abundance SUMO modified proteins could still be missed in mass spectrometry experiments.

| Comparison between the current study and the most up-to-date proteomics study | | |
|--|---|--|
| SUMOylation substrates | Current study: identification with MS and validation through IP & WB | Hendriks and Vertegaal, 2016 MS study and their referenced MS studies: identification only |
| Talin-1 | Identification in all three cell lines: MDA-MB-231, CMK11-5, platelets Validation in all three cell lines: MDA-MB-231, U2OS, platelets | Identification only Hela cells |
| Filamin A (Filamin-1) | Identification in MDA-MB-231 & CMK11-5 Validation in MDA-MB-231 and U2OS | Identification only |
| Cofilin-1 (non-muscle) | Identification in all three cell lines: MDA-MB-231, CMK11-5, platelets | Identification only |
| Profilin-1 | Identification in MDA-MB-231 & CMK11-5 | Identification only |
| Myosin-9 | Identification in MDA-MB-231 & CMK11-5 | Identification only |
| Myosin regulatory light chain 12A | Identification in CMK11-5 only | Identification only |
| Tubulin beta-4A chain | Identification in MDA-MB-231 only | Identification only |
| Tubulin alpha-4A chain | Identification in MDA-MB-231 & CMK11-5 | Identification only |
| Tubulin alpha-1B chain | Identification in MDA-MB-231 & platelets | Identification only |
| Fibrinogen gamma chain | Identification in CMK11-5 & Platelets | Identification only |
| Fibrinogen alpha chain | Identification in CMK11-5 only | Identification only |
| Vinculin | Identification in MDA-MB-231 & CMK11-5 for the first time Validation in MDA-MB-231 & U2OS | None |

Table 26. Summarising the comparisons between the identification of SUMOylated FA/FA-related proteins from Hendriks and Vertegaal's study in the MS analysis supplementary data and the current study of the identification and validation of SUMOylated FA proteins in MDA-MB-231, CMK11-5, platelets and U2OS cells

Some of the cytoplasmic SUMOylated proteins have been shown in Table 26 and compared to this current study for the identification and validation of the FA and FA-related proteins. Hendriks and Vertegaal's 2016 study has also identified the calpain inhibitor, calpastatin as well as calpain-2 as SUMOylation protein substrates, surprisingly as there has no published papers for the identification. The proteomics studies for identifying SUMOylation of filamin-1 has been published in 12 studies with no experimental validation (Bruderer et al., 2011, Golebiowski et al., 2009, Becker et al., 2013, Schimmel et al., 2014, Matic et al., 2008, Tatham et al., 2011, Schimmel et al., 2008, Impens et al., 2014, Hendriks et al., 2014, Hendriks et al., 2015c, Hendriks et al., 2015a, Xiao et al., 2015); the proteomics identification

of talin-1 SUMOylation has only been published in two studies with no experimental validation and no identification have been published for the SUMO modification site in talin-1 (Tatham et al., 2011, Becker et al., 2013); for Rac 1 SUMOylation, there has been only 1 paper published with experimental validation (Castillo-Lluva et al., 2010).

5.10 Software Prediction of SUMOylation Modified Sites in the FA Proteins

Protein SUMOylation is a very dynamic process, which is involved in many cellular activities. In order to determine the functional consequences of protein SUMOylation, it is important to determine which lysines are modified. Although mutational analysis and proteomics approaches have been used to identify the majority of known SUMOylated sites, it can be time consuming and labour intensive to analyse larger and more complex proteins, particularly those with dozens of potential consensus and non-consensus SUMOylation sites (Xu et al., 2008). Bioinformatics studies have also been used to identify protein SUMOylation sites and these approaches are considerably quicker and simpler to perform. In this study, SUMOplot and GPS SUMO have been used to predict the specific modified lysine residues in talin-1, vinculin and filamin-1. SUMOplot, along with GPS SUMO and MotifX, is one of the first methods available for SUMOylation site prediction, which has been performed on a very large test set (Xue et al., 2006). Many SUMOylation substrate sites follow a consensus motif ψ -K-X-E, but experimental data and mass spectrometry data have shown that some SUMOylation sites do not follow this motif, such as Rac1, where non-consensus sites were identified within the C-terminal polybasic region (PBR) of Rac1 as Rac1 lacks a consensus motif (Castillo-Lluva et al., 2010); therefore, with SUMO predicting software, sensitivity, specificity and accuracy will be important factors to determine its predicting power and not to generate false positive sites (Xue et al., 2006). However, additional large-scale and high throughput proteomic identification approach may still be required to exclude false negatives.

The SUMOplot and GPS SUMO have been used to predict the SUMOylation of p53, actin, cytoplasmic 1, Rac1 and FAK, which are known SUMOylated substrates. The predicted lysine positions in these substrates using these bioinformatics programmes have been identified and validated exactly as what have been predicted. p53 has been predicted with lysine K386 SUMO modified site using both programmes and this lysine has been identified and validated experimentally as a SUMO-1 conjugation site in the literature as the only SUMOylation site in p53 (Kwek et al., 2001, Melchior and Hengst, 2002, Gostissa et al., 1999, Rodriguez et al., 1999).

The N-terminal FERM (protein 4.1, ezrin, radixin and moesin homology) domain of FAK has been found to interact with the protein inhibitor of activated STAT1 (PIAS1, an E3-type

SUMO ligase) and this interaction was found to be direct; PIAS1 could induce the conjugation of SUMO-1 to FAK on K152 as a conserved residue in FAK and this lysine was highly likely to be the only one SUMOylation consensus motif and SUMOylated FAK was predominantly enriched in the nucleus (Kadaré et al., 2003, Mitra et al., 2005); this lysine has also been predicted with the highest probability, identified and validated experimentally. Interestingly, no predicted consensus motif have been predicted for Rac1, which is in agreement with the finding that Rac1 was SUMOylated in the non-consensus sites within the polybasic region of Rac1 as the main location for SUMO conjugation (Castillo-Lluva et al., 2010); actin has been predicted with K284 SUMO conjugation site using both programmes; K68 has been predicted using SUMOplot; site-directed mutagenesis has identified K284 and K68 as critical SUMO 2/3 modified sites in actin and both sites are required for the binding of SUMO enzymes; cooperativity between K68 and K284 is necessary for SUMO-2 and actin complex stability, which is required for the nuclear localization of actin (Hofmann et al., 2009).

The multiple sites for SUMO modifications have been collated comprehensively and shown 7327 SUMOylation sites in 3617 proteins (Hendriks and Vertegaal, 2016). The majority of the SUMOylated proteins are located in the nucleus and are linked to SUMO 1 rather than SUMO 2/3 modification; of all the proteins for which SUMOylation evidence exists, ~66% were nuclear (Hendriks and Vertegaal, 2016). However, in their study, they have summarised all the up-to-date references and listed the one identified SUMOylation modified site in filamin-1 as K299 (Schimmel et al., 2014, Hendriks et al., 2014, Hendriks et al., 2015b); filamin-1 has also been shown with K285 modified site (Hendriks et al., 2015c). None of the literature has directly identified any modified SUMOylation sites in talin or vinculin yet. There have also been no papers published identifying any SUMOylation modified sites for calpain and calpastatin.

In this study, talin and vinculin have been identified as SUMOylated substrates in three cell lines: the MDA-MB-231 cells, the U2OS cells, the CMK11-5 cells and the platelets. Talin-1, vinculin and filamin-1 SUMOylation have been validated in experiments for the first time in this study. There are multiple predicted SUMOylation modified sites in filamin-1 using the SUMOplot and GPS SUMO programmes and they have shown K865 and K876 are the highest probability SUMOylated lysine sites in filamin-1. Although K299 and K285 SUMO modified sites in filamin-1 came through the proteomic high throughput, none of the papers have validated filamin-1 SUMOylation experimentally. K299 was also predicted to be a SUMOylation site using GPS SUMO but not the SUMOplot. Similarly, more than one SUMO modifications and SIM sites for protein-protein interactions in filamin-1 have been predicted using SUMOplot and GPS SUMO. This suggests that numerous proteomics studies are

capable of identifying SUMOylated proteins and the majority of the SUMOylated proteins have been identified in the nucleus, however, the consensus motifs or non-consensus SUMO modified motifs in the identified SUMOylation protein and their role in the protein-protein interactions are much less identified and validated, particularly for the cytoplasmic proteins that have been identified to be SUMOylated.

Since p53, FAK, actin, cytoplasmic 1 and Rac1 have been predicted for their SUMOylation modified sites using the bioinformatics programmes and have validated the literature, this has suggested that the top predicted SUMOylation modified sites with the highest scores for talin (K841, K2445), vinculin (K731, K80 and K71) or filamin-1 (K2473, K876, K865 and K299) are reasonable, reliable and believable and they can be used and applied in the further experimental works. The next step for the validation of these predictions is site-directed mutagenesis.

The published proteomic studies have used several methods to identify and validate the putative SUMOylated proteins and SUMOylation modification sites. An advanced system-wide Protease-Reliant Identification of SUMO Modification (PRISM) with high-resolution MS has allowed for the detection of SUMOylated proteins as well as the identification of specific SUMO associated sites using wild-type SUMO on endogenous proteins in the cancerous HeLa cells (Hendriks et al., 2015b). In another study, a novel proteomics approach was developed to generate monoclonal antibodies, which could specifically recognize, capture and enrich the peptides containing SUMO remnant chains after tryptic digestion of SUMOylated proteins, followed by large-scale MS analysis of SUMO modified peptides (Lamoliatte et al., 2014). One study has also shown the development of stably transfected cell lines expressing a double-tagged modifier under the control of a tightly negatively regulated promoter; this has allowed the tagged modifier to be expressed and conjugated to the cellular proteins covalently and by tandem affinity purification of the protein pool and the identification of the modified proteins with LC and MS, 27 substrates were found to be modified by both SUMO-1 and SUMO-3, indicating the SUMO paralogues could be functionally distinct (Rosas-Acosta et al., 2005). SUMO-2 and SUMO-3 have been required for cells to survive heat shock identified in 766 putative substrates through quantitative labelling techniques, stringent purification of SUMOylated proteins, advanced MS technology and novel techniques of data analysis (Golebiowski et al., 2009). Many studies have been focused on the cell cycle, where an efficient tandem affinity purification strategy was developed characterizing SUMO 2/3 modified proteins in mitotic cells and in cells undergoing mitotic exit, therefore, combining this purification strategy with cell synchronization and quantitative MS (Schou et al., 2014). Similarly, quantitative MS approach has been

employed to identify SUMO-2 conjugated substrates during DNA damage (Hendriks et al., 2015c). High-resolution MS in a site-specific manner has been applied to study global SUMOylation in human cells, also including different PTMs that can cross talk with SUMO; they have also concluded that the SUMOylated lysines were frequently located in areas enriched for charged residues and the SUMOylated regions were depleted for phenylalanine, tryptophan, tyrosine, leucine and most particularly for cysteine (Hendriks et al., 2014).

Site-directed mutagenesis is the next approach to study protein SUMOylation. Currently, no studies have been performed on vinculin or talin SUMOylation using site directed mutagenesis. Vinculin can directly interact with talin and actin to control FA formation (Humphries et al., 2007). SUMOplot predicts 3 putative SUMOylation sites in talin with high probability as K841, K2445 and K2063. Talin rod contains ~11 vinculin binding sites, 2 actin binding sites and the binding site for β -integrin tails; talin R2R3 domain, each contains 2 vinculin binding sites and R2R3 binds to RIAM synergistically; also vinculin and RIAM can bind to the N-terminal region of talin rod by mutually exclusive mechanistic events (Goult et al., 2013b). This means that K841 lies in the talin rod R3 region, RIAM and vinculin binding site, K2445 is in the R13 region, where actin and vinculin binding site also lies; K2063 in the R11 region is in the RIAM, vinculin and β -integrin tail binding site (Goult et al., 2013b). As binding of talin to RIAM and vinculin regulates FAs assembly and turnover, where SUMOylation sites were found in these domains, this may be very important to the function of FA regulation and to individual FA proteins, i.e. talin and vinculin specifically, whether targeting SUMOylation sites could affect dynamic interactions in FA proteins.

The vinculin tail Vt competes with the talin rod domain for the binding to the vinculin head Vh D1 domain and in vinculin SUMO modification sites, the predicted SUMOylation sites K71 and K80 lie in the N-terminal vinculin head Vh D1 domain, where competition between talin tail binding domain and vinculin tail Vt binding to the vinculin head occurs. This suggests that SUMOylation may also be involved in the conformational changes of the vinculin molecule, where the vinculin head domain could be modified through SUMOylation and this can regulate the recruitment of talin-vinculin protein interactions. In the site mutagenesis study, it could be predicted to have an effect on vinculin recruitment to FA and disassembly events in the FA protein complex, if these SUMO modified sites were mutated.

5.11 Validation of the MS Data: Filamin-1 is a Substrate for SUMO Modification

Filamin 1 also known as filamin A, is an actin cross linking protein which acts as a scaffolding protein which could couple and mediate the transmembrane integrin signalling with the cell cytoskeleton and therefore regulate FA turnover (Xu et al., 2010). Filamin 1 is one of three filamin members of the filamin family (Critchley, 2000). Filamin can also bind to integrin β subunit at a site which overlaps with the talin binding sites and therefore filamin competes and interferes with talin binding (Calderwood et al., 2013). Filamin 1 and talin can both compete for integrin binding: when filamin 1 is bound with the integrin β cytoplasmic tail, it could form an extended β strand which would interact with β strands C and D of the filamin immunoglobulin-like domain (IgFLN) 21 and this interaction interface was found to be overlapped with that of the integrin-talin binding site; the integrin binding PTB-like domain of talin could cause inhibition of IgFLN 21 binding to β tail (Kiema et al., 2006). Filamin can also be cleaved by calpain; Filamin 1 and talin may compete for calpain-mediated cleavage, which would impact on FA disassembly (Xu et al., 2010).

Filamin 1 was identified as a SUMOylated protein during the mass spectrometry analysis. Filamin 1 was identified with high protein score and high coverage in both MDA-MB-231 and CMK11-5 cells. Further investigation validates that filamin 1 is indeed a SUMOylation substrate in both MDA-MB-231 and U2OS cells. The Co-IP results also suggested filamin 1 was present in the same complex with talin. These results implicate that both talin and filamin 1 can be SUMOylated in the focal adhesion, talin and filamin 1 may compete each other for integrin binding and SUMOylation of either protein is important in controlling FA turnover and cell migration and SUMOylation may be important in the regulation of their protein-protein interactions.

5.12 The String Network of the FA proteins

To investigate protein-protein interactions in the focal adhesion, talin and vinculin have been mapped into the STRING protein network with high STRING confidence all within 0.95-0.99 ranges. Talin-1 interacts with vinculin, integrin β 1, β 2, β 3, α 2b, actin α 1 subunit, calpain-2, paxillin, protein tyrosine kinase 2 (PTK2) and PIP5K1C (phosphatidylinositol-4-phosphate 5-kinase, type I, gamma) through a wide range of investigations including experimental determinations such as co-purification, co-crystallization, yeast2hybrid, genetic interactions etc from the primary resources; databases, such as through metabolic pathways, protein complexes, signal transduction pathways etc; through text mining or text data mining; through co-expression and co-occurrence, where the genes for the protein expressions are observed to be correlated in expression or the gene families with their occurrence patterns show similarities across a large number of experiments. These determined interactive

partners proposed by the STRING have been largely known FA proteins connected in the talin network. Many of them including vinculin, actin and calpain-2 could be SUMOylated either in the IP & WB experiments or in the prediction programmes & proteomic studies. This suggests that the overall role of SUMOylation is very important in the FA protein network and by changing protein-protein interactions through SUMOylation, it may be possible to affect the neighbouring protein in the network. Vinculin interacts with paxillin, talin-1, actin, protein tyrosine kinase 2 in the protein-protein network; similarly, if changing vinculin SUMOylation modification, it could affect the other neighbouring interactive partners. The talin network has been associated with several types of integrin, this could suggest that SUMOylation is probably involved in outside-in or inside-out integrin signalling cell migration pathways and from these information, it could be proposed that mutating talin SUMOylation or its predicted partners, it could probably alter the functions of these signalling molecules and therefore affecting cell migration.

5.13 Future Work: Talin and Vinculin Mutagenesis

Recently, the PIAS3-mediated SUMOylation of the GTPase Rac1 was reported to be required for optimal cell migration, invasion and lamellipodium protrusion indicating a role for SUMO in the regulation of cell migration and invasion (Steffen et al., 2013, Castillo-Lluva et al., 2010). The link between Rac 1 SUMOylation and FAs is unknown. Rac1^{-/-}MEF cells *in vitro* showed unaffected alterations in number, size and intensity in FAs, where Rac1 can contribute to but is not essential for FAs assembly (Steffen et al., 2013). Therefore, treatment with general SUMOylation inhibitors such as GA could also affect Rac1, complicating the interpretation of cell migration data. In addition, there are likely to be other FA proteins that are also regulated by SUMOylation, as well as vinculin and FAK, as suggested by this study.

To determine whether inhibiting SUMOylated talin in the cells can directly affect cell migration, another approach could be taken in the future work. For example, since talin 2445 lysine residue was shown to be highly likely to be SUMOylated in the GPS-SUMO database and the SUMOplot analysis, site-directed mutagenesis will be applied. This residue will be mutated, replaced with non-SUMOylation residues, such as arginine, resulting in a mutant talin that cannot be SUMOylated completely. This 2445 residue lies in the C-terminal actin binding domain of talin, which also contains a vinculin binding site VBS. By replacing this lysine, the interacting reactions of talin with vinculin, actin and integrin can also be determined. Talin lysine 841, 2063 and 441 were also predicted to be SUMOylated. Talin rod contains at least two actin binding sites and multiple vinculin binding sites VBSs, where the best studied lie in the C-terminal R13 domain (Gingras et al., 2008, Calderwood et al., 2013).

This would suggest that if the talin 2445 lysine residue could be SUMOylated, which is also in the R13 domain, this can be very important to explain how SUMOylation can affect protein-protein interaction. Creating talin mutants that cannot be SUMOylated will be able to investigate these issues. In this way, FA studies and cell migration will be conducted to confirm whether SUMOylation of talin (or vinculin) at this lysine residue is essential and required for cell migration.

Vinculin site-directed mutagenesis was investigated in preliminary studies as this molecule is nearly half the protein size compared to talin. Experimental works were started with the mEmerald vinculin plasmid. However, there were difficulties with the vinculin mutagenesis work. It required several primers with the point mutation inserted in each primer, a cloning vector with either ends cut complementary to the PCR products generated using these primers. The problem has been in the cloning process. Many attempts have been done but the cloning has not obtained the mutated amino acid exchanged for the original amino acid successfully. As a result, new methods will have to be developed and different cloning vector may also be used and a different mutagenesis kit will also be tried to use for future work. In vitro test and analysis could be done to express these newly cloned plasmids in the cells; cells would also be expressed with the wild type FA plasmid as a control for the test. Competition could happen between the wild type and mutated FA plasmid expressions in the cells; percentage of the mutation expression against normal expression, how non-SUMOylated mutated FA plasmid expression in the cells affects FA number, size, turnover, cell migration and protein-protein interactions could be analysed.

There have been studies on the promiscuity of the lysine modification, since lysine can be modified by SUMO and ubiquitin at a competitive level. A significant overlap of about 20% came through the proteomics study between ubiquitin and acetylation highlighting the extensive competitive crosstalk at site modification level; among SUMOylation and ubiquitination came through the mixed-chain conjugation interaction (Danielsen et al., 2011). Another study showed that the methyltransferase Ezh2-mediated talin 1 methylation on K2454 promoted turnover of focal complexes (Gunawan et al., 2015), where the predicted SUMO modification site K2445 is very close to K2454.

These suggest that even mutating a lysine resulting in non-SUMOylation function of the protein we cannot be too confident with the interpretation of outcome as the effects of the mutated lysine cannot be certain if it is directly due to SUMOylation or any types of post-translational modifications, such as ubiquitination. The single-point mutation experimental design can be time consuming and the interpretation of the data analysis has to be very

stringent based on the role of the crosstalk of the PTMs in the cells. As the bioinformatics data show that talin (K841, K2445) and vinculin (K731, K80) are SUMOylated at these lysine residues, firstly, experiments could be done to determine whether talin or vinculin can be ubiquitylated on these lysine residues in IP & WB experiments separately (acetylation, phosphorylation could also be tested), therefore, excluding the possibilities of the competitive lysine modification by different PTMs. Then, lysine-to-arginine mutagenesis could be done on these lysine residues in talin or vinculin and the interpretation can be confident that the modification is due to SUMOylation only. However, potential non-consensus SUMO modification motifs still need to be considered.

Chapter 6 – The Regulation of SUMOylation in Focal Adhesions in Platelets and the Megakaryocyte-like CMK11-5 Cells

6.1 Introduction and Hypothesis

Platelets originate from the cytoplasm of megakaryocytes in the bone marrow, where they circulate and guard the integrity of the blood vascular system (Ruggeri, 2002). Integrin-mediated platelet adhesion and aggregation are essential for shutting injured blood vessels and preventing excess blood loss. This process involves integrin activation or priming on the circulating platelets' surfaces at the site of the wounded blood vessel; the molecular mechanism is triggered with the binding of talin to the integrin β subunit cytoplasmic tail (Moser et al., 2008). In resting platelets, the integrins exhibit a low affinity state for ligand binding and they shift to a high affinity state when the platelets encounter a vascular wound; in mice lacking talin-1 platelets are unable to activate integrins in response to major platelet agonists including fibrinogen, fibronectin and von Willebrand factor (VWF) and this leads to severe haemostatic effects and complete resistance to arterial thrombosis (Nieswandt et al., 2007). In platelets, a process termed 'inside-out' signalling causes affinity alteration in integrin $\alpha\text{IIb}\beta\text{3}$ signalling (McDowall et al., 2003). RIAM, its overexpression together with talin recruitment to $\alpha\text{IIb}\beta\text{3}$ mediates agonist-induced $\alpha\text{IIb}\beta\text{3}$ activation (Watanabe et al., 2008). Purified talin was found to directly bind to synthetic peptides corresponding to GPIIb (P2b) and GPIIIa (P3a) cytoplasmic sequences (cytoplasmic domains of αIIb and β3), suggesting that both GPIIb and GPIIIa directly mediated this interaction with talin (Knezevic et al., 1996). The integrin $\alpha\text{IIb}\beta\text{3}$ plays a central role in platelet aggregation, haemostasis and thrombosis and this response requires the capacity to bind soluble ligands (MA et al., 2007).

The activation or conformation change of integrin $\alpha\text{IIb}\beta\text{3}$ is tightly regulated through inside-out signalling; vWF and fibrinogen binding can bridge the platelets together or vitronectin and fibronectin can modulate platelet aggregation; agonists such as ADP and thrombin which participate with G protein coupled receptors or with collagen or vWF, can involve GPIb-IX-V receptor complex or collagen receptors GPVI and all these lead to the activation of intracellular signalling events, such as reinforcement of adhesion and platelet activation, which feedback to the ligand binding competency and affinity to integrin $\alpha\text{IIb}\beta\text{3}$ extracellular domain (MA et al., 2007). At the vascular injury site, ADP, thrombin and TxA₂ release act in an autocrine and paracrine manner to amplify the activation signal, attract and recruit circulating platelets to the thrombus site (Rivera et al., 2009). A simplified diagram is shown in Figure 67.

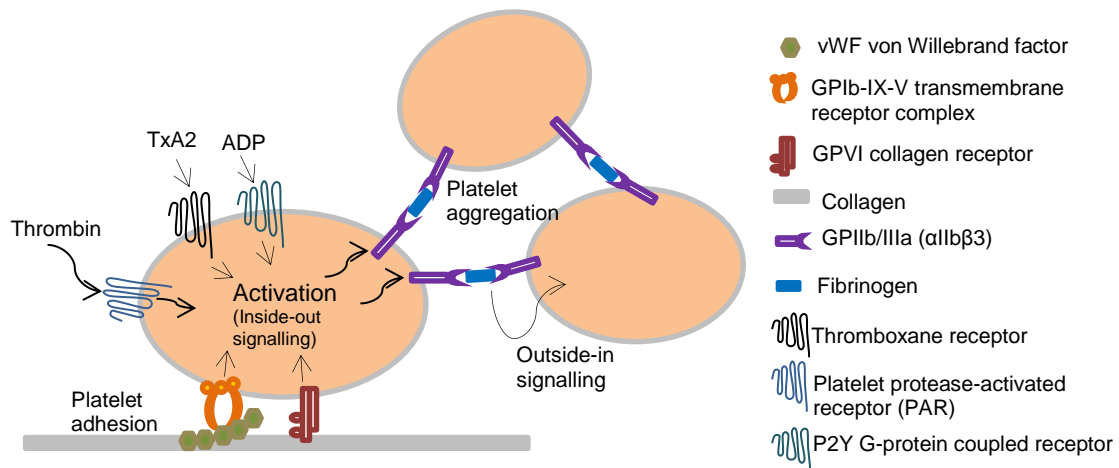


Figure 67. Signalling in platelet adhesion, activation and aggregation: platelets are adhered to collagen via GPIb-IX-V complex binding to vWF and GPVI collagen receptor signalling and platelets are activated by agonists such as thrombin, TxA2 (thromboxane A2) or ADP binding with their transmembrane receptors at the platelet membrane surface etc through inside-out signalling. Activation feeds back to activate platelet integrin $\alpha\text{IIb}\beta\text{3}$ which can bridge neighbouring platelets through fibrinogen binding leading to platelet aggregation

A human megakaryocyte-like cell line, CMK11-5 cells, has been used in this study, which is found to release platelet-like particles that have some of the same functions as normal platelets, for example, these CMK11-5 cells express the platelet antigens GP Ib, GP IIb/IIIa, and GP IV, indicating similar receptor characteristics between CMK11-5 and platelets and it can be a useful model to study megakaryocyte function (Sato et al., 1989, Greco, 1997). Disruption of the talin 1 gene in mouse platelet precursor megakaryocytes produces circulating platelets which exhibit normal morphology, however, these mice show spontaneous haemorrhage and pathological bleeding; this resulted from the loss of talin 1, which led to the inhibition of the activation of platelet β1 and β3 integrin in response to platelet agonists and severe impaired integrin $\alpha\text{IIb}\beta\text{3}$ -mediated platelet aggregation and β1 -mediated platelet adhesion (Petrich et al., 2007b). $\alpha\text{IIb}\beta\text{3}$ integrin activation is dependent on the talin association with the integrin β3 cytoplasmic tail *in vivo*, therefore, the modulation of β3 integrin and talin interactions could provide an attractive drug target for anti-thrombotics to achieve a reduced risk of pathological bleeding (Petrich et al., 2007a). Talin and kindlin-3 are crucial for integrin $\alpha\text{IIb}\beta\text{3}$ activation in CMK11-5 cells (Nakazawa et al., 2013).

Phorbol 12-myristate 13-acetate treatment (PMA) has been used in the experiments with the CMK11-5 cells. CMK11-5 cells are naturally grown in media suspension, the use of PMA helps the cells to adhere and spread on the plates to express their focal adhesions. Integrin $\alpha\text{IIb}\beta\text{3}$ expression in CMK cells with high GPIb expression can be activated by PMA (Kashiwagi et al., 2004). An acute treatment with PMA increases phosphorylation of focal adhesion kinase, paxillin, c-Src and cofilin and it could mediate cell spreading via the

activation of RhoA, which regulates actin reorganisation and FA formation (Lee et al., 2006). PMA has also been shown to modulate cell signalling through endogenous protein kinase C (PKC) and alternative fast diacylglycerol (DAG) signals could be transduced through the phorbol ester receptors, therefore affecting cell proliferation, differentiation, survival and transformation (Yang and Kazanietz, 2003). CMK11-5 cells are believed to have properties of megakaryocytic lineage including glycoprotein GPIIb / IIIa (integrin α IIb β 3) and platelets peroxidase activities and PMA treated CMK11-5 cells in conditioned medium could differentiate, stimulate and increase their GPIIb/IIIa antigen expressions but also PMA could induce the CMK11-5 cells to secrete hematopoietic growth factors including the GM-CSF (Komatsu et al., 1989).

The role of focal adhesions in platelets and CMK11-5 cells are different to those in the cancer cells. Focal adhesions are important in megakaryopoiesis, including megakaryocyte differentiation, maturation and spreading and platelet function such as spreading upon fibrinogen binding (Hitchcock et al., 2008). However, focal adhesions are involved in cell migration and metastasis in cancer cells. Calpain-2 is important in adhesion turnover in a variety of cells including platelets: vinculin can be proteolyzed by calpain during platelet aggregation into at least three fragments with the major fragment being 95kDa within 5 minutes upon platelets activation with thrombin or calcium ionophore; furthermore, the 95kDa cleaved vinculin fragment translocated from the membrane fraction to the cytoskeletal platelets, which may be important in the cytoskeletal remodelling of aggregating platelets (Serrano and Devine, 2004).

Hypothesis

Focal adhesions can be SUMOylated in MDA-MB-231 cells, U2OS cells, CMK11-5 cells and platelets. SUMOylated proteins have been identified in this study in platelets and CMK11-5 cells and in previous chapters SUMOylation has been shown to be involved in the regulation of FA dynamics and cell migration in the cancer cells. In platelets, SUMOylation could provide a novel mechanism for the integrin α IIb β 3-mediated activation of platelet adhesion and aggregation. In this study, the CMK11-5 cells and the platelets have been used to investigate whether inhibiting SUMOylation could affect the dynamic activities of the FAs. SUMOylation has been predicted to be involved in the regulation of FAs across different cell types; therefore, GA has been used in the experiments to determine its effects on the number and size of FAs in CMK11-5 cells and in platelet spreading. Cleavage of FA proteins resulted from the inhibition of SUMOylation.

6.2 Methods

6.2. 1 Treating CMK11-5 Cells for Spreading and Immunostaining Experiments

Fibrinogen Coating

10mg of fibrinogen (FN) was weighed and 1ml PBS was added to dissolve it (10 mg/ml). 200 µg/ml (1:50) was used as the working concentration. 130 µl FN was taken from the 10 mg/ml solution to mix with 6.5ml PBS. The glass coverslips were put into the 6-well plate and washed with methanol for 10 minutes. The methanol was removed and the coverslips were left to dry in the culture hood; 1ml FN (6.5ml) was added into each well and the coverslips were incubated with the FN for 1 hour at room temperature. Then the FN was removed and the coverslips washed with PBS once. The glass coverslips were blocked with 1% v/v BSA for 1 hour (0.1g BSA in 10ml PBS) at room temperature. After blocking, the BSA solution was removed; the CMK11-5 cells in RPMI media suspension were ready to be plated into the 6-well plate, 1×10^6 CMK11-5 cells were usually plated / well.

PMA treatment (Phorbol 12-myristate 13-acetate)

1 ml sterile DMSO was added to the PMA (Mass: 1mg, MW: 616.83, stock concentration: 1.6 mM). 160nM PMA working concentration was used for the CMK cell adhering and spreading (1:10000). For each well, 0.2µl (1:10000) of PMA was added in 2ml RPMI media for the CMK11-5 cells. The antibiotics (20µl pen/strep) were also added into the 2ml RPMI media for CMK11-5 cell growth. CMK11-5 cells were grown in RPMI media supplemented with 10% FBS at 37° C/5% CO₂ and passaged by dilution every 2-3 days at a density of 2×10^5 cells/ml. Differentiation of CMK11-5 cells was advanced by a two-step process. The cells were plated at a density of 2×10^6 cells per well in 6-well plates in RPMI media plus 160 nM PMA for 48h. On the third day, non-adherent cells were removed by aspiration and growth media was changed to IMDM supplemented with 10% v/v FBS in the presence of 160 nM PMA up to 5 days.

Immunostaining of CMK11-5 Cells

The CMK11-5 cells were grown to 70% confluence and incubated with 160nM PMA for 2 days. On the 3rd day the CMK11-5 cells were incubated with IMDM media (Gibco) containing 160nM PMA up to 3 days. Then CMK11-5 cells were treated with 100µM GA for 15, 30 and 60 minutes and were fixed and stained with antibodies (IHC: talin-1 antibody and Alexa 488 goat anti-mouse secondary antibody). The IHC steps were the same as in the IHC section (2.8. 2).

6.2. 2 CMK11-5 Cells: siRNA Treatment

CMK11-5 cells were treated with PMA as described previously and then treated with 0.2x Ubc9 siRNA (in Lipofectamine dilutions) for 48h. CMK11-5 whole cell lysates were made and labelled as negative control, scrambled siRNA and Ubc9 siRNA appropriately. The cell suspensions were centrifuged at 1500 rpm for 5 minutes. For each tube, the supernatant was removed and 200µl lysis buffer (1x RIPA, 1x PIC and 50mM NEM) was added to the cell pellet. The cells were resuspended in the lysis buffer immediately on ice. The cell lysates in each tube was transferred into eppendorf tubes and added with 1x SDS loading buffer. The samples were boiled at 95°C for 5 minutes and run on the gels afterwards.

6.2. 3 Platelet Spreading Assays

Platelets were previously taken from donors and the platelets were prepared according to the platelet isolation protocol (Professor Jon Gibbin's lab protocol). 50ml tyrodes with 0.045g glucose, 15ml ACD (anticoagulant acid citrate dextrose solution), 4ml 4% v/v citrate and 10µl prostacyclin x2 were prepared. Water bath at 30°C was switched on half an hour before use. 15ml ACD (against aggregation) was warmed up in water bath. Tyrodes with glucose was made up (Tyrode's buffer used for washing and isolation of platelets), mixed gently and put in water bath. Rack LP4 tubes (18 tubes for 50ml blood) were prepared. A beaker of Klorsept disinfectant was prepared. 4ml 4% citrate was sucked up into a 50ml syringe. 50ml blood was taken. 7.5ml of ACD was added to each 50ml syringe. Blood was divided up in each of the 18 tubes. Tubes were put into the centrifuge; empty tubes were added with water for balancing. The tubes were centrifuged for 20 minutes at 700rpm (102g) at 21°C.

New tubes, plastic pipettes and prostacyclin were prepared again. The contents were sucked off and the supernatant was kept (top layer of red blood was left = white blood cells) in one new 50ml falcon tube. 10µl prostacyclin was added and mixed carefully (inhibiting activation). The tubes were balanced and spun at 2600rpm (1413g) for 10 minutes at 24°C. After centrifugation the supernatant was discarded in Klorsept. The pellet was re-suspended with 25 ml tyrodes + glucose buffer; 3ml ACD was added. 10µl prostaglandin was added to platelets. Centrifugation was done at the 3rd time as before 2600rpm (1413g) for 10 minutes and supernatant was discarded. Platelets were re-suspended quickly in 5ml tyrodes and incubated at 31°C water bath for 30 minutes before starting experiment.

2x10⁸/ml washed platelets were left to adhere and spread on fibrinogen (100µg/ml) coated coverslips for 50 minutes at 37°C following three different treatments with or without 100µM GA. Non adherent platelets were removed and the coverslips were washed x3 with PBS, before fixing using 0.2% PFA for 10 minutes. The coverslips were then washed and treated

with 0.1% Triton-X100. The coverslips were washed x3 before IHC staining with Alexa 488 conjugated phalloidin for 1 hour at room temperature. The coverslips were then washed and mounted onto microscope slides. The adherent platelets were imaged with a 100x oil immersion lens on a Nikon A1-R confocal microscope.

Treatment 1: the platelets were pre-incubated with the control or 100 μ M GA for 30 minutes prior to exposure to fibrinogen. Treatment 2: the platelets were treated with the control or 100 μ M GA at the same time as they were added to fibrinogen coated coverslips. Treatment 3: the platelets were allowed to adhere for 20 minutes prior to treatment with the control or 100 μ M GA.

6.2. 4 Immunoprecipitation and Western Blotting with Platelets

The platelets were taken from different donors (different day/time, prepared in Jon's lab previously) and the platelet samples were prepared previously. The platelets were then treated with 100 μ M GA for 15 minutes. 5 μ l 100mM GA was diluted with 45 μ l tyrodes (1:10). Then for the treatments, 5 μ l of the diluted 100mM GA (1:10) was added in 495 μ l and the platelets were incubated with the GA for 15 minutes. 100 μ M TRAP (Thrombin receptor activator peptide) treatment was done to activate the platelets for 30 seconds. The samples were prepared for the IP and WB experiments.

6.2. 5 Platelets with the VIVAbind™-SUMO Kit

Platelets were taken from the donors and the platelet samples were prepared as described previously. The platelet samples were split into three samples: the control resting platelets, the GA 100 μ M treated samples and the TRAP 100 μ M activated samples. The platelets were treated with 100 μ M GA for 25 minutes. 5 μ l 100mM GA was diluted with 45 μ l tyrodes (1:10). Then for the treatment, 5 μ l of the diluted 100mM GA (1:10) was added in 495 μ l and the platelets were incubated with the GA for 25 minutes. For the TRAP activated platelets, the TRAP concentration was prepared the same as the GA, where 100 μ M TRAP was used. The TRAP was added nearly at the same time as the GA treatment was finished before loading the samples into the SUMO matrix columns. For the SUMO Kit, the concentration of the platelets was 0.6mg / 2ml. The cell lysates were made by adding the lysis buffer from the Kit provided. For each control, GA, and TRAP sample, 40 μ l SUMO matrix suspension was added and incubated overnight. The samples were prepared as the steps in the kit protocol described previously (Method 2.14 VIVAbind™-SUMO Kit). Lastly, the samples were added with the RSTB loading buffer and heated for 5 minutes at 95°C and the samples were ready to run on 4-20% PAGE gels.

6.3 Inhibition of SUMOylation Causes Increased Number and Size of Talin Containing FAs in CMK11-5 Cells

CMK11-5 cells were treated with 160nM PMA previously before they were treated with 100 μ M GA for 15, 30 and 60 minutes. This was to enable the CMK11-5 cells to adhere and spread. The CMK11-5 cells were then immunostained for talin using the talin-1 antibody. The immunostaining shows that after GA treatments, there is increased number and size of talin containing FAs in the CMK11-5 cells.

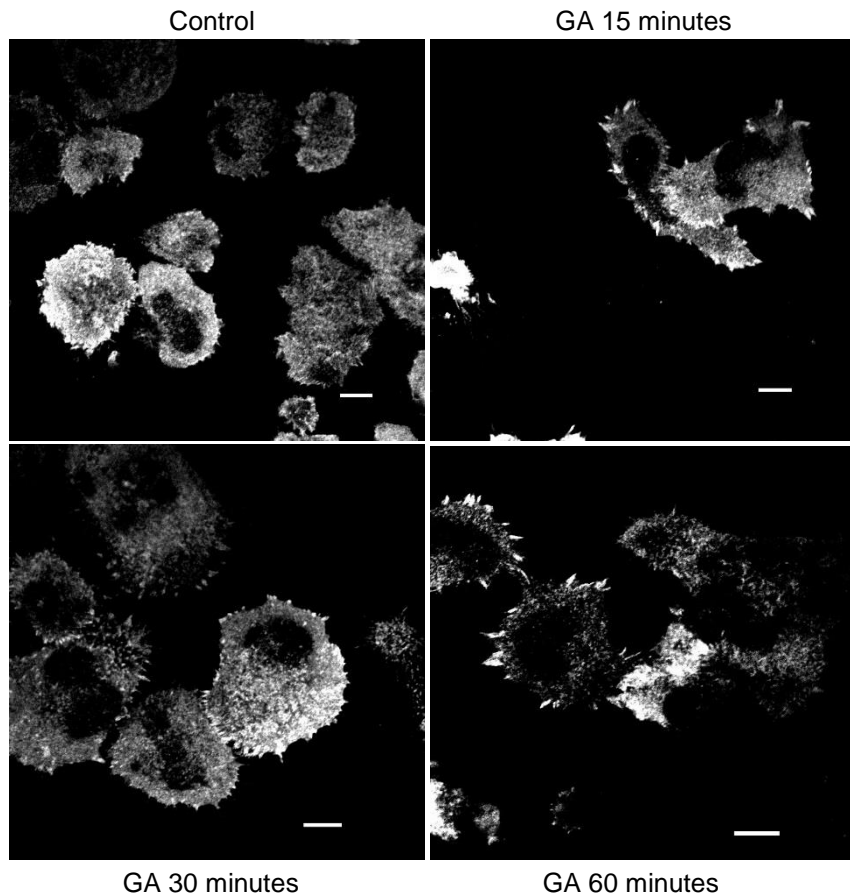
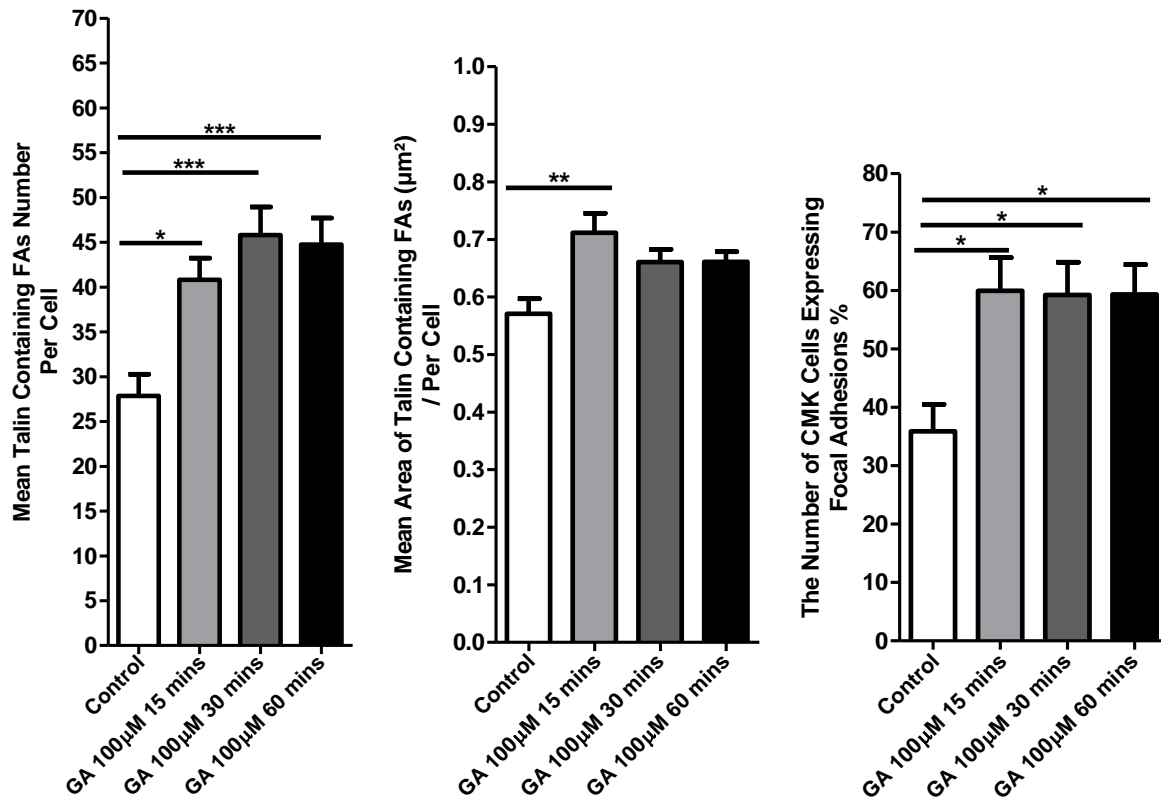


Figure 68. Immunostaining of talin in the CMK11-5 cells showing the talin containing FAs in the control compared to the 100 μ M GA treatments at 15, 30 or 60 minutes (n=3, individual replicates, representative images were shown, scale bar = 20 μ m).

In Figure 68, PMA treatments and fibrinogen binding has made the CMK11-5 cells to express their focal adhesions in the control and GA treated samples. The results were quantified and presented in Figure 69 as a total number of 3 combined experiments.



| Talin n=3 | Control | GA 15 minutes | GA 30 minutes | GA 60 minutes |
|--|---------------|---------------|---------------|---------------|
| Mean ± SE Number | 27.9 ± 2.43 | 40.8 ± 2.42 | 45.8 ± 3.14 | 44.7 ± 2.96 |
| Mean ± SE Size µm ² | 0.571 ± 0.026 | 0.712 ± 0.034 | 0.661 ± 0.022 | 0.661 ± 0.018 |
| Number of cells counted | 61 | 71 | 79 | 98 |
| The percentage of Cells Expressing FAs % | 35.9 ± 4.58 | 60.0 ± 5.68 | 59.3 ± 5.57 | 59.3 ± 5.12 |

Figure 69. Immunostaining of talin in CMK11-5 cells showing that compared to the untreated cells, after 100µM GA treatments at 15, 30 or 60 minutes, the mean number of the talin containing FAs were significantly increased; the mean size of the talin containing FAs was increased after 100 µM GA 15 minutes treatment. The percentage of the CMK11-5 cells expressing talin containing FAs in the control compared to the 100µM GA treatments were also increased at 15, 30 or 60 minutes (data was presented as mean ± SEM, $p < 0.0001$ ***, $n = 3$).

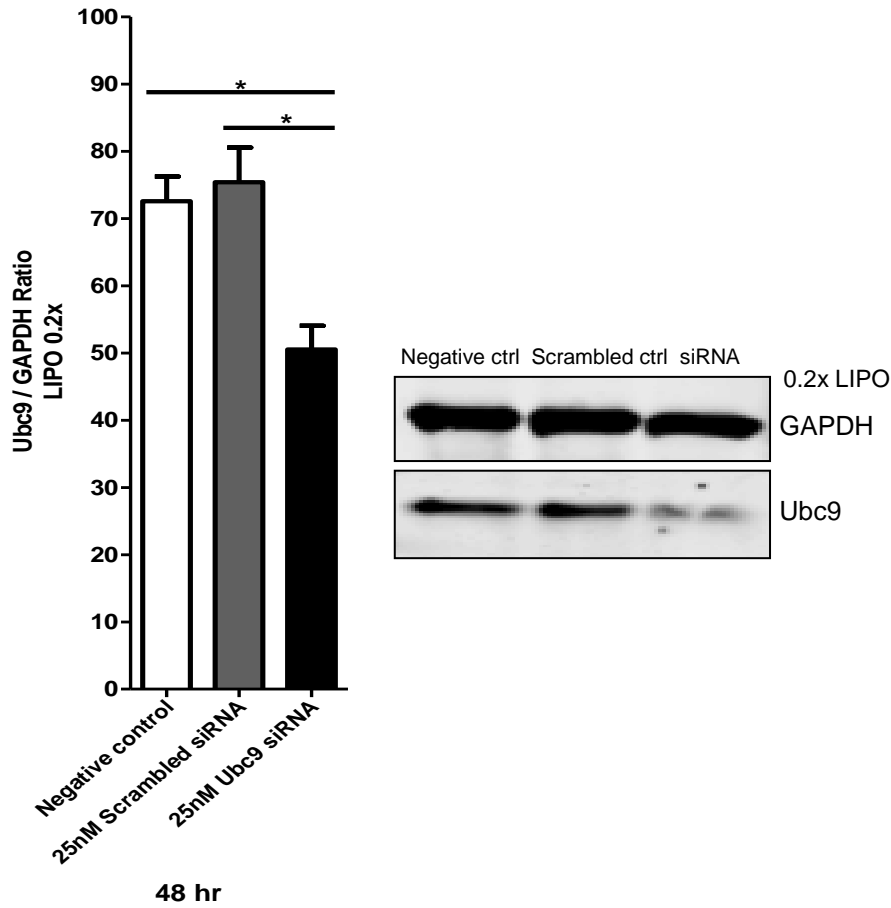
In Figure 69, compared to the untreated cells, after 15 minutes of 100µM GA treatments, the mean number of talin containing FAs was increased significantly from 27.9 ± 2.43 to 40.8 ± 2.42 (*); after 30 minutes of 100µM GA treatments, the mean number of talin containing FAs was increased significantly from 27.9 ± 2.43 to 45.8 ± 3.14 ($p < 0.0001$ ***); after 60 minutes of 100µM GA treatments, the mean number of talin containing FAs was increased significantly from 27.9 ± 2.43 to 44.7 ± 2.96 ($p < 0.0001$ ***). (The control was run for the total period of 1 hour).

Compared to the untreated cells, the mean size of talin containing FAs increased significantly after 15 minutes of 100 μ M GA treatments from 0.571 ± 0.026 to 0.712 ± 0.034 ($p=0.0029$ **).

Compared to the untreated cells, the percentage of the CMK11-5 cells expressing talin containing FAs after 15 minutes of 100 μ M GA treatment was significantly increased from 35.9 ± 4.58 % to 60.0 ± 5.68 % ($p=0.0055$ *); after 30 minutes of 100 μ M GA treatment, the percentage of the CMK11-5 cells expressing talin containing FAs was significantly increased from 35.9 ± 4.58 % to 59.3 ± 5.57 ($p=0.0055$ *); after 60 minutes of 100 μ M GA treatment, the percentage of the CMK11-5 cells expressing talin containing FAs was significantly increased from 35.9 ± 4.58 % to 59.3 ± 5.12 ($p=0.0055$ *).

6.4 Ubc9 siRNA Transfection Significantly Reduced the Ubc9 Enzyme Expression in CMK11-5 Cells

CMK11-5 cells were treated with PMA as described previously and then treated with 0.2x diluted Ubc9 siRNA (25nM) for 48 hours. Whole cell lysates were prepared for each treatment. The samples were run on the gels and blotted with Ubc9 antibody to determine the Ubc9 enzyme expression after the treatments. The results were quantified and presented as Ubc9 / GAPDH ratio as a total number of 3 combined experiments in Figure 70.



| Negative control | Scrambled siRNA | Ubc9 siRNA |
|------------------|-----------------|-------------|
| Mean ± SE | Mean ± SE | Mean ± SE |
| 72.6 ± 3.67 | 75.4 ± 5.17 | 50.5 ± 3.54 |

Figure 70. Western blot showing the negative control, scrambled siRNA and Ubc9 siRNA treatments for 48 hours in the CMK11-5 cells; the Ubc9 siRNA in 0.2x Lipofectamine diluted mixture treatment has caused the knockdown of Ubc9 E2 enzyme in the SUMOylation cycle. The bar chart was presented as Ubc9 vs. GAPDH ratio (n=3, data was presented as mean ± SEM, p=0.011 *).

In Figure 70, compared with the negative control, after 48 hours of 25nM Ubc9 siRNA treatments, the Ubc9 enzyme activity has decreased significantly as a ratio from 72.6 ± 3.67 to 50.5 ± 3.54 (p=0.011 *).

6. 5 Ginkgolic Acid Reduces Platelet Adhesion and Spreading upon Fibrinogen Binding

Platelets were previously taken from donors and prepared for isolation. 2×10^8 /ml washed platelets were left to adhere and spread on fibrinogen (100 μ g/ml) coated coverslips for 50 minutes at 37°C following three different treatments with or without 100 μ M GA. Platelets with 100 μ M GA treatments prior to fibrinogen binding or 100 μ M GA treatments at the same time as the platelets were exposed to fibrinogen binding completely abolished platelet spreading, i.e. no platelets left could be adhered.

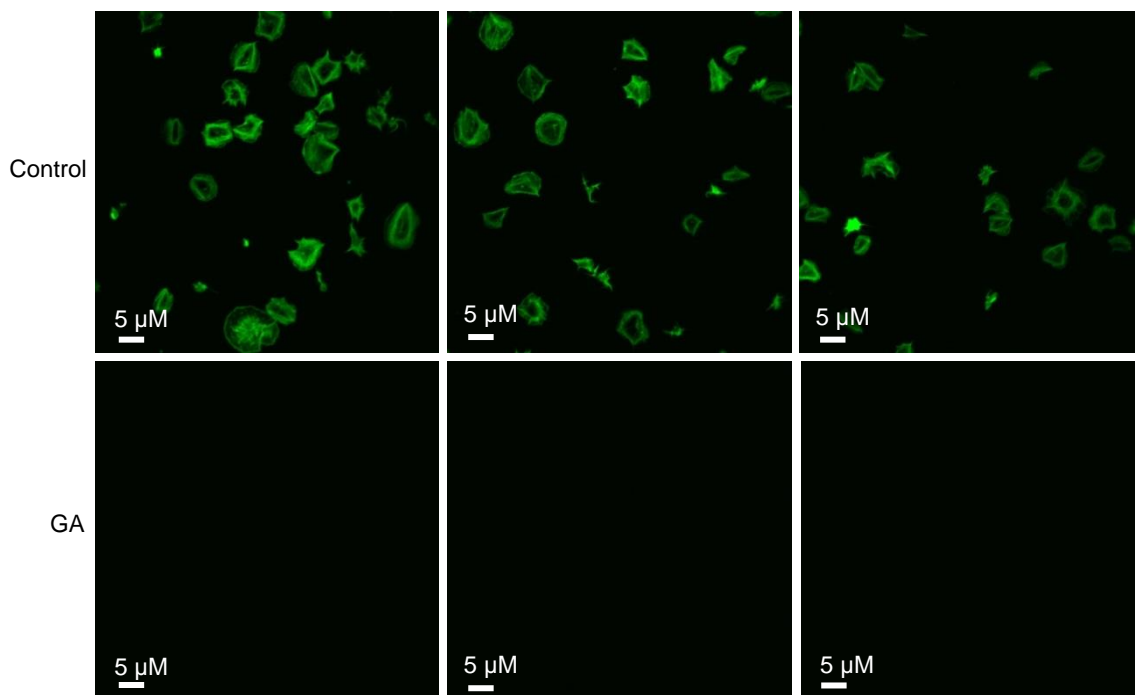


Figure 71. Platelets were left to pre-incubate with the control or 100 μ M GA for 30 minutes prior to exposure to fibrinogen for binding and incubated for a whole length of 50 minutes. Pre-treatments with 100 μ M GA has completely abolished platelets spreading on fibrinogen binding. Non-adhered platelets were removed and adhered platelets were fixed and stained with Alexa 488 conjugated phalloidin. Adhered platelets were imaged with a 100x oil immersion lens on a Nikon A1-R confocal microscope. Three representative images were presented and experiments were done on the same day.

In Figure 71, pre-treatment of platelets with 100 μ M GA for 30 minutes before being allowed to adhere and spread on fibrinogen for 50 minutes has completely ablated and prevented platelet adhesion to fibrinogen on the coverslips.

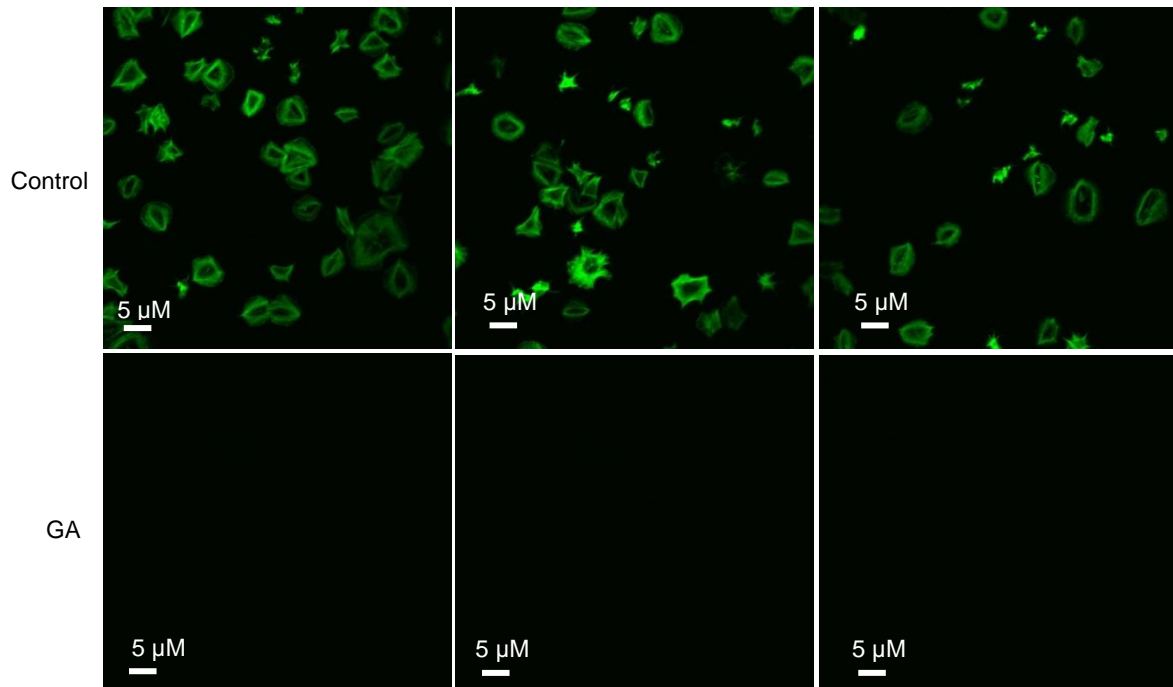


Figure 72. Platelets were treated with the control or 100 μ M GA at the same time as they were added to fibrinogen coated coverslips for binding for a whole incubation length of 50 minutes. Non-adhered platelets were removed and adhered platelets were fixed and stained with Alexa 488 conjugated phalloidin. Adhered platelets were imaged with a 100x oil immersion lens on a Nikon A1-R confocal microscope. Three representative images were presented and experiments were done on the same day.

In Figure 72, no pre-treatment of platelets with 100 μ M GA was done, but the treatment was added at the same time as the platelets were exposed to fibrinogen coated coverslips and then left to adhere and spread for 50 minutes, it has also completely ablated and prevented platelet adhesion to fibrinogen binding on the coverslips.

Treatment 3: the platelets were allowed to adhere for 20 minutes first on the fibrinogen coated coverslips prior to treatment with control or 100 μ M GA and left for incubation for a total of 50 minutes, i.e. the treatment with 100 μ M GA was 30 minutes followed after the first 20 minutes of platelets adhering to fibrinogen

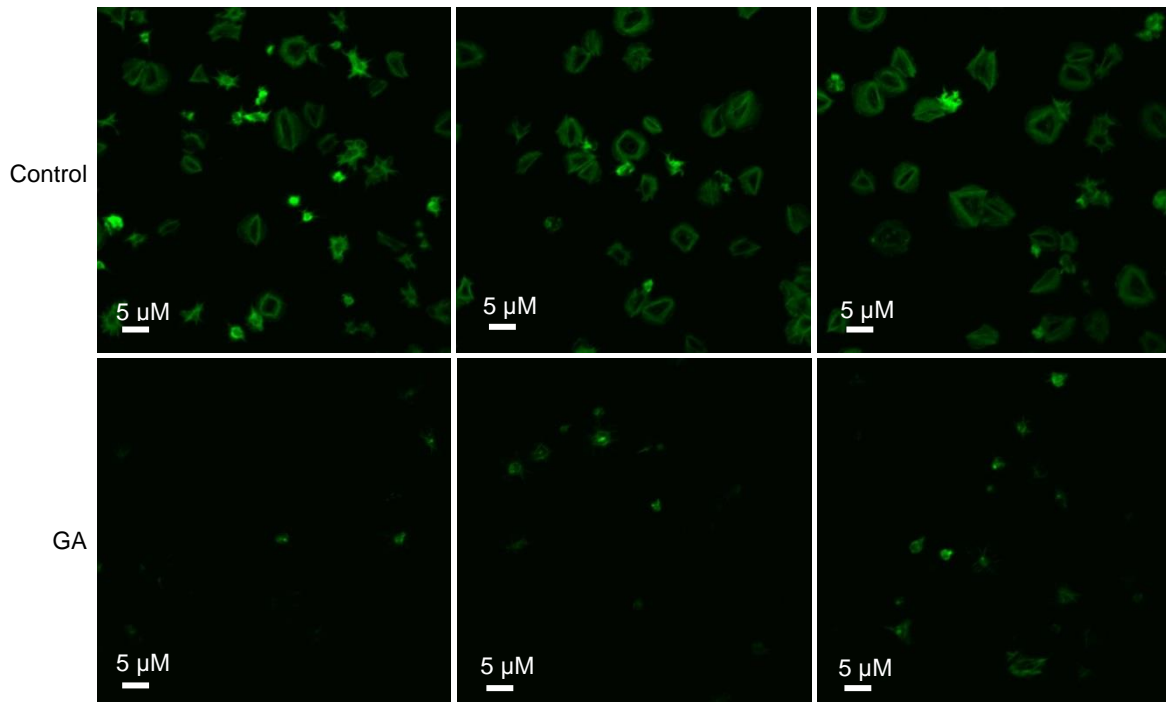


Figure 73. Platelets were left to adhere on fibrinogen for binding for 20 minutes first then followed by 30 minutes treatment with the control or 100 μ M GA; the total time for the platelets to fibrinogen binding was incubated for 50 minutes. Non-adhered platelets were removed and adhered platelets were fixed and stained with Alexa 488 conjugated phalloidin. Adhered platelets were imaged with a 100x oil immersion lens on a Nikon A1-R confocal microscope. Three representative images were presented and experiments were done on the same day.

In Figure 73, the addition of 100 μ M GA treatment following 20 minutes of platelet adhesion and spreading appeared to prevent further platelet adhesion and it has inhibited the spreading of these platelets that were already adhered previously.

6.6 GA Treatment of Platelets Induces Cleavage of Talin

IP SUMO 2/3, IB: Talin (c-9, N-terminal ab)

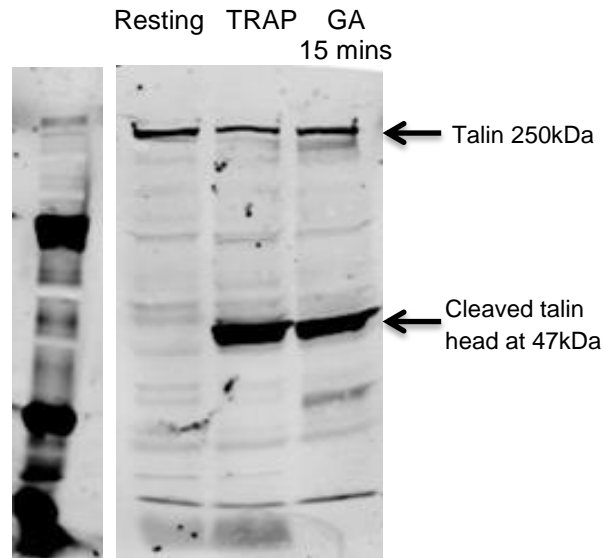


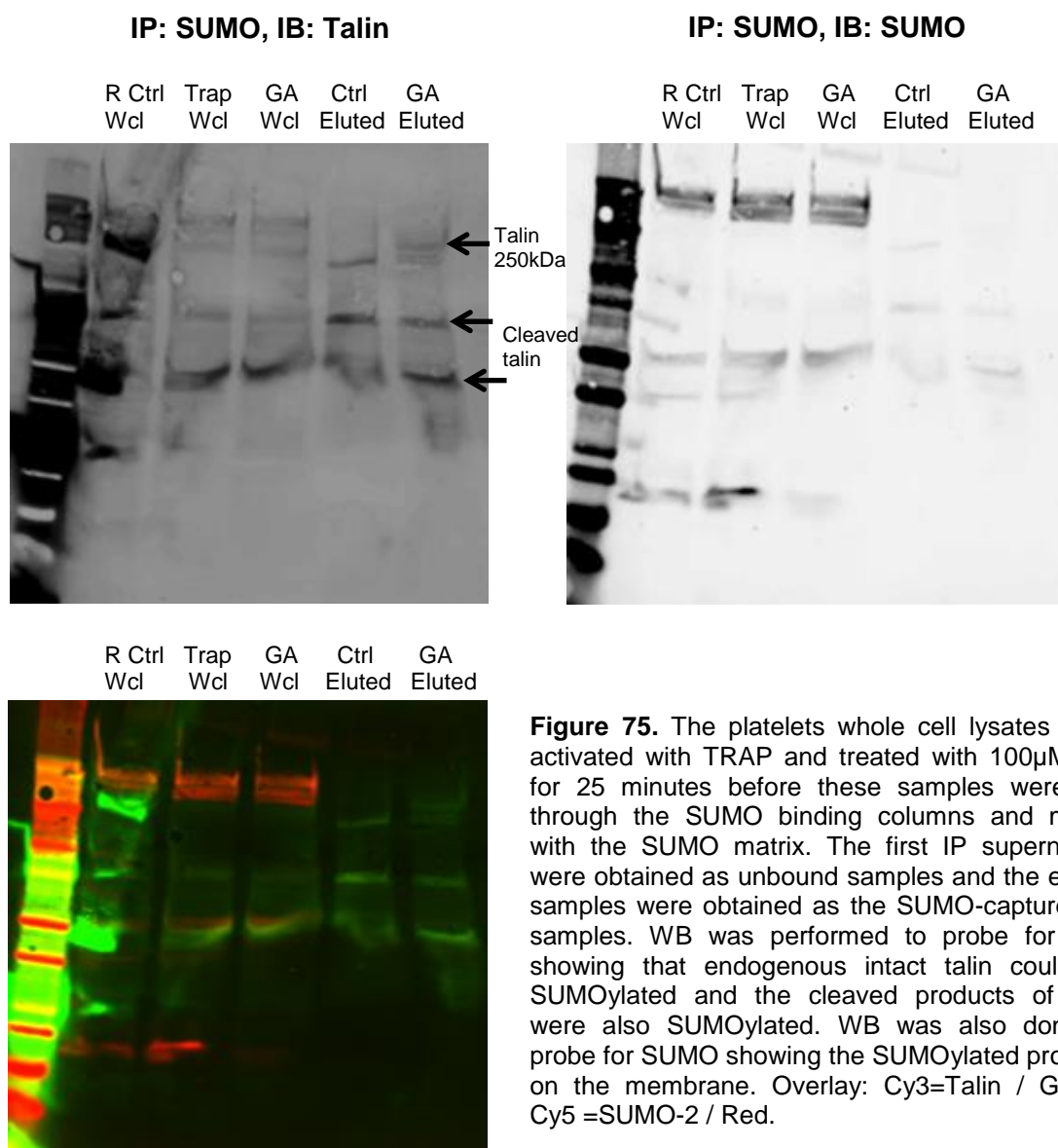
Figure 74. IP and WB showing that endogenous talin can be SUMOylated in resting platelets. Platelets were activated by 100 μ M TRAP treatment for 30 seconds showing a cleavage pattern in the talin detected by the N-terminal c-9 talin antibody. 15 minutes of 100 μ M GA treatment has also caused the cleavage pattern in talin as the intact talin 250kDa and a smaller band at 47kDa

The IP experiments with the platelets were done with Dr. Diana Barker alongside the IP experiments with MDA-MB-231 cells. Talin c-9 antibody detects the N-terminal end of the talin molecule. Talin can be SUMOylated in resting platelets and the intact talin was detected at 250kDa. In the TRAP (Thrombin receptor activator peptide) activated platelets, it has shown the 250kDa band as well as a smaller band at 47 kDa in Figure 74. This suggests that intact talin was SUMOylated and the cleaved talin was SUMOylated only at the smaller fragment (not in the resting platelets).

Platelets incubated with 100uM GA for 15 minutes also show the same cleavage pattern of talin. The same experiments were also done without the addition of TRAP activation and the platelets were treated with 100uM GA for 15, 30 and 60 minutes and it also shows the cleaved products of talin. Later, the cleaved smaller band was confirmed in mass spectrometry that it was SUMOylated cleaved talin as the talin head (experiments conducted by Dr. Diana Barker).

6.7 SUMO VIVA™ Binding Kit and Western Blotting Show SUMOylated Talin in Platelets

The platelets samples were prepared as described previously. The platelets were treated with 100µM GA for 25 minutes and activated with 100µM TRAP at the same time as the GA treatment. The platelets whole cell lysates samples were then prepared and put through with the SUMO binding columns and incubated with the SUMO matrix overnight. The next day, the samples were washed, bound and eluted using the SUMO binding kit washing buffers. The eluted samples and the whole cell lysates samples were both run on the gels and probed on the membranes using talin or SUMO antibodies.



In Figure 75, in the IP SUMO and IB talin membrane, intact talin was SUMOylated at 250kDa in both of the control eluted and 100µM GA eluted samples. In the 100µM GA 25 minutes treated eluted sample, the cleaved smaller fragment of talin head was also seen at 47kDa and this was SUMOylated.

Summary of effect of SUMOylation inhibitors on FA dynamics

| Inhibitors | Number of focal adhesions increased /per cell | Size of focal adhesions increased/µm ² | % Percentage expressing FAs | Platelets spreading inhibited |
|------------|--|--|---|---|
| GA (E1) | CMK+ 15, 30, 60 minutes 28 vs. 41, 46, 45 | CMK+ 15, 30, 60 minutes 0.57 vs. 0.71, 0.66, 0.66 | CMK+ 15, 30, 60 minutes 36% vs. 60% | Platelets not adhered to fibrinogen binding- 50 minutes |

Table 27. Summarising the effects of 100µM GA treatment in CMK11-5 cells and the platelets, the number and size of talin containing FAs were increased significantly and the percentage of the CMK cells expressing talin containing FAs was increased significantly; the platelet spreading was completely abolished after 100µM GA treatment

Discussion

6.8 SUMOylation Plays an Important Role in the Regulation of Focal Adhesions and Cell Spreading in CMK11-5 cells and Platelets

CMK11-5 cells express low levels of α IIb β 3 integrin and are thought to be more differentiated than the parent CMK cells from which they were derived (Komatsu et al., 1989). Since the CMK11-5 cells were naturally grown in suspension culture, this created difficulties to naturally induce them to express focal adhesions while in suspension. PMA was used to induce the activation and spreading of CMK11-5 cells onto the fibrinogen-coated coverslips. PMA could stimulate cell differentiation, spreading and cell surface expression of integrin α IIb β 3 during this time period (Kashiwagi et al., 2004). Also, non-adherent CMK11-5 cells were removed by aspiration and growth media was changed to IMDM containing PMA to achieve even higher levels of α IIb β 3 on the cell surface. In this way, the talin containing FAs could be expressed and measured upon integrin α IIb β 3 signalling. In the other cells, such as the human monocytic leukemia THP-1 cells, PMA induces the THP-1 cells to differentiate into macrophages and upregulate the p21^{WAF1/CIP1} promoter driven by a transcription factor Sp-1 (Traore et al., 2005). PMA was found to phosphorylate a number of cytosolic polypeptides, caused cell aggregations, lysosomal enzyme secretion and increased actin level associated with the cytoskeleton without the elevation of intracellular free Ca²⁺ in rabbit neutrophils (White et al., 1984). Short-term treatment with 100nM PMA activates PKC, ERK 1/2 (5 minutes treatment) and p38 MAP kinases (mitogen activated protein kinases, 1 hour treatment) independently in differentiated parental human colonic adenocarcinoma cell line Caco-2 (Jiang and Fleet, 2012). Long-term treatment with PMA up to 12 continuous days without passage in human melanocytes caused changes in cell morphology, cell cycle, cytoskeleton and the higher the PMA concentration (up to 170nM) the higher differentiation percentage in the melanocytes (Chao-Hsing and Hsin-Su, 1991). PMA is therefore a co-stimulator of cell differentiation. In this study, CMK11-5 cells not only were attached to the plastic coverslips from the suspension in the conditioned media but also were seen with irregular shaped morphology, indicating their differentiation.

The inhibition of protein SUMOylation made the CMK11-5 cells increase the number and size of their talin containing FAs after the first 15 minutes of 100 μ M GA treatment. This effect was induced after the use of PMA as PMA caused FAs to form as the cells were adhered.

The siRNA treatment reduced the Ubc9 expression after 48 hours in the CMK11-5 cells, indicating that the siRNA knockdown was effective. However, the knockdown was not

complete due to the length of the experiment and the nature of the cells and optimization needs further determination. CMK11-5 cells were grown in conditioned media and activated for 6-7 days before the siRNA knockdown effect was obtained. Therefore, siRNA was used to see if the Ubc9 expression was able to be reduced for the whole length of the 6 days experiments but it was not continuously used in the IHC experiments to count the FA number and size afterwards.

For platelets, the inhibition of protein SUMOylation completely inhibited platelets from spreading prior to fibrinogen binding or after the platelets had been bound with fibrinogen for 20 minutes. This suggests that SUMOylation was involved in integrin $\alpha\text{IIb}\beta\text{3}$ -cell adhesion interactions and platelets spreading. Platelet membrane receptors function to mediate the initial tethering of platelets to the wounded blood vessel wall or a lesion and this process is in three successive steps: platelet adhesion, activation and aggregation (Ruggeri, 2002). There are many signalling factors associated with the activation of the integrin $\alpha\text{IIb}\beta\text{3}$ and platelet membrane surface receptors. Several mechanisms are involved namely the VWF- GPIIb mediated platelet adhesion and aggregation; platelet-collagen adhesion mediated by the immunoglobulin (Ig) superfamily member GPVI receptor and integrin $\alpha\text{2}\beta\text{1}$, etc; the platelet adhesion to collagen requires the activation of integrin $\alpha\text{IIb}\beta\text{3}$ (GPIIb-IIIa) through inside-out signalling generated by GPVI and strengthened by the release of second mediators ADP (adenosine diphosphate) and thromboxane A2 (TxA2); platelets can adhere and aggregate to purified fibrinogen and fibrin under flow conditions, selectively mediated by $\alpha\text{IIb}\beta\text{3}$ (Nieswandt and Watson, 2003, Ruggeri and Mendolicchio, 2007). Platelet aggregation is a more complex process: platelet aggregation at low hemodynamic conditions (blood flow, blood vessel wall shear rate $< 1000 \text{ s}^{-1}$) is predominantly mediated by the integrin $\alpha\text{IIb}\beta\text{3}$ interaction with fibrinogen and this is independent of the von Willebrand factor (VWF) and glycoprotein Ib (GPIb, a membrane-bound platelet receptor) interaction in promoting initial platelet tethering to the blood vessel wall; at shear rates between $1000\text{-}10,000 \text{ s}^{-1}$, platelets tethering and the initial formation of discoid platelet aggregates is mediated by both GP Ib/V/IX and integrin $\alpha\text{IIb}\beta\text{3}$ and this becomes more VWF dependent progressively; at very high shear rates $> 10,000 \text{ s}^{-1}$, platelet aggregates does not require platelets activation and integrin $\alpha\text{IIb}\beta\text{3}$ however it is mostly mediated by VWF-GP Ib adhesive interactions (Jackson, 2007).

Talin can be SUMOylated in platelets. It indicates that the SUMOylation of talin in platelets may be involved in the activation of integrin $\alpha\text{IIb}\beta\text{3}$ signalling of the platelets leading to platelet spreading and aggregation. Inhibition of SUMOylation abolished the response of the integrin signalling therefore the platelets were completely incapable of fibrinogen binding.

6.9 Comparisons between Different Cell Types: the General Role of SUMOylation in the Regulation of Focal Adhesions

The agonist TRAP at 5 μ M can activate the platelets as quickly as 30 seconds (García et al., 2004). TRAP has been known as the thrombin receptor activating peptide, could mimic many effects of thrombin (McNicol and Robson, 1997) and once the platelets were activated, talin is cleaved with the talin head fragment being at 47kDa. Once talin is cleaved, it was the end-point of the activation of platelets.

Various inhibitors including GA, 2-D08, gossypetin and Ubc9 siRNA have been used in MDA-MB-231 cells and U2OS cells, with the use of GA in the CMKs and the platelets. SUMOylation plays an important regulatory role in FA disassembly in MDA-MB-231 cells and U2OS cells, where various inhibitors' treatments increased FA number and size. Similar effects were also seen in the CMK11-5 cells where 100 μ M GA treatment increased the number and size of talin containing FAs.

Talin exists in two states as an auto-inhibited form and the activated form in conformational structural change which causes an increase in its affinity to integrin β 3 binding and other ECM proteins during FA assembly (Ellis et al., 2013, Critchley and Gingras, 2008, Goult et al., 2013a). The binding of talin to the β 3 integrin tail is critical for the agonist-induced integrin α IIb β 3 activation (Petrich et al., 2007a). Since inhibiting SUMOylation leads to the cleavage of talin, this suggests that SUMOylation could be playing a role in the integrin α IIb β 3 and talin binding signalling axis and in the activation of talin, hence in the platelet spreading.

The regulatory mechanisms of SUMOylation of FAs in these cells were different. There were morphological changes regarding to the cell structure and alterations in the molecular integrin signalling pathway related in the talin functions. Talin was particularly investigated between the cancer cells and the platelets, where talin was obtained both of inactive non-cleaved state and cleaved conformational change in the platelets. Meanwhile, in cancer cells overexpressed with SUMO-2, the cancer cells consistently expressed cleaved talin, probably due to the fast speed of turnover required in the cancer cells. In platelets, talin cleavage resulted from the inhibition of SUMOylation was an all-or-nothing effect and the talin cleavage effect in the cancer cells could be regarded as a manifest exaggeration for the cells' functional requirement.

Role of SUMOylation in Platelets

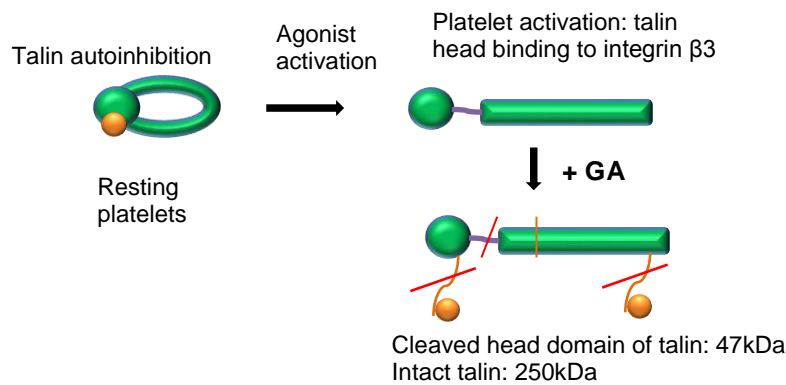


Figure 76. Talin is in its autoinhibition conformation in resting platelets. Upon agonist binding such as TRAP, platelets activation is through integrin $\alpha \text{IIb}\beta 3$ signalling which causes talin conformational change. After GA treatment, cleavage of talin is seen and both intact talin and the cleaved fragment of talin are SUMOylated

Talin was SUMOylated in both resting platelets and stimulated platelets. However, inhibiting SUMOylation after GA treatment caused cleavage of talin as the cleaved head domain as well as the intact talin. The N-terminal head of talin is ~47kDa and the C-terminal rod is ~190kDa (or 200kDa) (Yan et al., 2001). This may suggest SUMOylation is protective against talin cleavage. Talin cleavage may be an important function of the platelet activation in platelet adhesion, spreading and aggregation as inhibiting SUMOylation inhibited platelet spreading upon fibrinogen binding. This regulation of SUMOylation in FA proteins is a different process compared to the cancer cells.

The stimulation of platelets leads to the inside-out integrin $\alpha \text{IIb}\beta 3$ -FA signalling required for platelet aggregation with the neighbouring platelets to form a clot. This process is an all-or-nothing effect: the effect of talin SUMOylation in the activated platelets can be seen as an amplified signalling: all the talin proteins recruited at the integrin-FA assembly site can be SUMOylated; in resting platelets, SUMOylation protects against FA cleavage, however, talin can be cleaved by calpain-2 during platelet activation, since calpain activation is dependent on fibrinogen binding to integrin $\alpha \text{IIb}\beta 3$ (Schoenwaelder et al., 1997) and calpain cleavage promotes talin binding to integrin $\beta 3$ (Yan et al., 2001) and the cleaved talin is also SUMOylated. These cleaved SUMOylated talin are the endpoint of platelet activation which may contribute to the platelet adhesion and aggregation process. Inhibiting SUMOylation causes cleavage of talin and this effect is irreversible. Once the platelets were activated, the platelets could not be reverted back into their resting phase, i.e. once talin cleavage activation was stimulated, this was the endpoint of the inhibitory effects of the inhibitor.

The FA proteins in the cancer cells are involved in fast cell migration and metastasis, therefore their turnover requires consistent assembly and disassembly. SUMO-2 conjugation may be required for the FA disassembly consistently in cancer cells. However, the mechanism in platelets is that they require FA proteins in spreading and aggregation during wound healing; therefore, it is not a constant process, since when platelets are activated they cannot be reverted back to resting stage. The cancer cells require fast cell migration and their FA proteins may also be constantly recycled from the cytosol to the membrane leading to the consistent fast turnover event.

Talin, vinculin and filamin-1 have been identified as SUMOylation substrates in the MS analysis both in MDA-MB-231 and CMK11-5 cells. Talin and actin have been identified in MDA-MB-231 cells, CMK11-5 cells and platelets. Talin has been validated in the experiments to be a SUMOylation substrate. Interestingly, Integrin $\alpha\text{IIb}\beta\text{3}$ has been identified as a SUMOylation substrate in the MS analysis in both CMK11-5 cells and platelets. This suggests its overall role of integrin $\alpha\text{IIb}\beta\text{3}$ signalling in adhesion, activation and aggregation in megakaryocytes and platelets.

Talin has two fractions: the membrane-associated and cytosolic fractions, the membrane-associated talin was able to be cleaved into a 200kDa fragment similar to the calpain cleavage in CHO cells (Tranqui and Block, 1995). Talin was shown to be cleaved by calpain in skeletal muscle cells and released into the cytosol (Koh and Tidball, 2000). In resting platelets, talin was uniformly distributed throughout the cytoplasm; upon platelet activation, a significant amount of talin was rapidly redistributed to submembranous location (Bertagnolli et al., 1993). Talin and vinculin can both be cleaved by calpain (Franco et al., 2004). The membrane-associated talin and vinculin in the FAs in platelets are all SUMOylated at one time required for activation. Once stimulated, no cleaved fragments of talin can be obtained. Calpain activation, FA cleavage by calpain and the SUMOylation of talin may also be associated with the actin cytoskeleton rearrangement through integrin $\alpha\text{IIb}\beta\text{3}$ signalling during platelet aggregation process. However, the cleavage of talin is consistent and the cleaved talin fragments are SUMOylated and these may be important in actin-myosin network to achieve fast FA turnover e.g. FA disassembly in cancer cells during cancer cell migration.

The FA complex required for the platelet spreading may also be different to that of the FA assembling in the cancer cells. FAK is a key regulator for the FA complex formation; the calcium and integrin binding protein could regulate platelet spreading through FAK activity but only on immobilized fibrinogen binding to the platelet fibrinogen receptor $\alpha\text{IIb}\beta\text{3}$ / GPIIb-

IIIa (Naik and Naik, 2003). A megakaryocyte lineage-specific FAK-null mouse was generated, where FAK-null platelets exhibited diminished platelet spreading on immobilized fibrinogen indicating FAK role in megakaryocyte growth and platelet function *in vivo* (Hitchcock et al., 2008). Less was known about the role of vinculin in platelets; in one study, the vinculin gene was deleted in the megakaryocyte/platelet lineage in mice, in these vinculin-deficient platelets used from these mice, they displayed normal agonist-induced fibrinogen binding to $\alpha\text{IIb}\beta\text{3}$, normal platelet spreading and aggregation, actin polymerization, clot retraction and were capable of forming a pro-coagulant surface; they adhered to immobilized fibrinogen or collagen normally both under static and flow conditions, suggesting that vinculin may not be required for platelet $\alpha\text{IIb}\beta\text{3}$ function (Mitsios et al., 2010). However, vinculin was required for membrane cytoskeleton integrity: in thrombin-activated platelets vinculin was shown to be cleaved by calpain producing a major fragment at 95kDa with at least two other fragments during platelet aggregation, whereas in the resting platelets only full-length of vinculin was detectable; this 95kDa cleaved fragment was associated with the platelet cytoskeleton, where the cleaved vinculin fragments were transferred from the membrane to the cytoskeletal fractions in the aggregating platelets, suggesting that calpain cleavage of vinculin upon platelet stimulation may be involved in the actin cytoskeleton rearrangements important for platelet aggregation and motility; the calcium-dependent platelet protease, calpain was activated upon platelet activation and when the platelets were pre-incubated with its inhibitor calpeptin at 100 $\mu\text{g/ml}$ for 1 hour at 37°C then treated with 1 μM calcium ionophore abrogated vinculin cleavage to that level in the non-stimulated platelets (Serrano and Devine, 2004).

SUMOylation is required for megakaryocytes and platelet adhesion and spreading. For future work, how SUMOylation of talin is directly implicated in platelet adhesion and spreading needs to be determined. Moreover, the role of these cleaved talin fragments (or vinculin fragments) in the FA turnover and their functions in relation to the platelet activation, adhesion and aggregation can be determined further. Firstly, calpain inhibitors in combination with GA need to be used to determine if talin can still be cleaved in the activated and aggregated platelets; antibodies or molecular tags against the fragmented talin (head domain or rod domain of talin) can be used to determine their localization during platelet activation.

Chapter 7 - Overall Discussion and Future Perspectives

Metastasis contributes to high mortality rates of cancer which involves many highly regulated cell signalling processes. In this study, SUMOylation has been studied to look at its role in FAs and cancer cell migration. Talin, FAK and vinculin containing FAs have been shown to increase in number, size and turnover time after the SUMOylation inhibitor treatments, which has resulted in reduced speed of cell migration significantly. Inhibiting SUMOylation causes reduced FA turnover also indicating its role in FA disassembly. The SUMOylation of talin, vinculin and filamin-1 have been studied for the first time and validated in the MS studies. SUMOylation has been involved in the regulation of many FA proteins including talin, vinculin, filamin 1, actin and the integrin $\alpha 5\beta 3$ etc, which has suggested that SUMOylation has an overall diverse and crucial role in cell migration. Future experiments will be carried out to investigate closely how SUMOylation regulates FAs directly and its role in protein-protein interactions within FAs.

Site directed mutagenesis is the next step to determine if mutating lysines in part of the talin or vinculin molecule can directly impair cell migration; therefore, it can directly identify which lysines the talin molecule can be modified with SUMO 2/3. Since the bioinformatics tool are very stringent and reliable, it could suggest that what has been predicted to be the modified sites in the top list with the highest scores in the talin, vinculin or filamin-1 molecule could be genuine. This can also be used to determine whether mutating the predicted SUMOylated modified lysine residues in talin or vinculin could alter their localization in the cells, dynamics and turnover rates and their roles in adhesion signalling. However, IP & WB experiments also need to be done to investigate ubiquitination, phosphorylation or acetylation of FA proteins after mutagenesis of the speculated SUMO modified sites in FA proteins, since competition between PTMs could occur on the same lysine residue.

7.1 De-SUMOylation and its Focus

The SUMO de-conjugating enzymes are known as the Ulp and SENPs; in mammals, there are six SENPs: SENP1, SENP2, SENP3, SENP5, SENP6 and SENP7 (Wang and Dasso, 2009). The human proteases SENP1, SENP2, SENP3 and SENP5 are most closely related to yeast Ulp1 in sequence; human SENP6 and SENP7 are related to yeast Ulp2 (Hay, 2007). Some examples have been listed to discuss the roles of the SENPs. The SUMO modification of transcription factors could lead to their transcriptional activation mainly related as transcriptional repression, i.e. SUMOylation of transcription factors correlates with the inhibition of transcription and SUMOylation promotes the transcription factors to interact with the co-repressors therefore regulating gene function (Gill, 2005). Furthermore, the SUMO

conjugation with transcription factor can be reversibly removed by the SENPs, which would de-repress the transcription action and therefore it also regulates the gene expression (Hay, 2007). Uls/SENPs are highly specified towards SUMO paralogs, but also other functions are discriminated between processing, chain-editing reactions and deconjugation (Mukhopadhyay and Dasso, 2007). SUMO processing and deconjugation are essential proteolytic activities for nuclear metabolism and cell cycle progress in both higher eukaryotes and yeast; mutational analysis and biochemistry revealed the mechanism for SENP2 preferences to catalyze SUMO deconjugation over SUMO processing (Reverter and Lima, 2006). RanGAP1 could be modified by SUMO-1 and SUMO-2 *in vitro* and selectively modified by SUMO-1 *in vivo*; the RanGAP1-SUMO-1 conjugates could also form a more stable high affinity complex with the nucleoporin Nup358 (also known as RanBP2) than RanGAP1-SUMO-2, which protects RanGAP1 from the isopeptidases preferentially even in the presence of these isopeptidases: SENP1, 2 and 5; additionally, SENP1, 2 and 5 could efficiently deconjugate both SUMO-1 - and SUMO-2 – conjugated RanGAP1 in the absence of Nup358 and Ubc9 (Zhu et al., 2009).

SENP5 is required for cell division and mitochondrial function, previously, SENP5 has been reported to be present in the cytoplasm of oral squamous cell carcinoma (OSCC) predominantly, similarly, SENP3 was found to be overexpressed in OSCC (Sun et al., 2013, Ding et al., 2008); the inhibition of SENP5 could suppress cell growth, colony formation capacity and promote cell apoptosis i.e. an increase in caspase 3/7 activities and a decrease in cyclin B1 expression in serum-deprived osteosarcoma cells, U2OS cells and Saos-2 cells (Wang and Zhang, 2014). More specifically, knockdown of SENP5 using RNAi dramatically decreased proliferation in Hela cells and resulted in aberrant nuclei or multiple nuclei morphologies in many cells, especially multi-lobar nuclei indicating a defective mitosis or cytokinesis; whereas, the closet homolog SENP3 knockdown did not show this phenotype suggesting a unique role of SENP5 in the regulation of cell division (Di Bacco and Gill, 2006, Di Bacco et al., 2006). SENP1, 2, 3, 5 and 6 have SUMO-specific C-terminal hydrolase or isopeptidase activities; SENP5 was shown to remove SUMO-2 and SUMO-3 preferentially from SUMO-modified RanGAP1 *in vitro*; SENP5 RNAi led to an increase in SUMO-2 / SUMO-3 conjugated proteins than SUMO-1 conjugates (Di Bacco et al., 2006).

In the previous discussion in Chapter 3, de-SUMOylation has been briefly mentioned as whether inhibiting de-SUMOylation on the effects of FA dynamic activities could be reversible or not can be investigated in the future experiments. SENP1 and SENP2 are concentrated at the nuclear envelope through interactions with components of the nuclear pore complex; SENP6 and SENP7 mainly exhibit nucleoplasmic distribution; SENP3 and

SENP5 are compartmentalized in the nucleolus, where they play roles in early stages of ribosome maturation, however, a subfraction of SENP3 and SENP5 are also resided in the nucleoplasm and the cytoplasm (Nayak and Müller, 2014, Hickey et al., 2012). Consequently, the effects of knocking down SENP5 in the cancer cells, i.e. in the U2OS cells could also be determined in relation to the FA dynamic activities. One experiment could be done in the future is to determine the co-localization of these SENPs with the FA proteins such as talin or vinculin in the cells, to determine where they are de-SUMOylated in the cells i.e. in the FA or in the cytosol where they can be turned over; whether talin or SENP5 are localized together in the FA so that the FA turnover is dynamic. The NEM (N-Ethylmaleimide) has been used together with the PIC (protease inhibitor cocktail) in the preparation of the IP samples in this study (although the use of NEM with PIC or PIC alone gave similar amount of proteins in the whole cell lysates protected from the proteases inhibitors). This was to ensure that no protein de-SUMOylation or degradation before the SUMOylated proteins could be immunoprecipitated, captured and identified on the WB scanning. Whether enhancing de-SUMOylation of a protein could be achievable experimentally or increasing the time for a protein to stay SUMOylated i.e. increasing SUMOylation level of a protein could affect its localization, regulation or protein-protein interaction and function can also be further investigated. Since the SUMOylation of the cytoplasmic proteins are less understood, the identification of the comodulator of these SENPs which can prevent de-SUMOylation can be further investigated. SUMOylation is a very dynamic process and conjugation or de-conjugation of SUMO to the target proteins depends on the enzymatic and chemical conjugation steps. Therefore, the balance of SUMO conjugation and de-conjugation to the target proteins stays critical.

7.2 SUMOylation and Ubiquitination

Talin phosphorylation by Cdk5 regulates talin head ubiquitination, FA disassembly, lamellipodial dynamics and cell migration. The talin head can be cleaved by calpain-mediated proteolysis and the talin head binds to smurf1, an E3 ubiquitin ligase more than the full length talin leading to talin head ubiquitination and degradation (Huang et al., 2009). Therefore, ubiquitination is a crosstalk PTM that can regulate the same substrate protein. The substrate protein can be conjugated to ubiquitin and ubiquitin-like protein (UBL), which regulates its physiological function; the bound UBLs regulate their protein interactions with the proteasome, which the ubiquitination (also termed ubiquitylation) pathway also uses enzymes like E1, E2 and E3 enzymes to attach specific ubiquitin to the substrate proteins (Hochstrasser, 2009). Ubiquitin and UBL have been classified as two classes, which the SUMO belongs to the UBL class (Müller et al., 2001, Melchior, 2000). The ubiquitin is also usually attached to lysine side chains of the substrate target protein resulting in branched

isopeptide-ubiquitin-target protein conjugate and targeting it to the 26S proteasome for degradation (Müller et al., 2001). The effects of ubiquitination and SUMOylation are resulted from the specific interactive domains of the binding proteins mostly; both modifications are reversible and these have been largely studied in the nucleus (Gill, 2004). Some proteins can be modified on the same lysine by SUMO or ubiquitin but with different functions, such as I κ B α and γ PCNA (Mabb and Miyamoto, 2007, Bergink and Jentsch, 2009). I κ B α was primarily conjugated to SUMO-1 on K21, which was also utilized for ubiquitin modification, therefore, SUMO-1 conjugation to I κ B α could not be ubiquitinated and was resistant to proteasome-mediated degradation (Desterro et al., 1998). The proliferating cell nuclear protein (PCNA) has been one of the most striking examples of the control switch between ubiquitin and SUMO; PCNA is a DNA polymerase which encircles DNA acting as a processing factor for DNA polymerisation and as a moving platform for factors involved in DNA replication, synthesis and repair; PCNA could be modified on the same conserved lysine 164 either by monoubiquitylation, lysine 63-linked polyubiquitin chains or SUMO (lysine 164 is a non-consensus SUMO-conjugating site), which has been involved in DNA damage response (Bergink and Jentsch, 2009, Hoege et al., 2002).

In the previous discussion in Chapter 4, the total amount of protein stability has not been changed after the inhibition of protein SUMOylation globally suggesting that SUMOylation does not inhibit ubiquitination and therefore proteolysis of FA proteins. However, how ubiquitination of these FAs in cancer cells can have an impact on cell migration, parallel to their SUMOylation regulation have not been investigated yet. Since the talin head could be cleaved and can be regulated by SUMOylation and ubiquitination, this has raised interesting questions on how ubiquitin or SUMO could be regulating talin containing FA dynamic activities and therefore affecting cell migration. The ubiquitin C-terminal hydrolase-L1 deubiquitinating enzyme (UCH-L1) has been found to colocalize with FAK, p120-catenin and vinculin at the motile edge of the Hela cell membrane during the first phases of adhesion, enhance FA formation and FAK activation; UCH-L1 could promote survival, proliferation and metastatic potential and is a key regulator of tumour invasion and metastasis (Frisan et al., 2012, Kim et al., 2008).

As this study shows fast FA turnover requires consistent SUMO-2 conjugation of talin and the talin-vinculin interaction protein complex; the ubiquitination pathway may not function effectively in the cancer cells, whether any dysfunctions of ubiquitin are involved in FA dynamic turnover and cell migration can be considered, i.e. the role of talin ubiquitination in relation to talin SUMOylation in the FA dynamic turnover and its regulation may not be in balance. These effects can be further examined including the mechanistically similar

crosstalk but with different functions for these two pathways. Ubiquitination inhibitors could be used in the focal adhesion turnover assays to determine FA protein dynamic activities and in cell migration study after inhibition of protein ubiquitination; antibodies against ubiquitin can be used in the IP & WB experiments to determine FA (talin and vinculin) ubiquitination.

7.3. 1 Potential Drug Targets for Metastatic Cancers and Other Findings

The six hallmarks of cancer have been elucidated with two additional hallmarks added to the hallmark system recently. The factors that contribute to the tumour development have been growing on the lists. SUMOylation as a type of PTMs which has been studied exclusively in the nucleus has recently attracted attention to its role outside the nucleus such as in the regulation of cytoplasmic proteins, including the focal adhesions.

From this study, the pathway of SUMOylation in the regulation of FAs serves as a potential novel drug target for cancer treatments. There has only been one E2 enzyme in the SUMOylation conjugation pathway, interacting with nearly all the partners required for SUMOylation, which marks Ubc9 as a target for rational drug design (Duan et al., 2009). The cysteine 93 of Ubc9 serves as a covalent intermediate interaction; also, Ubc9 interacts with SUMO through non-covalent interaction but with high affinity, therefore, the virtual screening against the interface between the Ubc9 and SUMO, the covalent interactions between Ubc9 and substrates and the non-covalent interface can be possible targets (Duan et al., 2009).

Secondly, the activation of integrin requires talin phosphotyrosine-binding domain (PTB) binding to integrin β subunit cytoplasmic domains, knockdown of talin inhibited integrin activation; this serves as a therapeutic target to block talin from binding to integrin β subunit (Wegener et al., 2007, Tadokoro et al., 2003). Talin can be SUMOylated; from the previous experiments shown in this study, talin SUMOylation was consistently required in the cancer cells, i.e. talin was consistently in its conformational change and with SUMO-2 conjugation required for fast talin turnover.

Thirdly, this SUMOylation regulatory mechanism of FA serves as a prospective molecular target, which small molecules can be developed to stop consistent talin SUMOylation, such as the ginkgolic acid used experimentally to inhibit talin / FA disassembly and prevent fast talin turnover in the cancer cells. Clinical trials have been carried out indicating the potential therapeutic roles of *Ginkgo biloba* extract in cardiovascular diseases, since it has been reported to produce antioxidant effects, stress-alleviating effects, modify vasomotor function, reduce blood cell adhesion to endothelium, inhibit activation of platelets and smooth muscle

cells and prevent thrombosis (Zhou et al., 2004). The designated *Ginkgo biloba* extract EGb 761 is widely employed to treat cerebrovascular and peripheral vascular diseases and mild-to-moderate dementia (DeFeudis and Drieu, 2004, Smith and Luo, 2004). *Ginkgo biloba* extract is also reported to have anticancer properties to exhibit chemopreventive reactions and antiangiogenic effects (Mahadevan and Park, 2008). Although the long-term therapeutic use still needs to be evaluated.

From the literature, SUMOylation and anti-cancer drugs has become a more attractive area recently. Cancer treatment has included the anthracyclines and taxanes but the therapeutic efficacy has been a problem since DNA damage is associated with it, for example, the forkhead transcription factor (FoxM1) has been shown to have a critical role in resolving DNA damage response and genotoxic agents derived resistance (Khan et al., 2016). FoxM1 expression has been associated with epirubicin sensitivity and DNA double-strand breaks repair; ectopic FoxM1 expression could abolish the double-strand breaks sustained in MCF-7 breast cancer cells following epirubicin treatment and increase cell viability in response to enhanced DNA repair efficiency; however, FoxM1-null cells were hypersensitivity to DNA damage, epirubicin and γ -irradiation (Monteiro et al., 2013). In breast cancer, FoxM1 has been shown to be involved in endocrine, trastuzumab, cisplatin, paclitaxel, gefitinib and most recently in epirubicin resistance (Monteiro et al., 2013). FoxM1 inhibition could sensitize resistant glioblastoma cells to temozolomide by downregulating DNA repair response (Zhang et al., 2012). Recently, FoxM1 has been shown to be modified by SUMO-1 and FoxM1 SUMOylation was enhanced in MCF-7 breast cancer cells following epirubicin treatment and SUMOylation could inhibit FoxM1 activity and delay cancer cell mitotic activity in response to cytotoxic drugs (Myatt et al., 2014). This is more to do with SUMO-1 than SUMO 2/3.

Other studies have shown that increased Hsp90 (heat shock protein) SUMOylation could sensitize cancer cells to Hsp90 and therefore to Hsp90 inhibitors (Mollapour et al., 2014). Multiple myeloma patients have been found with decreased response to the proteasome inhibitor, bortezomib, which was found to specifically related to RNF4 belonging to the novel RING family Ub ligases, an E3 specific for poly-sumoylated proteins, which was induced in MM patients (Driscoll, 2012). The findings on SUMOylation of p53 oncogene can be important in the future p53 based anticancer therapies. Most cancer cells can activate telomerases to elongate telomeres and accomplish unlimited replicative potential, however, some cancer cells have to use telomere homologous recombination (HR) to elongate telomeres termed alternative lengthening of telomeres (ALT); the inhibition of TRF1 or TRF2 (telomere-binding protein) SUMOylation prevented APB formation (a hallmark of ALT cancer cells as the recruitment of telomeres to promyelocytic leukemia (PML) bodies, ALT-

associated PML bodies, APBs) (Potts and Yu, 2007). These studies have made the role of SUMOylation with more understanding in the drug treatment development of cancer.

From this study, therefore, SUMOylation of FA proteins can serve as novel drug target therapies as SUMOylation has been required for fast FA turnover, this mechanism can be served as a rational drug design i.e. to prevent consistent talin FA disassembly.

7.3. 2 Potential Drug Targets for Anti-Platelets Therapy

Platelets are key mediators of thrombosis and inflammation (Bhatt and Topol, 2003). The pathway of SUMOylation is also implicated in the potential drug target development for antiplatelet therapies to prevent thrombosis. The integrin $\beta 3$ has been implicated in many physiological and pathological functions including platelets aggregation, thrombosis ($\alpha \text{IIb}\beta 3$ only expressed on platelets and megakaryocytes), implantation, placentation, angiogenesis, bone remodelling and tumour progression ($\alpha \text{v}\beta 3$) (Hodivala-Dilke et al., 1999).

Targeting FA SUMOylation may aid the development of prospective molecular drug targets in platelets with abnormal integrin signalling. Reduction in the talin- $\alpha \text{IIb}\beta 3$ binding affinity could reduce integrin $\alpha \text{IIb}\beta 3$ activation; this can be considered as a way for the protection from arterial thrombosis (Stefanini et al., 2014). Loss of talin-1 in mice has been shown to abrogate integrin activation (to all known major agonists), platelet aggregation and thrombosis formation *in vitro* and *in vivo* (Nieswandt et al., 2007).

In platelet-mediated haemostasis and thrombosis, targeting talin SUMOylation may provide a mechanism in preventing the activation of platelets, i.e. targeting the talin cleavage and its downstream signalling pathway in platelets with upregulated integrin signalling, but the talin function is intact in the healthy resting platelets. Talin cleavage may be crucial for the FA turnover in the platelets. Inhibition of SUMOylation in platelets may assist in reducing platelet spreading; therefore it plays its role in the prevention of platelet adhesion and aggregation. In thrombosis, platelet aggregation is highly upregulated. Here, SUMOylation may serve as a novel drug target for the antiplatelet therapy.

In conclusion, as many of the FA proteins have been identified as SUMOylation substrates and each of these proteins plays a critical role in the cell migration signalling pathway, this gives very useful information in the further investigation of the role of SUMOylation being involved in the cell migration and broadening the understanding of the function of SUMOylation in the regulation of not just one FA protein but a group of the other signalling/adaptor/FA proteins together.

Acknowledgement

I thank Dr. Phil Dash for his guidance and supervision in my full 4-year PhD period and his support in the experimental work: in the first advice and guidance of working together on one of the first identification of talin SUMOylation among the focal adhesions using cancer cell lines; in the support of experimental studies: the live-cell imaging study, IHC study, FA dynamics study, FA isolation study, IP study (method developments and modifications), WB analysis and proteomics study; and throughout the period leading to the final writing stage: with many detailed supervision on the arrangements of the discussion contents and critical thinking development.

I thank Professor Jon Gibbins and Dr. Diana Barker for their collaborations together in this project: in the first collaboration on one of the first identification of talin SUMOylation, initially started in the platelets; I thank for Diana's support in the IP experiments and in the trying of the IP methods with SUMO immunoprecipitation in endogenous cells, which has helped myself to develop the transferrable experimental skills and in understanding the mechanism of talin SUMOylation in the cancer cells, completely different compared with the platelets; and their hospitality in supporting me with the use of their laboratory equipment, the Ubc9 siRNA reagents and SUMOylation inhibitors 2-D08 and gossypetin.

I sincerely thank my parents for their full support in my PhD studies and also they have contributed very much in accompanying in my previous studies and without their support I would not have been where I am.

I thank my Danial fellowship friends and my church for their support and encouragement spiritually, psychologically and physically as always.

Bibliography

- AHLEMEYER, B. & KRIEGLSTEIN, J. 2003. Neuroprotective effects of Ginkgo biloba extract. *Cellular and Molecular Life Sciences CMLS*, 60, 1779-1792.
- AHLEMEYER, B., SELKE, D., SCHAPER, C., KLUMPP, S. & KRIEGLSTEIN, J. 2001. Ginkgolic acids induce neuronal death and activate protein phosphatase type-2C. *European Journal of Pharmacology*, 430, 1-7.
- ALARCON-VARGAS, D. & RONAI, Z. E. 2002. SUMO in Cancer - Wrestlers Wanted. *Cancer Biology & Therapy*, 1, 237-242.
- ALONSO, A., GREENLEE, M., MATTS, J., KLINE, J., DAVIS, K. J. & MILLER, R. K. 2015. Emerging roles of sumoylation in the regulation of actin, microtubules, intermediate filaments, and septins. *Cytoskeleton*, 72, 305-339.
- AMRUTHA, K., NANJAN, P., SHAJI, S. K., SUNILKUMAR, D., SUBHALAKSHMI, K., RAJAKRISHNA, L. & BANERJI, A. 2014. Discovery of lesser known flavones as inhibitors of NF- κ B signaling in MDA-MB-231 breast cancer cells—A SAR study. *Bioorganic & Medicinal Chemistry Letters*, 24, 4735-4742.
- ANTHIS, N. J. & CAMPBELL, I. D. 2011. The tail of integrin activation. *Trends in Biochemical Sciences*, 36, 191-198.
- ANTHIS, N. J., WEGENER, K. L., YE, F., KIM, C., GOULT, B. T., LOWE, E. D., VAKONAKIS, I., BATE, N., CRITCHLEY, D. R., GINSBERG, M. H. & CAMPBELL, I. D. 2009. The structure of an integrin/talin complex reveals the basis of inside-out signal transduction. *EMBO J*, 28, 3623-3632.
- ARTYM, V. V. & MATSUMOTO, K. 2010. Imaging Cells in Three-Dimensional Collagen Matrix. *Current Protocols in Cell Biology*. John Wiley & Sons, Inc.
- AZUMA, Y., ARNAOUTOV, A. & DASSO, M. 2003. SUMO-2/3 regulates topoisomerase II in mitosis. *The Journal of Cell Biology*, 163, 477-487.
- BAEK, S. H. 2006. A Novel Link Between SUMO Modification and Cancer Metastasis. *Cell Cycle*, 5, 1492-1495.
- BAKOLITSA, C., COHEN, D. M., BANKSTON, L. A., BOBKOV, A. A., CADWELL, G. W., JENNINGS, L., CRITCHLEY, D. R., CRAIG, S. W. & LIDDINGTON, R. C. 2004. Structural basis for vinculin activation at sites of cell adhesion. *Nature*, 430, 583-586.
- BATE, N., GINGRAS, A. R., BACHIR, A., HORWITZ, R., YE, F., PATEL, B., GOULT, B. T. & CRITCHLEY, D. R. 2012. Talin Contains A C-Terminal Calpain2 Cleavage Site Important In Focal Adhesion Dynamics. *PLoS ONE*, 7, e34461.
- BAYANI, J., ZIELENSKA, M., PANDITA, A., AL-ROMAIIH, K., KARASKOVA, J., HARRISON, K., BRIDGE, J. A., SORENSEN, P., THORNER, P. & SQUIRE, J. A. 2003. Spectral karyotyping identifies recurrent complex rearrangements of chromosomes 8, 17, and 20 in osteosarcomas. *Genes, Chromosomes and Cancer*, 36, 7-16.
- BAYS, J. L., PENG, X., TOLBERT, C. E., GUILLUY, C., ANGELL, A. E., PAN, Y., SUPERFINE, R., BURRIDGE, K. & DEMALI, K. A. 2014. Vinculin phosphorylation differentially regulates mechanotransduction at cell–cell and cell–matrix adhesions. *The Journal of Cell Biology*, 205, 251-263.
- BECK, M., SCHMIDT, A., MALMSTROEM, J., CLAASSEN, M., ORI, A., SZYMBORSKA, A., HERZOG, F., RINNER, O., ELLENBERG, J. & AEBERSOLD, R. 2011a. The quantitative proteome of a human cell line. *Molecular Systems Biology*, 7, 549-549.
- BECK, M., SCHMIDT, A., MALMSTROEM, J., CLAASSEN, M., ORI, A., SZYMBORSKA, A., HERZOG, F., RINNER, O., ELLENBERG, J. & AEBERSOLD, R. 2011b. The quantitative proteome of a human cell line. *Molecular Systems Biology*, 7.
- BECKER, J., BARYSCH, S. V., KARACA, S., DITTNER, C., HSIAO, H.-H., DIAZ, M. B., HERZIG, S., URLAUB, H. & MELCHIOR, F. 2013. Detecting endogenous SUMO targets in mammalian cells and tissues. *Nat Struct Mol Biol*, 20, 525-531.

- BÉKÉS, M., PRUDDEN, J., SRIKUMAR, T., RAUGHT, B., BODDY, M. N. & SALVESEN, G. S. 2011. The Dynamics and Mechanism of SUMO Chain Deconjugation by SUMO-specific Proteases. *Journal of Biological Chemistry*, 286, 10238-10247.
- BENDORI, R., SALOMON, D. & GEIGER, B. 1989. Identification of two distinct functional domains on vinculin involved in its association with focal contacts. *The Journal of Cell Biology*, 108, 2383-2393.
- BERGERT, M., CHANDRADOSS, S. D., DESAI, R. A. & PALUCH, E. 2012. Cell mechanics control rapid transitions between blebs and lamellipodia during migration. *Proceedings of the National Academy of Sciences*, 109, 14434-14439.
- BERGINK, S. & JENTSCH, S. 2009. Principles of ubiquitin and SUMO modifications in DNA repair. *Nature*, 458, 461-467.
- BERNIER-VILLAMOR, V., SAMPSON, D. A., MATUNIS, M. J. & LIMA, C. D. 2002. Structural Basis for E2-Mediated SUMO Conjugation Revealed by a Complex between Ubiquitin-Conjugating Enzyme Ubc9 and RanGAP1. *Cell*, 108, 345-356.
- BERTAGNOLLI, M. E., LOCKE, S. J., HENSLER, M. E., BRAY, P. F. & BECKERLE, M. C. 1993. Talin distribution and phosphorylation in thrombin-activated platelets. *Journal of Cell Science*, 106, 1189-1199.
- BHATT, A., KAVERINA, I., OTEY, C. & HUTTENLOCHER, A. 2002. Regulation of focal complex composition and disassembly by the calcium-dependent protease calpain. *Journal of Cell Science*, 115, 3415-3425.
- BHATT, D. L. & TOPOL, E. J. 2003. Scientific and therapeutic advances in antiplatelet therapy. *Nat Rev Drug Discov*, 2, 15-28.
- BILIA, A. R. 2002. Ginkgo biloba L. *Fitoterapia*, 73, 276-279.
- BLOOM, R. J., GEORGE, J. P., CELEDON, A., SUN, S. X. & WIRTZ, D. 2008. Mapping Local Matrix Remodeling Induced by a Migrating Tumor Cell Using Three-Dimensional Multiple-Particle Tracking. *Biophysical Journal*, 95, 4077-4088.
- BOGGIO, R., COLOMBO, R., HAY, R. T., DRAETTA, G. F. & CHIOCCA, S. 2004. A Mechanism for Inhibiting the SUMO Pathway. *Molecular Cell*, 16, 549-561.
- BOHREN, K. M., NADKARNI, V., SONG, J. H., GABBAY, K. H. & OWERBACH, D. 2004. A M55V Polymorphism in a Novel SUMO Gene (SUMO-4) Differentially Activates Heat Shock Transcription Factors and Is Associated with Susceptibility to Type I Diabetes Mellitus. *Journal of Biological Chemistry*, 279, 27233-27238.
- BOIS, P. R. J., O'HARA, B. P., NIETLISPACH, D., KIRKPATRICK, J. & IZARD, T. 2006. The Vinculin Binding Sites of Talin and α -Actinin Are Sufficient to Activate Vinculin. *Journal of Biological Chemistry*, 281, 7228-7236.
- BORGON, R. A., VONRHEIN, C., BRICOGNE, G., BOIS, P. R. J. & IZARD, T. 2004. Crystal Structure of Human Vinculin. *Structure*, 12, 1189-1197.
- BORM, B., REQUARDT, R. P., HERZOG, V. & KIRFEL, G. 2005. Membrane ruffles in cell migration: indicators of inefficient lamellipodia adhesion and compartments of actin filament reorganization. *Experimental Cell Research*, 302, 83-95.
- BOSSIS, G. & MELCHIOR, F. 2006. SUMO: regulating the regulator. *Cell Division*, 1, 13.
- BOUAOUINA, M., GOULT, B. T., HUET-CALDERWOOD, C., BATE, N., BRAHME, N. N., BARSUKOV, I. L., CRITCHLEY, D. R. & CALDERWOOD, D. A. 2012. A Conserved Lipid-binding Loop in the Kindlin FERM F1 Domain Is Required for Kindlin-mediated α IIb β 3 Integrin Coactivation. *Journal of Biological Chemistry*, 287, 6979-6990.
- BOUDREAU, N. & MYERS, C. 2003. Breast cancer-induced angiogenesis: multiple mechanisms and the role of the microenvironment. *Breast Cancer Res*, 5.
- BRAKEBUSCH, C. & FÄSSLER, R. 2003. The integrin-actin connection, an eternal love affair. *The EMBO Journal*, 22, 2324-2333.
- BROUSSARD, J. A., WEBB, D. J. & KAVERINA, I. 2008. Asymmetric focal adhesion disassembly in motile cells. *Current Opinion in Cell Biology*, 20, 85-90.

- BROWN, C. M., HEBERT, B., KOLIN, D. L., ZARENO, J., WHITMORE, L., HORWITZ, A. R. & WISEMAN, P. W. 2006. Probing the integrin-actin linkage using high-resolution protein velocity mapping. *Journal of Cell Science*, 119, 5204-5214.
- BRUDERER, R., TATHAM, M. H., PLECHANOVOVA, A., MATIC, I., GARG, A. K. & HAY, R. T. 2011. Purification and identification of endogenous polySUMO conjugates. *EMBO reports*, 12, 142-148.
- BUSCHMANN, T., LERNER, D., LEE, C.-G. & RONAI, Z. E. 2001. The Mdm-2 Amino Terminus Is Required for Mdm2 Binding and SUMO-1 Conjugation by the E2 SUMO-1 Conjugating Enzyme Ubc9. *Journal of Biological Chemistry*, 276, 40389-40395.
- BUTT, T. R., EDAVETAL, S. C., HALL, J. P. & MATTERN, M. R. 2005. SUMO fusion technology for difficult-to-express proteins. *Protein Expression and Purification*, 43, 1-9.
- CALDERWOOD, D. A., CAMPBELL, I. D. & CRITCHLEY, D. R. 2013. Talins and kindlins: partners in integrin-mediated adhesion. *Nat Rev Mol Cell Biol*, 14, 503-517.
- CALDERWOOD, D. A., YAN, B., DE PEREDA, J. M., ALVAREZ, B. G., FUJIOKA, Y., LIDDINGTON, R. C. & GINSBERG, M. H. 2002. The Phosphotyrosine Binding-like Domain of Talin Activates Integrins. *J Biol Chem*, 277, 21749-21758.
- CAMPEAU, E. & GOBEIL, S. 2011. RNA interference in mammals: behind the screen. *Briefings in Functional Genomics*, 10, 215-226.
- CANCE, W. G., HARRIS, J. E., IACOCCA, M. V., ROCHE, E., YANG, X., CHANG, J., SIMKINS, S. & XU, L. 2000. Immunohistochemical analyses of focal adhesion kinase expression in benign and malignant human breast and colon tissues: correlation with preinvasive and invasive phenotypes. *Clin Cancer Res*, 6, 2417-2423.
- CANCE, W. G., KURENOVA, E., MARLOWE, T. & GOLUBOVSKAYA, V. 2013. Disrupting the Scaffold to Improve Focal Adhesion Kinase-Targeted Cancer Therapeutics. *Sci. Signal.*, 6, pe10-.
- CARISEY, A. & BALLESTREM, C. 2011. Vinculin, an adapter protein in control of cell adhesion signalling. *European Journal of Cell Biology*, 90, 157-163.
- CARRAGHER, N. O., WESTHOFF, M. A., FINCHAM, V. J., SCHALLER, M. D. & FRAME, M. C. 2003. A Novel Role for FAK as a Protease-Targeting Adaptor Protein: Regulation by p42 ERK and Src. *Current Biology*, 13, 1442-1450.
- CASTILLO-LLUVA, S., TATHAM, M. H., JONES, R. C., JAFFRAY, E. G., EDMONDSON, R. D., HAY, R. T. & MALLIRI, A. 2010. SUMOylation of the GTPase Rac1 is required for optimal cell migration. *Nat Cell Biol*, 12, 1078-1085.
- CHAFFER, C. L. & WEINBERG, R. A. 2011. A Perspective on Cancer Cell Metastasis. *Science*, 331, 1559-1564.
- CHAN, K. T., BENNIN, D. A. & HUTTENLOCHER, A. 2010. Regulation of Adhesion Dynamics by Calpain-mediated Proteolysis of Focal Adhesion Kinase (FAK). *Journal of Biological Chemistry*, 285, 11418-11426.
- CHAN, K. T., CORTESIO, C. L. & HUTTENLOCHER, A. 2009. FAK alters invadopodia and focal adhesion composition and dynamics to regulate breast cancer invasion. *The Journal of Cell Biology*, 185, 357-370.
- CHANG, C.-C., NAIK, MANDAR T., HUANG, Y.-S., JENG, J.-C., LIAO, P.-H., KUO, H.-Y., HO, C.-C., HSIEH, Y.-L., LIN, C.-H., HUANG, N.-J., NAIK, NANDITA M., KUNG, CAMY C. H., LIN, S.-Y., CHEN, R.-H., CHANG, K.-S., HUANG, T.-H. & SHIH, H.-M. 2011. Structural and Functional Roles of Daxx SIM Phosphorylation in SUMO Paralog-Selective Binding and Apoptosis Modulation. *Molecular Cell*, 42, 62-74.
- CHAO-HSING, K. & HSIN-SU, Y. 1991. A study of the effects of phorbol 12-myristate-13-acetate on cell differentiation of pure human melanocytes in vitro. *Archives of dermatological research*, 283, 119-124.
- CHAO, W.-T., ASHCROFT, F., DAQUINAG, A. C., VADAKKAN, T., WEI, Z., ZHANG, P., DICKINSON, M. E. & KUNZ, J. 2010. Type I Phosphatidylinositol Phosphate Kinase Beta Regulates Focal

- Adhesion Disassembly by Promoting β 1 Integrin Endocytosis. *Molecular and Cellular Biology*, 30, 4463-4479.
- CHARRAS, G. A. P., E. 2008a. Blebs lead the way: how to migrate without lamellipodia. *Nature Reviews Molecular Cell Biology*, 9, 730-736
- CHARRAS, G. T. 2008b. A short history of blebbing. *Journal of Microscopy*, 231, 466-478.
- CHARRAS, G. T., HU, C.-K., COUGHLIN, M. & MITCHISON, T. J. 2006. Reassembly of contractile actin cortex in cell blebs. *The Journal of Cell Biology*, 175, 477-490.
- CHEN, H., COHEN, D. M., CHOUDHURY, D. M., KIOKA, N. & CRAIG, S. W. 2005. Spatial distribution and functional significance of activated vinculin in living cells. *The Journal of Cell Biology*, 169, 459-470.
- CHEN, J.-H., TSAI, C.-W., WANG, C.-P. & LIN, H.-H. 2013. Anti-atherosclerotic potential of gossypetin via inhibiting LDL oxidation and foam cell formation. *Toxicology and Applied Pharmacology*, 272, 313-324.
- COHEN, D. M., CHEN, H., JOHNSON, R. P., CHOUDHURY, B. & CRAIG, S. W. 2005. Two Distinct Head-Tail Interfaces Cooperate to Suppress Activation of Vinculin by Talin. *Journal of Biological Chemistry*, 280, 17109-17117.
- COLL, J., BEN-ZE'EV, A., EZZELL, R., FERNANDEZ, J. R., BARIBAULT, H., OSHIMA, R. & ADAMSON, E. 1995. Targeted disruption of vinculin genes in F9 and embryonic stem cells changes cell morphology, adhesion, and locomotion. *Proceedings of the National Academy of Sciences*, 92, 9161-9165.
- COLLAVIN, L., GOSTISSA, M., AVOLIO, F., SECCO, P., RONCHI, A., SANTORO, C. & DEL SAL, G. 2004. Modification of the erythroid transcription factor GATA-1 by SUMO-1. *Proceedings of the National Academy of Sciences of the United States of America*, 101, 8870-8875.
- COLÓ, G. P., HERNÁNDEZ-VARAS, P., LOCK, J., BARTOLOMÉ, R. A., ARELLANO-SÁNCHEZ, N., STRÖMBLAD, S. & TEIXIDÓ, J. 2012. Focal adhesion disassembly is regulated by a RIAM to MEK-1 pathway. *Journal of Cell Science*, 125: 5338-5352.
- CRITCHLEY, D. R. 2000. Focal adhesions – the cytoskeletal connection. *Current Opinion in Cell Biology*, 12, 133-139.
- CRITCHLEY, D. R. 2004. Cytoskeletal proteins talin and vinculin in integrin-mediated adhesion. *Biochemical Society Transactions*, 32, 831-836.
- CRITCHLEY, D. R. & GINGRAS, A. R. 2008. Talin at a glance. *Journal of Cell Science*, 121, 1345-1347.
- CUKIERMAN, E., PANKOV, R. & YAMADA, K. M. 2002. Cell interactions with three-dimensional matrices. *Current Opinion in Cell Biology*, 14, 633-640.
- DA SILVA-FERRADA, E., LOPITZ-OTSOA, F., LANG, V., Rodríguez, M. S. & MATTHIESEN, R. 2012. Strategies to Identify Recognition Signals and Targets of SUMOylation. *Biochemistry Research International*, 2012, 16.
- DA SILVA-FERRADA, E., XOLALPA, W., LANG, V., AILLET, F., MARTIN-RUIZ, I., DE LA CRUZ-HERRERA, C. F., LOPITZ-OTSOA, F., CARRACEDO, A., GOLDENBERG, S. J., RIVAS, C., ENGLAND, P. & RODRIGUEZ, M. S. 2013. Analysis of SUMOylated proteins using SUMO-traps. *Sci. Rep.*, 3, 1690.
- DANIELSEN, J. M. R., SYLVESTERSEN, K. B., BEKKER-JENSEN, S., SZKLARCZYK, D., POULSEN, J. W., HORN, H., JENSEN, L. J., MAILAND, N. & NIELSEN, M. L. 2011. Mass Spectrometric Analysis of Lysine Ubiquitylation Reveals Promiscuity at Site Level. *Molecular & Cellular Proteomics*, 10 (3).
- DAVID, G., NEPTUNE, M. A. & DEPINHO, R. A. 2002. SUMO-1 Modification of Histone Deacetylase 1 (HDAC1) Modulates Its Biological Activities. *Journal of Biological Chemistry*, 277, 23658-23663.
- DEAKIN, N. O. & TURNER, C. E. 2011. Distinct roles for paxillin and Hic-5 in regulating breast cancer cell morphology, invasion, and metastasis. *Molecular Biology of the Cell*, 22, 327-341.

- DEBRAND, E., EL JAI, Y., SPENCE, L., BATE, N., PRAEKELT, U., PRITCHARD, C. A., MONKLEY, S. J. & CRITCHLEY, D. R. 2009. Talin 2 is a large and complex gene encoding multiple transcripts and protein isoforms. *FEBS Journal*, 276, 1610-1628.
- DEFEUDIS, F. V. & DRIEU, K. 2004. "Stress-alleviating" and "vigilance-enhancing" actions of Ginkgo biloba extract (EGb 761). *Drug Development Research*, 62, 1-25.
- DEFEUDIS, F. V., PAPADOPOULOS, V. & DRIEU, K. 2003. Ginkgo biloba extracts and cancer: a research area in its infancy. *Fundamental & Clinical Pharmacology*, 17, 405-417.
- DELON, I. & BROWN, N. H. 2007. Integrins and the actin cytoskeleton. *Current Opinion in Cell Biology*, 19, 43-50.
- DEMALI, K. A. & BURRIDGE, K. 2003. Coupling membrane protrusion and cell adhesion. *Journal of Cell Science*, 116, 2389-2397.
- DENISON, C., RUDNER, A. D., GERBER, S. A., BAKALARSKI, C. E., MOAZED, D. & GYGI, S. P. 2005. A Proteomic Strategy for Gaining Insights into Protein Sumoylation in Yeast. *Molecular & Cellular Proteomics*, 4, 246-254.
- DESGROSELLIER, J. S. & CHERESH, D. A. 2010. Integrins in cancer: biological implications and therapeutic opportunities. *Nat Rev Cancer*, 10, 9-22.
- DESTERRO, J. M. P., RODRIGUEZ, M. S. & HAY, R. T. 1998. SUMO-1 Modification of I κ B α Inhibits NF- κ B Activation. *Molecular Cell*, 2, 233-239.
- DI BACCO, A. & GILL, G. 2006. SUMO-Specific Proteases and the Cell Cycle. *Cell Cycle*, 5, 2310-2313.
- DI BACCO, A., OUYANG, J., LEE, H.-Y., CATIC, A., PLOEGH, H. & GILL, G. 2006. The SUMO-Specific Protease SENP5 Is Required for Cell Division. *Molecular and Cellular Biology*, 26, 4489-4498.
- DING, X., SUN, J., WANG, L., LI, G., SHEN, Y., ZHOU, X. & CHEN, W. 2008. Overexpression of SENP5 in oral squamous cell carcinoma and its association with differentiation. *Oncol Rep*, 20, 1041-5.
- DISCHER, D. E., JANMEY, P. & WANG, Y.-L. 2005. Tissue Cells Feel and Respond to the Stiffness of Their Substrate. *Science*, 310, 1139-1143.
- DOMADIA, P. N., LI, Y.-F., BHUNIA, A., MOHANRAM, H., TAN, S.-M. & BHATTACHARJYA, S. 2010. Functional and structural characterization of the talin FOF1 domain. *Biochemical and Biophysical Research Communications*, 391, 159-165.
- DONG, M., PANG, X., XU, Y., WEN, F. & ZHANG, Y. 2013. Ubiquitin-Conjugating Enzyme 9 Promotes Epithelial Ovarian Cancer Cell Proliferation in Vitro. *International Journal of Molecular Sciences*, 14, 11061-11071.
- DRAG, M. & SALVESEN, G. S. 2008. DeSUMOylating enzymes—SENPs. *IUBMB Life*, 60, 734-742.
- DRISCOLL, J. J. 2012. *The SUMOylation Pathway as a Potential Therapeutic Target in Multiple Myeloma*, INTECH Open Access Publisher.
- DRISCOLL, J. J., PELLURU, D., LEFKIMMIATIS, K., FULCINITI, M., PRABHALA, R. H., GREIPP, P. R., BARLOGIE, B., TAI, Y.-T., ANDERSON, K. C., SHAUGHNESSY, J. D., ANNUNZIATA, C. M. & MUNSHI, N. C. 2010. The sumoylation pathway is dysregulated in multiple myeloma and is associated with adverse patient outcome. *Blood*, 115, 2827-2834.
- DUAN, X., TRENT, J. O. & YE, H. 2009. Targeting the SUMO E2 Conjugating Enzyme Ubc9 Interaction for Anti-Cancer Drug Design. *Anti-Cancer Agents in Medicinal Chemistry- Anti-Cancer Agents*, 9, 51-54.
- ELLIOTT, P. R., GOULT, B. T., KOPP, P. M., BATE, N., GROSSMANN, J. G., ROBERTS, G. C. K., CRITCHLEY, D. R. & BARSUKOV, I. L. 2010. The Structure of the Talin Head Reveals a Novel Extended Conformation of the FERM Domain. *Structure*, 18, 1289-1299.
- ELLIS, S. J., GOULT, B. T., FAIRCHILD, M. J., HARRIS, N. J., LONG, J., LOBO, P., CZERNIECKI, S., VAN PETEGEM, F., SCHOCK, F., PEIFER, M. & TANENTZAPF, G. 2013. Talin autoinhibition is required for morphogenesis. *Curr Biol*, 23, 1825-33.
- ENTSCHLADEN, F., DRELL IV, T. L., LANG, K., MASUR, K., PALM, D., BASTIAN, P., NIGGEMANN, B. & ZAENKER, K. S. 2005. Analysis methods of human cell migration. *Experimental Cell Research*, 307, 418-426.

- ESCOBAR-CABRERA, E., OKON, M., LAU, D. K. W., DART, C. F., BONVIN, A. M. J. J. & MCINTOSH, L. P. 2011. Characterizing the N- and C-terminal Small Ubiquitin-like Modifier (SUMO)-interacting Motifs of the Scaffold Protein DAXX. *Journal of Biological Chemistry*, 286, 19816-19829.
- FERNÁNDEZ, J. L. R., GEIGER, B., SALOMON, D. & BEN - ZE'EV, A. 1992. Overexpression of vinculin suppresses cell motility in BALB/c 3T3 cells. *Cell motility and the cytoskeleton*, 22, 127-134.
- FRACKLER, O. T. A. G., R. J. 2008. Cell motility through plasma membrane blebbing. *Cell Biol.*, 181, 879 - 884.
- FRALEY, S. I., FENG, Y., KRISHNAMURTHY, R., KIM, D.-H., CELEDON, A., LONGMORE, G. D. & WIRTZ, D. 2010. A distinctive role for focal adhesion proteins in three-dimensional cell motility. *Nat Cell Biol*, 12, 598-604.
- FRALEY, S. I., FENG, Y., WIRTZ, D. & LONGMORE, G. D. 2011. Reply: reducing background fluorescence reveals adhesions in 3D matrices. *Nat Cell Biol*, 13, 5-7.
- FRAME, M. C., FINCHAM, V. J., CARRAGHER, N. O. & WYKE, J. A. 2002. v-Src's hold over actin and cell adhesions. *Nature Reviews Molecular Cell Biology*, 3, 233-245.
- FRANCIS, A. R., SHETTY, T. K. & BHATTACHARYA, R. K. 1989. Modulating effect of plant flavonoids on the mutagenicity of N-methyl-N' -nitro-N-nitrosoguanidine. *Carcinogenesis*, 10, 1953-1955.
- FRANCO, S. J. & HUTTENLOCHER, A. 2005. Regulating cell migration: calpains make the cut. *Journal of Cell Science*, 118, 3829-3838.
- FRANCO, S. J., RODGERS, M. A., PERRIN, B. J., HAN, J., BENNIN, D. A., CRITCHLEY, D. R. & HUTTENLOCHER, A. 2004. Calpain-mediated proteolysis of talin regulates adhesion dynamics. *Nat Cell Biol*, 6, 977-983.
- FRIEDL, P. 2004. Prespecification and plasticity: shifting mechanisms of cell migration. *Current Opinion in Cell Biology*, 16, 14-23.
- FRIEDL, P., HEGERFELDT, Y. & TUSCH, M. 2004. Collective cell migration in morphogenesis and cancer. *International Journal of Developmental Biology*, 48, 441-449.
- FRIEDL, P. A. A., S. 2011. Cancer invasion and the microenvironment: plasticity and reciprocity. *Cell*, 147, 992-1009.
- FRIEDL, P. A. W., K. 2010. Plasticity of cell migration: a multiscale tuning model. *The Journal of Cell Biology*, 188, 11-19.
- FRIEDLAND, J. C., LEE, M. H. & BOETTIGER, D. 2009. Mechanically activated integrin switch controls alpha5beta1 function. *Science (New York, N.Y.)*, 323, 642-644.
- FRISAN, T., COPPOTELLI, G., DRYSELIUS, R. & MASUCCI, M. G. 2012. Ubiquitin C-terminal hydrolase-L1 interacts with adhesion complexes and promotes cell migration, survival, and anchorage independent growth. *The FASEB Journal*, 26, 5060-5070.
- FUKUDA, I., ITO, A., HIRAI, G., NISHIMURA, S., KAWASAKI, H., SAITOH, H., KIMURA, K.-I., SODEOKA, M. & YOSHIDA, M. 2009a. Ginkgolic Acid Inhibits Protein SUMOylation by Blocking Formation of the E1-SUMO Intermediate. *Chemistry & Biology*, 16, 133-140.
- FUKUDA, I., ITO, A., URAMOTO, M., SAITOH, H., KAWASAKI, H., OSADA, H. & YOSHIDA, M. 2009b. Kerriamycin B inhibits protein SUMOylation. *J Antibiot*, 62, 221-224.
- GALBRAITH, C. G., YAMADA, K. M. & GALBRAITH, J. A. 2007. Polymerizing Actin Fibers Position Integrins Primed to Probe for Adhesion Sites. *Science*, 315, 992-995.
- GALISSON, F., MAHROUCHE, L., COURCELLES, M., BONNEIL, E., MELOCHE, S., CHELBI-ALIX, M. K. & THIBAUT, P. 2011. A Novel Proteomics Approach to Identify SUMOylated Proteins and Their Modification Sites in Human Cells. *Molecular & Cellular Proteomics*, 10 (2).
- GANESAN, A. K., KHO, Y., KIM, S. C., CHEN, Y., ZHAO, Y. & WHITE, M. A. 2007. Broad spectrum identification of SUMO substrates in melanoma cells. *PROTEOMICS*, 7, 2216-2221.
- GARCÍA-ALVAREZ, B., DE PEREDA, J. M., CALDERWOOD, D. A., ULMER, T. S., CRITCHLEY, D., CAMPBELL, I. D., GINSBERG, M. H. & LIDDINGTON, R. C. 2003. Structural Determinants of Integrin Recognition by Talin. *Molecular Cell*, 11, 49-58.
- GARCÍA, A., PRABHAKAR, S., HUGHAN, S., ANDERSON, T. W., BROCK, C. J., PEARCE, A. C., DWEK, R. A., WATSON, S. P., HEBESTREIT, H. F. & ZITZMANN, N. 2004. Differential proteome analysis

- of TRAP-activated platelets: involvement of DOK-2 and phosphorylation of RGS proteins. *Blood*, 103, 2088-2095.
- GAREAU, J. R. & LIMA, C. D. 2010. The SUMO pathway: emerging mechanisms that shape specificity, conjugation and recognition. *Nat Rev Mol Cell Biol*, 11, 861-871.
- GEIGER, B., SPATZ, J. P. & BERSHADSKY, A. D. 2009. Environmental sensing through focal adhesions. *Nat Rev Mol Cell Biol*, 10, 21-33.
- GEIGER, B. A. Y., K.M. 2011. Molecular architecture and function of matrix adhesions. *Cold Spring Harb Perspect Biol* 3, 1-22.
- GEISS-FRIEDLANDER, R. & MELCHIOR, F. 2007. Concepts in sumoylation: a decade on. *Nature reviews Molecular cell biology*, 8, 947-956.
- GERALDO, S., SIMON, A., ELKHATIB, N., LOUVARD, D., FETLER, L. & VIGNJEVIC, D. M. 2012. Do cancer cells have distinct adhesions in 3D collagen matrices and in vivo? *European Journal of Cell Biology*, 91, 930-937.
- GIANNONE, G., DUBIN-THALER, B. J., ROSSIER, O., CAI, Y., CHAGA, O., JIANG, G., BEAVER, W., DÖBEREINER, H.-G., FREUND, Y., BORISY, G. & SHEETZ, M. P. 2007. Lamellipodial Actin Mechanically Links Myosin Activity with Adhesion-Site Formation. *Cell*, 128, 561-575.
- GILL, G. 2004. SUMO and ubiquitin in the nucleus: different functions, similar mechanisms? *Genes & development*, 18, 2046-2059.
- GILL, G. 2005. Something about SUMO inhibits transcription. *Current Opinion in Genetics & Development*, 15, 536-541.
- GINGRAS, A. R., BATE, N., GOULT, B. T., HAZELWOOD, L., CANESTRELLI, I., GROSSMANN, J. G., LIU, H., PUTZ, N. S. M., ROBERTS, G. C. K., VOLKMANN, N., HANEIN, D., L., B. I. & R., C. D. 2008. The structure of the C-terminal actin-binding domain of talin. *EMBO J*, 27, 458-469.
- GINGRAS, A. R., VOGEL, K.-P., STEINHOFF, H.-J., ZIEGLER, W. H., PATEL, B., EMSLEY, J., CRITCHLEY, D. R., ROBERTS, G. C. K. & BARSUKOV, I. L. 2006. Structural and Dynamic Characterization of a Vinculin Binding Site in the Talin Rod. *Biochemistry*, 45, 1805-1817.
- GINGRAS, A. R., ZIEGLER, W. H., FRANK, R., BARSUKOV, I. L., ROBERTS, G. C. K., CRITCHLEY, D. R. & EMSLEY, J. 2005. Mapping and Consensus Sequence Identification for Multiple Vinculin Binding Sites within the Talin Rod. *Journal of Biological Chemistry*, 280, 37217-37224.
- GLADING, A., LAUFFENBURGER, D. A. & WELLS, A. 2002. Cutting to the chase: calpain proteases in cell motility. *Trends in Cell Biology*, 12, 46-54.
- GOKSOY, E., MA, Y. Q., WANG, X., KONG, X., PERERA, D., PLOW, E. F. & QIN, J. 2008. Structural basis for the autoinhibition of talin in regulating integrin activation. *Mol Cell*, 31, 124-33.
- GOLDMANN, W. H. & INGBER, D. E. 2002. Intact Vinculin Protein Is Required for Control of Cell Shape, Cell Mechanics, and rac-Dependent Lamellipodia Formation. *Biochemical and Biophysical Research Communications*, 290, 749-755.
- GOLEBIEWSKI, F., MATIC, I., TATHAM, M. H., COLE, C., YIN, Y., NAKAMURA, A., COX, J., BARTON, G. J., MANN, M. & HAY, R. T. 2009. System-Wide Changes to SUMO Modifications in Response to Heat Shock. *Science Signaling*, 2, 24.
- GOLUBOVSKAYA, V., KAUR, A. & CANCE, W. 2007. Cloning and characterization of the promoter region of human focal adhesion kinase gene: nuclear factor kappa B and p53 binding sites. *Biochimica et Biophysica Acta (BBA) - Gene Structure and Expression*, 1678, 111-125.
- GOLUBOVSKAYA, V. M., FINCH, R., ZHENG, M., KURENOVA, E. V. & CANCE, W. G. 2008. The 7-amino-acid site in the proline-rich region of the N-terminal domain of p53 is involved in the interaction with FAK and is critical for p53 functioning. *Biochem J*, 411, 151-160.
- GOSTISSA, M., HENGSTERMANN, A., FOGAL, V., SANDY, P., SCHWARZ, S. E., SCHEFFNER, M. & DEL SAL, G. 1999. Activation of p53 by conjugation to the ubiquitin-like protein SUMO-1. *EMBO J*, 18, 6462-6471.
- GOULT, B. T., BOUAQUINA, M., ELLIOTT, P. R., BATE, N., PATEL, B., GINGRAS, A. R., GROSSMANN, J. G., ROBERTS, G. C. K., CALDERWOOD, D. A., CRITCHLEY, D. R. & BARSUKOV, I. L. 2010.

- Structure of a double ubiquitin - like domain in the talin head: a role in integrin activation. *The EMBO Journal*, 29, 1069-1080.
- GOULT, B. T., XU, X.-P., GINGRAS, A. R., SWIFT, M., PATEL, B., BATE, N., KOPP, P. M., BARSUKOV, I. L., CRITCHLEY, D. R., VOLKMANN, N. & HANEIN, D. 2013a. Structural studies on full-length talin1 reveal a compact auto-inhibited dimer: Implications for talin activation. *Journal of Structural Biology*, 184, 21-32.
- GOULT, B. T., ZACHARCHENKO, T., BATE, N., TSANG, R., HEY, F., GINGRAS, A. R., ELLIOTT, P. R., ROBERTS, G. C. K., BALLESTREM, C., CRITCHLEY, D. R. & BARSUKOV, I. L. 2013b. RIAM and Vinculin Binding to Talin Are Mutually Exclusive and Regulate Adhesion Assembly and Turnover. *Journal of Biological Chemistry*, 288, 8238-8249.
- GRASHOFF, C., HOFFMAN, B. D., BRENNER, M. D., ZHOU, R., PARSONS, M., YANG, M. T., MCLEAN, M. A., SLIGAR, S. G., CHEN, C. S., HA, T. & SCHWARTZ, M. A. 2010. Measuring mechanical tension across vinculin reveals regulation of focal adhesion dynamics. *Nature*, 466, 263-266.
- GRECO, N. J. 1997. Functional Expression of a P2T ADP Receptor in Xenopus Oocytes Injected With Megakaryocyte (CMK 11-5) RNA. *Arteriosclerosis, Thrombosis, and Vascular Biology*, 17, 769-777.
- GRÉGOIRE, S., TREMBLAY, A. M., XIAO, L., YANG, Q., MA, K., NIE, J., MAO, Z., WU, Z., GIGUÈRE, V. & YANG, X.-J. 2006. Control of MEF2 Transcriptional Activity by Coordinated Phosphorylation and Sumoylation. *Journal of Biological Chemistry*, 281, 4423-4433.
- GRUNERT, S., JECHLINGER, M. & BEUG, H. 2003. Diverse cellular and molecular mechanisms contribute to epithelial plasticity and metastasis. *Nat Rev Mol Cell Biol*, 4, 657-665.
- GU, Z., LIU, F., TONKOVA, E. A., LEE, S. Y., TSCHUMPERLIN, D. J. & BRENNER, M. B. 2014. Soft matrix is a natural stimulator for cellular invasiveness. *Molecular Biology of the Cell*, 25, 457-469.
- GUNAWAN, M., VENKATESAN, N., LOH, J. T., WONG, J. F., BERGER, H., NEO, W. H., LI, L. Y. J., LA WIN, M. K., YAU, Y. H., GUO, T., SEE, P. C. E., YAMAZAKI, S., CHIN, K. C., GINGRAS, A. R., SHOCHAT, S. G., NG, L. G., SZE, S. K., GINHOUX, F. & SU, I. H. 2015. The methyltransferase Ezh2 controls cell adhesion and migration through direct methylation of the extranuclear regulatory protein talin. *Nat Immunol*, 16, 505-516.
- GUPTON, S. L. & WATERMAN-STORER, C. M. 2006. Spatiotemporal Feedback between Actomyosin and Focal-Adhesion Systems Optimizes Rapid Cell Migration. *Cell*, 125, 1361-1374.
- HÁKONARDÓTTIR, G. K., LÓPEZ-CEBALLOS, P., HERRERA-REYES, A. D., DAS, R., COOMBS, D. & TANENTZAPF, G. 2015. In vivo quantitative analysis of Talin turnover in response to force. *Molecular Biology of the Cell*, 26, 4149-4162.
- HANAHAAN, D. & WEINBERG, ROBERT A. 2011. Hallmarks of Cancer: The Next Generation. *Cell*, 144, 646-674.
- HANG, J. & DASSO, M. 2002. Association of the Human SUMO-1 Protease SENP2 with the Nuclear Pore. *Journal of Biological Chemistry*, 277, 19961-19966.
- HARUNAGA, J. S. & YAMADA, K. M. 2011. Cell-matrix adhesions in 3D. *Matrix Biology*, 30, 363-368.
- HAVAKI, S., KOULOUKOUSSA, M., AMAWI, K., DROSOS, Y., ARVANITIS, L., GOUTAS, N., VLACHODIMITROPOULOS, D., VASSILAROS, S., KATSANTONI, E. & VOLOUDAKIS-BALTATZIS, I. 2007. Altered expression pattern of integrin $\alpha\beta 3$ correlates with actin cytoskeleton in primary cultures of human breast cancer. *Cancer Cell International*, 7.
- HAY, R. T. 2005. SUMO: A History of Modification. *Molecular Cell*, 18, 1-12.
- HAY, R. T. 2007. SUMO-specific proteases: a twist in the tail. *Trends in Cell Biology*, 17, 370-376.
- HEGERFELDT, Y., TUSCH, M., BRÖCKER, E.-B. & FRIEDL, P. 2002. Collective Cell Movement in Primary Melanoma Explants. *Plasticity of Cell-Cell Interaction, $\beta 1$ -Integrin Function, and Migration Strategies*, 62, 2125-2130.
- HENDRIKS, I. A., D'SOUZA, R. C., CHANG, J.-G., MANN, M. & VERTEGAAL, A. C. O. 2015b. System-wide identification of wild-type SUMO-2 conjugation sites. *Nature Communications*, 6, 7289.

- HENDRIKS, I. A., D'SOUZA, R. C. J., YANG, B., VERLAAN-DE VRIES, M., MANN, M. & VERTEGAAL, A. C. O. 2014. Uncovering Global SUMOylation Signaling Networks in a Site-Specific Manner. *Nature structural & molecular biology*, 21, 927-936.
- HENDRIKS, IVO A., TREFFERS, LOUISE W., VERLAAN-DE VRIES, M., OLSEN, JESPER V. & VERTEGAAL, ALFRED C. O. 2015c. SUMO-2 Orchestrates Chromatin Modifiers in Response to DNA Damage. *Cell Reports*, 10, 1778-1791.
- HENDRIKS, I. A. & VERTEGAAL, A. C. O. 2016. A comprehensive compilation of SUMO proteomics. *Nat Rev Mol Cell Biol*, 17, 581-595.
- HENLEY, J. M., CRAIG, T. J. & WILKINSON, K. A. 2014. Neuronal SUMOylation: Mechanisms, Physiology, and Roles in Neuronal Dysfunction. *Physiological Reviews*, 94, 1249-1285.
- HICKEY, C. M., WILSON, N. R. & HOCHSTRASSER, M. 2012. Function and Regulation of SUMO Proteases. *Nature reviews. Molecular cell biology*, 13, 755-766.
- HIETAKANGAS, V., ANCKAR, J., BLOMSTER, H. A., FUJIMOTO, M., PALVIMO, J. J., NAKAI, A. & SISTONEN, L. 2006. PDSM, a motif for phosphorylation-dependent SUMO modification. *Proceedings of the National Academy of Sciences of the United States of America*, 103, 45-50.
- HILGARTH, R. S., MURPHY, L. A., SKAGGS, H. S., WILKERSON, D. C., XING, H. & SARGE, K. D. 2004. Regulation and Function of SUMO Modification. *Journal of Biological Chemistry*, 279, 53899-53902.
- HIROHAMA, M., KUMAR, A., FUKUDA, I., MATSUOKA, S., IGARASHI, Y., SAITOH, H., TAKAGI, M., SHINYA, K., HONDA, K., KONDOH, Y., SAITO, T., NAKAO, Y., OSADA, H., ZHANG, K. Y. J., YOSHIDA, M. & ITO, A. 2013. Spectomycin B1 as a Novel SUMOylation Inhibitor That Directly Binds to SUMO E2. *ACS Chemical Biology*.
- HITCHCOCK, I. S., FOX, N. E., PRÉVOST, N., SEAR, K., SHATTIL, S. J. & KAUSHANSKY, K. 2008. Roles of focal adhesion kinase (FAK) in megakaryopoiesis and platelet function: studies using a megakaryocyte lineage-specific FAK knockout. *Blood*, 111, 596-604.
- HOCHSTRASSER, M. 2009. Origin and function of ubiquitin-like proteins. *Nature*, 458, 422-429.
- HODIVALA-DILKE, K. M., MCHUGH, K. P., TSAKIRIS, D. A., RAYBURN, H., CROWLEY, D., ULLMAN, C., XE, MOLLIE, ROSS, F. P., COLLIER, B. S., TEITELBAUM, S. & HYNES, R. O. 1999. β 3-integrin-deficient mice are a model for Glanzmann thrombasthenia showing placental defects and reduced survival. *The Journal of Clinical Investigation*, 103, 229-238.
- HOEGE, C., PFANDER, B., MOLDOVAN, G.-L., PYROWOLAKIS, G. & JENTSCH, S. 2002. RAD6-dependent DNA repair is linked to modification of PCNA by ubiquitin and SUMO. *Nature*, 419, 135-141.
- HOELLEIN, A., FALLAHI, M., SCHOEFFMANN, S., STEIDLE, S., SCHAUB, F. X., RUDELIUS, M., LAITINEN, I., NILSSON, L., GOGA, A., PESCHEL, C., NILSSON, J. A., CLEVELAND, J. L. & KELLER, U. 2014. Myc-induced SUMOylation is a therapeutic vulnerability for B-cell lymphoma. *Blood*, 124, 2081-2090.
- HOFMANN, W. A., ARDUINI, A., NICOL, S. M., CAMACHO, C. J., LESSARD, J. L., FULLER-PACE, F. V. & DE LANEROLLE, P. 2009. SUMOylation of nuclear actin. *The Journal of Cell Biology*, 186, 193-200.
- HSIA, D. A., MITRA, S. K., HAUCK, C. R., STREBLOW, D. N., NELSON, J. A., ILIC, D., HUANG, S., LI, E., NEMEROW, G. R., LENG, J., SPENCER, K. S. R., CHERESH, D. A. & SCHLAEPFER, D. D. 2003. Differential regulation of cell motility and invasion by FAK. *The Journal of Cell Biology*, 160, 753-767.
- HU, K., JI, L., APPEGATE, K. T., DANUSER, G. & WATERMAN-STORER, C. M. 2007. Differential Transmission of Actin Motion Within Focal Adhesions. *Science*, 315, 111-115.
- HUANG, C., RAJFUR, Z., YOUSEFI, N., CHEN, Z., JACOBSON, K. & GINSBERG, M. H. 2009. Talin phosphorylation by Cdk5 regulates Smurf1-mediated talin head ubiquitylation and cell migration. *Nat Cell Biol*, 11, 624-630.

- HUMPHRIES, J. D., WANG, P., STREULI, C., GEIGER, B., HUMPHRIES, M. J. & BALLESTREM, C. 2007. Vinculin controls focal adhesion formation by direct interactions with talin and actin. *The Journal of Cell Biology*, 179, 1043-1057.
- HUNTER, T. 2007. The age of crosstalk: phosphorylation, ubiquitination, and beyond. *Molecular cell*, 28, 730-738.
- HUTTENLOCHER, A. A. H., A.R. 2011. Integrins in cell migration. *Cold Spring Harb Perspect Biol*, 3, 1-17.
- HUVENEERS, S. & DANEN, E. H. J. 2009. Adhesion signaling – crosstalk between integrins, Src and Rho. *Journal of Cell Science*, 122, 1059-1069.
- IMPENS, F., RADOSHEVICH, L., COSSART, P. & RIBET, D. 2014. Mapping of SUMO sites and analysis of SUMOylation changes induced by external stimuli. *Proceedings of the National Academy of Sciences*, 111, 12432-12437.
- IZARD, T. & VONRHEIN, C. 2004. Structural Basis for Amplifying Vinculin Activation by Talin. *Journal of Biological Chemistry*, 279, 27667-27678.
- JACKSON, S. P. 2007. The growing complexity of platelet aggregation. *Blood*, 109, 5087-5095.
- JANSSEN, M. E. W., KIM, E., LIU, H., FUJIMOTO, L. M., BOBKOV, A., VOLKMANN, N. & HANEIN, D. 2006. Three-Dimensional Structure of Vinculin Bound to Actin Filaments. *Molecular Cell*, 21, 271-281.
- JEONG, H. J., RYU, Y. B., PARK, S.-J., KIM, J. H., KWON, H.-J., KIM, J. H., PARK, K. H., RHO, M.-C. & LEE, W. S. 2009. Neuraminidase inhibitory activities of flavonols isolated from *Rhodiola rosea* roots and their in vitro anti-influenza viral activities. *Bioorganic & Medicinal Chemistry*, 17, 6816-6823.
- JIANG, Y. & FLEET, J. C. 2012. Effect of phorbol 12-myristate 13-acetate activated signaling pathways on 1α , 25 dihydroxyvitamin D(3) regulated human 25-hydroxyvitamin D(3) 24-hydroxylase gene expression in differentiated Caco-2 cells. *Journal of cellular biochemistry*, 113, 1599-1607.
- JOHNSON, E. S. 2004. Protein modification by SUMO. *Annu. Rev. Biochem.*, 73, 355-382.
- JOHNSON, R. P. & CRAIG, S. W. 1994. An intramolecular association between the head and tail domains of vinculin modulates talin binding. *Journal of Biological Chemistry*, 269, 12611-9.
- KADARÉ, G., TOUTANT, M., FORMSTECHE, E., CORVOL, J.-C., CARNAUD, M., BOUTTERIN, M.-C. & GIRAULT, J.-A. 2003. PIAS1-mediated Sumoylation of Focal Adhesion Kinase Activates Its Autophosphorylation. *Journal of Biological Chemistry*, 278, 47434-47440.
- KALLI, A. C., WEGENER, K. L., GOULT, B. T., ANTHIS, N. J., CAMPBELL, I. D. & SANSOM, M. S. P. 2010. The Structure of the Talin/Integrin Complex at a Lipid Bilayer: An NMR and MD Simulation Study. *Structure*, 18, 1280-1288.
- KALLURI, R. & WEINBERG, R. A. 2009. The basics of epithelial-mesenchymal transition. *The Journal of Clinical Investigation*, 119, 1420-1428.
- KANAI, K., REZA, H. M., KAMITANI, A., HAMAZAKI, Y., HAN, S.-I., YASUDA, K. & KATAOKA, K. 2010. SUMOylation negatively regulates transcriptional and oncogenic activities of MafA. *Genes to Cells*, 15, 971-982.
- KANCHANAWONG, P., SHTENGEL, G., PASAPERA, A. M., RAMKO, E. B., DAVIDSON, M. W., HESS, H. F. & WATERMAN, C. M. 2010. Nanoscale architecture of integrin-based cell adhesions. *Nature*, 468, 580-584.
- KASHIWAGI, H., SHIRAGA, M., HONDA, S., KOSUGI, S., KAMAE, T., KATO, H., KURATA, Y. & TOMIYAMA, Y. 2004. Activation of integrin $\alpha\text{IIb}\beta\text{3}$ in the glycoprotein Ib-high population of a megakaryocytic cell line, CMK, by inside-out signaling. *Journal of Thrombosis and Haemostasis*, 2, 177-186.
- KERSCHER, O. 2007. SUMO junction—what's your function? New insights through SUMO-interacting motifs. *EMBO Reports*, 8, 550-555.
- KESSLER, J. D., KAHLE, K. T., SUN, T., MEERBREY, K. L., SCHLABACH, M. R., SCHMITT, E. M., SKINNER, S. O., XU, Q., LI, M. Z., HARTMAN, Z. C., RAO, M., YU, P., DOMINGUEZ-VIDANA, R., LIANG, A.

- C., SOLIMINI, N. L., BERNARDI, R. J., YU, B., HSU, T., GOLDING, I., LUO, J., OSBORNE, C. K., CREIGHTON, C. J., HILSENBECK, S. G., SCHIFF, R., SHAW, C. A., ELLEDGE, S. J. & WESTBROOK, T. F. 2012. A SUMOylation-Dependent Transcriptional Subprogram Is Required for Myc-Driven Tumorigenesis. *Science*, 335, 348-353.
- KHAN, F. A., PANDUPUSPITASARI, N. S., HUANG, C.-J., HAO, X. & ZHANG, S. 2016. SUMOylation: A link to future therapeutics. *Current issues in molecular biology*, 18, 49-56.
- KIEMA, T., LAD, Y., JIANG, P., OXLEY, C. L., BALDASSARRE, M., WEGENER, K. L., CAMPBELL, I. D., YLÄNNE, J. & CALDERWOOD, D. A. 2006. The Molecular Basis of Filamin Binding to Integrins and Competition with Talin. *Molecular Cell*, 21, 337-347.
- KIM, C., YE, F. & GINSBERG, M. H. 2011. Regulation of Integrin Activation. In: SCHEKMAN, R., GOLDSTEIN, L. & LEHMANN, R. (eds.) *Annual Review of Cell and Developmental Biology*, Vol 27. Palo Alto: Annual Reviews.
- KIM, D.-H., KHATAU, S. B., FENG, Y., WALCOTT, S., SUN, S. X., LONGMORE, G. D. & WIRTZ, D. 2012. Actin cap associated focal adhesions and their distinct role in cellular mechanosensing. *Scientific Reports*, 2, 555.
- KIM, H. J., KIM, Y. M., LIM, S., NAM, Y. K., JEONG, J., KIM, H. J. & LEE, K. J. 2008. Ubiquitin C-terminal hydrolase-L1 is a key regulator of tumor cell invasion and metastasis. *Oncogene*, 28, 117-127.
- KIM, J. B. 2005. Three-dimensional tissue culture models in cancer biology. *Seminars in Cancer Biology*, 15, 365-377.
- KIM, Y. S., KEYSER, S. G. L. & SCHNEEKLOTH JR, J. S. 2014. Synthesis of 2',3',4'-trihydroxyflavone (2-D08), an inhibitor of protein sumoylation. *Bioorganic & Medicinal Chemistry Letters*, 24, 1094-1097.
- KIM, YEONG S., NAGY, K., KEYSER, S. & SCHNEEKLOTH JR, JOHN S. 2013. An Electrophoretic Mobility Shift Assay Identifies a Mechanistically Unique Inhibitor of Protein Sumoylation. *Chemistry & Biology*, 20, 604-613.
- KIRSH, O., SEELER, J.-S., PICHLER, A., GAST, A., MULLER, S., MISKA, E., MATHIEU, M., HAREL-BELLAN, A., KOUZARIDES, T., MELCHIOR, F. & DEJEAN, A. 2002. The SUMO E3 ligase RanBP2 promotes modification of the HDAC4 deacetylase. *EMBO J*, 21, 2682-2691.
- KNEZEVIC, I., LEISNER, T. M. & LAM, S. C.-T. 1996. Direct Binding of the Platelet Integrin α IIb β 3 (GPIIb-IIIa) to Talin: EVIDENCE THAT INTERACTION IS MEDIATED THROUGH THE CYTOPLASMIC DOMAINS OF BOTH α IIb AND β 3. *Journal of Biological Chemistry*, 271, 16416-16421.
- KNUESEL, M., CHEUNG, H. T., HAMADY, M., BARTHEL, K. K. B. & LIU, X. 2005. A Method of Mapping Protein Sumoylation Sites by Mass Spectrometry Using a Modified Small Ubiquitin-like Modifier 1 (SUMO-1) and a Computational Program. *Molecular & Cellular Proteomics*, 4, 1626-1636.
- KOH, T. J. & TIDBALL, J. G. 2000. Nitric oxide inhibits calpain-mediated proteolysis of talin in skeletal muscle cells. *American Journal of Physiology - Cell Physiology*, 279, C806-C812.
- KOMATSU, N., SUDA, T., MOROI, M., TOKUYAMA, N., SAKATA, Y., OKADA, M., NISHIDA, T., HIRAI, Y., SATO, T. & FUSE, A. 1989. *Growth and differentiation of a human megakaryoblastic cell line, CMK*.
- KOTAJA, N., KARVONEN, U., JÄNNE, O. A. & PALVIMO, J. J. 2002. PIAS Proteins Modulate Transcription Factors by Functioning as SUMO-1 Ligases. *Molecular and Cellular Biology*, 22, 5222-5234.
- KRAYNOV, V. S., CHAMBERLAIN, C., BOKOCH, G. M., SCHWARTZ, M. A., SLABAUGH, S. & HAHN, K. M. 2000. Localized Rac Activation Dynamics Visualized in Living Cells. *Science*, 290, 333-337.
- KUBOW, K. E. & HORWITZ, A. R. 2011. Reducing background fluorescence reveals adhesions in 3D matrices. *Nat Cell Biol*, 13, 3-5.

- KUNG, CAMY C.-H., NAIK, MANDAR T., WANG, S.-H., SHIH, H.-M., CHANG, C.-C., LIN, L.-Y., CHEN, C.-L., MA, C., CHANG, C.-F. & HUANG, T.-H. 2014. Structural analysis of poly-SUMO chain recognition by the RNF4-SIMs domain. *Biochemical Journal*, 462, 53-65.
- KUO, J.-C., HAN, X., HSIAO, C.-T., YATES III, J. R. & WATERMAN, C. M. 2011. Analysis of the myosin-II-responsive focal adhesion proteome reveals a role for [beta]-Pix in negative regulation of focal adhesion maturation. *Nat Cell Biol*, 13, 383-393.
- KUO, J.-C., HAN, X., YATES, J. R. & WATERMAN, C. M. 2012. Isolation of Focal Adhesion Proteins for Biochemical and Proteomic Analysis. In: SHIMAOKA, M. (ed.) *Integrin and Cell Adhesion Molecules: Methods and Protocols*. Totowa, NJ: Humana Press.
- KWEK, S. S., DERRY, J., TYNER, A. L., SHEN, Z. & GUDKOV, A. V. 2001. Functional analysis and intracellular localization of p53 modified by SUMO-1. *Oncogene*, 20, 2587-2599.
- LAMMERMANN, T. A. S., M. 2009. Mechanical modes of 'amoeboid' cell migration. *Current Opinion in Cell Biology*, 21, 636-644.
- LAMOLIATTE, F., CARON, D., DURETTE, C., MAHROUCHE, L., MAROUI, M. A., CARON-LIZOTTE, O., BONNEIL, E., CHELBI-ALIX, M. K. & THIBAUT, P. 2014. Large-scale analysis of lysine SUMOylation by SUMO remnant immunoaffinity profiling. *Nature Communications*, 5, 5409.
- LEBART, M.-C. & BENYAMIN, Y. 2006. Calpain involvement in the remodeling of cytoskeletal anchorage complexes. *FEBS Journal*, 273, 3415-3426.
- LEBER, M. F. & EFFERTH, T. 2009a. Molecular principles of cancer invasion and metastasis (review). *International journal of oncology*, 34, 881.
- LEE, M. S., KIM, Y. B., LEE, S. Y., KIM, J. G., KIM, S. H., YE, S. K. & LEE, J. W. 2006. Integrin signaling and cell spreading mediated by phorbol 12-myristate 13-acetate treatment. *J Cell Biochem*, 99.
- LEGATE, K. R. & FÄSSLER, R. 2009. Mechanisms that regulate adaptor binding to β -integrin cytoplasmic tails. *Journal of Cell Science*, 122, 187-198.
- LEGATE, K. R., MONTANEZ, E., KUDLACEK, O. & FUSSLER, R. 2006. ILK, PINCH and parvin: the tIPP of integrin signalling. *Nat Rev Mol Cell Biol*, 7, 20-31.
- LEVINSON, H., HOPPER, J. E. & EHRlich, H. P. 2002. Overexpression of integrin α v promotes human osteosarcoma cell populated collagen lattice contraction and cell migration. *Journal of Cellular Physiology*, 193, 219-224.
- LI, H., NIU, H., PENG, Y., WANG, J. & HE, P. 2013a. Ubc9 promotes invasion and metastasis of lung cancer cells. *Oncol Rep*, 29, 1588-94.
- LI, R., WEI, J., JIANG, C., LIU, D., DENG, L., ZHANG, K. & WANG, P. 2013b. Akt SUMOylation Regulates Cell Proliferation and Tumorigenesis. *Cancer Research*, 73, 5742-5753.
- LIN, H.-H. 2015. In Vitro and in Vivo Atheroprotective Effects of Gossypetin against Endothelial Cell Injury by Induction of Autophagy. *Chemical Research in Toxicology*, 28, 202-215.
- LING, K., DOUGHMAN, R. L., FIRESTONE, A. J., BUNCE, M. W. & ANDERSON, R. A. 2002. Type I[gamma] phosphatidylinositol phosphate kinase targets and regulates focal adhesions. *Nature*, 420, 89-93.
- LING, K., DOUGHMAN, R. L., IYER, V. V., FIRESTONE, A. J., BAIRSTOW, S. F., MOSHER, D. F., SCHALLER, M. D. & ANDERSON, R. A. 2003. Tyrosine phosphorylation of type I γ phosphatidylinositol phosphate kinase by Src regulates an integrin-talin switch. *The Journal of Cell Biology*, 163, 1339-1349.
- LIU, X. & SCHNELLMANN, R. G. 2003. Calpain Mediates Progressive Plasma Membrane Permeability and Proteolysis of Cytoskeleton-Associated Paxillin, Talin, and Vinculin during Renal Cell Death. *Journal of Pharmacology and Experimental Therapeutics*, 304, 63-70.
- LOCK, J. G., HALLER, B.W. AND STROMBLAD, S. 2008. Cell-matrix adhesion complexes: Master control machinery of cell migration. *Seminars in Cancer Biology*, 18, 65-76.
- LORENTZEN, A., BAMBER, J., SADOK, A., SCHWAB, L.E. AND MARSHALL, C.J. 2011. An ezrin-rich, rigid uropod-like structure directs movement of amoeboid blebbing cells. *Journal of Cell Science*, 124, 1256-1267.

- LU, P. F., WEAVER, V.M. AND WERB, Z. J. 2012. The extracellular matrix: A dynamic niche in cancer progression. *Cell. Biol.*, 196, 395-406.
- LUNDBERG, E., FAGERBERG, L., KLEVEBRING, D., MATIC, I., GEIGER, T., COX, J., ÄLGENÄS, C., LUNDEBERG, J., MANN, M. & UHLEN, M. 2010. Defining the transcriptome and proteome in three functionally different human cell lines. *Molecular Systems Biology*, 6, 450.
- MA, Y. Q., QIN, J. & PLOW, E. 2007. Platelet integrin $\alpha\text{IIb}\beta\text{3}$: activation mechanisms. *Journal of Thrombosis and Haemostasis*, 5, 1345-1352.
- MABB, A. M. & MIYAMOTO, S. 2007. SUMO and NF- κ B ties. *Cellular and Molecular Life Sciences*, 64, 1979-1996.
- MAHADEVAN, S. & PARK, Y. 2008. Multifaceted Therapeutic Benefits of Ginkgo biloba L.: Chemistry, Efficacy, Safety, and Uses. *Journal of Food Science*, 73, R14-R19.
- MAKHNEVYCH, T., SYDORSKY, Y., XIN, X., SRIKUMAR, T., VIZEACOMAR, F. J., JERAM, S. M., LI, Z., BAHR, S., ANDREWS, B. J., BOONE, C. & RAUGHT, B. 2009. Global Map of SUMO Function Revealed by Protein-Protein Interaction and Genetic Networks. *Molecular Cell*, 33, 124-135.
- MARTEL, V., VIGNOUD, L., DUPE, S., FRACHET, P., BLOCK, M. R. & ALBIGES-RIZO, C. 2000. Talin controls the exit of the integrin alpha 5 beta 1 from an early compartment of the secretory pathway. *Journal of Cell Science*, 113, 1951-1961.
- MARTIN, S., WILKINSON, K. A., NISHIMUNE, A. & HENLEY, J. M. 2007. Emerging extranuclear roles of protein SUMOylation in neuronal function and dysfunction. *Nat Rev Neurosci*, 8, 948-959.
- MATIC, I., SCHIMMEL, J., HENDRIKS, I. A., VAN SANTEN, M. A., VAN DE RIJKE, F., VAN DAM, H., GNAD, F., MANN, M. & VERTEGAAL, A. C. O. 2010. Site-Specific Identification of SUMO-2 Targets in Cells Reveals an Inverted SUMOylation Motif and a Hydrophobic Cluster SUMOylation Motif. *Molecular Cell*, 39, 641-652.
- MATIC, I., VAN HAGEN, M., SCHIMMEL, J., MACEK, B., OGG, S. C., TATHAM, M. H., HAY, R. T., LAMOND, A. I., MANN, M. & VERTEGAAL, A. C. O. 2008. In Vivo Identification of Human Small Ubiquitin-like Modifier Polymerization Sites by High Accuracy Mass Spectrometry and an in Vitro to in Vivo Strategy. *Molecular & Cellular Proteomics*, 7, 132-144.
- MCDOWALL, A., INWALD, D., LEITINGER, B., JONES, A., LIESNER, R., KLEIN, N. & HOGG, N. 2003. A novel form of integrin dysfunction involving β1 , β2 , and β3 integrins. *The Journal of Clinical Investigation*, 111, 51-60.
- MCNICOL, A. & ROBSON, C. A. 1997. Thrombin Receptor-Activating Peptide Releases Arachidonic Acid from Human Platelets: A Comparison with Thrombin and Trypsin. *Journal of Pharmacology and Experimental Therapeutics*, 281, 861-867.
- MELCHIOR, F. 2000. SUMO-nonclassical ubiquitin. *Annual review of cell and developmental biology*, 16, 591-626.
- MELCHIOR, F. & HENGST, L. 2002. SUMO-1 and p53. *Cell Cycle*, 1, 243-247.
- MEYER, A. S., HUGHES-ALFORD, S. K., KAY, J. E., CASTILLO, A., WELLS, A., GERTLER, F. B. & LAUFFENBURGER, D. A. 2012. 2D protrusion but not motility predicts growth factor-induced cancer cell migration in 3D collagen. *The Journal of Cell Biology*, 197, 721-729.
- MIERKE, C. T., FREY, B., FELLNER, M., HERRMANN, M. & FABRY, B. 2011. Integrin $\alpha\text{5}\beta\text{1}$ facilitates cancer cell invasion through enhanced contractile forces. *Journal of Cell Science*, 124, 369-383.
- MILLER, G. J., DUNN, S. D. & BALL, E. H. 2001. Interaction of the N- and C-terminal Domains of Vinculin: CHARACTERIZATION AND MAPPING STUDIES. *Journal of Biological Chemistry*, 276, 11729-11734.
- MITCHISON, T. J. & CRAMER, L. P. 1996. Actin-Based Cell Motility and Cell Locomotion. *Cell*, 84, 371-379.
- MITRA, S. K., HANSON, D. A. & SCHLAEPFER, D. D. 2005. Focal adhesion kinase: in command and control of cell motility. *Nat Rev Mol Cell Biol*, 6, 56-68.
- MITRA, S. K. A. S., D.D. 2006. Integrin-regulated FAK-Src signalling in normal and cancer cells. *Current Opinion in Cell Biology*, 18, 516-523.

- MITSIOS, J. V., PRÉVOST, N., KASIRER-FRIEDE, A., GUTIERREZ, E., GROISMAN, A., ABRAMS, C. S., WANG, Y., LITVINOV, R. I., ZEMLIJIC-HARPF, A., ROSS, R. S. & SHATTIL, S. J. 2010. What Is Vinculin Needed for in Platelets? *Journal of thrombosis and haemostasis : JTH*, 8, 2294-2304.
- MO, Y.-Y., YU, Y., EE, P. L. R. & BECK, W. T. 2004. Overexpression of a Dominant-Negative Mutant Ubc9 Is Associated with Increased Sensitivity to Anticancer Drugs. *Cancer Research*, 64, 2793-2798.
- MO, Y.-Y., YU, Y., THEODOSIOU, E., RACHEL EE, P. L. & BECK, W. T. 2005. A role for Ubc9 in tumorigenesis. *24*, 2677-2683.
- MOCELLIN, S. & PROVENZANO, M. 2004. RNA interference: learning gene knock-down from cell physiology. *Journal of Translational Medicine*, 2 (1), 39.
- MOES, M., RODIUS, S., COLEMAN, S. J., MONKLEY, S. J., GOORMAGHTIGH, E., TREMUTH, L., KOX, C., VAN DER HOLST, P. P. G., CRITCHLEY, D. R. & KIEFFER, N. 2007. The Integrin Binding Site 2 (IBS2) in the Talin Rod Domain Is Essential for Linking Integrin β Subunits to the Cytoskeleton. *Journal of Biological Chemistry*, 282, 17280-17288.
- MOHSENY, A. B., HOGENDOORN, P.C.W. AND CLETON-JANSEN, A.M. 2012. Osteosarcoma Models: From Cell Lines to Zebrafish. *Sarcoma*, 2012.
- MOHSENY, A. B., MACHADO, I., CAI, Y., SCHAEFER, K.-L., SERRA, M., HOGENDOORN, P. C. W., LLOMBART-BOSCH, A. & CLETON-JANSEN, A.-M. 2011. Functional characterization of osteosarcoma cell lines provides representative models to study the human disease. *Lab Invest*, 91, 1195-1205.
- MOLLAPOUR, M., BOURBOULIA, D., BEEBE, K., WOODFORD, MARK R., POLIER, S., HOANG, A., CHELLURI, R., LI, Y., GUO, A., LEE, M.-J., FOTOOH-ABADI, E., KHAN, S., PRINCE, T., MIYAJIMA, N., YOSHIDA, S., TSUTSUMI, S., XU, W., PANARETOU, B., STETLER-STEVENSON, WILLIAM G., BRATSLAVSKY, G., TREPPEL, JANE B., PRODRMOU, C. & NECKERS, L. 2014. Asymmetric Hsp90 N Domain SUMOylation Recruits Aha1 and ATP-Competitive Inhibitors. *Molecular Cell*, 53, 317-329.
- MONTANEZ, E., USSAR, S., SCHIFFERER, M., BÖSL, M., ZENT, R., MOSER, M. & FÄSSLER, R. 2008. Kindlin-2 controls bidirectional signaling of integrins. *Genes & Development*, 22, 1325-1330.
- MONTEIRO, L. J., KHONGKOW, P., KONGSEMA, M., MORRIS, J. R., MAN, C., WEEKES, D., KOO, C.-Y., GOMES, A. R., PINTO, P. H. & VARGHESE, V. 2013. The Forkhead Box M1 protein regulates BRIP1 expression and DNA damage repair in epirubicin treatment. *Oncogene*, 32, 4634-4645.
- MORINI, M., MOTTOLESE, M., FERRARI, N., GHIORZO, F., BUGLIONI, S., MORTARINI, R., NOONAN, D. M., NATALI, P. G. & ALBINI, A. 2000. The $\alpha 3\beta 1$ integrin is associated with mammary carcinoma cell metastasis, invasion, and gelatinase B (mmp-9) activity. *International Journal of Cancer*, 87, 336-342.
- MOSCHOS, S. J., SMITH, A. P., MANDIC, M., ATHANASSIOU, C., WATSON-HURST, K., JUKIC, D. M., EDINGTON, H. D., KIRKWOOD, J. M. & BECKER, D. 2007. SAGE and antibody array analysis of melanoma-infiltrated lymph nodes: identification of Ubc9 as an important molecule in advanced-stage melanomas. *Oncogene*, 26, 4216-4225.
- MOSER, M., NIESWANDT, B., USSAR, S., POZGAJOVA, M. & FASSLER, R. 2008. Kindlin-3 is essential for integrin activation and platelet aggregation. *Nat Med*, 14, 325-330.
- MUKHOPADHYAY, D. & DASSO, M. 2007. Modification in reverse: the SUMO proteases. *Trends in Biochemical Sciences*, 32, 286-295.
- MÜLLER, S., BERGER, M., LEHEMBRE, F., SEELER, J.-S., HAUPT, Y. & DEJEAN, A. 2000. c-Jun and p53 Activity Is Modulated by SUMO-1 Modification. *Journal of Biological Chemistry*, 275, 13321-13329.
- MÜLLER, S., HOEGE, C., PYROWOLAKIS, G. & JENTSCH, S. 2001. Sumo, ubiquitin's mysterious cousin. *Nat Rev Mol Cell Biol*, 2, 202-213.
- MYATT, S. S., KONGSEMA, M., MAN, C. W. Y., KELLY, D. J., GOMES, A. R., KHONGKOW, P., KARUNARATHNA, U., ZONA, S., LANGER, J. K., DUNSBY, C. W., COOMBES, R. C., FRENCH, P.

- M., BROSENS, J. J. & LAM, E. W. F. 2014. SUMOylation inhibits FOXM1 activity and delays mitotic transition. *Oncogene*, 33, 4316-4329.
- NAIK, M. U. & NAIK, U. P. 2003. Calcium-and integrin-binding protein regulates focal adhesion kinase activity during platelet spreading on immobilized fibrinogen. *Blood*, 102, 3629-3636.
- NAKAZAWA, T., TADOKORO, S., KAMAE, T., KIYOMIZU, K., KASHIWAGI, H., HONDA, S., KANAKURA, Y. & TOMIYAMA, Y. 2013. Agonist stimulation, talin-1, and kindlin-3 are crucial for α IIb β 3 activation in a human megakaryoblastic cell line, CMK. *Experimental Hematology*, 41, 79-90.e1.
- NAYAK, A. & MÜLLER, S. 2014. SUMO-specific proteases/isopeptidases: SENPs and beyond. *Genome Biology*, 15, 422.
- NGOC, K. V. N., CHEUNG, K.J., BRENOT, A., SHAMIR, E.R., GRAY, R.S., HINES, W.C., YASWEN, P., WERB, Z. AND EWALD, A.J. 2012. ECM microenvironment regulates collective migration and local dissemination in normal and malignant mammary epithelium. *PNAS* 109, E2595-2604.
- NGUYEN, V., NGUYEN, A., MEYERS, C. A., SHEN, J., SCOTT, M. A. & JAMES, A. W. 2016. The Role of Integrins in Osteosarcoma. *International Journal of Orthopaedics*, 3, 544-548.
- NIE, M., XIE, Y., LOO, J. A. & COUREY, A. J. 2009. Genetic and Proteomic Evidence for Roles of Drosophila SUMO in Cell Cycle Control, Ras Signaling, and Early Pattern Formation. *PLoS ONE*, 4, e5905.
- NIESWANDT, B., MOSER, M., PLEINES, I., VARGA-SZABO, D., MONKLEY, S., CRITCHLEY, D. & FÄSSLER, R. 2007. Loss of talin1 in platelets abrogates integrin activation, platelet aggregation, and thrombus formation in vitro and in vivo. *The Journal of Experimental Medicine*, 204, 3113-3118.
- NIESWANDT, B. & WATSON, S. P. 2003. Platelet-collagen interaction: is GPVI the central receptor? *Blood*, 102, 449-461.
- NIFOROU, K. N., ANAGNOSTOPOULOS, A. K., VOUGAS, K., KITTAS, C., GORGOLIS, V. G. & TSANGARIS, G. T. 2008. The Proteome Profile of the Human Osteosarcoma U2OS Cell Line. *Cancer Genomics - Proteomics*, 5, 63-77.
- OSULA, O., SWATKOSKI, S. & COTTER, R. J. 2012. Identification of protein SUMOylation sites by mass spectrometry using combined microwave-assisted aspartic acid cleavage and tryptic digestion. *Journal of mass spectrometry : JMS*, 47, 644-654.
- PANKOV, R., CUKIERMAN, E., KATZ, B.-Z., MATSUMOTO, K., LIN, D. C., LIN, S., HAHN, C. & YAMADA, K. M. 2000. Integrin Dynamics and Matrix Assembly: Tensin-Dependent Translocation of α 5 β 1 Integrins Promotes Early Fibronectin Fibrillogenesis. *The Journal of Cell Biology*, 148, 1075-1090.
- PANSE, V. G., HARDELAND, U., WERNER, T., KUSTER, B. & HURT, E. 2004. A Proteome-wide Approach Identifies Sumoylated Substrate Proteins in Yeast. *Journal of Biological Chemistry*, 279, 41346-41351.
- PARSONS, J. T. 2003. Focal adhesion kinase: the first ten years. *Journal of Cell Science*, 116, 1409-1416.
- PARSONS, J. T., HORWITZ, A. R. & SCHWARTZ, M. A. 2010. Cell adhesion: integrating cytoskeletal dynamics and cellular tension. *Nat Rev Mol Cell Biol*, 11, 633-643.
- PATEL, B., GINGRAS, A. R., BOBKOV, A. A., FUJIMOTO, L. M., ZHANG, M., LIDDINGTON, R. C., MAZZEO, D., EMSLEY, J., ROBERTS, G. C. K., BARSUKOV, I. L. & CRITCHLEY, D. R. 2006. The Activity of the Vinculin Binding Sites in Talin Is Influenced by the Stability of the Helical Bundles That Make Up The Talin Rod. *Journal of Biological Chemistry*, 281, 7458-7467.
- PENTIKÄINEN, U. & YLÄNNE, J. 2009. The Regulation Mechanism for the Auto-Inhibition of Binding of Human Filamin A to Integrin. *Journal of Molecular Biology*, 393, 644-657.
- PETIT, V. & THIERY, J.-P. 2000. Focal adhesions: Structure and dynamics. *Biology of the Cell*, 92, 477-494.
- PETRICH, B. G., FOGELSTRAND, P., PARTRIDGE, A. W., YOUSEFI, N., ABLOOGLU, A. J., SHATTIL, S. J. & GINSBERG, M. H. 2007a. The antithrombotic potential of selective blockade of talin-

- dependent integrin $\alpha\text{IIb}\beta\text{3}$ (platelet GPIIb-IIIa) activation. *The Journal of Clinical Investigation*, 117, 2250-2259.
- PETRICH, B. G., MARCHESE, P., RUGGERI, Z. M., SPIESS, S., WEICHERT, R. A. M., YE, F., TIEDT, R., SKODA, R. C., MONKLEY, S. J., CRITCHLEY, D. R. & GINSBERG, M. H. 2007b. Talin is required for integrin-mediated platelet function in hemostasis and thrombosis. *The Journal of Experimental Medicine*, 204, 3103-3111.
- PETRIE, R. J., DOYLE, A. D. & YAMADA, K. M. 2009. Random versus directionally persistent cell migration. *Nat Rev Mol Cell Biol*, 10, 538-549.
- PETRIE, R. J. & YAMADA, K. M. 2012. At the leading edge of three-dimensional cell migration. *Journal of Cell Science*, 125, 5917-5926.
- POLLARD, T. D. & BORISY, G. G. 2003. Cellular Motility Driven by Assembly and Disassembly of Actin Filaments. *Cell*, 112, 453-465.
- PONTI, A., MACHACEK, M., GUPTON, S. L., WATERMAN-STORER, C. M. & DANUSER, G. 2004. Two Distinct Actin Networks Drive the Protrusion of Migrating Cells. *Science*, 305, 1782-1786.
- POPOWICZ, G. M., SCHLEICHER, M., NOEGEL, A. A. & HOLAK, T. A. 2006. Filamins: promiscuous organizers of the cytoskeleton. *Trends in Biochemical Sciences*, 31, 411-419.
- POTTS, P. R. & YU, H. 2007. The SMC5/6 complex maintains telomere length in ALT cancer cells through SUMOylation of telomere-binding proteins. *Nature structural & molecular biology*, 14, 581-590.
- PRASS, M., JACOBSON, K., MOGILNER, A. & RADMACHER, M. 2006. Direct measurement of the lamellipodial protrusive force in a migrating cell. *The Journal of Cell Biology*, 174, 767-772.
- QIN, Y., XU, J., AYSOLA, K., BEGUM, N., REDDY, V., CHAI, Y., GRIZZLE, W. E., PARTRIDGE, E. E., REDDY, E. S. P. & RAO, V. N. 2011. Ubc9 mediates nuclear localization and growth suppression of BRCA1 and BRCA1a proteins. *Journal of Cellular Physiology*, 226, 3355-3367.
- QIN, Y., XU, J., AYSOLA, K., OPREA, G., REDDY, A., MATTHEWS, R., OKOLI, J., CANTOR, A., GRIZZLE, W. E. & PARTRIDGE, E. E. 2012. BRCA1 proteins regulate growth of ovarian cancer cells by tethering Ubc9. *Am J Cancer Res*, 2, 540-548.
- RAM, S. E. A. Y., K.M. 2005. Cell migration in 3D matrix. *Current Opinion in Cell Biology*, 17, 524-532.
- REN, X. D., KIOSSES, W. B., SIEG, D. J., OTEY, C. A., SCHLAEPFER, D. D. & SCHWARTZ, M. A. 2000. Focal adhesion kinase suppresses Rho activity to promote focal adhesion turnover. *Journal of Cell Science*, 113, 3673-3678.
- REVERTER, D. & LIMA, C. D. 2006. Structural basis for SENP2 protease interactions with SUMO precursors and conjugated substrates. *Nature structural & molecular biology*, 13, 1060-1068.
- RIDLEY, A. J. 2011. Life at the Leading Edge. *Cell*, 145, 1012-1022.
- RIVERA, J., LOZANO, M. L., NAVARRO-NÚÑEZ, L. & VICENTE, V. 2009. Platelet receptors and signaling in the dynamics of thrombus formation. *Haematologica*, 94, 700-711.
- ROBERTS, G. C. K. & CRITCHLEY, D. R. 2009. Structural and biophysical properties of the integrin-associated cytoskeletal protein talin. *Biophysical Reviews*, 1, 61-69.
- RODIUS, S., CHALOIN, O., MOES, M., SCHAFFNER-RECKINGER, E., LANDRIEU, I., LIPPENS, G., LIN, M., ZHANG, J. & KIEFFER, N. 2008. The Talin Rod IBS2 α -Helix Interacts with the β3 Integrin Cytoplasmic Tail Membrane-proximal Helix by Establishing Charge Complementary Salt Bridges. *Journal of Biological Chemistry*, 283, 24212-24223.
- RODRÍGUEZ FERNÁNDEZ, J., GEIGER, B., SALOMON, D. & BEN-ZE'EV, A. 1993. Suppression of vinculin expression by antisense transfection confers changes in cell morphology, motility, and anchorage-dependent growth of 3T3 cells. *The Journal of Cell Biology*, 122, 1285-1294.
- RODRIGUEZ, M. S., DESTERRO, J. M. P., LAIN, S., MIDGLEY, C. A., LANE, D. P. & HAY, R. T. 1999. SUMO-1 modification activates the transcriptional response of p53. *EMBO J*, 18, 6455-6461.
- ROSAS-ACOSTA, G., RUSSELL, W. K., DEYRIEUX, A., RUSSELL, D. H. & WILSON, V. G. 2005. A Universal Strategy for Proteomic Studies of SUMO and Other Ubiquitin-like Modifiers. *Molecular & Cellular Proteomics*, 4, 56-72.

- ROULEAU, N., WANG, J., KARRAS, L., ANDREWS, E., BIELEFELD-SEVIGNY, M. & CHEN, Y. 2008. Highly sensitive assays for SUMOylation and small ubiquitin-like modifier-dependent protein-protein interactions. *Analytical Biochemistry*, 375, 364-366.
- RUGGERI, Z. M. 2002. Platelets in atherothrombosis. *Nature medicine*, 8, 1227-1234.
- RUGGERI, Z. M. & MENDOLICCHIO, G. L. 2007. Adhesion Mechanisms in Platelet Function. *Circulation Research*, 100, 1673-1685.
- SABEH, F., SHIMIZU-HIROTA, R. & WEISS, S. J. 2009. Protease-dependent versus -independent cancer cell invasion programs: three-dimensional amoeboid movement revisited. *The Journal of Cell Biology*, 185, 11-19.
- SAHAI, E. A. M., C.J. 2003. Different modes of tumour cell invasion have distinct requirements for Rho/ROCK signalling and extracellular proteolysis. *Nature Cell Biology*, 5, 711 - 719.
- SAITOH, H. & HINCHEY, J. 2000. Functional Heterogeneity of Small Ubiquitin-related Protein Modifiers SUMO-1 versus SUMO-2/3. *Journal of Biological Chemistry*, 275, 6252-6258.
- SAKAMOTO, S., MCCANN, R. O., DHIR, R. & KYPRIANOU, N. 2010. Talin1 Promotes Tumor Invasion and Metastasis via Focal Adhesion Signaling and Anoikis Resistance. *Cancer Research*, 70, 1885-1895.
- SAMPSON, D. A., WANG, M. & MATUNIS, M. J. 2001. The Small Ubiquitin-like Modifier-1 (SUMO-1) Consensus Sequence Mediates Ubc9 Binding and Is Essential for SUMO-1 Modification. *Journal of Biological Chemistry*, 276, 21664-21669.
- SANSING, H. A., SARKESHIK, A., YATES, J. R., PATEL, V., GUTKIND, J. S., YAMADA, K. M. & BERRIER, A. L. 2011. Integrin $\alpha\beta 1$, $\alpha\beta 2$, $\alpha\beta 3$ effectors p130Cas, Src and talin regulate carcinoma invasion and chemoresistance. *Biochemical and Biophysical Research Communications*, 406, 171-176.
- SATO, T., FUSE, A., EGUCHI, M., HAYASHI, Y., RYO, R., ADACHI, M., KISHIMOTO, Y., TERAMURA, M., MIZOGUCHI, H., SHIMA, Y., KOMORI, I., SUNAMI, S., OKIMOTO, Y. & NAKAJIMA, H. 1989. Establishment of a human leukaemic cell line (CMK) with megakaryocytic characteristics from a Down's syndrome patient with acute megakaryoblastic leukaemia. *British Journal of Haematology*, 72, 184-190.
- SAUNDERS, R. M., HOLT, M. R., JENNINGS, L., SUTTON, D. H., BARSUKOV, I. L., BOBKOV, A., LIDDINGTON, R. C., ADAMSON, E. A., DUNN, G. A. & CRITCHLEY, D. R. 2006. Role of vinculin in regulating focal adhesion turnover. *European Journal of Cell Biology*, 85, 487-500.
- SCHALLER, M. D. 2001. Paxillin: a focal adhesion-associated adaptor protein. *Oncogene*, 20, 6459-6472.
- SCHIMMEL, J., EIFLER, K., SIGURÐSSON, JÓN O., CUIJPERS, SABINE A. G., HENDRIKS, IVO A., VERLAAN-DE VRIES, M., KELSTRUP, CHRISTIAN D., FRANCAVILLA, C., MEDEMA, RENÉ H., OLSEN, JESPER V. & VERTEGAAL, ALFRED C. O. 2014. Uncovering SUMOylation Dynamics during Cell-Cycle Progression Reveals FoxM1 as a Key Mitotic SUMO Target Protein. *Molecular Cell*, 53, 1053-1066.
- SCHIMMEL, J., LARSEN, K. M., MATIC, I., VAN HAGEN, M., COX, J., MANN, M., ANDERSEN, J. S. & VERTEGAAL, A. C. O. 2008. The Ubiquitin-Proteasome System Is a Key Component of the SUMO-2/3 Cycle. *Molecular & Cellular Proteomics*, 7, 2107-2122.
- SCHÖBER, M., RAGHAVAN, S., NIKOLOVA, M., POLAK, L., PASOLLI, H. A., BEGGS, H. E., REICHARDT, L. F. & FUCHS, E. 2007. Focal adhesion kinase modulates tension signaling to control actin and focal adhesion dynamics. *The Journal of Cell Biology*, 176, 667-680.
- SCHOENWAEELDER, S. M., YUAN, Y., COORAY, P., SALEM, H. H. & JACKSON, S. P. 1997. Calpain Cleavage of Focal Adhesion Proteins Regulates the Cytoskeletal Attachment of Integrin $\alpha\text{IIb}\beta 3$ (Platelet Glycoprotein IIb/IIIa) and the Cellular Retraction of Fibrin Clots. *Journal of Biological Chemistry*, 272, 1694-1702.
- SCHOROVA, L. & MARTIN, S. 2016. Sumoylation in Synaptic Function and Dysfunction. *Frontiers in Synaptic Neuroscience*, 8, 9.

- SCHOU, J., KELSTRUP, C. D., HAYWARD, D. G., OLSEN, J. V. & NILSSON, J. 2014. Comprehensive Identification of SUMO2/3 Targets and Their Dynamics during Mitosis. *PLoS ONE*, 9, e100692.
- SEELER, J. S. & DEJEAN, A. 2003. Nuclear and unclear functions of SUMO. *Nat Rev Mol Cell Biol*, 4.
- SEONG, J., TAJIK, A., SUN, J., GUAN, J.-L., HUMPHRIES, M. J., CRAIG, S. E., SHEKARAN, A., GARCÍA, A. J., LU, S., LIN, M. Z., WANG, N. & WANG, Y. 2013. Distinct biophysical mechanisms of focal adhesion kinase mechanoactivation by different extracellular matrix proteins. *Proceedings of the National Academy of Sciences*, 110, 19372-19377.
- SERRANO, K. & DEVINE, D. V. 2004. Vinculin is proteolyzed by calpain during platelet aggregation: 95 kDa cleavage fragment associates with the platelet cytoskeleton. *Cell Motility and the Cytoskeleton*, 58, 242-252.
- SEYOUM, A., ASRES, K. & EL-FIKY, F. K. 2006. Structure–radical scavenging activity relationships of flavonoids. *Phytochemistry*, 67, 2058-2070.
- SHAN, G. 2010. RNA interference as a gene knockdown technique. *The international journal of biochemistry & cell biology*, 42, 1243-1251.
- SHATTIL, S. J., KIM, C. & GINSBERG, M. H. 2010. The final steps of integrin activation: the end game. *Nat Rev Mol Cell Biol*, 11, 288-300.
- SHIIO, Y. & EISENMAN, R. N. 2003. Histone sumoylation is associated with transcriptional repression. *Proceedings of the National Academy of Sciences*, 100, 13225-13230.
- SLAMON, D., CLARK, G., WONG, S., LEVIN, W., ULLRICH, A. & MCGUIRE, W. 1987. Human breast cancer: correlation of relapse and survival with amplification of the HER-2/neu oncogene. *Science*, 235(4785): 177-82.
- SLOAN, E., POULIOT, N., STANLEY, K., CHIA, J., MOSELEY, J., HARDS, D. & ANDERSON, R. 2006. Tumor-specific expression of $\alpha v \beta 3$ integrin promotes spontaneous metastasis of breast cancer to bone. *Breast Cancer Research*, 8.
- SMITH, J. V. & LUO, Y. 2004. Studies on molecular mechanisms of Ginkgo biloba extract. *Applied Microbiology and Biotechnology*, 64, 465-472.
- SONG, J., DURRIN, L. K., WILKINSON, T. A., KRONTIRIS, T. G. & CHEN, Y. 2004. Identification of a SUMO-binding motif that recognizes SUMO-modified proteins. *Proceedings of the National Academy of Sciences of the United States of America*, 101, 14373-14378.
- STANKOVIC-VALENTIN, N., DELTOUR, S., SEELER, J., PINTE, S., VERGOTEN, G., GUÉRARDEL, C., DEJEAN, A. & LEPRINCE, D. 2007. An Acetylation/Deacetylation-SUMOylation Switch through a Phylogenetically Conserved ψ KXEP Motif in the Tumor Suppressor HIC1 Regulates Transcriptional Repression Activity. *Molecular and Cellular Biology*, 27, 2661-2675.
- STEFANINI, L., YE, F., SNIDER, A. K., SARABAKHSH, K., PIATT, R., PAUL, D. S., BERGMEIER, W. & PETRICH, B. G. 2014. A talin mutant that impairs talin-integrin binding in platelets decelerates $\alpha IIb \beta 3$ activation without pathological bleeding. *Blood*, 123, 2722-2731.
- STEFFEN, A., LADWEIN, M., DIMCHEV, G. A., HEIN, A., SCHWENKMEZGER, L., ARENS, S., LADWEIN, K. I., MARGIT HOLLEBOOM, J., SCHUR, F., VICTOR SMALL, J., SCHWARZ, J., GERHARD, R., FAIX, J., STRADAL, T. E. B., BRAKEBUSCH, C. & ROTTNER, K. 2013. Rac function is crucial for cell migration but is not required for spreading and focal adhesion formation. *Journal of Cell Science*, 126, 4572-4588.
- SUN, Z., HU, S., LUO, Q., YE, D., HU, D. & CHEN, F. 2013. Overexpression of SENP3 in oral squamous cell carcinoma and its association with differentiation. *Oncology reports*, 29, 1701-1706.
- TADOKORO, S., SHATTIL, S. J., ETO, K., TAI, V., LIDDINGTON, R. C., DE PEREDA, J. M., GINSBERG, M. H. & CALDERWOOD, D. A. 2003. Talin Binding to Integrin β Tails: A Final Common Step in Integrin Activation. *Science*, 302, 103-106.
- TAHERIAN, A., LI, X., LIU, Y. & HAAS, T. A. 2011. Differences in integrin expression and signaling within human breast cancer cells. *BMC Cancer*, 11, 1-15.
- TAMMSALU, T., MATIC, I., JAFFRAY, E. G., IBRAHIM, A. F. M., TATHAM, M. H. & HAY, R. T. 2014. Proteome-Wide Identification of SUMO2 Modification Sites.

- TATHAM, M. H., JAFFRAY, E., VAUGHAN, O. A., DESTERRO, J. M. P., BOTTING, C. H., NAISMITH, J. H. & HAY, R. T. 2001. Polymeric Chains of SUMO-2 and SUMO-3 Are Conjugated to Protein Substrates by SAE1/SAE2 and Ubc9. *Journal of Biological Chemistry*, 276, 35368-35374.
- TATHAM, M. H., MATIC, I., MANN, M. & HAY, R. T. 2011. Comparative proteomic analysis identifies a role for SUMO in protein quality control. *Sci Signal*, 4, rs4.
- TENG, S., LUO, H. & WANG, L. 2012. Predicting protein sumoylation sites from sequence features. *Amino Acids*, 43, 447-455.
- TRANQUI, L. & BLOCK, M. R. 1995. Intracellular Processing of Talin Occurs within Focal Adhesions. *Experimental Cell Research*, 217, 149-156.
- TRAORE, K., TRUSH, M. A., GEORGE JR, M., SPANNHAKE, E. W., ANDERSON, W. & ASSEFFA, A. 2005. Signal transduction of phorbol 12-myristate 13-acetate (PMA)-induced growth inhibition of human monocytic leukemia THP-1 cells is reactive oxygen dependent. *Leukemia Research*, 29, 863-879.
- UCHIMURA, Y., NAKAO, M. & SAITOH, H. 2004. Generation of SUMO-1 modified proteins in E. coli: towards understanding the biochemistry/structural biology of the SUMO-1 pathway. *FEBS Letters*, 564, 85-90.
- ULLMANN, R., CHIEN, CHRISTOPHER D., AVANTAGGIATI, MARIA L. & MULLER, S. 2012. An Acetylation Switch Regulates SUMO-Dependent Protein Interaction Networks. *Molecular Cell*, 46, 759-770.
- VELLON, L., MENENDEZ, J. A. & LUPU, R. 2006. A bidirectional " $\alpha\text{v}\beta\text{3}$ integrin-ERK1/ERK2 MAPK" connection regulates the proliferation of breast cancer cells. *Mol Carcinog*, 45.
- VERTEGAAL, A. C. O., ANDERSEN, J. S., OGG, S. C., HAY, R. T., MANN, M. & LAMOND, A. I. 2006. Distinct and Overlapping Sets of SUMO-1 and SUMO-2 Target Proteins Revealed by Quantitative Proteomics. *Molecular & Cellular Proteomics*, 5, 2298-2310.
- VERTEGAAL, A. C. O., OGG, S. C., JAFFRAY, E., RODRIGUEZ, M. S., HAY, R. T., ANDERSEN, J. S., MANN, M. & LAMOND, A. I. 2004. A Proteomic Study of SUMO-2 Target Proteins. *Journal of Biological Chemistry*, 279, 33791-33798.
- WANG, J., CHEN, L., WEN, S., ZHU, H., YU, W., MOSKOWITZ, I. P., SHAW, G. M., FINNELL, R. H. & SCHWARTZ, R. J. 2011. Defective sumoylation pathway directs congenital heart disease. *Birth Defects Research Part A: Clinical and Molecular Teratology*, 91, 468-476.
- WANG, J., LI, A., WANG, Z., FENG, X., OLSON, E. N. & SCHWARTZ, R. J. 2007. Myocardin sumoylation transactivates cardiogenic genes in pluripotent 10T1/2 fibroblasts. *Molecular and cellular biology*, 27, 622-632.
- WANG, J. & SCHWARTZ, R. J. 2010. Sumoylation and Regulation of Cardiac Gene Expression. *Circulation Research*, 107, 19-29.
- WANG, K. U. N. & ZHANG, X.-C. 2014. Inhibition of SENP5 suppresses cell growth and promotes apoptosis in osteosarcoma cells. *Experimental and Therapeutic Medicine*, 7, 1691-1695.
- WANG, L., ZHANG, J., BANERJEE, S., BARNES, L., SAJJA, V., LIU, Y., GUO, B., DU, Y., AGARWAL, M. K., WALD, D. N., WANG, Q. & YANG, J. 2010. Sumoylation of Vimentin³⁵⁴ Is Associated with PIAS3 Inhibition of Glioma Cell Migration.
- WANG, Y. & DASSO, M. 2009. SUMOylation and deSUMOylation at a glance. *Journal of Cell Science*, 122, 4249-4252.
- WANG, Y. K., WANG, Y.H., WANG, C.Z., SUNG, J.M., CHIU, W.T., LIN, S.H., CHANG, Y.H. AND TANG, M.J. 2003. Rigidity of collagen fibrils controls collagen gel-induced down-regulation of focal adhesion complex proteins mediated by $\alpha\text{2}\beta\text{1}$ integrin. *The Journal of Biological Chemistry*, 278 21886-21892.
- WATANABE, N., BODIN, L., PANDEY, M., KRAUSE, M., COUGHLIN, S., BOUSSIOTIS, V. A., GINSBERG, M. H. & SHATTIL, S. J. 2008. Mechanisms and consequences of agonist-induced talin recruitment to platelet integrin $\alpha\text{IIb}\beta\text{3}$. *The Journal of Cell Biology*, 181, 1211-1222.
- WEBB, D. J., PARSONS, J. T. & HORWITZ, A. F. 2002. Adhesion assembly, disassembly and turnover in migrating cells—over and over and over again. *Nature cell biology*, 4, E97-E100.

- WEGENER, K. L., PARTRIDGE, A. W., HAN, J., PICKFORD, A. R., LIDDINGTON, R. C., GINSBERG, M. H. & CAMPBELL, I. D. 2007. Structural Basis of Integrin Activation by Talin. *Cell*, 128, 171-182.
- WEIGELT, B., PETERSE, J. L. & VAN'T VEER, L. J. 2005. Breast cancer metastasis: markers and models. *Nat Rev Cancer*, 5, 591-602.
- WESTHOFF, M. A., SERRELS, B., FINCHAM, V. J., FRAME, M. C. & CARRAGHER, N. O. 2004. Src-Mediated Phosphorylation of Focal Adhesion Kinase Couples Actin and Adhesion Dynamics to Survival Signaling. *Molecular and Cellular Biology*, 24, 8113-8133.
- WHITE, J. R., HUANG, C. K., HILL, J. M., NACCACHE, P. H., BECKER, E. L. & SHA'AFI, R. I. 1984. Effect of phorbol 12-myristate 13-acetate and its analogue 4 alpha-phorbol 12,13-didecanoate on protein phosphorylation and lysosomal enzyme release in rabbit neutrophils. *Journal of Biological Chemistry*, 259, 8605-8611.
- WILKINSON, K. A. & HENLEY, J. M. 2010. Mechanisms, regulation and consequences of protein SUMOylation. *Biochemical Journal*, 428, 133-145.
- WIRTZ, D., KONSTANTOPOULOS, K. & SEARSON, P. C. 2011. The physics of cancer: the role of physical interactions and mechanical forces in metastasis. *Nat Rev Cancer*, 11, 512-522.
- WISNIEWSKI, J. R., ZOUGMAN, A., NAGARAJ, N. & MANN, M. 2009. Universal sample preparation method for proteome analysis. *Nat Meth*, 6, 359-362.
- WOHLSCHLEGEL, J. A., JOHNSON, E. S., REED, S. I. & YATES, J. R. 2004. Global Analysis of Protein Sumoylation in *Saccharomyces cerevisiae*. *Journal of Biological Chemistry*, 279, 45662-45668.
- WOLF, K., ALEXANDER, S., SCHACHT, V., COUSSENS, L.M., VON ANDRIAN, U.H., VAN RHEENEN, J., DERYUGINA, E. AND FRIEDL, P. 2009. Collagen-based cell migration models in vitro and in vivo. *Seminars in Cell & Developmental Biology*, 20, 931-941.
- WOLF, K., MAZO, I., LEUNG, H., ENGELKE, K., ANDRIAN, U.H.V., DERYUGINA, E.I., STRONGIN, A.Y., BROCKER, E.B. AND FRIEDL, P. 2003. Compensation mechanism in tumour cell migration: mesenchymal-amoeboid transition after blocking of pericellular proteolysis. *The Journal of Cell Biology* 160 267-277.
- WOOD, C. K., TURNER, C. E., JACKSON, P. & CRITCHLEY, D. R. 1994. Characterisation of the paxillin-binding site and the C-terminal focal adhesion targeting sequence in vinculin. *Journal of Cell Science*, 107, 709-717.
- WOZNIAK, K., KRUPA, R., SYNOWIEC, E. & MORAWIEC, Z. 2014. Polymorphism of UBC9 Gene Encoding the SUMO-E2-Conjugating Enzyme and Breast Cancer Risk. *Pathology & Oncology Research*, 20, 67-72.
- WOZNIAK, M. A., MODZELEWSKA, K., KWONG, L. & KEELY, P. J. 2004. Focal adhesion regulation of cell behavior. *Biochimica et Biophysica Acta (BBA) - Molecular Cell Research*, 1692, 103-119.
- WU, F., ZHU, S., DING, Y., BECK, W. T. & MO, Y.-Y. 2009. MicroRNA-mediated Regulation of Ubc9 Expression in Cancer Cells. *Clinical Cancer Research*, 15, 1550-1557.
- WYKOFF, D. D. & O'SHEA, E. K. 2005. Identification of Sumoylated Proteins by Systematic Immunoprecipitation of the Budding Yeast Proteome. *Molecular & Cellular Proteomics*, 4, 73-83.
- XIAO, Z., CHANG, J.-G., HENDRIKS, I. A., SIGURÐSSON, J. O., OLSEN, J. V. & VERTEGAAL, A. C. O. 2015. System-wide Analysis of SUMOylation Dynamics in Response to Replication Stress Reveals Novel Small Ubiquitin-like Modified Target Proteins and Acceptor Lysines Relevant for Genome Stability. *Molecular & Cellular Proteomics*, 14, 1419-1434.
- XU, J., HE, Y., QIANG, B., YUAN, J., PENG, X. & PAN, X.-M. 2008. A novel method for high accuracy sumoylation site prediction from protein sequences. *BMC Bioinformatics*, 9, 8.
- XU, W., COLL, J. L. & ADAMSON, E. D. 1998. Rescue of the mutant phenotype by reexpression of full-length vinculin in null F9 cells; effects on cell locomotion by domain deleted vinculin. *Journal of Cell Science*, 111, 1535-1544.
- XU, Y., BISMAR, T. A., SU, J., XU, B., KRISTIANSEN, G., VARGA, Z., TENG, L., INGBER, D. E., MAMMOTO, A., KUMAR, R. & ALAOUI-JAMALI, M. A. 2010. Filamin A regulates focal

- adhesion disassembly and suppresses breast cancer cell migration and invasion. *The Journal of Experimental Medicine*, 207, 2421-2437.
- XUE, Y., ZHOU, F., FU, C., XU, Y. & YAO, X. 2006. SUMOsp: a web server for sumoylation site prediction. *Nucleic Acids Research*, 34, W254-W257.
- YAMAGUCHI, H. & CONDEELIS, J. 2007. Regulation of the actin cytoskeleton in cancer cell migration and invasion. *Biochimica et Biophysica Acta (BBA) - Molecular Cell Research*, 1773, 642-652.
- YAMAGUCHI, H., LORENZ, M., KEMPIAK, S., SARMIENTO, C., CONIGLIO, S., SYMONS, M., SEGALL, J., EDDY, R., MIKI, H., TAKENAWA, T. & CONDEELIS, J. 2005. Molecular mechanisms of invadopodium formation: the role of the N-WASP-Arp2/3 complex pathway and cofilin. *The Journal of Cell Biology*, 168, 441-452.
- YAN, B., CALDERWOOD, D. A., YASPAN, B. & GINSBERG, M. H. 2001. Calpain Cleavage Promotes Talin Binding to the β 3Integrin Cytoplasmic Domain. *Journal of Biological Chemistry*, 276, 28164-28170.
- YANG, C. & KAZANIETZ, M. G. 2003. Divergence and complexities in DAG signaling: looking beyond PKC. *Trends in Pharmacological Sciences*, 24, 602-608.
- YANG, S., ZHANG, J. J. & HUANG, X.-Y. 2009. Orai1 and STIM1 Are Critical for Breast Tumor Cell Migration and Metastasis. *Cancer Cell*, 15, 124-134.
- YANG, Y., KITAGAKI, J., DAI, R.-M., TSAI, Y. C., LORICK, K. L., LUDWIG, R. L., PIERRE, S. A., JENSEN, J. P., DAVYDOV, I. V., OBEROI, P., LI, C.-C. H., KENTEN, J. H., BEUTLER, J. A., VOUSDEN, K. H. & WEISSMAN, A. M. 2007. Inhibitors of Ubiquitin-Activating Enzyme (E1), a New Class of Potential Cancer Therapeutics. *Cancer Research*, 67, 9472-9481.
- YAO, M., GOULT, B. T., CHEN, H., CONG, P., SHEETZ, M. P. & YAN, J. 2014. Mechanical activation of vinculin binding to talin locks talin in an unfolded conformation. *Sci. Rep.*, 4.
- YAO, Q., LI, H., LIU, B.-Q., HUANG, X.-Y. & GUO, L. 2011. SUMOylation-regulated Protein Phosphorylation, Evidence from Quantitative Phosphoproteomics Analyses. *Journal of Biological Chemistry*, 286, 27342-27349.
- YOSHIDA, K. & SOLDATI, T. 2006. Dissection of amoeboid movement into two mechanically distinct modes. *Journal of Cell Science*, 119, 3833-3844.
- ZAIDEL-BAR, R., BALLESTREM, C., KAM, Z. & GEIGER, B. 2003. Early molecular events in the assembly of matrix adhesions at the leading edge of migrating cells. *Journal of Cell Science*, 116, 4605-4613.
- ZAIDEL-BAR, R. & GEIGER, B. 2010. The switchable integrin adhesome. *Journal of Cell Science*, 123, 1385-1388.
- ZAMAN, M. H., TRAPANI, L. M., SIEMINSKI, A. L., MACKELLAR, D., GONG, H., KAMM, R. D., WELLS, A., LAUFFENBURGER, D. A. & MATSUDAIRA, P. 2006. Migration of tumor cells in 3D matrices is governed by matrix stiffness along with cell-matrix adhesion and proteolysis. *Proceedings of the National Academy of Sciences*, 103, 10889-10894.
- ZAMIR, E. & GEIGER, B. 2001. Molecular complexity and dynamics of cell-matrix adhesions. *Journal of Cell Science*, 114, 3583-3590.
- ZHANG, J. L., QIAN, Y. B., ZHU, L. X. AND XIONG, Q. R. 2011. Talin1, a Valuable Marker for Diagnosis and Prognostic Assessment of Human Hepatocellular Carcinomas *Asian Pacific Journal of Cancer Prevention*
12, 3265-3269.
- ZHANG, N., WU, X., YANG, L., XIAO, F., ZHANG, H., ZHOU, A., HUANG, Z. & HUANG, S. 2012. FoxM1 inhibition sensitizes resistant glioblastoma cells to temozolomide by downregulating the expression of DNA-repair gene Rad51. *Clinical cancer research*, 18, 5961-5971.
- ZHANG, X.-D., GOERES, J., ZHANG, H., YEN, T. J., PORTER, A. C. G. & MATUNIS, M. J. 2008a. SUMO-2/3 Modification and Binding Regulate the Association of CENP-E with Kinetochores and Progression through Mitosis. *Molecular Cell*, 29, 729-741.

- ZHANG, X., JIANG, G., CAI, Y., MONKLEY, S. J., CRITCHLEY, D. R. & SHEETZ, M. P. 2008b. Talin depletion reveals independence of initial cell spreading from integrin activation and traction. *Nat Cell Biol*, 10, 1062-1068.
- ZHAO, Q., XIE, Y., ZHENG, Y., JIANG, S., LIU, W., MU, W., LIU, Z., ZHAO, Y., XUE, Y. & REN, J. 2014. GPS-SUMO: a tool for the prediction of sumoylation sites and SUMO-interaction motifs. *Nucleic Acids Research*, 42, W325-W330.
- ZHOU, A.-X., HARTWIG, J. H. & AKYÜREK, L. M. 2009. Filamins in cell signaling, transcription and organ development. *Trends in Cell Biology*, 20, 113-123.
- ZHOU, W., CHAI, H., LIN, P. H., LUMSDEN, A. B., YAO, Q. & CHEN, C. 2004. Clinical Use and Molecular Mechanisms of Action of Extract of Ginkgo biloba Leaves in Cardiovascular Diseases. *Cardiovascular Drug Reviews*, 22, 309-319.
- ZHU, S., GOERES, J., SIXT, K. M., BÉKÉS, M., ZHANG, X.-D., SALVESEN, G. S. & MATUNIS, M. J. 2009. Protection from Isopeptidase-Mediated Deconjugation Regulates Paralog-Selective Sumoylation of RanGAP1. *Molecular Cell*, 33, 570-580.
- ZHU, S., SACHDEVA, M., WU, F., LU, Z. & MO, Y. Y. 2010. Ubc9 promotes breast cell invasion and metastasis in a sumoylation-independent manner. *Oncogene*, 29, 1763-1772.
- ZIEGLER, WOLFGANG H., GINGRAS, ALEX R., CRITCHLEY, DAVID R. & EMSLEY, J. 2008. Integrin connections to the cytoskeleton through talin and vinculin. *Biochemical Society Transactions*, 36, 235-239.
- ZIEGLER, W. H., LIDDINGTON, R. C. & CRITCHLEY, D. R. 2006. The structure and regulation of vinculin. *Trends in Cell Biology*, 16, 453-460.